SYNTHESIS, PHOTOISOMERIZATION AND ANTIMALARIAL ACTIVITIES OF CINNAMOYL CHLOROQUINOLINE HYBRIDS

By

NEMUDZIVHADI ANZA IMANUEL

(16000452)

A dissertation submitted in fulfilment of the requirements for the degree of Master of Science

In the

Department of Chemistry

Faculty of Science, Engineering and Agriculture

University of Venda

Thohoyandou, Limpopo

South Africa

Supervisor

Dr MV Bvumbi

Co-supervisor

Prof SS Mnyakeni Moleele

DECLARATION

I, **Nemudzivhadi Anza Imanuel** hereby declare that this thesis titled "**synthesis, photoisomerization and antimalarial activities of cinnamic acid/chloroquinoline analogues"** is my own work done under the supervisions of **Dr MV Bvumbi and Prof SS Mnyakeni Moleele** and this work has not been submitted before to this or any other university for any degree or examination. All the referenced material has been duly acknowledged. This work is being submitted for a degree **MSc in chemistry** in the University of Venda, Faculty of Science, Engineering and Agriculture at the department of chemistry.

Signature: 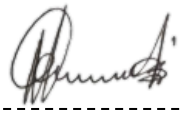 **Date**: 16/02/2024

Abstract

The primary aim of this project was to synthesize a series of cinnamoyl chloroquinoline hybrids employing a technique of molecular hybridization. Cinnamoyl chloroquinoline hybrids are compounds with the heteroaromatic core of amino-7-chloroquinoline, linked to differently substituted cinnamic acid groups by flexible primary diamines. In this study, three series (n=2, 3 and 6) of nineteen cinnamoyl chloroquinoline hybrids **18-36** were successfully synthesized by modifying known conventional methods with yields ranging from 24-74%. The structures of synthesized compounds were characterized by a combination of ^{1}H NMR, ^{13}C NMR, HRMS and IR analysis.

Hybrids **18-36** were found to isomerize when exposed to light to form mixture of *cis* and *trans* isomers. Through chromatographic mass spectrometry (LC-MS), these isomers were studied and LC-Q-TOF-MS/MS analyses of the photo-products revealed the emergence of *cis* isomer which eluted before its synthesized *trans* counterpart, suggesting a reduced polarity. The polarity of the compounds was significantly influenced by the nature of the substituents attached to the phenyl ring. Electron-withdrawing groups such as Cl, NO_2, and F increased polarity in contrast to electron donating group OCH_3 which reduced polarity. The concept of photoisomerization of cinnamoyl chloroquinoline hybridswere validated by the measurement of the transformation of *trans* to *cis* isomers using ^{1}H NMR.

Compounds **18-36** were tested against wild-type drug-sensitive strain (NF54) and multidrug-resistant isolate (K1) of the human malaria parasite *Plasmodium falciparum*. Compounds with longer alkyl carbon chain linkers demonstrated greater antiplasmodial activity compared to those with shorter chain linkers. The *in vitro* studies revealed that compound **32** showed the most potent activity (*in vitro* 50% inhibitory concentration, 0,012 µM for strain NF54 and 0,009 µM for strain K1 and resistance index of 0.717 as a potential antimalarial agent. Other compounds (compounds **34** and **35**) also showed moderate activity against a CQ-sensitive strain (NF54) and superior activity against a CQ-resistant strain (K1) of *Plasmodium falciparum*.

Acknowledgements

I express my gratitude to the almighty God for bestowing upon me the opportunity, strength and perseverance to successfully finish this MSc project. The following individuals are highly appreciated for their invaluable personal contributions that greatly facilitated the successful completion of this dissertation.

- I would like to extend my utmost gratitude to my supervisor, **Dr. Mpelegeng Victoria Bvumbi**, for her comprehensive guidance, support, patience, wisdom, and perceptive remarks throughout every phase of this project. I sincerely appreciate your perseverance and support during the period of sluggish or unproductive progress in this project. You assumed a maternal role in my life by consistently providing me with constructive feedback regarding both academic and general life matters. I express my gratitude to you.

- I wish to express my profound appreciation to my co-supervisor, **Prof. SS Mnyakeni Moleele,** for his tremendous guidance, counsel, and assistance. His profound expertise and extensive experience have greatly assisted me in this project.
- I express my gratitude to **Prof. Ntakadzeni Edwin Madala** for the collaborative partnership that facilitated our access to his laboratory. The collaboration yielded exceptional outcomes. Thank you for conducting high-resolution mass spectrometry (HRMS) analysis on all of our synthesised compounds and assisting me in their analysis. I greatly appreciate your efforts in enhancing my cognitive abilities.

- I would like to express my deepest gratitude to **Mr. Patrick Pandelani**, our NMR technician, for his unwavering dedication to ensuring the timely delivery of our results and the flawless operation of NMR at all times.

- To our Lab technicians **Mr Fhumulani Mutshaeni** and **Ms Nontlantla Regina Maseko**, thank you so much for keeping our instruments safe and functional. Once again thank you for your assistance in providing the much-needed resources to carry this study.

❖ I would like to express my gratitude to the **Design, Synthesis, and Biomolecular (DSB)** and **Drug Synthesis and Isolation (DSI)** research groups, as well as the Chemistry department, for their invaluable support. Working with all of you has been a delightful experience.

❖ I express my utmost gratitude to my mother, **Ms Ennie Mihloti Chauke**, for consistently motivating me to complete this project.

❖ I would also like to extend my appreciation to my life partner and my best friend, **Ms. Unarine Tshishonga** for her unwavering support and serving as my source of inspiration throughout the duration of this project. I am grateful to my son, **Mr. Mukundi Nemudzivhadi**, for inspiring me to endure difficult circumstances.

❖ Dear **H3D** at University of Cape Town, I would like to express my gratitude for conducting screenings on our compounds to determine their antiplasmodial activities.

❖ I express my gratitude to the **National Research Foundation of South Africa (NRF)** for their generous financial support.

Conference proceedings and publication

Conference proceedings

1. AI Nemudzivhadi, MV Bvumbi, SS Mnyakeni Moleele. Poster presentation: Synthesis and Photoisomerization of Conjugated Cinnamic Acid/Chloroquinoline as Potential Antimalarial Agents. 44th South African Chemical Institute (SACI) National Convention, Stellenbosch, South Africa, 8-13 January **2023**.
2. Anza Imanuel Nemudzivhadi, MV Bvumbi, SS Mnyakeni Moleele. *Stereochemistry in the synthesis of Cinnamic acid/chloroquinoline conjugates as potential antimalarial agents.* SACI National Young Chemists' Symposium South Africa (held virtually), 3-4 October **2022.**

Publication

1. MM Kabanda, AI Nemudzivhadi, MV Bvumbi, NE Madala, *Rationalizing the formation of quasi-molecular anions due to tautomerization of chloroquine-cinnamide hybrid molecule during analysis by electrospray ionization (ESI) – mass spectrometry (MS) and through density functional theory (DFT) calculations, Journal of Molecular Structure*,1291 (**2023**).

Glossary of Abbreviations/Acronyms

ACQ: 4-amino-7-chloroquinoline

ACT: Artemisinin-based comination therapies

Arts: Artesunate

BOP: (Benzotriazol-1-yloxytris(dimethylamino)phosphonium hexafluorophosphate)

CA/CQ: Cinnamoyl-chloroquine hybrids

CH_2Cl_2: Dichloromethane

CO_2: Carbon dioxide

CQ: Chloroquine

DABCO: 1,4-Diazabicyclo[2.2.2]octane

DCC: N,N′-Dicyclohexylcarbodiimide

DCM: Dichloromethane

DIEA: N-ethyl-N,N-diisopropylamine

DMSO: Dimethyl Sulfoxide

DMF: N,N-Dimethylformamide

DFT: Density functional theory

ESI-MS: Electrospray ionization Mass spectrometry

EtOAc: Ehtyl acetate

Et3N: Triethyl amine

EtOH: Ethanol

FTIR: Fourier Transformed Infrared

H2O: Water

HEDI-CIN: heterocyclic-dipeptide-cinnamic acid conjugates

HOBT: Hydroxy Benzotriazole

IPr: Isopropyl

IUPAC: International Union of Pure and Applied Chemistry

IC50: Half Maximal Inhibitory Concentration

K1: resistant strain

LC-ESI-qTOF-MS/MS: High-performance liquid chromatography coupled with electrospray ionization-quadrupole-time of flight-mass spectrometry

LC: Liquid chromatography

MBC: Minimum bacterial concentration

MeOH: Methanol

MgSO4: Magnesium Sulphate

MP*:* Melting Point

MHz: Megahertz

μM: Nanomolar

NF54: wild-type drug sensitive strain

$NaHCO_3$: Sodium hydrogen carbonate

NMR**:** Nuclear Magnetic Resonance

NaOH: sodium hydroxide

Na2CO3: Sodium Carbonate

PfCRT: *plasmodium falciparum chloroquine-resistant transporter*

Ph: Phenyl

PyBOP: benzotriazol-1-yloxytripyrrolidinophosphonium hexafluorophosphate

RBC: Red blood cells

Ri: Resistant index

***$SOCl_2$*:** Thionyl chloride

TBTU: O-(benzotriazol-1-yl)-N,N,N′,N′-tetramethyluronium tetrafluoroborate

TEA: Triethylamine

TFA: Trifluoroacetic acid

TLC: Thin layer chromatography

UV: Ultraviolet

UHPLC-QTOF-MS: Ultra-high performance liquid chromatography-quadrupole time-of-flight mass spectrometry

^{1}H NMR: Proton Nuclear Magnetic Resonance

^{13}C NMR: Carbon Nuclear Magnetic Resonance

WHO: World Health Organisation

Table of Contents

CHAPTER 1

INTRODUCTION AND LITERATURE REVIEW

1. INTRODUCTION

1.1 Malaria burden and epidemiology

Malaria is a parasitic disease with high rate of mortality and morbidity caused by parasitic protozoan of the genus *Plasmodium*.[1–3] Pregnant women, children, and immune-compromised individuals have the highest morbidity and mortality, and Africa bears the heaviest burden.[4] According to WHO report 2022, over the last two decades, the number of malaria cases have declined by 1.5 billion cases. 7.6 million lives were saved in the process of fighting against the spread of malaria. It was reported in 2022 malaria impacted nearly half of the global population, resulting in 247 million clinical cases and 619,000 fatalities.[5]

From 2000 to 2019, there was a decline in case incidence in the WHO African Region, going from 370 to 226 per 1000 population at risk.[6] However, in 2020, there was a slight increase to 232 per 1000 population at risk. This increase can be attributed to the disruptions caused by the COVID-19 pandemic, which affected healthcare services.[7] In 2022, the number of reported cases dropped to 223 per 1000 people at risk. The number of malaria deaths in the WHO African Region saw a decline from 808,000 in 2000 to 548,000 in 2017, only to rise again to 604,000 in 2020. The number of estimated deaths has once again decreased to 580,000 in 2022. There has been a significant decline in the malaria mortality rate over the years. Between 2000 and 2019, the rate dropped by 60%, going from 143 to 57 deaths per 100,000 population at risk. However, there was a slight increase to 61 deaths in 2020, followed by a decrease to 56 deaths in 2022.[8]

There are five species of the genus Plasmodium which are known to cause malaria to human beings, namely *P. falciparum*, *P. vivax*, *P. ovale*, *P. malariae* and *P. knowlesi.* The most fatal species is *P. falciparum.*[9–11] Current information suggests that *P. knowlesi* malaria does not spread from person to person, but rather is transmitted by an *Anopheles* mosquito from infected monkey.[4] *Plasmodium falciparum* and *P. vivax* malaria pose the greatest public health challenge**.** *P. falciparum* is most prevalent in Africa and is responsible for most deaths from malaria. This is predominantly due to its ability to sequester in the microvasculature, with these occlusions playing a role in the development of severe malaria.

P. vivax has a wider geographical distribution than *P. falciparum* because it can develop in the *Anopheles* mosquito vector at lower temperatures.[12,13] It also has a dormant liver stage (known as a hypnozoite) that can activate months after an initial infection, causing a relapse of symptoms. The dormant stage enables *P. vivax t*o survive for long periods when *Anopheles* mosquitoes are not present[13,14]

Although *P. vivax* can occur throughout Africa, the risk of infection with this species is quite low because of the absence in many African populations of the Duffy gene, which produces a protein necessary for *P. vivax* to invade red blood cells. In many areas outside Africa, infections due to *P. vivax* are more common than those caused by *P. falciparum,* and they result in substantial morbidity. However, *P. vivax* have low fatality rate as compared to *P. falciparum.*[15]

1.2 Transmission of malaria

Generally, the parasites are transmitted by the female *Anopheles* mosquito as shown in **figure 1** below. *Plasmodium* parasites depends on two hosts, first of which is the sexual cycle taking place in the *Anopheles* mosquito and followed the asexual cycle in the human as the intermediate host.[16] During a blood meal by the infected female *Anopheles* mosquito, sporozoites enter the human host and infect the liver cells. Then in the liver stage, sporozoites mature into tissue schizonts, which rupture and release merozoites. In this stage, some species of *Plasmodium* can form hypnozoites, which can remain dormant in the liver for many weeks or years.

Thereafter, merozoites move into blood, where they infect the red blood cells and form trophozoites. The ring stage trophozoites mature into blood schizonts (blood stage). These red blood cells rupture and infect the healthy red blood cells. In this stage, some trophozoites convert into gametocytes. If an *Anopheles* mosquito bites an infected person, the sexual cycle of the parasite in the mosquito begins.[17]

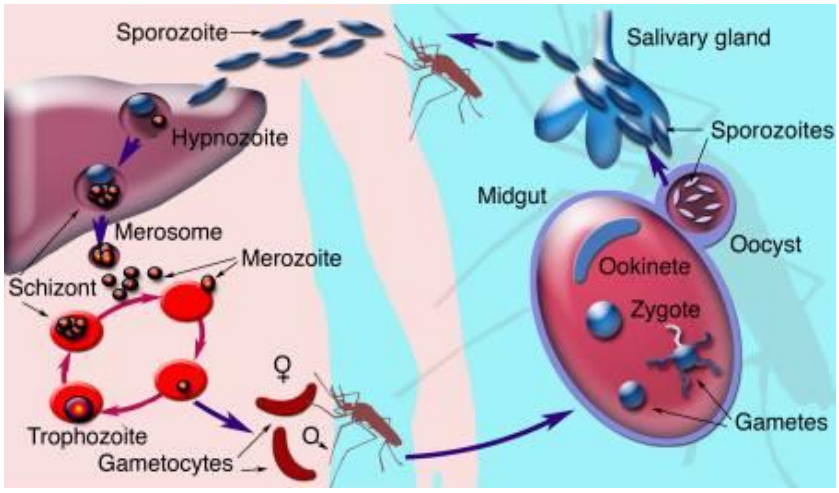

***Figure 1**: The life cycle of plasmodium parasite.*[18]

1.3 Treatment of malaria

Due to the unavailability of effective vaccines, chemotherapy remains the mainstay for the treatment of malaria. Malaria in most instances is a curable disease if it is diagnosed in time and treated with proper medication. However, the rapid development of drug resistance has compromised the use of conventional antimalarial drugs such as chloroquine, amodiaquine, pamaquine, mefloquine and pyrimethamine[19].

For hundreds of years prior to the discovery of the mosquito cycle, two herbal remedies, *cinchona* bark and *qinghao*, were used to effectively cure malaria.[20] Most of the antimalarial drugs used to treat and prevent malaria infection target the erythrocytic stage of infection, which is the stage of infection that causes symptomatic illness. The extent of hepatic stage activity for most antimalarial drugs on the market is unknown.[21]

Malaria must be treated at the acute blood stage. Infections caused by *Plasmodium ovale* or *Plasmodium vivax* also necessitate terminal prophylaxis.[22] This could be accomplished by using a drug that is effective against hypnozoites, which can remain dormant in the liver for months or even years after infection. Several medications, either alone or in combination, have shown efficacy and have been regarded as the cornerstone of malaria treatment. However, drug or multi-drug resistance to these agents has grown and poses a significant challenge in malaria treatment.[23,24]

1.3.1 Current therapeutic method for treatment of malaria.

According to the WHO, the best treatment option for treating the uncomplicated malaria is artemisinin-based combination therapies (ACTs).[25,26] The therapies include fast acting artemisinin, artemether or artesunate along with other drugs such as lumefantrine, mefloquine, amodiaquine, sulfadoxine, pyrimethamine, **Figure 2.**[6] Although ACTs are highly effective and decrease the chances of resistance development, few cases of artemisinin resistance have recently been reported in some south-east Asian countries.[27,28] The high costs of ACTs is a major limitation for its use in underdeveloped or developing countries especially in Africa.

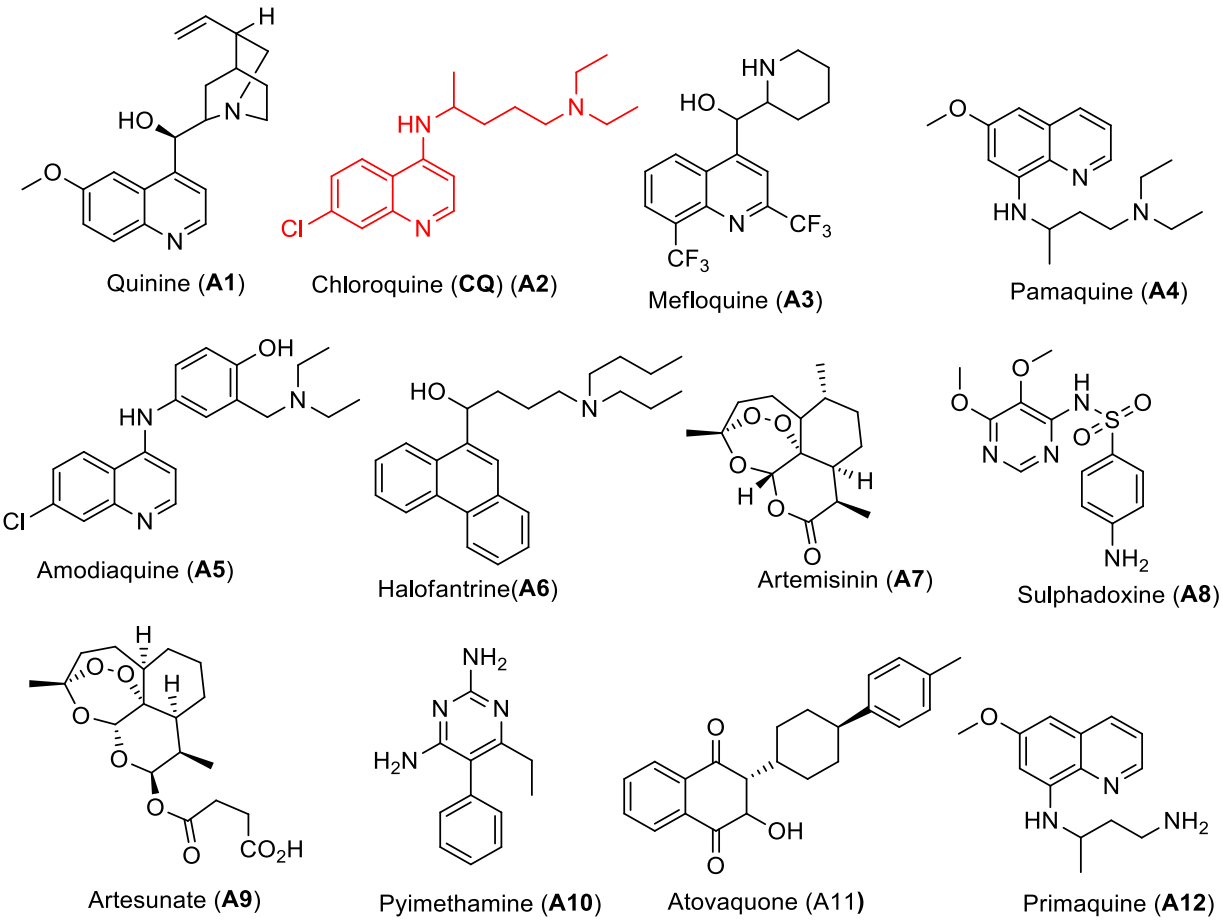

***Figure 2**: Commercially available antimalarial drugs.*

Almost all the first-line antimalarial medications, including chloroquine (CQ), artemisinin (ART), sulfadoxine, and pyrimethamine have been rendered ineffective (**Figure 2**)[29]. Additionally, the overuse of antimalarial medications, insufficient or ineffective therapeutic approaches to infections, and high levels of parasite adaptability at the genetic and metabolic levels all contributed to the resilience of

malarial parasites to these medications[30]. As a result, Artemisinin combination therapy (ACT), a combination of medications, is now frequently used to treat malaria. This combination of medications, which includes artemether-lumefantrine, artesunate-mefloquine, artesunate-sulfadoxine-pyrimethamine, atovaquone-proguanil, quinine-doxycycline, clindamycin, or mefloquine is the most preferred medicines for the curative treatment of malaria[31]. But, the common side effects of these currently marketed drugs include nausea, vomiting, headache, dizziness, heart block, insomnia, pneumonia, abdominal pain, etc [32]. Hence, the search for a novel, safe, and affordable antimalarial drug effective against multidrug-resistant malaria is urgently needed as these antimalarial medications lose their efficacy due to resistance.

1.4. Molecular hybridization

Many scientists around the world use innovative approaches to develop antimalarial medicines. They employ various methods such as repurposing drugs, developing analogues of existing drugs, optimising therapies with available drugs and assessing and employing chemosensitizers (drug-resistance reversers).[33] There is, however, another strategy that has gained much attention in the field of contemporary medicinal chemistry. The strategy is called molecular hybridization and it involves the combination of two biologically active molecules (pharmacophores) into one single hybrid entity with a dual mode of action.[34] These novel hybrid molecules have the potential to enhance efficacy, improve safety, be cost-effective and reduce the propensity to elicit resistance relative to the parent drugs.[35]

These hybrid compounds are typically formed by linking the structural domains of two or more compounds, either directly or through a linker, resulting in a potent and efficient drug.[36] In this research project we utilized the use of hybrid molecules as potential antimalarial agents.

1.4.1 Advantage of hybrid molecules

Typically, a combination therapy is used to overcome drug resistance in treating complex diseases like cancer. The selection of drugs and doses for combination therapy is challenging due to differences in solubility, stability, and pharmacokinetic properties. In addition, developing an optimal combination therapy is costly and may cause additive toxic side effects due to drug interactions. By merging multiple active chemicals into a single molecule, it is possible to address the limitations of combination

therapy and enhance overall effectiveness.[37,38] Furthermore, the possibility of adverse effects induced by drug-drug interactions is substantially reduced when treatment is carried out using a hybrid molecule rather than two distinct medications in combination. One intriguing possibility is that a hybrid molecule may still maintain the synergistic action of the two medications from which the two distinct pharmacophores were formed.[39]

Given the thorough study of hybrid molecule templates regarding their pharmacological and toxicological characteristics, it is possible to develop a hybrid chemical library including potentially beneficial and safe compounds. Consequently, this may greatly expedite the process of discovering new drugs.

1.4.2 Classification of hybrid molecules according to hybrid chemical structures

Hybrid molecules may be classified according to their distinct chemical compositions, which may include the entire chemical structure(s) of the original source(s) or only a portion of the source(s). The joining mode of two or more chemicals can be direct conjugation, through a linking arm, or by blending different haptophoric moieties of two or more different drugs. Hybrid compounds can be classified in various ways as shown in **figure 3**.[40] Hybrid drugs are classified based on the manner in which they are linked to each other. The two agents can be linked directly or via a spacer or linker.

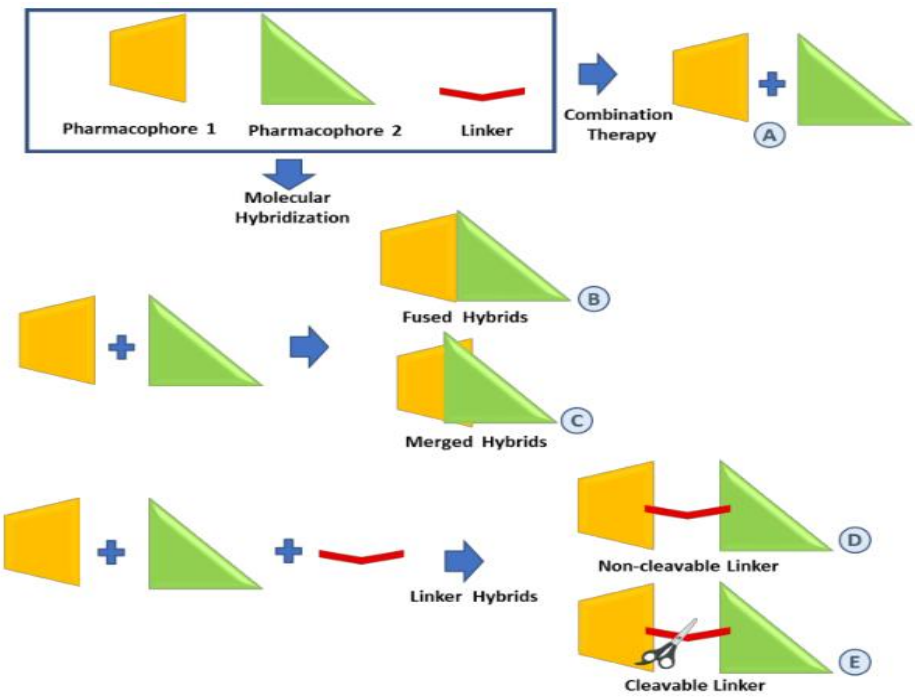

Figure 3: *Strategies for the combination of pharmacophores. (**A**): combination therapy, (**B–E**): molecular hybridization approaches*[41]

- **Fused hybrids**: In the case of directly linked hybrids (as shown in **Figure 3B**), the two molecular units are fused together without the use of any linkers. This means that each molecule contributes a functional group to form a bond, typically resulting in an ester, carbamate, or amide that can be hydrolyzed by enzymes.
- **Merged hybrids**: The formation of merged hybrids (**Figure 3C**) occurs when the structural motifs of both pharmacophores overlap, potentially leading to either the retention or loss of the original functional activities.
- **Linker hybrids**: they are distinguished by the presence of easily recognisable linkers that are categorised as either (i) non-cleavable or (ii) cleavable linker.
    i. A **non-cleavable linker** (**Figure 3D**) results in a hybrid that is capable of preserving the biological activity and affinity for the biological target of the individual units. This is achieved by maintaining the structure of the hybrid or potentially introducing a novel biological action.
    ii. A **cleavable linker** (depicted in **Figure 3E**) has been designed to release the parent agents, each with its own distinct mode of action, in response to physiological or enzymatic conditions.

1.5. Chloroquine (CQ)

Chloroquine (**A2**) belongs to the 4-aminoquinoline family of antimalarial agents and was the first-line drug for the treatment of malaria infection because of its safety and effectiveness in eradicating blood schizont of all strains of malaria parasites.[19,42] It was initially synthesized in 1934 as a potential alternative to quinine.[19] Due to its relative safety and efficacy especially to pregnant women and children, it was considered as a relevant choice of treatment for malaria until the emergence of CQ resistance plasmodium strain in 1961[43]. Thus, the use of chloroquine became limited to those CQ sensitive parasites. It was well established that drug structural modification is particularly vital when the resistance is transport mediated in nature, as with CQ resistance.[44]

1.5.1 Chloroquine mechanism of action

Chloroquine inhibits plasmodium parasites from converting heme to hemozoin. Heme poisons and kills plasmodium parasite. This occurs during malaria's erythrocytic stage. The parasite degrades haemoglobin in its digestive vacuole. Degradation produces heme, which is toxic to parasites. Since malaria parasites lack heme-deactivating enzymes, they polymerize heme to hemozoin. **Figure 4** shows that CQ acts by inhibiting hemozoin formation. At cellular level, CQ is easily transported into the digestive vacuole and doubly protonated in the digestive vacuole. This doubly protonated CQ complexes with heme and prevents hemozoin formation due to its high affinity for heme.[45]

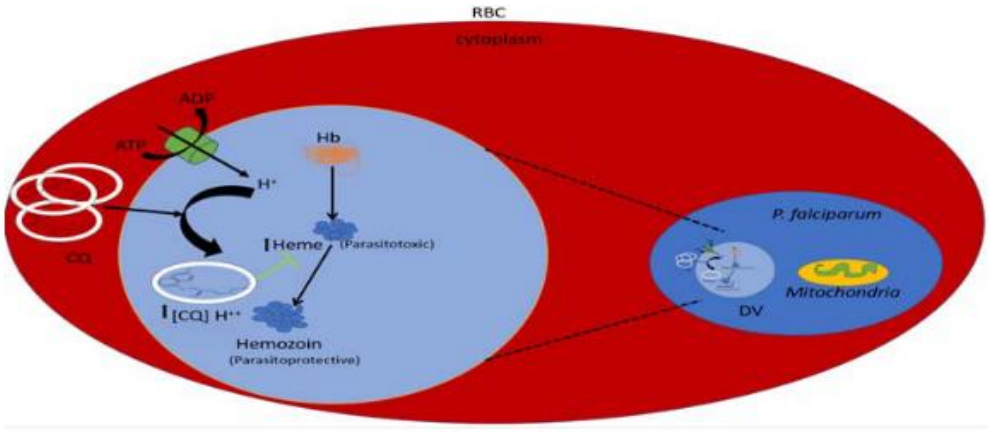

***Figure 4**: Mechanism of Chloroquine. After P. falciparum enters the host red blood cell (RBC), it engulfs and degrades Hb. Heme from proteolysis accumulates and kills malaria parasites. Parasites polymerize heme to Parasitoprotective hemozoin to avoid parasiticides. CQ prevents heme from becoming hemozoin, killing the parasite.*

1.5.2 Mechanism of chloroquine resistance

The development of resistant strains of the malaria parasite has slowed down the progress that has been made towards controlling the spread of malaria. A mutated *Plasmodium falciparum* CQ-resistant transporter (PfCRT) reduced CQ concentration in the parasite digestive vacuole. As the amount of CQ decreases, the polymerization of heme to hemozoin keeps going. The parasite is able to survive the therapeutic concentration of CQ because parasitotoxic heme is lost and parasitoprotective hemozoin builds up. This means that the parasite has developed CQ resistance. The digestive vacuole efflux mechanism for CQ is unknown. However, altering hydrogen ion concentration potentials in the parasite digestive vacuole may affect CQ accumulation as shown in **figure 5**.[46] PfCRT-mediated CQ resistance has stopped this drug from being used. Other than PfCRT, few other receptor/pumps are associated with CQ resistance, such as Pgh-1 and ATPase pump.[45]

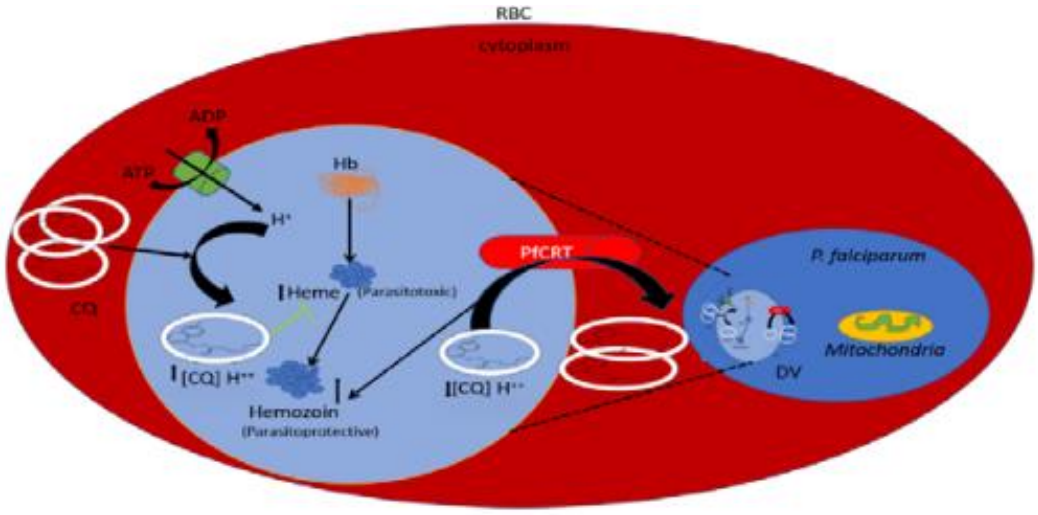

***Figure 5**: A schematic diagram showing the mechanism of Chloroquine resistance. The P. falciparum developed a survival tactics in the presence of CQ through formation of P. falciparum CQ resistance transporter (PfCRT) which mediates efflux of CQ out of the parasite digestive vacuole. As the CQ concentration drops, polymerization of heme to hemozoin continues. Depletion of parasitotoxic heme and accumulation of Parasitoprotective hemozoin allows the parasite to survive the therapeutic concentration of CQ and is said to have developed CQ resistance.*

1.5.3 Biological activities of some quinoline-based antimalarial hybrid compounds.

Compound **B1** exhibited the highest level of antiplasmodial activity against the K1 strain, with an IC_{50} value of 71.16 nM. This activity was approximately four times more potent than that of CQ, which had an IC_{50} value of 255 nM. Furthermore, it exhibited the highest binding ability to hematin, which was equivalent to that of CQ (LogK: 5.52 ± 0.02).

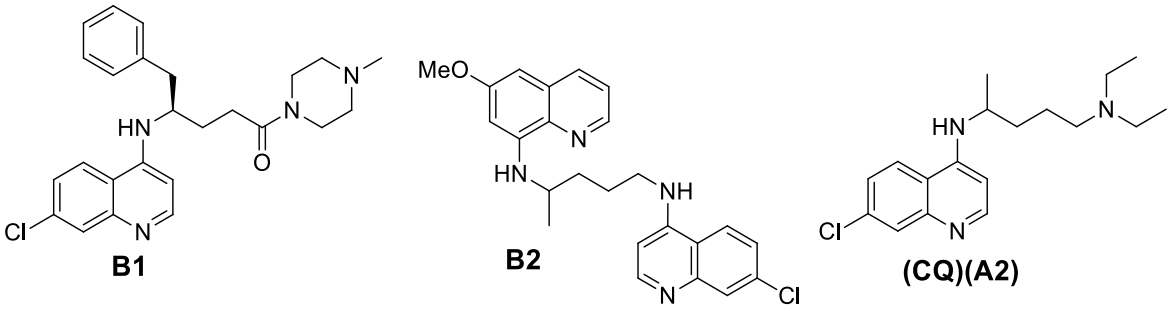

***Figure 6**: Quinoline-based antimalarial hybrid compounds.*

Compound **B2** was synthesized by Lödige et al.,[47] displaying a moderate antimalarial activity. It revealed strong inhibitory activity against the liver-stage development in vitro, but it did not have a notable impact on sporozoite motility or the invasion of hepatocytes. Furthermore, it showed activity against *Plasmodium berghei* liver stages in vivo, effectively preventing blood stage patency. Additionally, it exhibited therapeutic effects on the symptoms of experimental cerebral malaria.[48]

1.6. Cinnamic acid

Cinnamic acids and their derivatives are products of secondary metabolism that are found in abundance throughout the plant kingdom. The term "cinnamic" is derived from the spice cinnamon (Cinnamomum zeilanicum), which has been used since antiquity as a flavouring agent as well as for its stimulant, carminative, antiseptic, and insecticide properties.[49] Trans-cinnamic acid ((2E)-3-phenylprop-2-enoic acid) **C1** (**Figure 7**) is the simplest naturally occurring aromatic carboxylic acid.[50] It can be found in the bark of various Cinnamomum tree species or in the resinous exudates of Liquidamber trees. Other hydroxycinnamic acids, such as p-coumaric, caffeic, ferulic, and sinapic acids, and compounds that are derived from them, are found in many parts of plants, such as fruits, leaves, flowers, and more.[49,51]

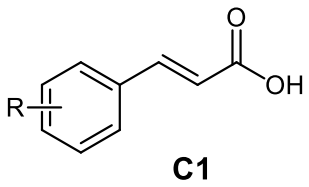

C1

Figure 7: *General structure of cinnamic acid.*

The presence of an acrylic acid group to the phenyl ring results in cinnamic having either a *cis* or a *trans* configuration, with the latter being more commonly observed.[51] The benzene ring and a short unsaturated hydrocarbon chain of cinnamic acids determines their low polarity and low water solubility.[52] Due to the presence of the alkene double bond which does not permit rotation, cinnamic acids and their derivatives are prone to geometrical isomerization which is induced by sunlight (UV radiation).[53]

1.6.1. Geometrical isomerization

The utilisation of isomerization, specifically photochemical isomerization, has demonstrated efficacy in pharmaceutical drug delivery systems due to the distinct pharmacokinetic and pharmacodynamic properties of isomers. Drug isomerism has ushered in an innovative era of drug development. Currently, the understanding of isomerism has facilitated the development of safer and more efficacious alternatives for existing and new drugs.[54]

The cis-trans photo isomerization of functionalized molecules induces a change in dipole moments, which determines whether the trans and cis isomers are hydrophobic or hydrophilic. Geometrical isomerization has proven to be a key factor in drug design and development due to the enhancement of specific physicochemical properties such as dipole moments, affinity to polar molecules, drug orientation (structural conformation), and thus the accessibility of functional groups (atom specificity) on the compound by the target.[55]

Conversion of *trans* isomer into *cis* isomer is possible if either isomer is heated to a high temperature or it absorbed light at a specific wavelength. This process of converting *trans* to *cis* isomer is called photoisomerization and will be explained fully explained in chapter 3.

1.6.2 Biological activities of cinnamic acids

Research has shown that cinnamic acid has a wide range of beneficial properties, including antioxidant, antimicrobial, anticancer, neuroprotective, anti-inflammatory, and antidiabetic properties.[56,57] Additionally, they have shown efficacy against malaria.[58] Their therapeutic value has been extensively documented through the work of several researchers and are found to possess various medicinal properties.[45]

Trans-cinnamic acid (**C2**) shown in **figure 8** exhibited a slight antibacterial effect against most types of Gram-negative and Gram-positive bacteria, with MIC values above 5.0 mM. Similar levels of the efficacy were seen against the fish pathogens *Aeromonas hydrophila, Aeromonas salmonicida*, and *Edwardiella tarda*, with MIC values ranging from 5.6 to 7.7 mM.[59–61] On the other hand, cinnamic acid demonstrated significantly higher activity against the bacteria responsible for tuberculosis, specifically *Mycobacterium tuberculosis* H37Rv strain. Its efficacy was measured with MIC values ranging from 270 to 675 µM using the SPOTi and radiometric Bactec assays. Both the free carboxylic acid and the presence of the α,β-unsaturation were essential for the anti-TB activity, as observed in the study.[49]

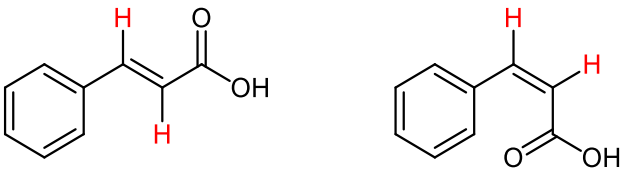

trans-cinnamic acid (**C2**) *cis*-cinnamic acid (**C3**)

***Figure 8**: Chemical structures of trans-cinnamic acid(**C2**) and cis-cinnamic acid(**C3**).*

Guzman reported that the geometric isomer cis-cinnamic acid (**C3**), exhibited a level of activity that was approximately 120 times higher than that of the trans isomer (**C2**).[49] The minimum bactericidal concentrations (MBC) values for cis-cinnamic acid were 16.9 µM, while the MBC values for trans-cinnamic acid were 2.0 mM. These results were obtained against a multidrug-resistant strain of *M. tuberculosis*.[62]

1.6.3 Cinnamoylated chloroquinoline hybrid agents

Cinnamoyl chloroquinoline hybrids are compounds with the heteroaromatic core of amino-7-chloroquinoline (highlighted in blue in **figure 9**), linked to differently substituted cinnamic acid groups (highlighted in red in **figure 9**). The two pharmacophoric moieties can either be conjugated directly (fused) or through different

flexible diamines spacer. Incorporating cinnamic acid into hybrid molecules is extremely valuable. The electron donation from cinnamic acid effectively disrupts radical chain reactions, resulting in the formation of stable products.[52,63]

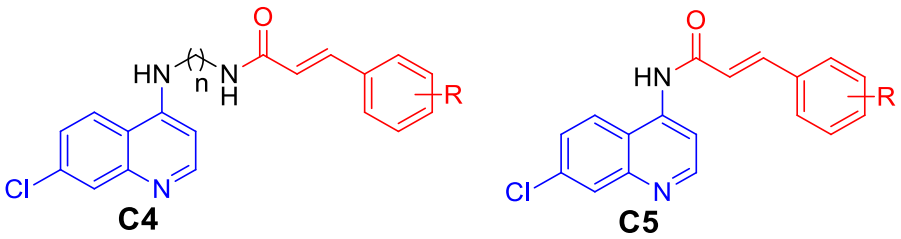

***Figure 9**: General structures of cinnamoylated chloroquinoline hybrids.*

1.6.3.1 Antimalarial activities of cinnamic acid-chloroquinoline hybrid drugs

The concept of "covalent biotherapy" was applied by Pérez, *et al*., when they combine the individual efficacy of two different drug in a single molecule by linking the active part of one to the other.[64] Through this approach, the group prepared a dozen of new CQ bioconjugates containing amino-7-chloroquinoline in aminobutyl mediated covalent linkage with various substituted cinnamoyl functional groups as shown in **figure 10**.

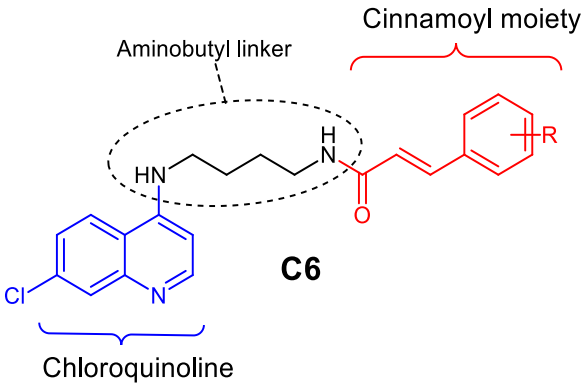

Hybrid compounds	R substituents
C6-a	H
C6-b	p-methyl
C6-c	p-isopropyl
C6-d	p-methoxy
C6-e	p-amino
C6-f	m-fluoro
C6-g	p-fluoro
C6-h	p-chloro
C6-i	p-bromo
C6-j	o-nitro
C6-k	m-nitro
C6-l	p-nitro

***Figure 10**: structure of CQ-cinnamic acid hybrids.*

The dual anti-*P falciparum* bioactivity incorporated in the CQ-cinnamic acid conjugates is inhibition of both hemozoin formation and new permeability pathway. This pathway was believed to develop following parasite invasion of the red blood cell. The bioconjugates were tested for anti-plasmodial activity against CQ-resistant *P.*

falciparum (W2) in vitro. All the conjugates **C6** produced IC_{50} of < 60 nM which was less than 183 nM produced by the standard CQ. The most potent conjugate was found to be the compound, **C6-c** (IC_{50} = 11.0 nM). The presence of the linker between the two pharmacophore was necessary for anti-plasmodial effect in a similar way lipophilicity of bioconjugates determines their therapeutic potential.

In another study by Pérez and co-workers,[65] (**figure 11**) 4-amino-7-chloroquinoline core was linked to a trans-cinnamic acid moiety through a dipeptide spacer to get compound **C7**. Direct coupling of aminoquinoline to cinnamic acid derivatives was also achieved to get compound **C8**. Compounds **C7** and **C8** were evaluated for their in vitro antimalarial activity against the blood-stage CQR W2 strain of *P. falciparum*. The resulting activity profile revealed a complete lack of activity for compound **C8**, which correlated with their inability to inhibit heme polymerization. Furthermore, compound **C7** inhibited heme polymerization in vitro and displayed IC_{50} values between 1 and 11 nM, suggesting that this inhibitory activity is at least in part accountable for their antimalarial activity.

Conjugates **C9** and **C10** were evaluated for their in vitro antimalarial potency and hybrids **C9** displayed activities between 15 and 141 nM against the sensitive 3D7 parasite strain and between 11 and 111 nM against the resistant W2 strain of *P. falciparum*, which are higher potencies than CQ (IC_{50} (W2) = 138 nM). Compound **C10** completely lacked activity. The compounds' activities were also evaluated against liver stage P. berghei parasites and most conjugates displayed outstanding potency against both erythrocytic and liver stages of the parasite. The most potent compounds **C9-c** and **C9-e** were confirmed to be active in vivo against a blood-stage infection in a *P. berghei* rodent malaria model, as they extended survival with two to seven days when treated with doses of 30 mg/kg/day for two days. Hybrid **C9-c** was highly toxic when administered in doses of 100 mg/kg/day, while hybrid **C9-e** did not appear to be toxic at any tested dosage.[66] The cinnamoyl core thus appears to be a valuable pharmacophore to enhance the antiplasmodial potency of chloroquine.

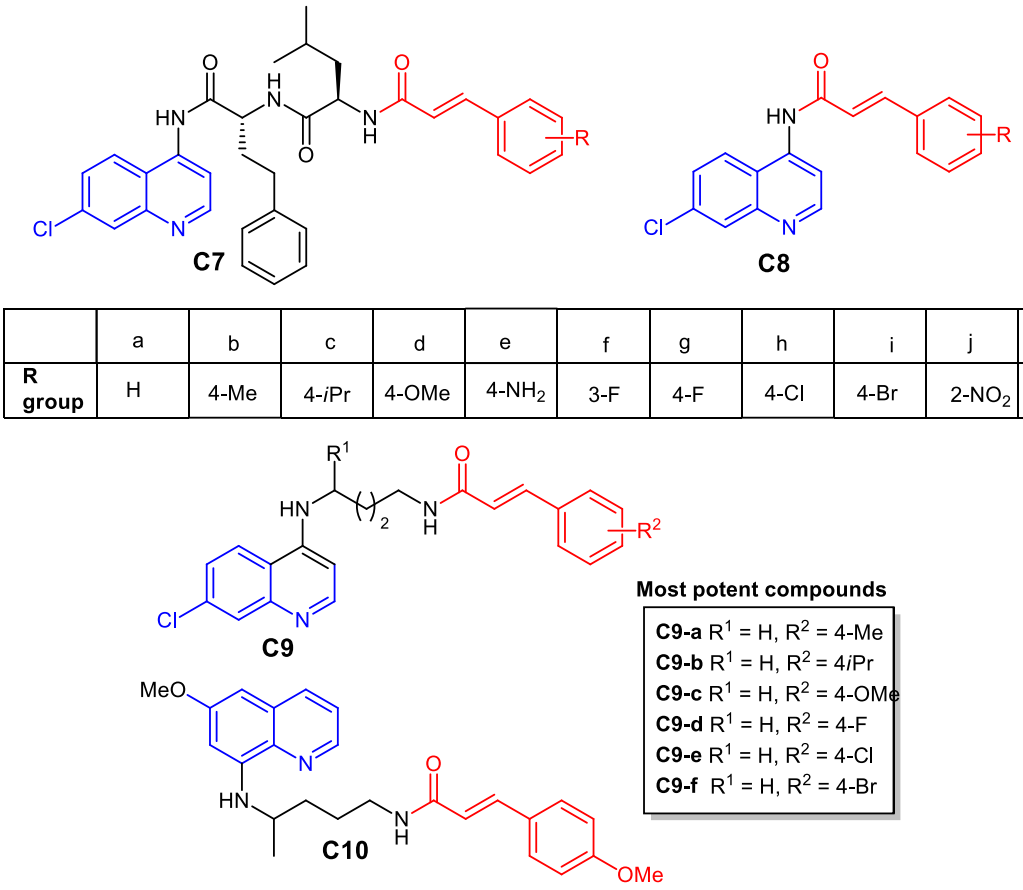

	a	b	c	d	e	f	g	h	i	j	k	l
R group	H	4-Me	4-*i*Pr	4-OMe	4-NH_2	3-F	4-F	4-Cl	4-Br	2-NO_2	3-NO_2	4-NO_2

***Figure 11**: Examples of chloroquinoline-cinnamic acid hybrids.*

1.7. Synthetic methods towards the assembly of cinnamoyl-chloroquine hybrids.

The emergence of resistance to antimalarial drugs is a serious problem, leading to search for new drugs that can overcome the resistance. Not surprisingly, the utilization of CQ pharmacophore has been one of the main approaches in this effort, as CQ has been used to control malaria for many decades without serious problems. In this effort, a molecular hybridization approach using a CQ pharmacophore and other cinnamic moieties as antimalarial agents have been extensively examined.[36]

As mentioned before, the use of molecular hybridization techniques to synthesize cinnamoylated-chloroquinoline analogues has been reported. Below is a brief review of some hybridization methods that have been used in the past to synthesize cinnamic acid-chloroquinoline hybrid drugs.

1.7.1. Perez *et al.*'s method of cinnamic acid-chloroquinoline

1.7.1.1 First generation heterocyclic-cinnamic acid conjugates

Perez *et al.*[65] successfully synthesised a novel group of heterocyclic-dipeptide-cinnamic (HEDI-CIN) acid conjugates, **scheme 1**. These conjugates were synthesised by linking 4-amino-7-chloroquinoline **D2** core to a trans-cinnamic acid moiety using a dipeptide spacer. This was accomplished by linking two amino acids to a 4-amino-7-chloroquinoline core and then combining this quinolinyl dipeptide with cinnamic acid. The conjugation was done using benzotriazol-1-yloxytripyrrolidinophosphonium hexafluorophosphate (PyBOP) as a coupling agent. Similarly, HECIN acid derivatives **D7** were also synthesized. HECIN are analogues of these hybrids but do not contain the dipeptide spacer. This was also achieved by directly coupling aminoquinoline to cinnamic acid derivatives using PyBOP as a coupling agent.[65]

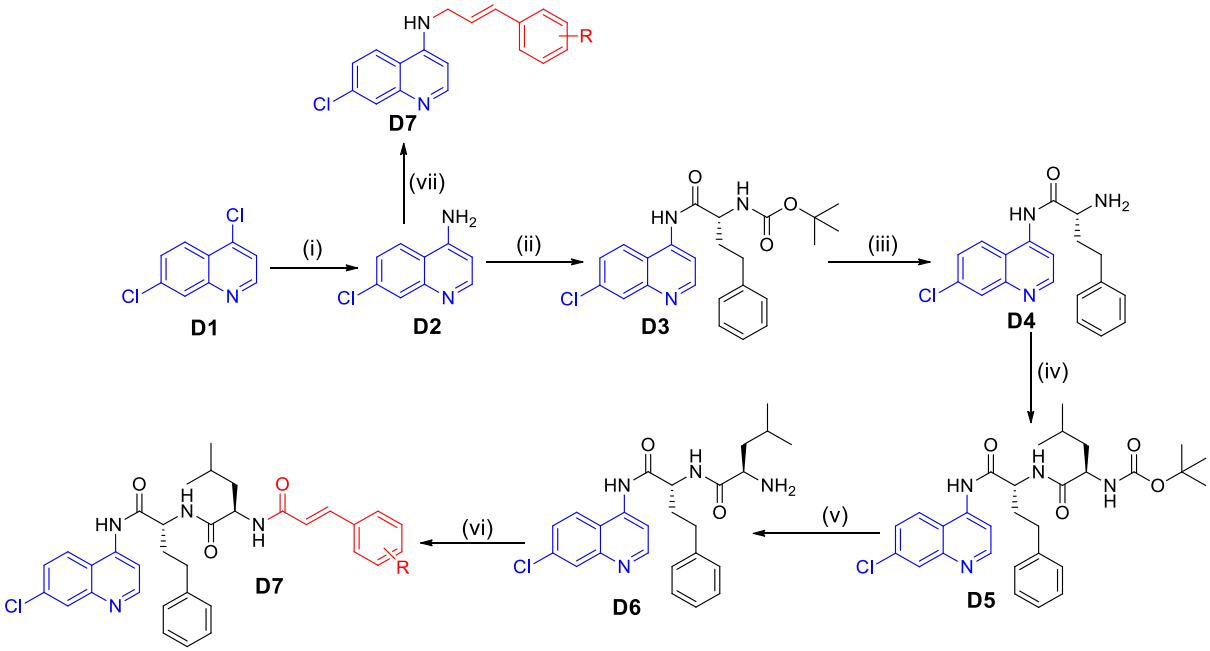

***Scheme 1**: Reagent conditions: (i) NH_3 (g), phenol, 150 °C, 2 h; (ii) TBTU, Boc-D-homoPhenylalanine, DIEA, DMF, 1 day; (iii) TFA, 2 h; (iv) PyBOP, DIEA, DCM, 1 day; (v) TFA, 2 h; (vi) PyBOP, corresponding cinnamic acid, DIEA, DCM, 3 days; (vii) PyBOP, corresponding cinnamic acid, DIEA, DMF, 24 hours.*

1.7.1.2. Second generation heterocycle−cinnamic acid conjugates

In pursuit of synthesizing more lead *N*-cinnamoylated chloroquine analogues, Perez *et al.*[64] reported a series of compounds ,**scheme 2**. Based on the findings of the

previous study,[65] it was determined that having a spacer between the heterocycle and the cinnamoyl motif was necessary for the antimalarial activity. To achieve this, the cinnamoyl group was coupled to a 4-aminoquinoline core using a flexible and more hydrophobic butylamine/butyloxy chain, resulting in the synthesis of hybrids **E5**. The chloroquinoline and cinnamoyl cores remained unchanged in the second-generation conjugates. However, the rigid and hydrophilic dipeptide spacer found in the first-generation conjugates **D7** was substituted with a flexible and more hydrophobic butyl chain **E2**. This substitution enhanced the overall basicity of the compounds.

Compound **E5** was synthesised through a two-step process. Firstly, a nucleophilic aromatic substitution reaction was carried out between the suitable diaminoalkane (1,3-diaminopropane, 1,4-diaminobutane, or 1,5-diaminopentane) and 4,7-dichloroquinoline **E1**. Then, the resulting compounds **E3** were coupled with the appropriate cinnamic acids **E4**, using TBTU/DIEA as an activating agent[66].

Compound **F2** was synthesised by performing a single amide coupling reaction between the parent drug primaquine **F1** and cinnamic acid. This reaction was carried out using standard peptide coupling conditions, which involved activating the cinnamic acid with O-(benzotriazol-1-yl)-N,N,N′,N′-tetramethyluronium tetrafluoro-borate (TBTU) in the presence of N-ethyl-N,N-diisopropylamine (DIEA), followed by adding PQ.

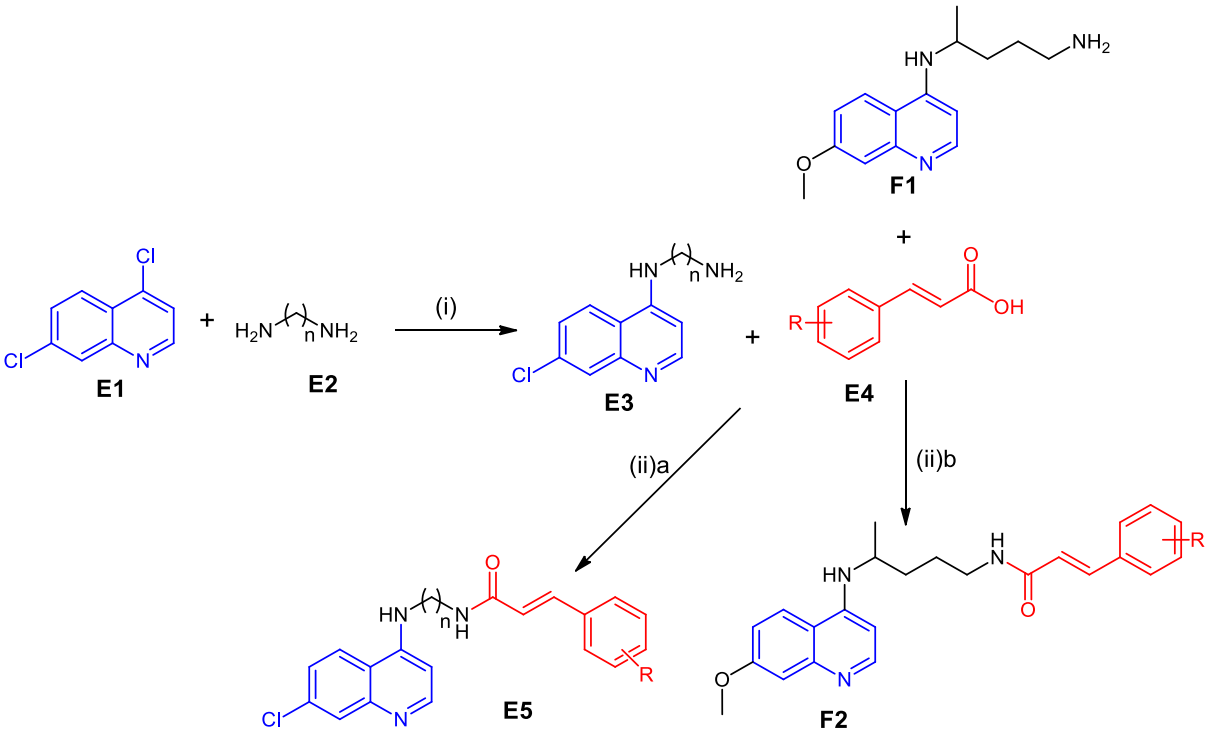

***Scheme 2**: Synthesis of a) 4-amino-7-chloroquinoline/cinnamic acid conjugates **E5** and b) 8-amino-6-methoxyquinoline analogue 8. Reagents and conditions: (i) 100 ^{O}C, 2 h ;(ii)a and b TBTU/DIEA, RT, 24 h, **F3** (R=p-iPr).*

1.7.2 Gayam and Ravi's method of cinnamoylated chloroquine analogues

Gayam and Ravi synthesised a novel class of cinnamoylated chloroquine hybrid analogues by employing an alternative method from the one used by Perez *et al*[64,65]. The procedure for synthesising the target and intermediate compounds is outlined in **Scheme 3**. The nucleophilic substitution of 1,2-diaminoethane **G2** at the 4th position of 4,7-dichloroquinoline **G1** formed intermediate **G3**. The synthesis of the trans cinnamic acid derivatives **G6** involved the utilisation of malanoic acid **G5** and substituted aldehydes **G4** in DMF. The 1,4-Diazabicyclo[2.2.2]octane (DABCO) served as the catalyst for the reaction. The final cinnamoylated chloroquine analogues, **G7**, were synthesised using a coupling reagent consisting of 1-Hydroxybenzotriazole (HOBT) and N,N′-Dicyclohexylcarbodiimide (DCC).[67]

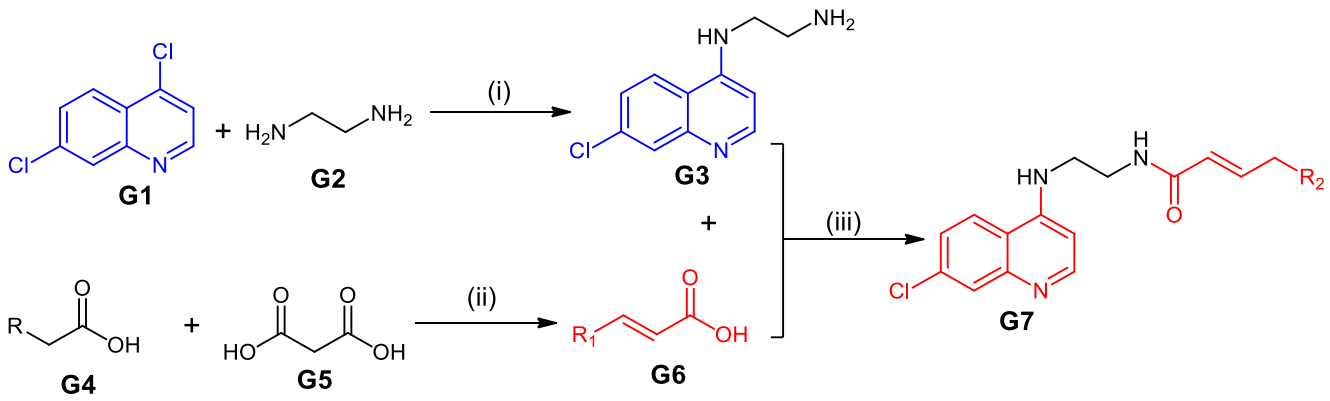

Scheme 3. *Reagents and conditions: (i) 110 °C, overnight; (ii) DABCO, DMF, 110 °C, 2.0 h; (iii) DCC, HOBT, THF, 0 °C, 1.0 h then r.t overnight.*

1.8 Aims and Objectives

The fact that different cinnamoylated-chloroquinoline analogues (**figures 10** and **11**) have shown anti-malarial efficacy equal or better than chloroquine, encouraged us to investigate and expand these compounds even further in our project.

In addition to their antimalarial activities, we wanted to explore the compounds' isomerism when exposed to light as well as their structural behaviours. As a result, the general approach to the compounds were based on mainly 3 features as projected in **Figure 12**.

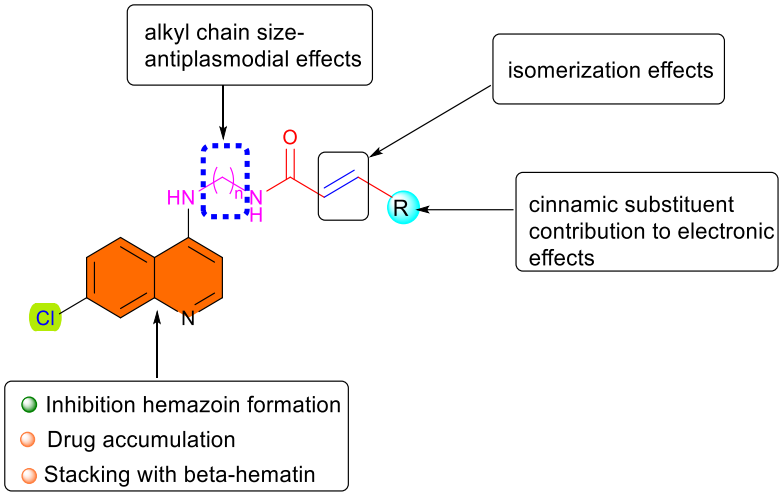

***Figure 12**: General overview of the cinnamoylated-chloroquine structure studied.*

Due to its well documented and known effects, the chloroquinoline moiety was not studied in this project. However, 3 other parts were the focus of this study and are elaborated as part of our aims.

1.8.1 *Part 1: Effect of different linkers*

Generally, it has been established that the presence of the linker between the two pharmacophore has antiplasmodial effects. Consequently, we wanted to investigate to what extent does different linkers in terms of the alkyl chain sizes affects the chemistry, photoisomerization and the antiplasmodial activities of these compounds.

1.8.2 *Part 2: Effect of the olefinic/alkenic bond on trans/cis geometrical isomerization*

Currently there are no reports showing that photoisomerization work has been done on these compounds. We aimed to study their isomerization by exposing them to UV

light and using UHPLC-QTOF-MS as an analytical tool to observe the chromatographs obtained. The aim was to observe different isomers attained and also to study their polarities.

1.8.3 *Part 3: Effects of the groups/atoms on the cinnamic motif.*

Many cinnamic acid derivatives have different biological activities and have been attributed to the nature and positions of the substituent groups.[52] The aim of using different substituents (electron withdrawing/donating) was to study the electron effects that these groups might bring to the overall conjugated compounds in terms of activity and the polarity effects.

Our main **objectives** were as follows:

- Synthesis of trans cinnamoyl chloroquinoline hybrids.
- Purification of CA/CQ analogues using column chromatography, flash chromatography and recrystallization.
- Photoisomerization of trans cinnamoyl chloroquinoline hybrids with analysis by UHPLC.
- Characterization of final compounds using a combination of NMR (^{1}H and ^{13}C), IR Spectroscopies as well as HRMS.
- To screen (at UCT's H3D labs) the antiplasmodial activities of final compounds against chloroquine sensitive (NF54) and resistant (K1) strains of *P. falciparum.*

CHAPTER 2

SYNTHESIS OF CINNAMOYL-CHLOROQUINE HYBRIDS

2.1. CHEMISTRY

The generally known synthetic methods offered tremendous flexibility in preparing the analogues required for the study. Thus, the analogues were prepared using the general retrosynthetic method depicted in **Scheme 4**.

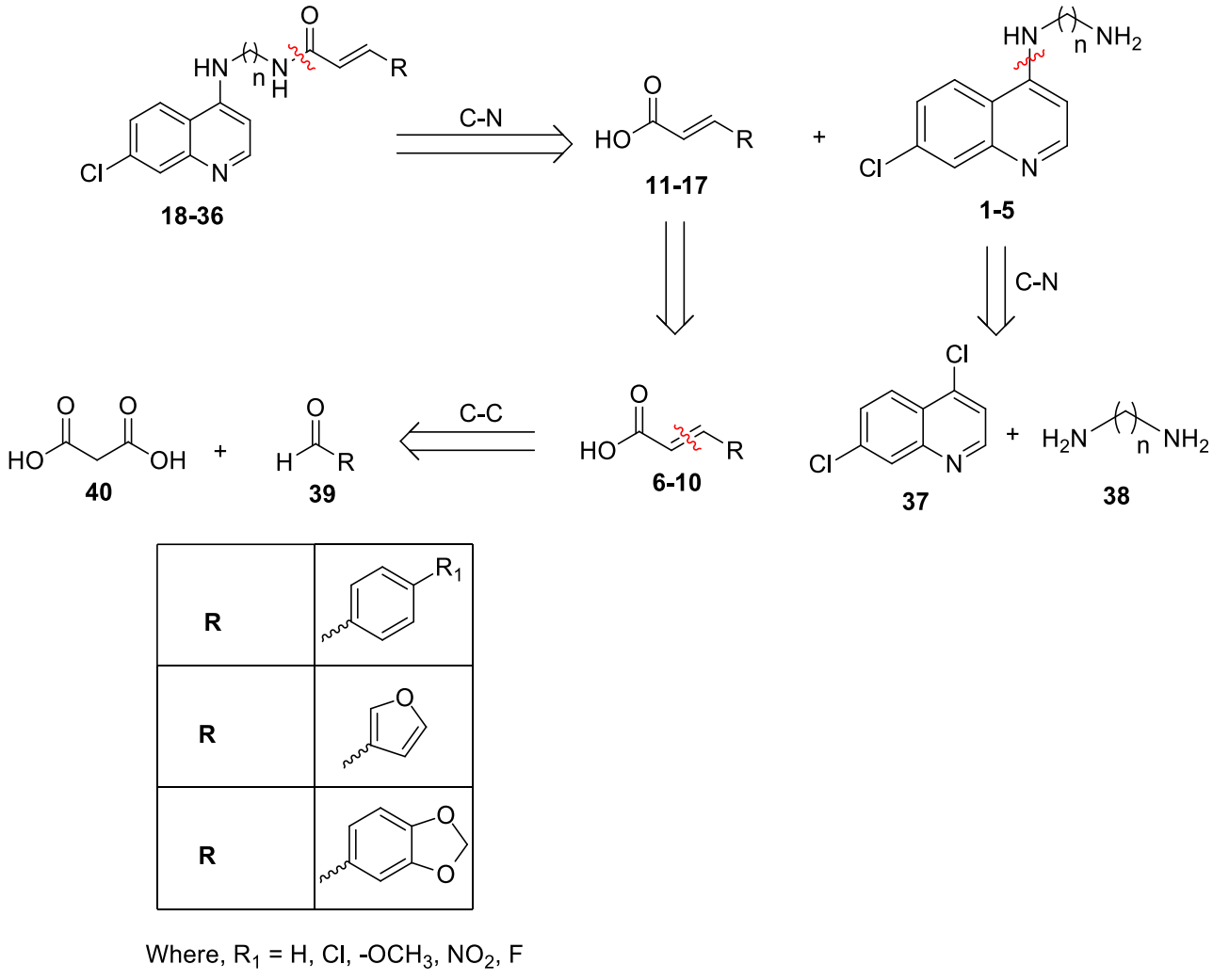

Where, R_1 = H, Cl, -OCH_3, NO_2, F

***Scheme 4**: Retrosynthetic analysis of cinnamic/chloroquinoline analogues*.

Two pharmacophoric scaffolds (4,7-dichloroquinoline (**37**) and cinnamic acids derivatives (**6-10**) were conjugated through diaminoalkanes (**38**) to form cinnamoyl chloroquinoline hybrids (**18-36**). Target compounds **18-36** could be derived from acyl chlorides (**11-17**) and *N*-(7-Chloroquinoline-4-yl) diaminoalkanes (**1-5**) by cleavage of the carbon-nitrogen single bond. *N*-(7-Chloroquinoline 4yl) diaminoalkanes (**1-5**) could be prepared by substitution reaction from the cleavage of the carbon-nitrogen single bond to get two commercially available 4,7-dichloroquinoline (**37**) and diaminoalkanes (**38**). On the other hand, the functional group interchanged could be applied from acyl

chlorides (**11-17**) to cinnamic acid derivatives (**6-10**). Furthermore, the cinnamic acid derivatives could be obtained from aldehydes (**39**) and malonic acids (**40**) via Knoevenagel condensation.

2.1.1. The approach towards the synthesis of cinnamoylated-chloroquinoline analogues

2.1.1.1. Synthesis of cinnamic acids via Knoevenagel condensation

In addition to the commercially available cinnamic acids, more were synthesized from malonic acid and different aldehydes. The structure-activity analysis (SAR) showed that the substituents on the para position of the phenyl ring exhibited a wide range of biological activities as compared to ortho and meta positions. According to Assaleh *et al*, methoxy and chloro groups are widely recognized as highly active cinnamic acid substituents, hence they were also chosen in this project. [68]

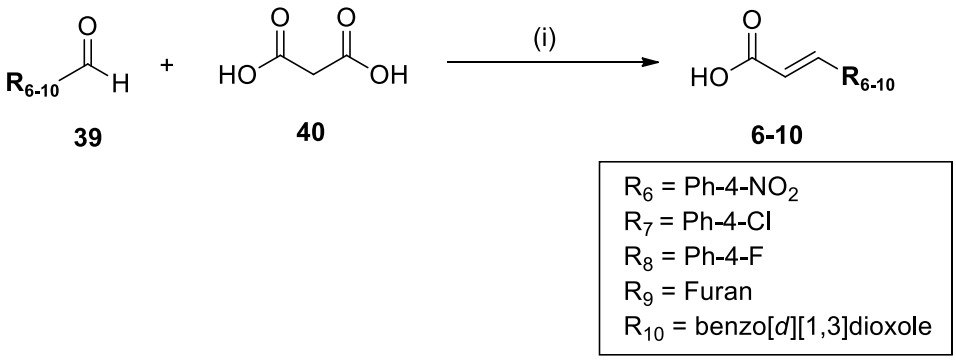

Scheme 5*: General reaction scheme for Knoevenagel condensation. Reagents and conditions: (i) piperidine, pyridine, reflux, 6 h,* ***6-10*** *(81-97%).*

Using Doebner-Knoevenagel condensation over malonic acid, a series of cinnamic acids derivatives were obtained in high yield and purity in the base-catalyzed medium. The condensation reaction used pyridine as the solvent and a trace of piperidine as the catalyst[69] (**scheme 5**).

***Table 1**: characterization of cinnamic acid derivatives **6-10**.*

Compounds	R	Percentage yield (%)	Morphology
6	Ph-4-NO_2	83.60	Yellow solid
7	Ph-4-Cl	97.24	White solid
8	Ph-4-F	88.39	White solid
9	Furan	90.43	Dark brown solid
10	Benzo[*d*][1,3]dioxole	80.96	Black solid

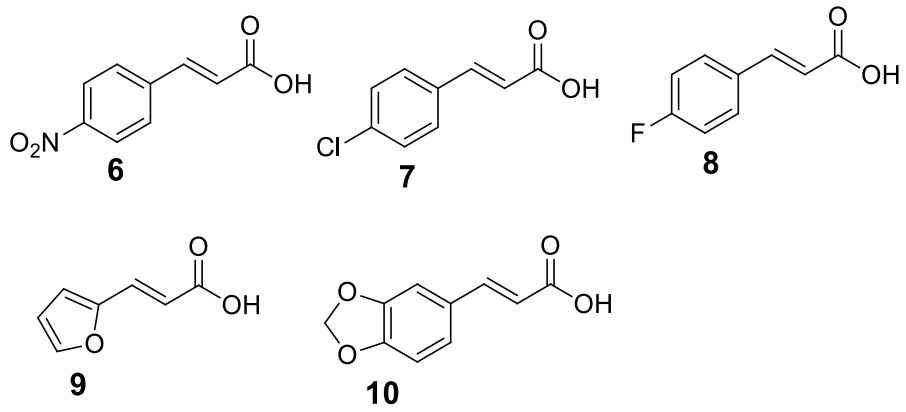

***Figure 13**: structures of synthesized cinnamic acid derivatives.*

The proposed mechanism for the synthesis of cinnamic acid derivatives is shown in **Scheme 6**. The active methylene hydrogen atom is abstracted by the base, resulting in the enolate ion (**I**). Because of extensive delocalization and the intramolecular hydrogen bonding, the enolate formed in this case is a stable dianion (**II**). The dianion acts as a nucleophile on the aldehyde's electrophilic carbonyl carbon, and after proton abstraction from the medium (**III**), the aldol (**IV**) is formed (monocarboxylate in this basic solution). From the aldol (**IV**), the next step to take place is decarboxylation and dehydration which occur via a cyclic transition state (**V**). CO_2 from either of the two -COOH groups could occur, resulting in either an E or Z double bond in the product. However, because the product has trans geometry, a lower energy transition state is involved, resulting in a more stable E alkenoic acid (**VI**) as the product.

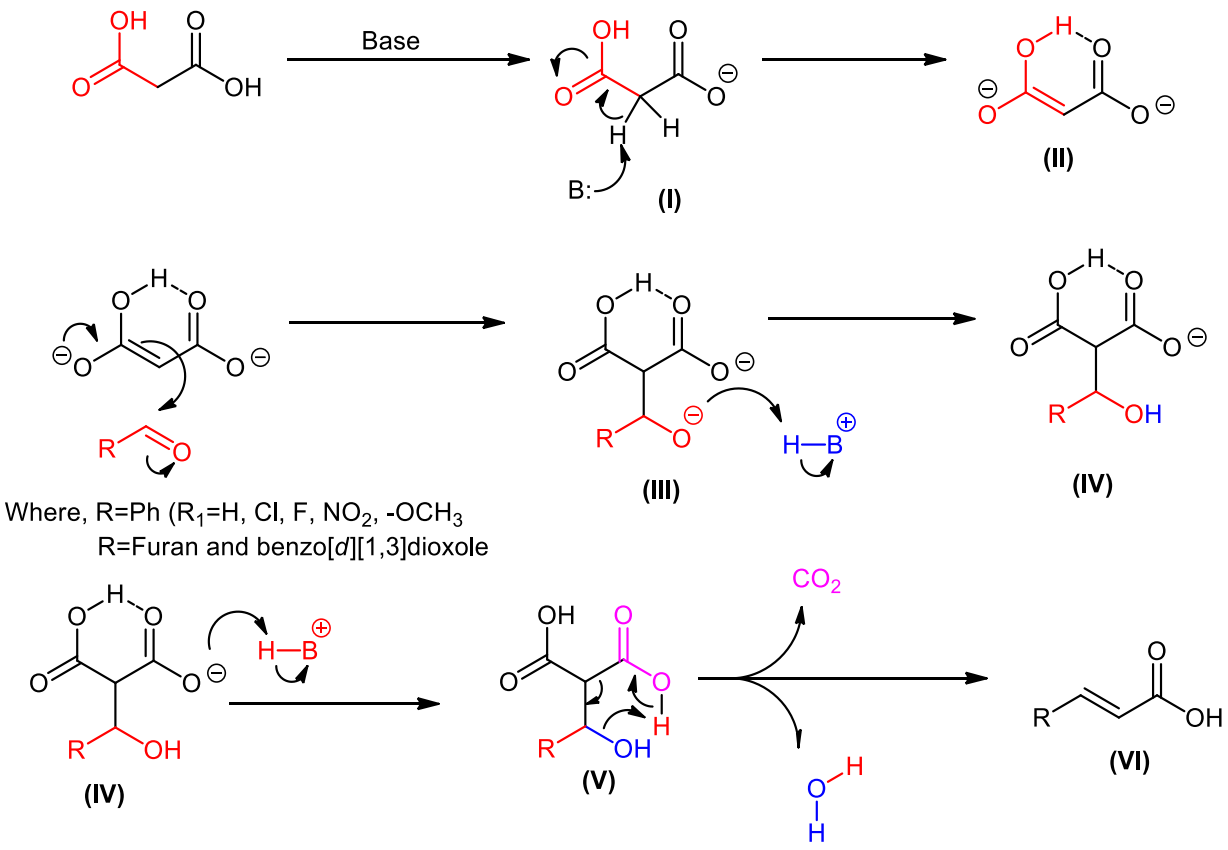

***Scheme 6**: The Doebner-Knoevenagel condensation reaction mechanism*.

Compounds **6-10** were confirmed by ^{1}H and ^{13}C NMR spectroscopy. The ^{1}H NMR revealed that the aldehydic peak which is usually found at 9-10 ppm has been replaced by the carboxylic acid moiety of cinnamic acid as shown by the broad singlet peak at ≈12 ppm integrating for one proton. The presence of the -CH=CH- proton peaks of the cinnamic acids at 6.4-7.7 ppm indicated the formation of olefinic carbons. The coupling constant of these olefinic protons for the compounds were between 15.8-16.1 Hz suggesting that the cinnamic acids derivatives were *trans*-oriented. Depending on what R represented on each cinnamic acid, 3 carbon signals were observed in all the ^{13}C NMR. They all represented the carbonyl carbon at 167.0 ppm to 167.9 ppm and the two alkenic ones at 123.6 ppm and 141.3 ppm for compound **6,** 120.1 ppm and 142.5 ppm for compound **7**, 116 ppm and 130.9 ppm for compound **9**,117.1 ppm and 143.9 ppm for compound **10**.

2.1.1.2. Aromatic nucleophilic substitution of chlorine

In this project, we have added flexible straight-chain diaminoalkanes (1,2-diaminoalkane, 1,3-propane-diamine, propane-1,2-diamine, N^{1}-methylpropane-1,3-

diamine and 1,6-hexanediamine) employing aromatic nucleophilic substitution at position four of 4,7-dichloroquinoline, **scheme 7**.

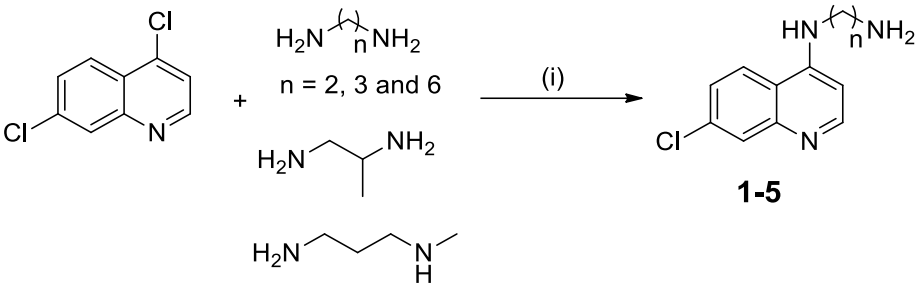

***Scheme 7**: General synthesis of the amination of 4,7-dichloroquinoline. Reagents and conditions: (i) 165 °C, 8 h, (23-89%).*

The N-(7- Chloroquinoline-4-yl) alkane-diamines (**1-5**) compounds were synthesized from commercially available 4,7-dichloroquinoline and different linkers of diamines. The Compoundss were obtained in poor to good yield based on the type of diaminoalkane used (**Table 2**). Compounds (**1-5**) showed the expected signals for the diamines side chain in the ^{1}H and ^{13}C NMR spectra, confirming that substitution had occurred.

***Table 2**: Characterization data of N-(7- Chloroquinoline-4-yl) alkane-diamines **1-5**.*

Compounds	Diamines	Percentage yield (%)	Morphology
1	*N*^{1}-(7-chloroquinolin-4-yl)ethane-1,2-diamine	23	Yellow solid
2	*N*^{1}-(7-chloroquinolin-4-yl)propane-1,3-diamine	89	White solid
3	*N*^{1}-(7-chloroquinolin-4-yl)propane-1,2-diamine	74	Pale-yellow solid
4	*N*^{1}-(7-chloroquinolin-4-yl)-*N*^{3}-methylpropane-1,3-diamine	79	Pale-yellow solid
5	*N*^{1}-(7-chloroquinolin-4-yl)hexane-1,6-diamine	57	Yellow solid

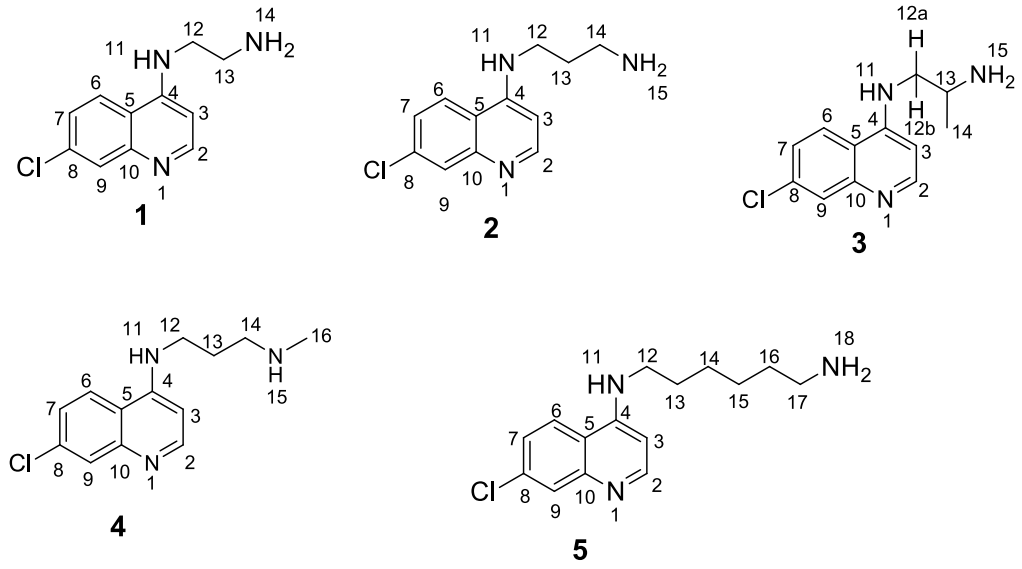

***Figure 14**: Structures of N-(7- Chloroquinoline 4yl) alkane-diamines (**1-5**).*

The absorption frequencies in the 3350-3200 cm^{-1} region, which is linked to N-H stretching, were widely observed in the IR spectra of compounds **1-5**. The expected signals were 4 doublets for H-2, H-3, H-6 and H-7 and a singlet for H-9, but due to long-range meta coupling the singlet H-9 at 7.78 ppm is a doublet and one of the doublets H-7 at 7.42 ppm is a doublet of doublet. The doublets H-2, H-3 and H-6 resonated at 8.38pm, 6.45 ppm and 8.24 ppm respectively.

The ^{13}C NMR of each compound showed four different tertiary carbons C-4 at 152.4 ppm, C-10 at 149.5 ppm, C-8 at 133.8 ppm, C-5 at 117.9 ppm which further supported the presence of the quinoline moiety. Carbons of the various methylene linkers were confirmed on ^{13}C NMR and DEPT135 between 21.5–51.2 ppm. DEPT135 confirmed the methylene peaks of compound **2** C-12, C-13 and C-14 at 41.07 ppm, 31.5 ppm and 39.3 ppm, respectively. DEPT135 of compound **3** exhibited only two peaks C-12 at 51.2 ppm and C-13 at 45.1 ppm. DEPT135 of compound **4** showed three peaks being C-12, C-13 and C-14 at 41.1 ppm, 27.6 ppm and 499.4 ppm, respectively. Compound **5** showed signal C-12 at 41.8 ppm, C-17 at 33.4 ppm, C-13 at 29.5 ppm, C-16 at 28.2 ppm, C-14 at 27.1 ppm, and C-15 at 26.6 ppm.

As shown by ^{1}H NMR spectrum (**Figure 15**), compound **1** was characterized by broad triplet peak NH-11 at 7.28 ppm integrating for one proton. The NH-11 peak is triplet due to H-12 and broad as the proton is coupled to heteroatomic atom (nitrogen). In the aliphatic region broad NH_2-14 singlet peak appeared at 3.38 ppm integrating to two protons. Two methylene protons appeared at 3.26 and 2.81 ppm respectively. H-12

appeared as doublet of doublet integrating for two protons and H-13 as a triplet integrating two protons. In the aromatic region, four doublets and one doublet of doublet were observed at 8,37 ppm, 8,27 ppm, 7.78 ppm, 7,43 ppm, 6.49 ppm, respectively.

Compound **1** was further confirmed by ^{13}C NMR which exhibited eleven peaks. Quaternary carbons were observed with C-4 at 152.3 ppm, C-10 at 149.4 ppm, C-8 at 133.8 ppm, C-5 at 117.8 ppm and five C=C double bond signals. The methylene carbons C-12 and C-13 resonated at 46.1 ppm and 40.4 ppm.

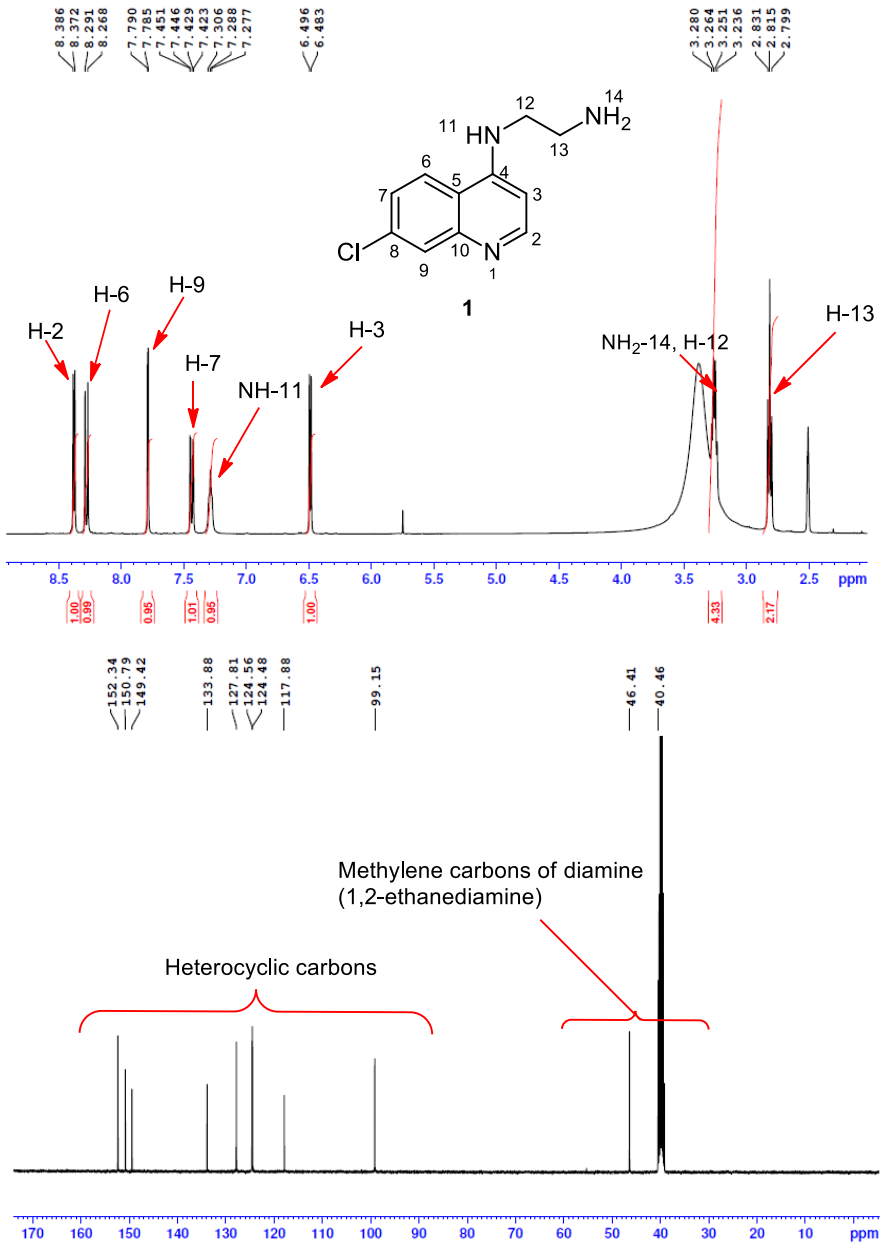

***Figure 15**: ^{1}H and ^{13}C NMR of N-(7- Chloroquinoline-4-yl) ethyl-diamine (**1**).*

2.1.1.3. Formation of Acyl chlorides from cinnamic acid derivatives

Initially, the cinnamic acids derivatives were being coupled directly with the N-(7-chloroquinoline-4-yl) alkane-diamines (**1-5**) using the coupling agent 2-(1H-Benzotriazole-1-yl)-1,1,3,3-tetramethylaminium-tetrafluoroborate (TBTU) and *N, N*-Diisopropylethylamine (DIEA) for 24 hours at room temperature following a method by Perez *et al.*[64] (**scheme 8**). To our surprise, the expected products gave very low yields which were very difficult to separate.

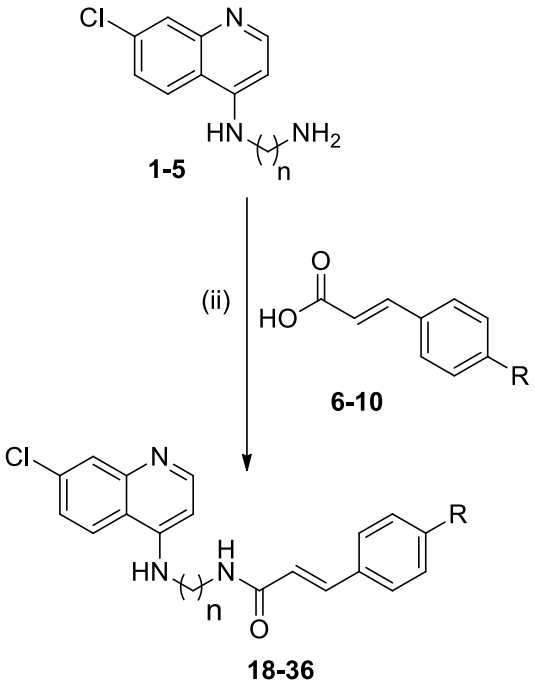

***Scheme 8**: Synthesis of 4-amino-7-chloroquinoline/cinnamic acid conjugate. Reagents and conditions: (i) 100 ˚C, 2 h, (ii) 2-(1H-Benzotriazole-1-yl)-1,1,3,3-tetramethylaminium-tetrafluoroborate (TBTU)/ N, N-Diisopropylethylamine (DIEA), RT, 24 h.*

Alternatively, an approach to first chlorinate the cinnamic acids were envisaged. As a results, thionyl chloride ($SOCl_2$) was used to generate acyl chlorides from corresponding cinnamic acids derivatives as shown in **Scheme 9**. It reacted with carboxylic acids in the presence of co-solvent DMF to give an acid chloride, sulfur dioxide (SO_2) and HCl.[70] The mechanism of acid chloride formation using thionyl chloride is illustrated in **Scheme 10.** The aim of converting the carboxylic acid into acid chloride was to optimize the yield, reduce the amount of by-products, facilitate the final purification, and exploit more economical reagents.

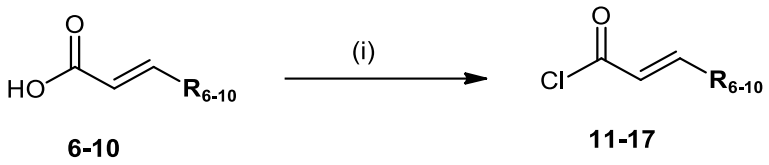

6-10 **11-17**

Scheme 9*: Acylation of cinnamic acid derivatives. Reagents and conditions: anhydrous toluene, Thionyl chloride ($SOCl_2$), 2-3 drops of DMF, RT, 8 h.*

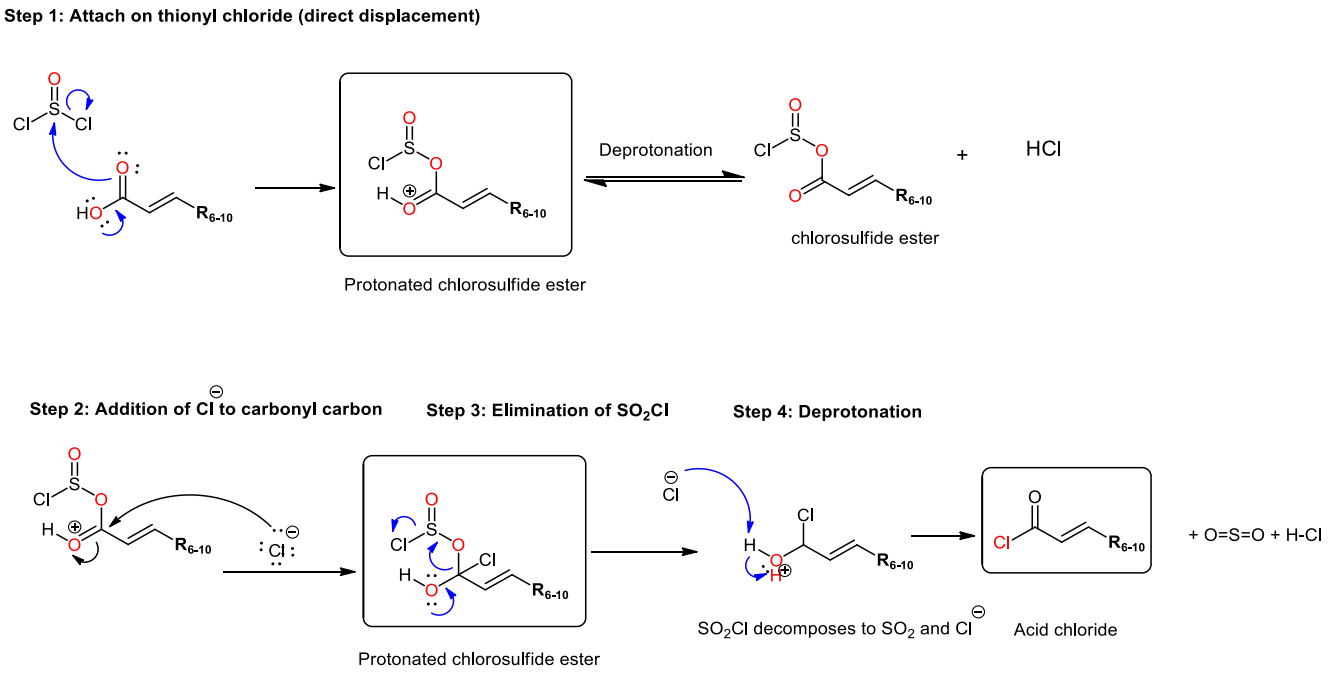

Scheme 10*: Proposed mechanism for acyl chloride formation using thionyl chloride.*

The carboxylic acid, acting as a nucleophile, attacks the sulfur atom (electrophile), leading in the replacement of H with SO_2Cl. The carbonyl oxygen serves as the nucleophile in the first step. Once the chlorosulfite ester is formed, the acid chloride is formed through a conventional addition-elimination mechanism, in which the chloride ion attacks the carbonyl carbon, resulting in the formation of C-Cl, the breakage of C-O (pi), and the C-O pi bond being re-formed, and the C-O bond being broken. The resulting (protonated) acid chloride is subsequently deprotonated by Cl to form the acid chloride.

2.1.1.4. Conjugation of Acyl chlorides and N-(7-Chloroquinoline-4-yl) alkyl-diamine

The conjugation of acyl chlorides with N-(7-chloroquinoline-4-yl) alkyl-diamine is a crucial synthetic strategy used in this project. The synthesis involved the reaction of 4-aminochloroquinolines and acyl chlorides in the presence of a triethylamine and dichloromethane as shown in **scheme 11**. Aluminium foil was used to cover the flasks to prevent or minimise exposing the reaction to light. The precaution was taken in line with the imminent isomerization that could take place when exposed to light. The products were obtained pure after purified by flash chromatography using 5-30% (v/v) ethyl acetate/ methanol to yield compounds **18-36**.

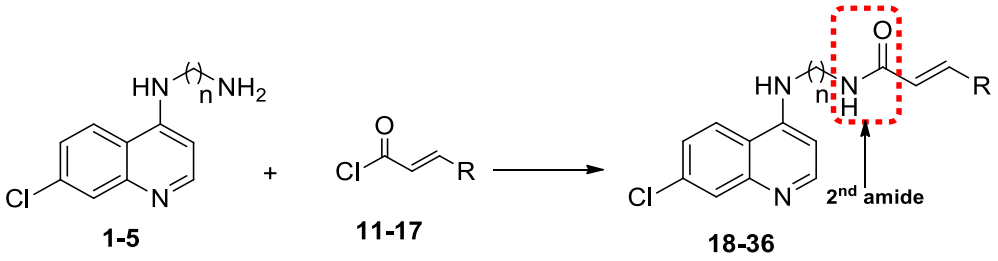

***Scheme 11**: Nucleophilic substitution of acyl chlorides and N-(7-Chloroquinoline-4-yl) alkyl-diamines. Reagents and conditions: Dry DCM, Triethylamine (Et_3N), RT, 24 h.*

Amide compounds are formed through the net substitution reaction between acid chlorides and amines. The process involves the nucleophilic addition of an amine (nucleophile) to the carbonyl carbon (electrophile), resulting in the formation of an intermediate compound that releases a chloride anion. Subsequently, the chloride ion undergoes a nucleophilic attack on the carbonyl, leading to deprotonation and the formation of the amide and HCl, **Scheme 12**.

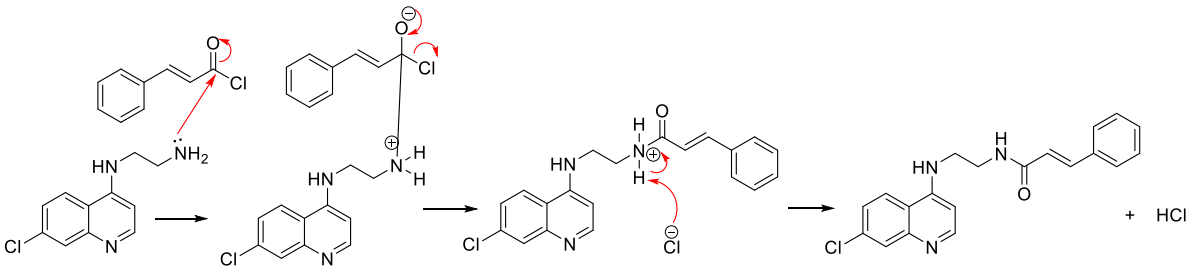

***Scheme 12:** Proposed mechanism for synthesis of cinnamoyl chloroquinoline hybrids **18-36**.*

2.1.1.4.1. Cinnamoyl chloroquinoline hybrids (18-24) with ethane-1,2-diamine linker

The chemical structures of compounds **18-24** shown in **figure 16** were confirmed by NMR, FTIR and HRMS data. In the ^{1}H NMR spectra of compounds **18-24**, the quinoline moiety was confirmed by four distinctive doublet signals (H-2, H-3, H-16 and H-9) and one doublet of doublet (H-7) signal in the downfield region of the spectra from 6.30 to 8.35 ppm. The number of signals observed in the ^{13}C NMR spectra of quinoline moiety is in agreement with the structures of the compounds as shown by four different tertiary carbons C-4 at 152.4 ppm, C-10 at 149.5 ppm, C-8 at 133.8 ppm, C-5 at 117.9 ppm and five =C-H peaks.

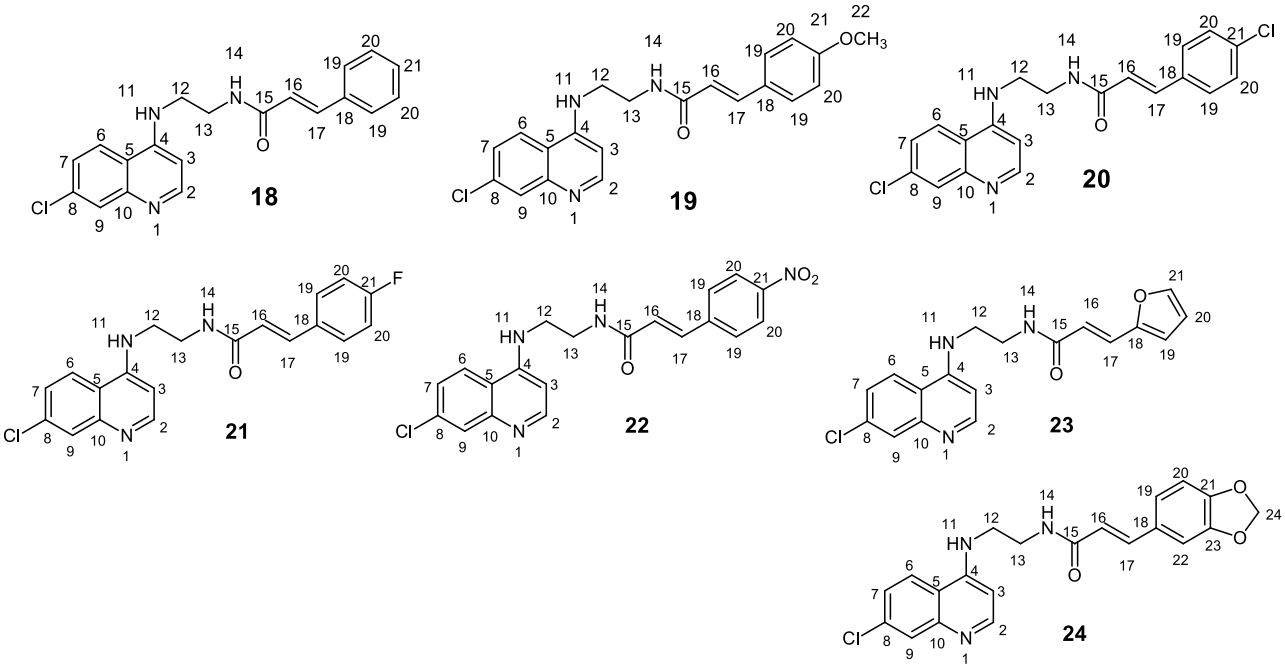

***Figure 16**: Cinnamoyl chloroquinoline hybrids (**18-24**) with ethane-1,2-diamine linker.*

Generally, ^{1}H NMR spectra of compounds **18-24** showed two multiplets H-12 and H-13 of the ethane-1,2-diamine integrating to four protons between 3.56-3,36 ppm. Two distinct methylene carbons were shown on the DEPT NMR at a region between 42.7 ppm and 37.9 ppm for C-12 and C-13, respectively. Distinctive doublet peaks H-16 and H-17 of cinnamic acid olefinic hydrogens were present in all spectra at 6.62-6.65 ppm and 7.52-7.77 ppm. The value of the $^{3}J_{HH}$ coupling constant of approximately 16 Hz in all of the compounds indicated that they are trans isomers.

The IR spectra of compounds **18-24** displayed all bands characteristic for the amide group NH stretch peak at 3310-3333 cm^{-1}, aromatic C-H stretch at 2907-2986 cm^{-1}. A

strong absorption band between 1657-1686 cm^{-1} was attributed to the C=O stretching vibration of the amide group. Bands around 1550-1586 cm^{-1} and 1222-1343 cm^{-1} were attributed to the C=N and C-N respectively. In the fingerprint region of the spectra, there were peaks representing the R groups on the cinnamic acids, i.e., C-F stretch at 513 cm^{-1}, C-Cl at 429 cm^{-1}, nitro group C-N at 1229-1299 cm^{-1} and C-O at 1035 cm^{-1}. HRMS confirmed the molecular ions which were consistent with the calculated mass as represented in **Table 3**.

Table 3**: characterization of data of compound **18-24.

Compound	n	R	% Yield	HRMS (m/z)	Mp (ºC)
18	2	Ph-4-H	59	352.1338 (found), 351.8294 (calcd.)	252-258
19	2	Ph-4-OCH_3	68	382.1443 (found), 381.8554 (calcd.)	235-236
20	2	Ph-4-Cl	63	387.0855 (found), 386.2745 (calcd.)	251-252
21	2	Ph-4-F	37	370.1126 (found), 369.8199 (calcd.)	246-249
22	2	Ph-4-NO_2	41	397.1194 (found), 396.8270 (calcd.)	241-243
23	2	-C_4H_4O	42	342.1032 (found), 341.7915 (calcd.)	240-242
24	2	-$C_7H_6O_2$	54	396.1240 (found), 395.8389 (calcd.)	252-254

The cinnamoyl moiety of compounds **23** and **24** were obtained from furfural and piperonal. The furan and benzo[*d*][1,3]dioxole rings were introduced to see how compounds with different R from the phenyl ring would behave in terms of their reactivity and their biological activity.

Compound **23** was isolated as brown solid (42%) with a melting point of 240-242 ºC. It was confirmed by ^{1}H NMR, ^{13}C NMR spectroscopy, as well as mass and infra-red spectroscopy. ^{1}H NMR spectrum (**figure 17**) revealed four doublets and one doublet of doublet in the quinoline moiety, H-2 at 8.42 ppm, H-3 at 6.60 ppm, H-6 at 8.21 ppm, H-9 at 7.16 ppm, and H-7 at 7.47 ppm, respectively and both peaks integrate for one proton. Proton H-9 coupled weakly to H-7 giving H-7 the multiplicity of doublet of doublet with *J* coupling constant of 2.3 Hz. The reaction took place at NH-14 on Compound **1**. This was confirmed by chemical shift that shifted downfield from 3.38 ppm as a broad singlet integrating for two protons to broad triplet NH-14 at 8.28 ppm

integrating to one proton. Methylene peaks of the amino-1,2-diamines H-12 and H-13 appeared as a multiplet at 3.55–3.42 integrating for four protons. The cinnamoyl moiety showed two olefinic peaks, two doublet and one doublet of doublet peaks of furan ring: Characteristic doublet peaks H-16 and H-17 of cinnamic acid olefinic hydrogens were observed at 6.47 ppm and 7.39 ppm respectively. The value of the $^{3}J_{HH}$ coupling constant of 15.7 Hz was observed in both H-16 and H-17. H-19 and H-21 appeared as doublet, accounting for one proton at 6.94 ppm and 7.80 respectively. H-20 is doublet of doublet due to H-19 and H-21 at 7.07 ppm.

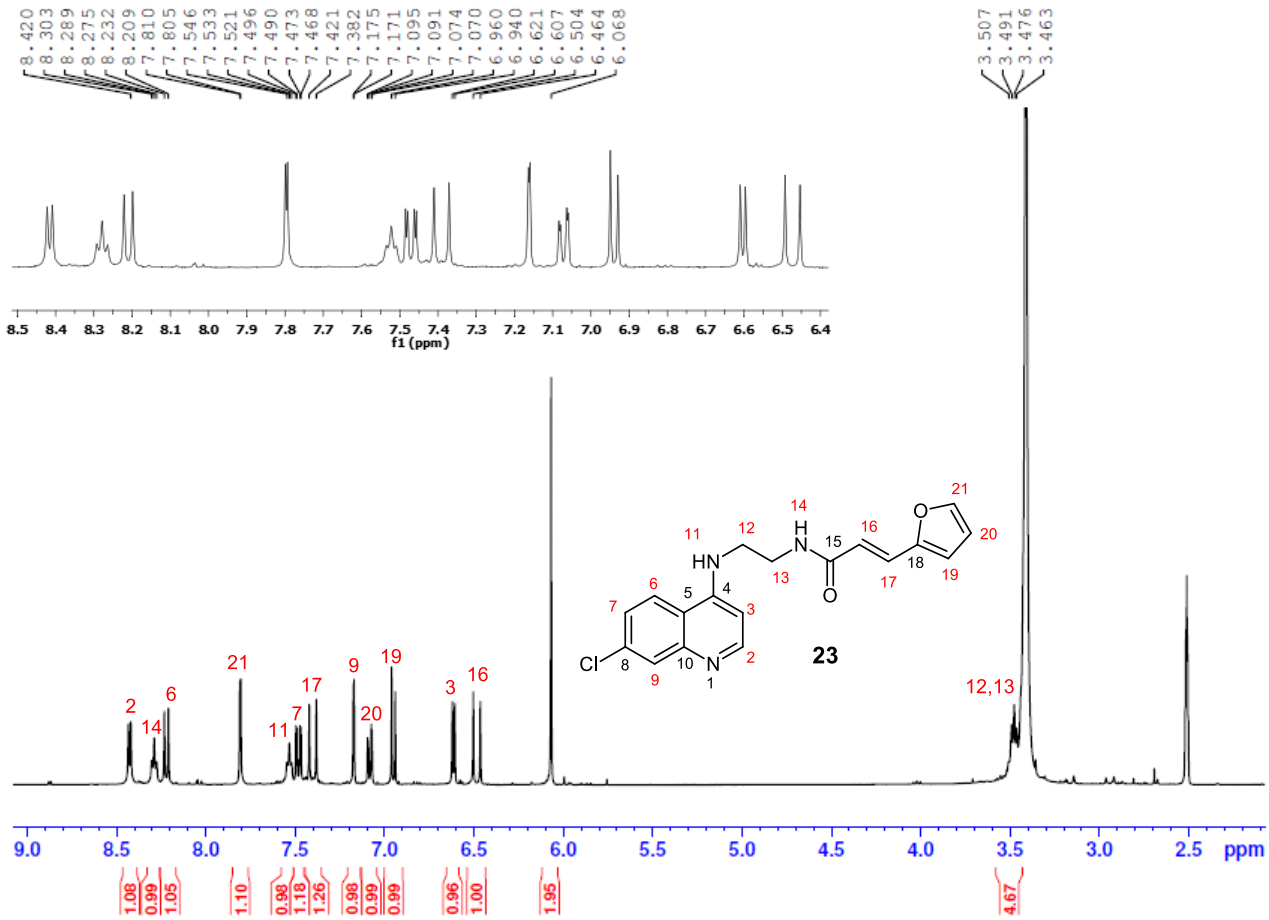

Figure 17: ^{1}H NMR of (E)-N-(2-((7-chloroquinolin-4-yl)amino)ethyl)-3-(furan-2-yl)acrylamide (**23**) in DMSO-d6.

The ^{13}C NMR spectrum showed 16 peaks in the aromatic region with a quaternary carbonyl peak C-15 of the amide group at 165.6 ppm. Tertiary carbons C-4 at 150.9 ppm, C-10 at 149.1 ppm, C-8 at 133.5 ppm, C-5 at 117.5 ppm further supported the presence of the quinoline moiety. Methylene signals C-12 and C-13 of the diamine moiety were confirmed on ^{13}C NMR and DEPT135 at 42.3 ppm and 37.5 ppm. Other

peaks of the furan ring were all well accounted for with C-21, C-19 and C-20 at 144.8 ppm, 113.9 ppm and 112.4 ppm, respectively as shown in **figure 18**.

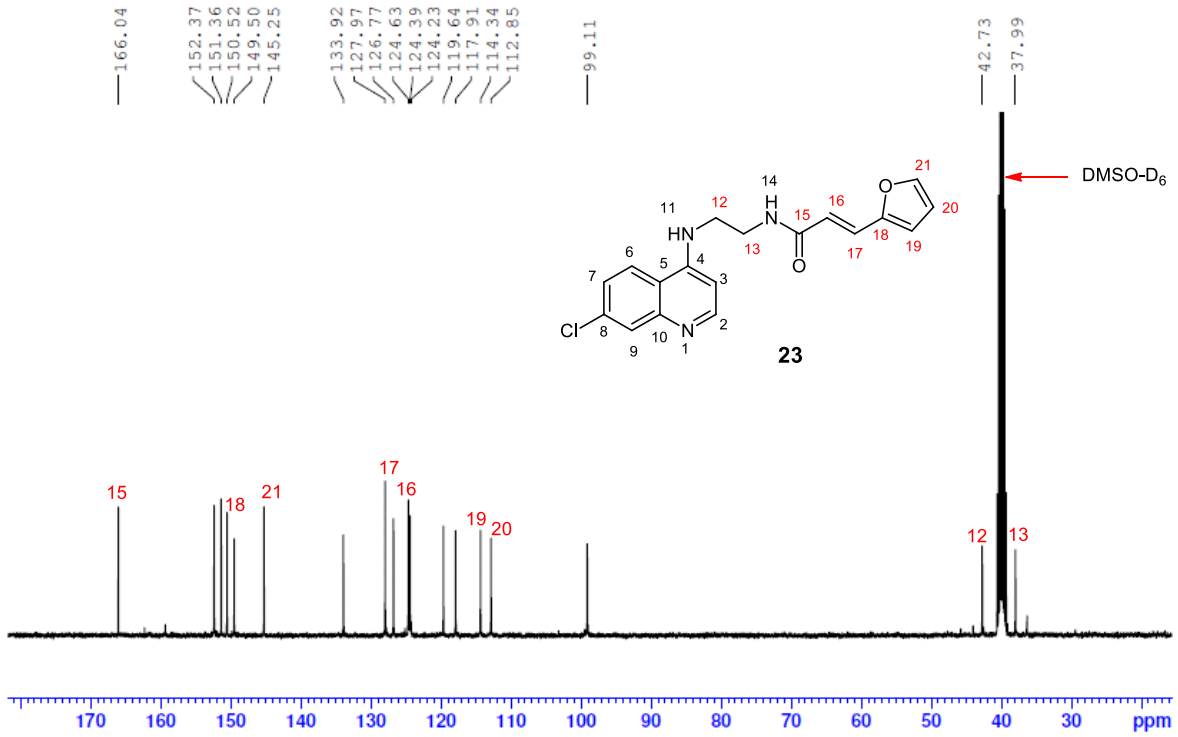

***Figure 18**: ^{13}C NMR of (E)-N-(2-((7-chloroquinolin-4-yl)amino)ethyl)-3-(furan-2-yl)acrylamide (**23**) in DMSO-d6.*

The IR spectrum of **23** showed an N-H stretch peak at 3324 cm^{-1}, aromatic =C-H stretch at 2983 cm^{-1}, carbonyl group C=O at 1666 cm^{-1}, C=N stretch at 1586 cm^{-1}, aromatic C=C stretch at 1533 cm^{-1}, C-N at 1238 cm^{-1} and C-O vibration at 1136 cm^{-1}. The HRM confirmed the mass of 341.1032 relative to the calculated mass of 341.79.

Compound **24** afforded a light brown solid (54%), and ^{1}NMR and ^{13}C NMR spectroscopy confirmed the product. The ^{1}H NMR showed four signals in the benzo[*d*][1,3]dioxole ring. Two doublets integrated to 1 proton, H-22 at 7.17 ppm and H-20 at 6.94 ppm, one doublet of doublet H-19 due to H-22 and H-20 at 7.08 ppm. and a singlet at 6.06 integrating to two protons. The other signals of interest were the characteristic doublet peaks of cinnamic acid olefinic hydrogens H-16 and 17 at 6.48 and 7.39 with $^{3}J_{HH}$ coupling of 15.8 Hz and 15.7 Hz, respectively. Broad triplet N-H at 8.30 ppm is where the conjugation occurred from primary amine (NH_2). Signals of the linker were observed as a multiplet between 3.56 – 3.44 ppm. Other peaks of the quinoline ring are also well accounted for.

The ^{13}C NMR further confirm compound **24** by showing 21 carbon peaks as expected with 7 carbons in the benzo[*d*][1,3]dioxole ring, 3 of which are quaternary cabrons C-23, C-21 and at 148.5 ppm, 147.9 ppm and 129.2 ppm respectively. Other peaks are C-19 at 123.9, C-20 at 108.6 ppm, C-22 at 106.2 and C-24 at 101.4 ppm. Distinctive carbonyl peak C-15 appeared at 166.0 ppm and unsaturated olefinic carbons C-16 and C-17 appeared at 120.0 ppm and 138.8 ppm. The IR spectrum further confirmed the structure by showing bands around 1686 cm^{-1} and 3310 cm^{-1} which were attributed to the amide group's C=O and N-H stretching vibrations, respectively. HRMS confirmed a molecular ion of *m/z* 395.1240 (MH-), consistent with a molecular mass of 395.84.

2.1.1.4.2. Cinnamoyl chloroquinoline hybrids (25-27) with a propane-1,2-diamine linker.

Compounds **25**-**27** shown in **figure 19** were synthesized in moderate yields (**table 4**) through amide bond formation between the acid chlorides of the cinnamic acids (**11-13**) and the *N*^{1}-(7-chloroquinolin-4-yl) propane-1,2-diamine (**3**). The introduction of NH_2 group in position 2 of propane brought the stereochemistry (chirality) in compounds **25-27**.

***Table 4**: Characterization data of compounds **25**-**27**.*

Compound	N	R	% Yield	HRMS (m/z)	Mp (ºC)
25	3	Ph	50	366.1375 (found), 365.8560 (calcd.)	152-153
26	3	Ph-4-Cl	48	401.1014 (found), 400.3011 (calcd.)	237-240
27	3	Ph-4-OCH_3	46	396.1823 (found), 395.8820 (calcd.)	212-216

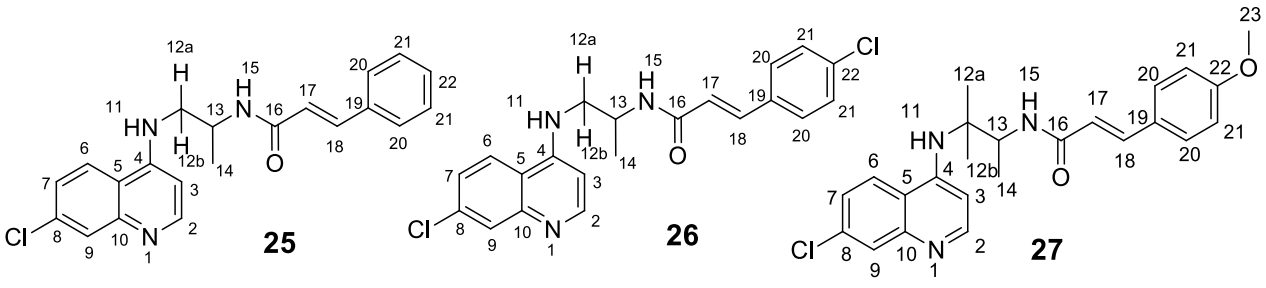

***Figure 19**: Cinnamoyl chloroquinoline hybrids (**25-27**) with a propane-1,2-diamine linker.*

Compounds **25-27** were confirmed by ^{1}H NMR, ^{13}C NMR spectroscopy (**figure 20 and 21**), as well as IR spectroscopy and HRMS.

The IR spectra of compounds **25-27** commonly showed the presence of absorption frequencies in the 3351–3325 cm^{-1} region, which is associated with N–H stretching and C=O stretch at 1659-1644 cm^{-1}. In the fingerprint region the characteristic C-Cl vibration appeared at 848 cm^{-1} and C-O of the methoxy group at 1367 cm^{-1} for compounds **26** and **27**, respectively.

The quinoline moiety was clearly identified from the presence of four doublets and one doublet of doublet, assigned to signals of the heterocyclic proton H-2, H-3, H-6, H-9 and H-7, respectively, in the ^{1}H spectra.

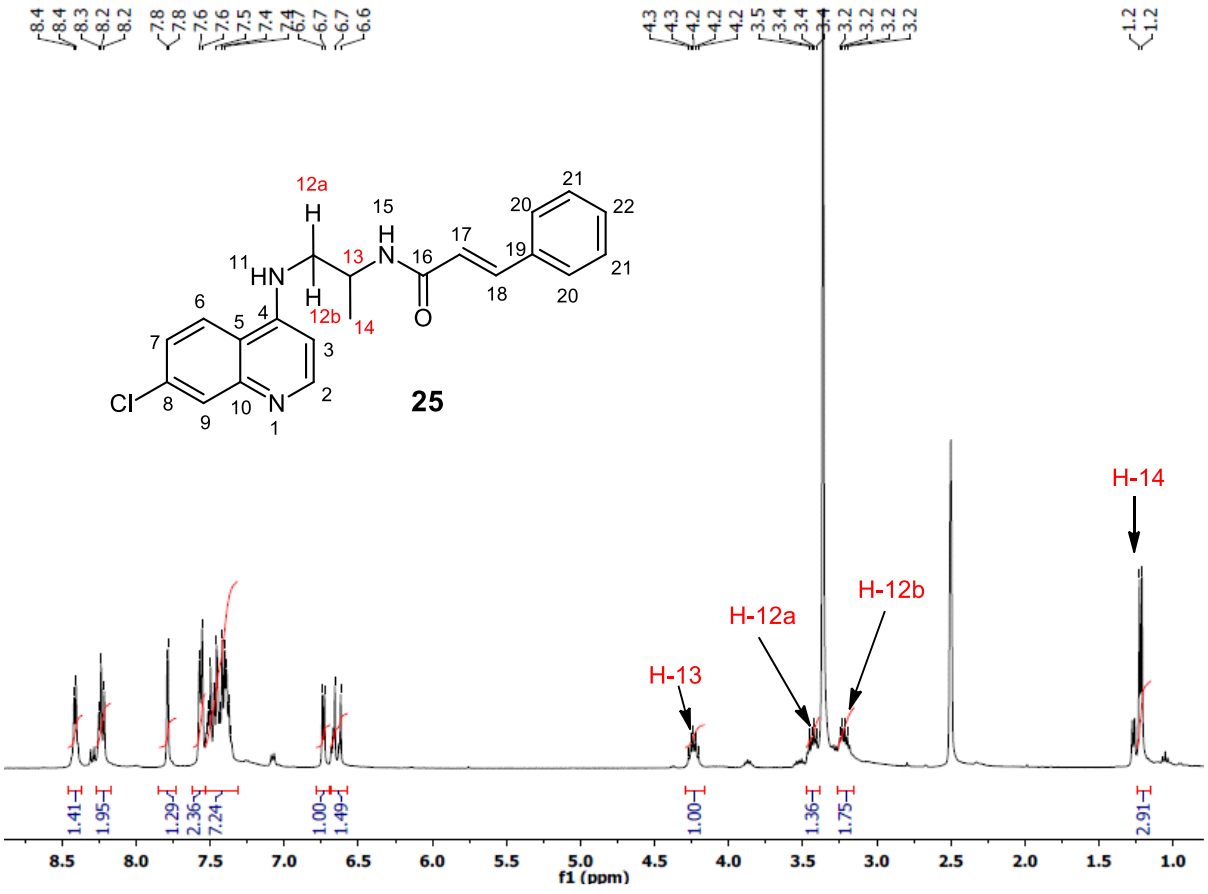

***Figure 20**: ^{1}H NMR of N-(1-((7-chloroquinolin-4-yl)amino)propan-2-yl)cinnamamide(**25**) in DMSO-d6.*

Figure 20 is the ^{1}H NMR of compound **25** mainly showing the proton siganals of the propane-1,2-diamine linker which on both compounds **25-27**, the protons were identified on a region 3.8–1.7 ppm. On compound **25**, H-13 appeared as quintet

integrating to 1 proton with a *J* coupling constant of 6.7 Hz. Two signals H-12a and H-12b appeared as doublet of a doublet at 3.43 and 3.22 ppm, respectively and both integrating to 1 proton each. Proton H-14 integrated for three protons and had multiplicity of doublet due to H-13. The disappearance and chemical shift of primary amine (NH_2) which appeared as a doublet from Compound **3** at 1.20 ppm to being a doublet upfield the spectrum at 8.22 ppm, indicated that the was attachment of cinnamoyl moiety.

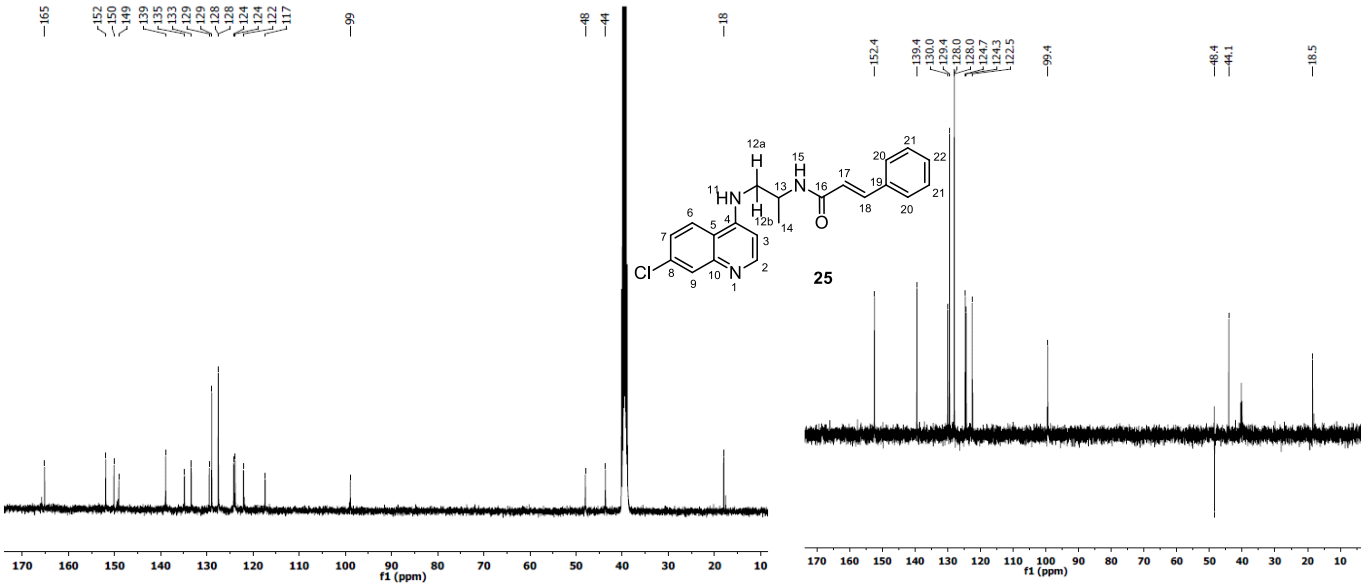

***Figure 21**: ^{13}C NMR and DEPT 135 of N-(1-((7-chloroquinolin-4-yl)amino)propan-2-yl)cinnamamide(**25**) in DMSO-d6.*

The DEPT 135 of both compounds **25-27** showed five different tertiary aryl carbons, C-2, C-3, C-6, C-7 and C-9 at 152-99 ppm, as well as four quaternary carbons, C-4, C-10, C-8 and C-5 in the region between 150.2-117.4 ppm which further supported the presence of the quinoline moiety. Methylene carbon peaks of propane-1,2-diamine linker, were identified on DEPT135 between 17.9-48.2 ppm.

2.1.1.4.3. Cinnamoyl chloroquinoline hybrids (28 and 29) with a propane-1,3-diamine linker

Compounds **28** and **29** (**figure 22**) were synthesized by reacting *N*^{1}-(7-chloroquinolin-4-yl) propane-1,3-diamine (**2**) and cinnamoyl chlorides **11** and **12** at room temperature for 8 hours in the presence of triethylamine.

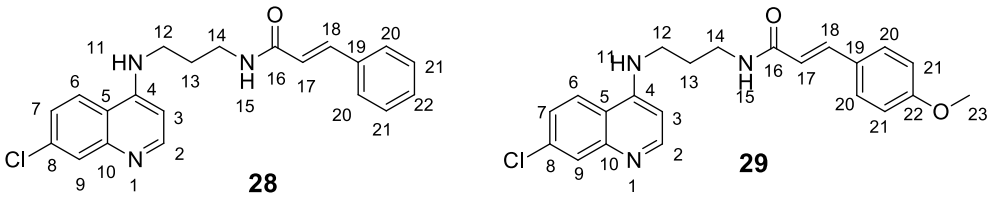

***Figure 22**: Cinnamoyl chloroquinoline hybrids (28 and 29) with a propane-1,3-diamine linker.*

Compound **28** afforded a white solid (54%) with a melting point of 190-192 ^{o}C. The product was confirmed by ^{1}H NMR, ^{13}C NMR spectroscopy, IR spectroscopy and HRMS. The ^{13}C NMR showed nine carbon peaks in the quinoline ring's aromatic region, of which four were quaternary carbons, C-4, C-5, C-8 and C-10 at 165.2, 117.5, 133.4 and 149.0 ppm, respectively. Four tertiary carbons, C-2, C-3, C-6, C-7 and C-9 in the quinoline ring also appeared at 151.9, 98.7, 124.1, 124.0 and 129.4 ppm, respectively. DEPT 135 confirmed the CH_2 peaks, namely C-14, C-12 and C-13, at 40.1 ppm, 36.7 ppm and 27.9 ppm, which belonged to the diamine moiety. The presence of carbonyl carbon at 165.2 ppm confirmed the formation of an amide group. Furthermore, two distinct olefinic carbons, C-17 and C-18, were observed at 122.2 and 138.6 ppm, respectively. The peaks of the cinnamoyl ring were all well accounted for with one quaternary (C-19) and 3 CH's C-20, C-21 and C-22 at 128.9 ppm, 127.5 ppm and 127.4 ppm.

^{1}H NMR spectrum showed 15 signals; the first signal confirming the structure of compound **28** was the disappearance of the primary amine NH_2-15 to form the secondary amine NH-15, which also showed a chemical shift from 3.35 ppm to 8.26 ppm and appeared as a multiplet overlapping with H-6. In the aromatic region, H-6, H-21, H-18, H-7, H-22 and NH-11 appeared as a multiplet between 7.48-7.32 ppm. In the diamine moiety, H-12 and H-14 appeared to be doublet integrating to four protons, and H-13 appeared as a quartet due to H-12 and H-14 integrating for 2 protons. Only one olefinic proton H-17 was visible, appearing at 6.64 ppm as a doublet due to one proton of H-18 with a *J* coupling constant of 15.8 Hz. The presence of the N-H stretch of the secondary amine in the IR spectrum at 3337 cm^{-1} and characteristic C-H and C=C stretch at 3048 cm^{-1} and 1537 cm^{-1}, respectively, further confirmed compound **28**. The mass spectrum also confirmed the molecular ion m/z 366.1408 compared to the calculated mass of 365.8560.

Compound **29**, isolated as a white solid with a melting point of 196-198 ^{o}C, had an additional proton (H-23) of the methoxy group attached in the para position of the benzene ring in the aliphatic region of its ^{1}H NMR spectrum. The H-23 signal appeared as a singlet integrating to three protons bit downfield at 3.77 ppm due to heteroatomic atom oxygen. The presence of the methoxy group made a chemical shift on C-22 from 127.4 ppm in compound **28** to 160.8 ppm in compound **29**. DEPT NMR showed the additional $\underline{C}H_3$ peak at 55.7 ppm; all other ^{1}H NMR and ^{13}C NMR are well accounted for. All characteristic bands of the N-H group and C-H stretch were observed at 3351 cm^{-1} and 3062 cm^{-1}, the distinct band of C-O of the methoxy group was observed at 1367 cm^{-1} of the IR spectrum. The molecular ion of the compound was reported in **table 5**.

***Table 5**: Characterization data of compounds **28** and **29**.*

Compound	n	R	% Yield	HRMS (m/z)	Mp (^{o}C)
28	3	Ph	53	366.1408 (found), 365.8560 (calcd.)	190-192
29	3	Ph-4-OCH3	54	396.1820 (found), 395.8820 (calcd.)	196-198

2.1.1.4.4. Cinnamoyl chloroquinoline hybrids (30-36) with hexane-1,6-diamine linker

The quinoline-cinnamoyl hybrids **30-36** (**figure 23**) were prepared by covalently binding the two motifs with 1,6-hexanediamine linker to afford cinnamoyl chloroquinoline hybrids **30-36** in low to good yield (**table 6**).

Table 6**: characterization of data of compounds **30-36.

compound	N	R	% Yield	HRMS (m/z)	Mp (^{o}C)
30	6	Ph-4-H	70	408.1963 (found), 407.9357 (calcd.)	174-175
31	6	Ph-4-OCH_3	74	438.1980 (found), 437.9617 (calcd.)	107-109
32	6	Ph-4-Cl	60	443.1484 (found), 442.3808 (calcd.)	183-185
33	6	Ph-4-F	25	426.1751 (found), 425.9333(calcd.)	150-153
34	6	Ph-4-NO_2	46	453.1696 (found), 452.9333 (calcd.)	136-140
35	6	-C_4H_4O	41	398.1746 (found), 397.8979(calcd.)	120-123

36	6	$-C_7H_6O_2$	54	452.1746 (found), 451.9452(calcd.)	168-170

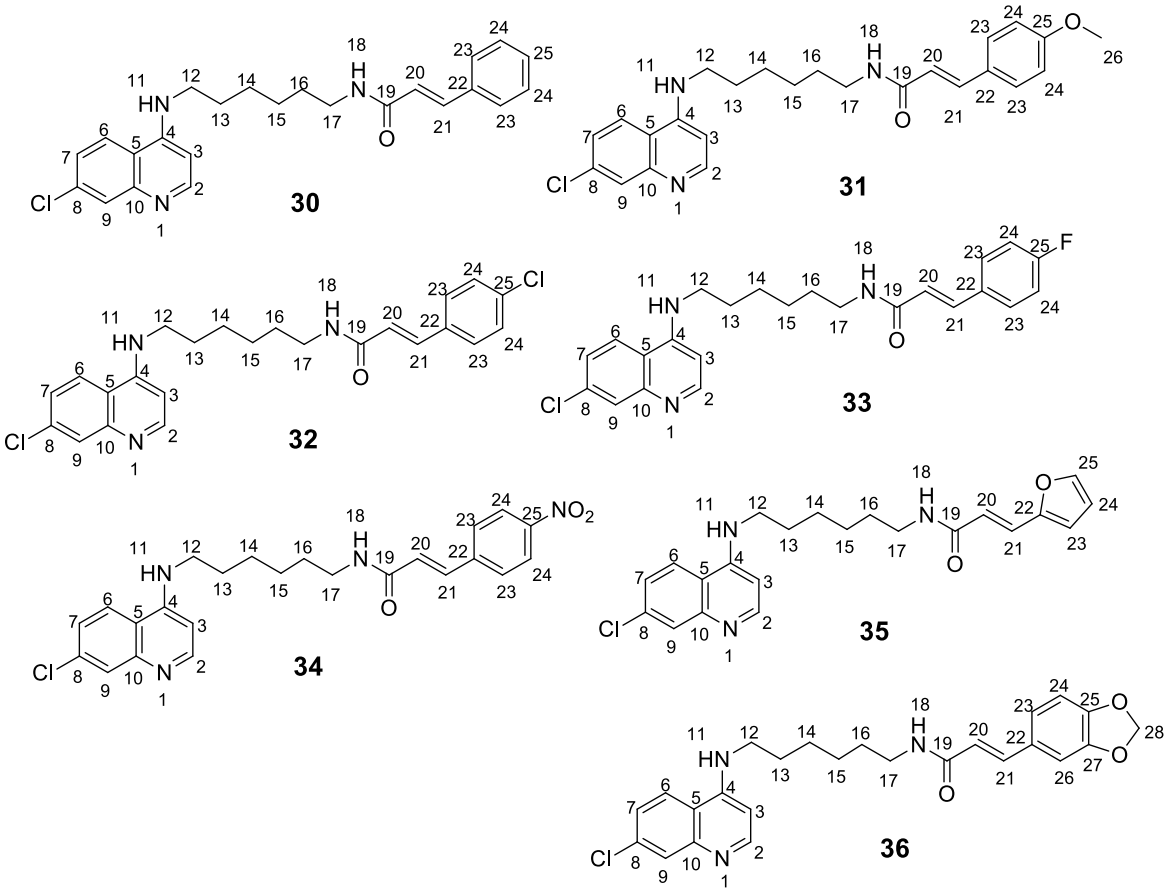

***Figure 23**: Cinnamoyl chloroquinoline hybrids (**30-36**) with hexane-1,6-diamine linker.*

Compound **31** afforded a light-yellow solid (74%) with a melting point of 107-109 ^{o}C. It was confirmed by ^{1}H NMR, ^{13}C NMR spectroscopy, and mass and IR spectroscopy. In addition to a singlet at 3.78 ppm integrating for 3Hs (Ph-4-OCH_3), the ^{1}H NMR spectrum showed 17 other protons: 4 doublets and 1 doublet of doublet for the quinoline moiety at 8.32 ppm, 8.28 ppm, 7.78 ppm, 6.44 and 7.44 for H-2, H-6, H-9, H-3 and H-7, respectively. Both NH groups (NH-11 and NH-18) were clearly displayed on the spectrum as broad triplets at chemical shifts of 7.50 and 8.04 ppm respectively. two olefinic doublets (H-20 and H-21) integrating to 1 proton at 6.47 ppm and 7.35 ppm had a coupling constant of 15.9 Hz. Furthermore, two doublets (H-23 and H-24) in the benzene ring appeared at 7.50 ppm and 6.96 ppm, respectively and integrated to two protons. In the diamine moiety, 3 doublet of doublets and a multiplet signals were observed. H-12 integrated to two protons t 3.25 ppm with a multiplicity of doublet of doublet. H-17 also appeared as doublet of doublet at3.17 ppm. H-13 and H-16 were

also observed at1.64 ppm and1.46 ppm, respectively. Multiplet signals between 1.36-1.30 ppm exhibited H-15 & H-14, respectively.

The ^{13}C NMR spectrum showed a carbonyl peak (HN-C=O) at 165.6 ppm, plus 6 quaternary carbons C-25, C-4, C-10, C-8, C-5, and C-22 at 160.7-99.0 ppm. Nine CH peaks were observed in the region of 152.3 to 117.9 ppm for C-2, C-6, C-7, C-9, C-23, C-24 and C-3. DEPT 135 NMR proved the existence of 6 methylene carbons (CH_2) of 1,6-hexanediamine linker. The IR spectrum of **31** showed the presence of the N-H stretch of the secondary amine at 3355 cm^{-1} and characteristic C-H and C=O stretch at 2905 cm^{-1} and 1657 cm^{-1}, respectively. The mass spectrum also confirmed the molecular ion *m/z* 438.1980 compared to the calculated mass of 437.9617.

As with compound **31**, compounds **30, 32, 33** and **34** were also confirmed by ^{1}H NMR, ^{13}C NMR spectroscopy, IR spectroscopy and HRMS data. Generally, in the ^{1}H NMR spectrum of compounds **30, 32, 33** and **34**, the quinoline moiety was identified by four distinctive doublet signals (H-2, H-3, H-6 and H-9) and one doublet of doublet (H-7) signal at 7.43 ppm that accounts for the aromatic hydrogens. In case where R was methoxy there was an additional singlet at 3.78 ppm assigned to H-26 and where R was chlorine at para position of the benzene ring there was a deficit of a proton signal as compared to other compounds. It was the same case in the ^{13}C NMR spectrum for compound **31** to have a distinct signal (C-26) deshielded at 114.8 ppm due to the presence of heteroatomic oxygen atom of the methoxy group. ^{13}C NMR further confirmed the quinoline moiety by the signals in the region of 152.3, 150.5, 149.1, 133.8, 127.6, 124.5, 124.4, 117.8 and 98.9 ppm, which corresponds to the aromatic carbons: C-2, C-14, C-10, C-8, C-6, C-7, C-14, C-5 and C-3. The presence of 1,6-hexanediamine moiety was determined by six signals in the 42.8, 39.1, 29.5, 28.1, 26.8, 26.7 ppm region corresponding to the methylene carbons, C-12, C-17, C-13, C-16, C-15 and C-14 ppm, respectively. The IR spectra of compounds **30, 32, 33** and **34** showed a characteristic NH and C=O stretch of the amide group at 3344-3359 cm^{-1}, and 1636-1665 cm^{-1}, respectively. HRMS of all the compounds gave further evidence of the successful synthesis of compounds **30, 32, 33** and **34** as shown in **table 6**.

Compound **33** was isolated as light yellow solid (25%) with a melting point of 150.-153°C. It was confirmed by ^{1}H NMR,^{13}C NMR and IR spectroscopy. Seventeen proton signals were observed on ^{1}H NMR spectrum as expected. The conjugation of

cinnamoyl moiety and aminoquinoline took place at 8.46 ppm showing a broad triplet peak (NH-18) due to H-17. Two aromatic proton signals H-23 and H-24 on the cinnamoyl moiety integrated to two protons and showed a multiplicity of doublet of doublet with *J* values of 5.6 Hz and 6.0 Hz, respectively. The ^{13}C NMR spectrum showed 22 carbon peaks. What is important to notice was the presence of fluorine atom which splits the signals for the *ipso*-, *ortho*-, *meta*-and *para*- carbons into doublets with typical coupling constants. Doublet at 161.6 ppm (J_{C-F} = 159.3 Hz) was due to the *ipso* C-25. The carbon ortho to the fluorine atom (C-24) also exhibited a doublet at 115.9 ppm (J_{C-F} = 21.7 Hz). The two equivalent carbons which are *meta* (C-23) to the fluorine atom also split into doublet at 129.6 with J_{C-F} = 8.5 Hz. Finally, the quaternary carbon (C-22) which was para to the fluorine atom was observed at 131.6 ppm and just like the others, it also split to doublet with a coupling constant of J_{C-F} = 2.9 Hz. The general observation was that the *ipso* carbon had higher coupling constant while the further carbon, e.g the *para* one had lower coupling constant. The rest of the carbon signals in the spectrum were self-explained. The IR spectrum of 33 further confirmed the compound by the presence of C-F stretch at 513 cm^{-1}.

As with compounds **23** and **24,** different rings (furan and benzo[*d*][1,3]dioxole) were introduced to compounds **35** and **36** to see how compounds with different R group from the phenyl ring and longer chain would behave in terms of their reactivity and their biological activity.

Compound **35** was isolated as brown solid (41%) with a melting point of 120-123 ^{o}C. It was confirmed by ^{1}H NMR, ^{13}C NMR spectroscopy, mass and infra-red spectroscopy. ^{1}H NMR spectrum revealed four doublets, and one doublet of a doublet in the quinoline moiety, H-2 at 8.37 ppm, H-3 at 6.44 ppm, H-6 at 8.28 ppm, H-9 at 7.74 ppm, and H-7 at 7.42 ppm, respectively and both peaks integrate for one proton. Proton H-9 coupled weakly to H-7 giving H-7 the multiplicity of doublet of doublet with *J* coupling constant of 2.1 Hz. The reaction took place at NH_2-18 on Compound **5**. This was confirmed by chemical shift shifted downfield from 2.45 ppm as a broad singlet integrating for two protons to broad triplet NH-18 at 8.14 ppm integrating to one proton. Methylene peaks of the 1.6-hexanediamine appeared as a multiplets: H-12 and H-17 at 3.36-3.10 ppm integrating for 4Hs, H-13 at 1.76-1.52 integrating foe 2Hs, H-16, H-14 and H-15 integrating for 6Hs at 1.51-1.25 ppm. The cinnamic acid moiety was showed by the presence of two olefinic peaks, two doublets and one doublet of doublet

peaks of furan ring: Characteristic doublet peaks H-20 and H-21 of cinnamic acid olefinic hydrogens were observed at 6.43 ppm and 7.22 ppm (15.7 Hz), respectively. H-23 and H-25 appeared as doublet, accounting for one proton at 6.74 ppm and 7.78 ppm, respectively. H-24 is doublet of doublet due to H-23 and H-25 at 6.56 ppm.

The ^{13}C NMR spectrum showed 16 peaks in the aromatic region with a quaternary carbonyl peak C-19 at 165.2 ppm. Tertiary carbons C-4 at 151.5 ppm, C-10 at 149.3 ppm, C-8 at 133.9 ppm, C-5 at 117.9 ppm further supported the presence of the quinoline moiety. Methylene signals C-12, C-13, C-14, C-15, C-16 and C-17 were observed on ^{13}C NMR and DEPT135 in the aliphatic region from 42.8 to 26.7 ppm. Other carbon signals of the furan ring were all well accounted for with C-25, C-23 and C-24 at 145.1 ppm, 113.9 ppm and 112.8 ppm, respectively.

The IR spectrum of **35** showed an N-H stretch peak at 3284 cm^{-1}, aromatic =C-H stretch at 2928 cm^{-1}, carbonyl group C=O at 1656 cm^{-1}, C=N stretch at 1575 cm^{-1}, aromatic C=C stretch at 1450 cm^{-1}, C-N at 1230 cm^{-1} and C-O vibration at 1136 cm^{-1}. The HRM confirmed the mass of 398.1676 relative to the calculated mass of 397.8979.

Compound **36** afforded a light brown solid (54%), and ^{1}NMR and ^{13}C NMR spectroscopy, IR spectroscopy and HRMS confirmed the product. The ^{1}H NMR showed four signals in the benzo[*d*][1,3]dioxole ring: two doublets integrated to 1 proton, H-26 at 7.12 ppm and H-24 at 6.93 ppm, one doublet of doublet H-23 due to H-24 and H-26 at 7.04 ppm, and a singlet (H-28) at 6.05 integrating to two protons. The other signals of interest were the characteristic doublet signals of the olefinic hydrogens H-20 and H-21 at 6.45 and 7.23 ppm, the $^{3}J_{HH}$ coupling constant were not visible as the peaks were appearing as multiplets. Broad triplet NH-18 at 8.00 ppm is where the conjugation occurred from primary amine (NH_2). Signals of the linker were observed as a multiplets between 3.32-3.10 ppm for H-12 and H-17, 1.73-1.57 ppm for H-13, 1.55-1.40 ppm for H-16, 1.41-1.26 ppm for H-14 and H-15 integrating for 4Hs. Other peaks of the quinoline ring are also well accounted for like reported in the previous compounds.

The ^{13}C NMR further confirmed compound **36** by showing 25 carbon peaks as expected. seven carbons were observed in the benzo[*d*][1,3]dioxole ring, 3 of which are quaternary cabrons C-22, C-25 and C-27 at 129.4 ppm, 147.9 ppm and 148.3 ppm respectively. Other peaks are C-23 at 123.9, C-24 at 108.5 ppm, C-26 at 106.1 and

C-28 at 101.4 ppm. Distinctive carbonyl peak C-19 appeared at 165.0 ppm. unsaturated olefinic carbons was observed on DEPT 135 spectrum as follows: 42.4 ppm (C-12), 38.6 ppm (C-17), 29.2 ppm (C-13), 27.7 ppm (C-16), 26.3 ppm (C-14), and 26.2 ppm (C-15). The IR spectrum further confirmed the structure by showing bands around 3343 cm^{-1} and 1620 cm^{-1} which were attributed to the amide group's N-H and C=O stretching vibrations, respectively. HRMS confirmed molecular ion of *m/z* 452.1746 (M+H) which was consistent with a molecular mass of 451.9452.

2.1.2. Summary

Three series of nineteen hybrid cinnamoyl chloroquinoline hybrids **18-36** were successfully synthesized by employing known conventional methods. These compounds were variously modified at different positions as outlined in the aims section representing diversity of substitution. Four steps were followed en route to these compounds **18-36**, with overall yields of 24-74%. The key steps included (i) the nucleophilic (Cl) substitution, (ii) acyl chloride formation and (iii) conjugation reactions. A direct conjugation of cinnamic acids with 4-aminochloroquinolines by coupling agents as reported by *Perez et al* was problematic, hence the option to generate acyl chlorides which were used without further purification.

Modifications of a range of carbon chain (with lengths 2-6) linkers as well as different R- groups substituted at the cinnamoyl ring afforded a range of compounds.

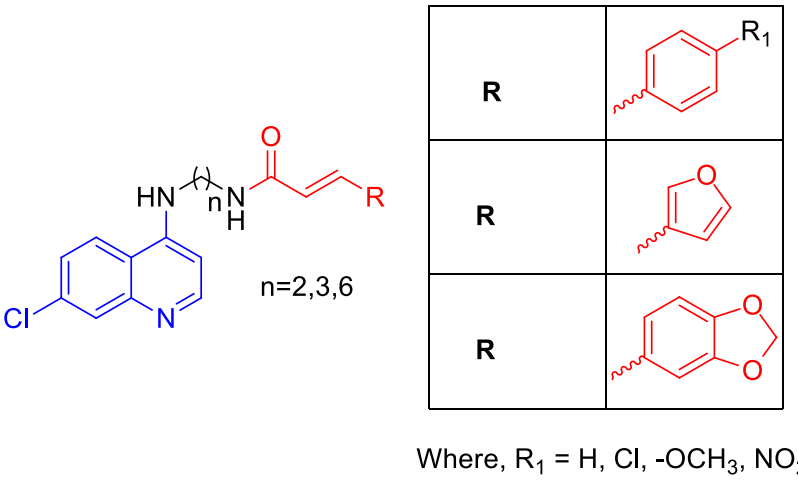

***Figure 24**: General structure of cinnamoyl chloroquinoline hybrids (**18-36**).*

It was observed that when R_1 is the same, but the number of carbons on a chain linker are increasing, the proton atoms gain more energy and cause a change in the chemical shifts from left to the right (deshielded). For example, when (R_1=H) and (n) increases from 2 to 6, the protons meta to that hydrogen gained higher frequency and moves downfield the NMR spectra. i.e. in compounds **18** (H-19 at 7.57 ppm), **25** (H-20 at 7,56 ppm), **28** (H-20 at 7.56 ppm) and **30** (H-23 at 7.55 ppm).

The presence of specific functional groups can have significant effects on the nuclear magnetic resonance (NMR) spectra of organic compounds. Electron-withdrawing groups like chlorine atoms are known for their electronegativity that can cause deshielding effects on nearby protons, resulting in downfield shifts in the NMR spectrum. The deshielding effect is the result of electronegative atom pulling the electron density away from the nuclei of ^{1}H atoms and exposing them more to the magnetic field, which "deshields" the nuclei and shifting the peak downfield.[71] On the contrary, Fluorine (F) atoms exhibit a strong electronegativity and can induce substantial deshielding, leading to more pronounced downfield shifts. The presence of nitro (NO_2) groups can result in significant deshielding effects, causing nearby protons to experience downfield shifts. Electron-donating groups like methoxy (OCH_3) groups can cause a shielding effect on nearby protons, resulting in upfield shifts in the NMR spectrum.[72] The effect of R groups on the cinnamoyl-chloroquine compounds is shown in the **Table 7** below.

Table 7: *Chemical shifts of the proton atoms meta to the specific R_1 group.*

n	R_1=H	R_1=Cl	R_1=F	R_1=NO_2	R_1=OCH_3
	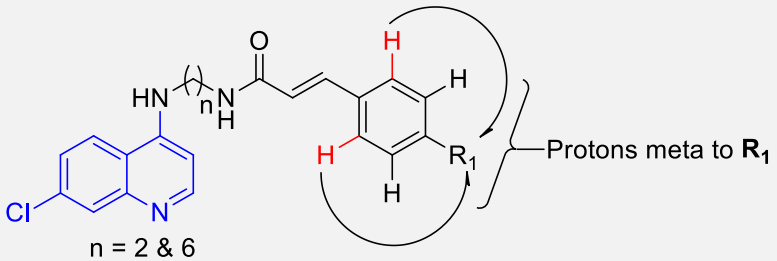 n = 2 & 6				
6	**30** (7.55 ppm)	**32** (7.58 ppm)	**33** (7.60 ppm)	**34** (7.82 ppm)	**31** (7.50 ppm)
2	**18** (7.57 ppm)	**20** (7.61 ppm)	**21** (7.65 ppm)	**22** (7.85 ppm)	**19** (7.52 ppm)

When n=6, the chemical shift of the proton *meta* to electron-withdrawing groups dishielded downfield increasing from hydrogen (H) in compound 30 at 5.55 ppm all the way to 7.88 ppm in compound **34** were R_1=NO_2 but was shielded upfield in compound **31** caused by electron donating methoxy group (OCH_3). Similar trend was observed in the case where carbon linker chain was equal to two (n=2). In conclusion, shorter carbon chain linker (n=2) and electron withdrawing groups caused a great shift (downfield) in the chemical environment of proton atoms and also carbons of cinnamoyl chloroquinoline hybrids **18-36**.

2.2 Miscellaneous results

2.2.1 Discovery of the formation of quasi-molecular ions due to tautomerization of compound 18

In the work that was not part of the objectives of this project, **18** was observed to generate strong quasi-molecular anions during ESI-MS, despite not being predisposed to anion formation based on its structural configuration.[73] Although the visual inspection of the structural configuration **18** makes it impossible to ionize in negative ESI mode, due to its lack of possible functional groups that can easily be deprotonated, is was found to have resulted in formation of intense quasi-molecular anions of this molecule which was detected at m/z 350.104, **Figure 25**.

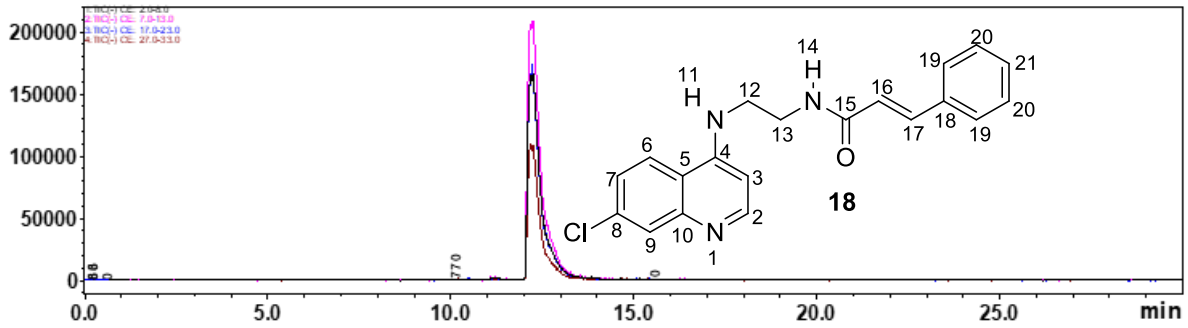

***Figure 25**: Representative base peak ion chromatogram showing detection of a quasi-molecular anion of **18** through LC-ESI-qTOF-MS/MS at various collision energies.*

In order to rationalise the formation of these anions, it was therefore hypothesised that the molecule underwent tautomerization which is a phenomenon identical with amide containing molecules.[74,75]

A further interpretation of the mechanism behind formation of the observed quasi-molecular anions was done on the density functional theory (DFT) study that determined the activation energy for the interconversion between the amide and the imidic acid tautomeric isomers, with optimised geometries shown in **Figure 26**.

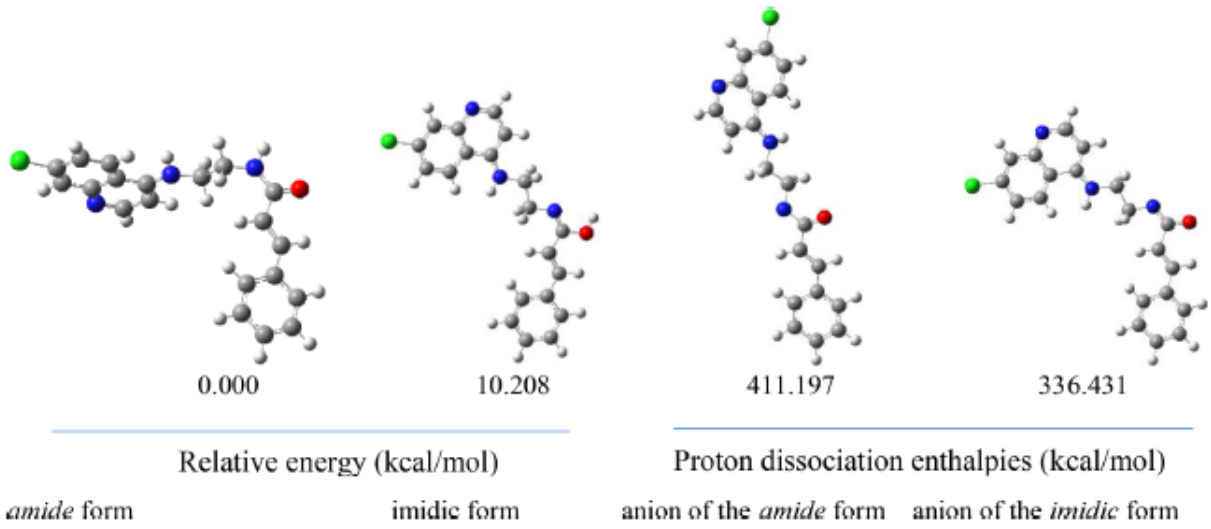

Figure 26: Optimised amide and imidic species for **18** and their corresponding anion species.

Furthermore, the relative stability between the amide and imidic conformers as well as the dissociation enthalpy related to the formation of the quasi-molecular anion systems were estimated and reported in **Table 8**.

Table 8: *Relative energies (kcal/mol) and relative activation energies for the reaction species in the amide ↔ imidic tautomeric mechanism. Calculations with 6-31++G(d,p) basis set.*

structure	B3LYP/6-31++G(d,p) results		M06–2X/ 6-31++G(d,p) results	
	ΔE (kcal/mol)	ΔG (kcal/mol)	ΔE (kcal/mol)	ΔG (kcal/mol)
Amide	0.000	0.000	0.000	0.000
Transition state	37.245	37.119	38.527	37.903
Imidic	9.775	9.800	8.988	9.0819

Further validation of the conversion mechanism of the amide to the imidic form was studied, **Figure 27**. The activation barrier height was estimated to be at 37.3 kcal/mol, suggesting the stability of the amide form and also the possibility form of imidic, although not an easy one, and that the two isomers may co-exist in vacuum.

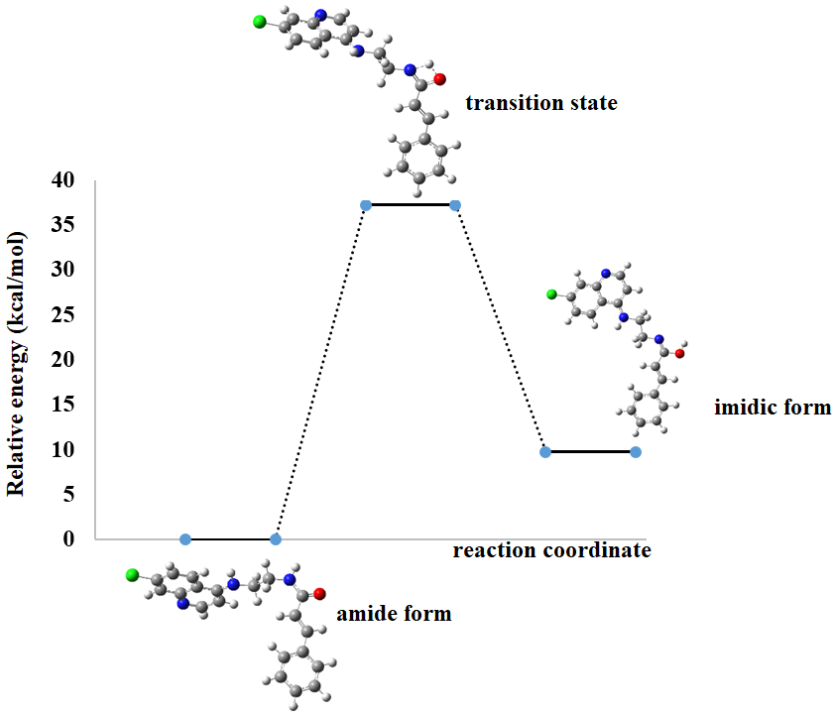

Figure 27: *Energy profile (relative energy against reaction coordinate) for the amide ↔ imidic tautomeric mechanism.*

2.2.2 Conclusion

At the end, the DFT investigation into the formation of quasi-molecular anion species in LC-ESI-MS experiments of **18** has provided valuable insights. The study aimed to confirm the existence of amide-imidic tautomers and elucidate the mechanism behind the observed anion species formation. The results revealed that the amide tautomeric form is more energetically favourable than its imidic counterpart, supported by a high activation energy barrier for the conversion from amide to imidic form. The estimated proton dissociation enthalpy suggests that the imidic form is the likely origin of the quasi-molecular anion species observed during ionization in LC-ESI-MS experiments. This investigation not only enhances our understanding of the molecular dynamics but also contributes to the broader field of analytical chemistry, providing crucial information for the interpretation of experimental results in mass spectrometry studies.

Resultantly, this work was published in Journal of Molecular Chemistry [See Appendix section].

CHAPTER 3

ISOMERIZATION OF CINNAMOYL-CHLOROQUINE HYBRIDS

3.1. Photoisomerization of cinnamoyl-chloroquine hybrids

Photoisomerization is a process which happens when a molecule changes structurally upon exposure to light.[76] As a potent tool for adjusting the pharmacological characteristics of bioactive compounds, it plays a crucial role in drug development.[68] It is possible to control drug release, improve therapeutic efficacy, and reduce side effects by taking advantage of this light-induced molecular transformation, in which molecules change their structural characteristics when exposed to particular wavelengths of light.[68,77] Researchers can develop novel photo-switchable drugs with precise temporal and spatial control over their biological activity by leveraging the principles of photoisomerization.[78] From targeted drug delivery to personalized medicine, this innovative approach has enormous potential for addressing a range of drug development challenges. Recent studies have illuminated the significance of photoisomerization as a flexible and effective tool in the pharmaceutical industry.[79–81]

Cinnamoylated-4-amino-7-chloroquinoline hybrid compounds have characteristics of being photo-pharmacological agents that are brought by olefinic protons in the cinnamic acid. These types of compounds have photoactive group that must absorb light at a desired wavelength and reorganize the molecular structure after photo-activation.

Because the photoisomerization of cinnamoyl chloroquinoline hybrids has not been studied, as a result this project embarked on investigating their photo-switchable effects. In addition to the known structural activities brought by the chloroquinoline moiety, the design of the compounds also looked at structural properties such as alkyl chain linkers and substituents on cinnamic acids, **Figure 28**.

3.2. Irradiation Methodology

A 2 mg/mL solution of compound (**18-36**) *trans* positional isomer were prepared with 100% absolute ethanol. Irradiation of samples were conducted by placing the solution (trans isomer) in a Spectroline UV lamp operating at 254 nm with an intensity of 390 μW/cm^2. Irradiation was conducted for 24 hours. All the samples were filtered and placed in amber vials and subjected to UHPLC-QTOF-MS.

3.3. Photoisomerization of Cinnamoylated-chloroquinoline compounds18-36.

Nineteen (19) cinnamoylated-chloroquinoline compounds were irradiated under UV as mentioned above and the following results were obtained.

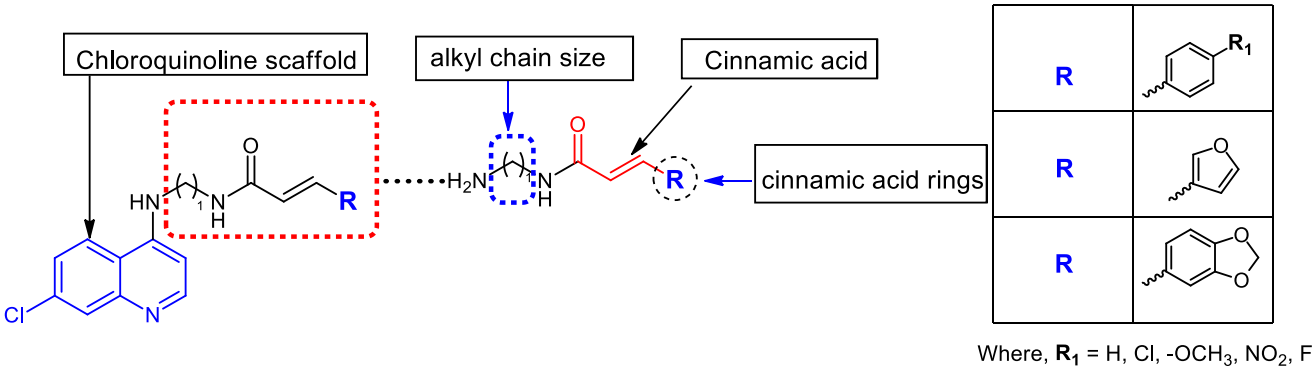

***Figure 25**: Structural parameters considered in the study.*

The observations were made prior and after UV irradiation (**figure 29** and **figure 30**, respectively).

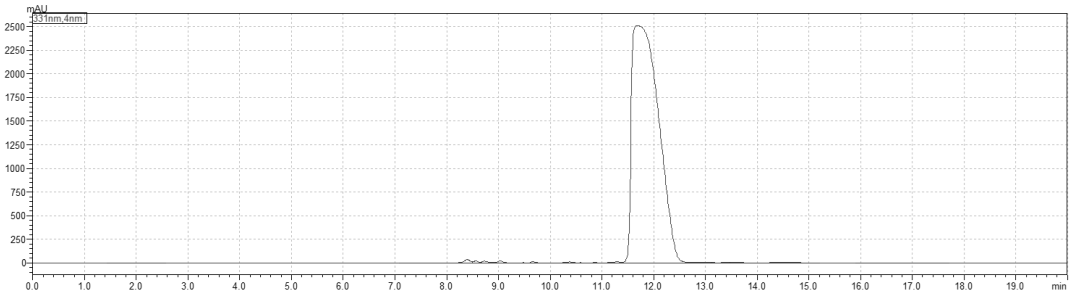

***Figure 26**: Representative UHPLC-QTOF-MS chromatograph showing trans isomer of (**20a**) before UV irradiation.*

Prior to UV irradiation, the chromatograph showed mainly a single peak which corresponds to the *trans* isomer as indicated in **figure 29**.

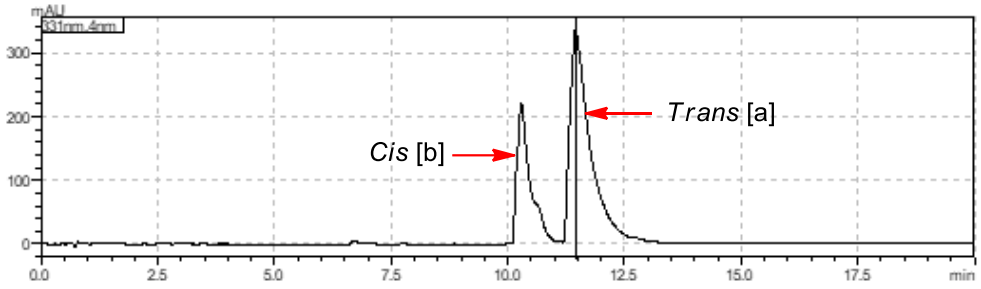

***Figure 27**: Representative UHPLC-QTOF-MS chromatograph showing mainly cis and trans isomer peaks of **20** after 24 hours UV treated. The two peaks are represented as **20a** and **20b** indicating both trans and cis isomers.*

After the compounds were subjected to UV irradiation, The chromatograph (**Figure 30**) showed the peaks representing the mixture of both cis and trans isomers after irradiation. Despite the presence of a dominating trans isomer at 12.0 minutes, a significant characteristic peak appeared at 10.5 minutes and was related with the cis isomer. The pattern was seen in all compounds, see the appendix section. This showed that even after UV irradiation of the solutions, there was no 100% conversion from trans to cis isomer. The length of the chain linkers and the substituents on the phenyl ring of the cinnamoyl moiety are the only differences between these compounds, as shown in **Scheme 13**. These physical features were shown to influence their behavior in terms of elution retention times.

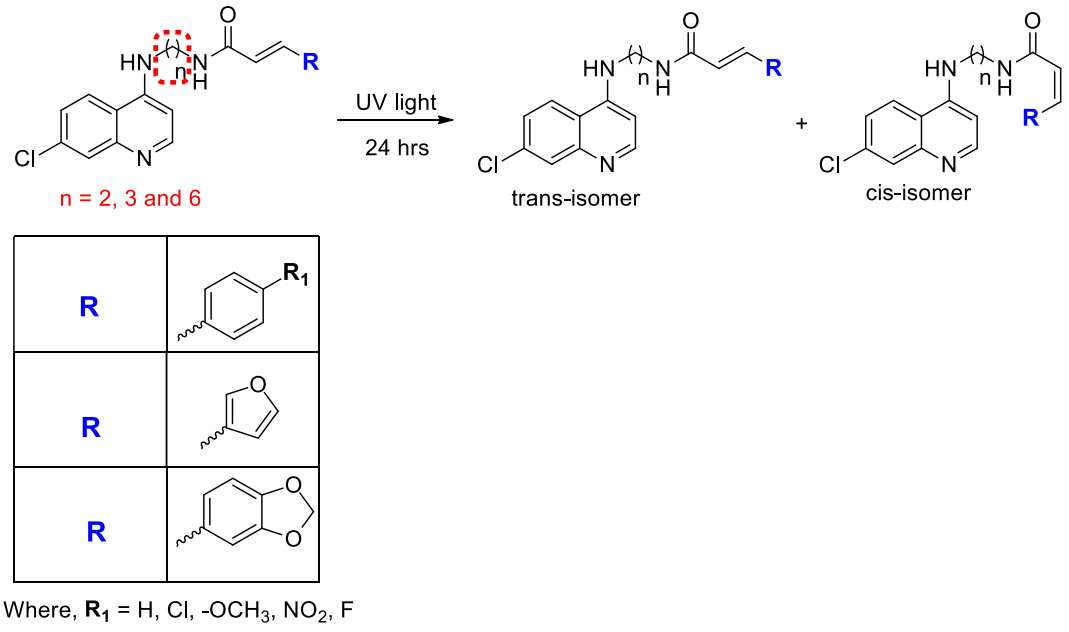

***Scheme 13**: Schematic representation showing both trans and cis structures after UV irradiation.*

The results (**Table 9**) are showing chromatographic retention times for various compounds **18-24** with different R groups. In the chromatography, the retention time is the time it takes for a compound to travel through the chromatographic column and reach the detector. Differences in retention times can provide information about the relative polarities or interactions of the compounds with the stationary phase in the column.

Table 9: *Characterizations of cinnamoylated compounds after isomerization with ethane-1,2-diamine(n=2) spacer/linker.*

Entry	Compound	R group	Linker (n)	Isomer	Retention time/min
1	**18a**	**Ph-4-H**	**2**	*Trans*	12.50
2	**18b**	**Ph-4-H**	**2**	*Cis*	11.50
3	**19a**	**Ph-4-OCH_3**	**2**	*Trans*	11.50
4	**19b**	**Ph-4-OCH_3**	**2**	*Cis*	10.50
5	**20a**	**Ph-4-Cl**	**2**	*Trans*	12.00
6	**20b**	**Ph-4-Cl**	**2**	*Cis*	11.50
7	**21a**	**Ph-4-F**	**2**	*Trans*	13.00
8	**21b**	**Ph-4-F**	**2**	*Cis*	11.50
9	**22a**	**Ph-4-NO_2**	**2**	*Trans*	11.50
10	**22b**	**Ph-4-NO_2**	**2**	*Cis*	10.50
11	**23a**	**-C_4H_4O**	**2**	*Trans*	11.00
12	**23b**	**-C_4H_4O**	**2**	*Cis*	9.00
13	**24a**	**-$C_7H_6O_2$**	**2**	*Trans*	11.50
14	**24b**	**-$C_7H_6O_2$**	**2**	*Cis*	10.50

The chromatographs generally revealed that the compounds eluted at retention times ranging from 9 to 13.50 minutes, as shown in **Table 9**. The compounds with the substituent /R group -Cl and -F connected on the para position of the phenyl ring are the most polar of the compounds with the ethane-1,2-diamine linker. This was demonstrated by longer retention times of 13.50 and 13.00, respectively, when compared to **18a, 19a, 22a, 23a, and 24a**. Because chlorine and fluorine are electronegative atoms, their presence increased the overall polarity of compounds **20a** and **21a**. In certain instances, it might increase dipole moments and higher intermolecular forces. Across all compounds, the cis isomers eluted before their trans counterparts. This observation is consistent with previous findings that trans-cinnamic acid has a longer retention time than its cis counterpart.[76,82]

Regarding the elution retention times, the substituents on the phenyl groups of OCH_3, NO_2, and $C_7H_6O_2$ on compounds **19a, 22a, and 24a** displayed intriguing patterns since they displayed the same retention times on both trans and cis isomers (11.50 and 10.50 minutes). The subtle interaction between the electronegativity and the electron-donating or electron-withdrawing characteristics of substituents results in the polarity shift between cis and trans isomers. The arrangement and molecular structure of these substituents can affect the specific effects.

***Table 10**: Characterizations of cinnamoylated compounds after isomerization with propane-1,3-diamine and propane-1,2-diamine (n=3) spacer/linker.*

Entry	Compound	R group	Linker (n)	Isomer	Retention time/min
1	**25a**	**Ph-4-H**	**3(Branched)**	*Trans*	12.50
2	**25b**	**Ph-4-H**	**3(Branched)**	*Cis*	11.50
3	**26a**	**Ph-4-Cl**	**3(Branched)**	*Trans*	14.00
4	**26b**	**Ph-4-Cl**	**3(Branched)**	*Cis*	12.00
5	**27a**	**-OCH_3**	**3(Branched)**	*Trans*	11.50
6	**27b**	**-OCH_3**	**3(Branched)**	*Cis*	9.50
7	**28a**	**Ph-4-H**	**3**	*Trans*	11.50
8	**28b**	**Ph-4-H**	**3**	*Cis*	10.00
9	**29a**	**-OCH_3**	**3**	*Trans*	13.50
10	**29b**	**-OCH_3**	**3**	*Cis*	12.00

Compounds **28a** and **28b** (n=3, R=Ph-4-H) had a retention time of 11.50 minutes and 10.00 minutes, respectively, while compounds **25a** and **25b** had a retention time of 12.50 and 11.50 minutes, respectively. The *trans* and *cis* isomers differ by 1.5 and 1 minute, respectively. The difference in this compound is due to a change in the diamine linker, which on **25a** contains methyl on position 2 of the chain, causing the linker to be branched. Because hydrogen is a nonpolar element, its presence did not affect the polarity of the cis and trans isomers. Hydrogen's effect on polarity is probably less than that of the other substituents (Cl and OCH_3). Once more, the electronegative atom chlorine demonstrated its ability to increase the polarity of these compounds, with **26a**

exhibiting the highest RT value (14.00 min). In general, the presence of chlorine in a molecule increases polarity.

***Table 11**: Characterizations of cinnamoylated compounds after isomerization with Hexane-1,6-diamine (n=6) spacer/linker.*

Entry	Compound	R group	Linker (n)	Isomer	Retention time/min
1	30a	Ph-4-H	6	*Trans*	13.50
2	30b	Ph-4-H	6	*Cis*	12.00
3	31a	Ph-OCH_3	6	*Trans*	12.00
4	31b	Ph-OCH_3	6	*Cis*	9.50
5	32a	Ph-4-Cl	6	*Trans*	14.00
6	32b	Ph-4-Cl	6	*Cis*	9.50
7	33a	Ph-4-F	6	*Trans*	13.50
8	33b	Ph-4-F	6	*Cis*	12.00
9	34a	Ph-4-NO_2	6	*Trans*	14.00
10	34b	Ph-4-NO_2	6	*Cis*	9.50
11	35a	-C_4H_4O	6	*Trans*	12.00
12	35b	-C_4H_4O	6	*Cis*	9.50
13	36a	-$C_7H_6O_2$	6	*Trans*	12.50
14	36b	-$C_7H_6O_2$	6	*Cis*	9.50

The retention time of compounds **30a** and **30b** (n=6, R=Ph-4-H) is 13.50 and 12.00 minutes, respectively. As the length of the chain increases, so does the retention time. In both trans and cis isomers, compounds **32a** and **34a** have the same RT (14.00 and 9.50 min). According to this data, the length of the alkyl chain (n) appeared to affect the polarity of these compounds, with shorter chained compounds being less polar than longer chained compounds. This conclusion is based on the observation that shorter chain compounds eluted earlier (have shorter retention times) than their longer chain counterparts, which is consistent with the general trend in chromatography in which less polar compounds move through the column more quickly.

To summarize, chromatographic behaviour is intricately linked to compound molecular structure. The observed retention time differences are influenced by substitute type, alkyl chain length, branching, and isomerism. The polarity of the compounds is

significantly influenced by the nature of the substituent attached to the phenyl ring. For example, the presence of electron-withdrawing groups such as Cl, NO_2, and F (compounds **20a, 20b, 22a, 22b, 26a, 26b, 28a, 28b, 31a, 31b, 33a, 33b**) generally results in increased polarity, thus longer retention times. In contrast, substituents such as OCH_3, as found in compounds (**18a, 18b, 25a, 25b, 27a, 27b**) appear to reduce polarity.

Longer alkyl chains have longer retention times, implying increased polarity, i.e., from n=2 to n=6. The polarity switching associated with geometrical isomerization was confirmed by the elution of the newly formed cis isomer at a shorter retention time than the trans isomer. Furthermore, the length of the alkyl covalent linkers (2-carbon and 6-carbon chains) that fused the pharmacophoric units, 4,7-dichloroquinoline, and cinnamic acid played a role in isomerization and helped to identify or establish their polarity. For instance, compounds **30a**-**36a** would be identified as increased lipophilic compounds due to their longer alkyl chain linker that resulted in longer retention times for both isomers than their shorter alkyl linked compounds (**18a-29a**). This data provides valuable insights for chromatographic analysis, aiding in identifying, separating, and characterizing compounds in analytical chemistry studies.

3.4. Proton NMR measurements

For each hour interval, an aliquot was collected and reduced to dryness under vacuum. The solid samples were dissolved in DMSO-d_6 and ^{1}H NMR spectra were run on a Bruker Advance 400 MHz.

3.4.1 ^{1}H NMR measurement of the trans–cis mixtures of photoisomerized of cinnamic acid/chloroquinoline analogues

The use of NMR spectroscopy in this study serves as a powerful tool, allowing for precise characterization of the isomeric changes and shedding light on the mechanistic complexities underlying the photoisomerization process. The photoisomerization of chloroquinoline-cinnamic acid analogues were validated by the measurement of the transformation of trans to cis isomers using ^{1}H NMR.

The examination of UV irradiated samples with thin layer chromatography was ineffective because both isomers demonstrated the same relative mobility on silica gel with several eluent systems. Therefore ^{1}H NMR spectroscopy was used to monitor the progress of isomerization. Aliquots were taken periodically before and after the

irradiation (2-hour intervals, indicated as t = 0, t = 1, t = 3 and t = 5) and the spectra (**Figure 31**) display the progression of the photochemically induced isomerization.

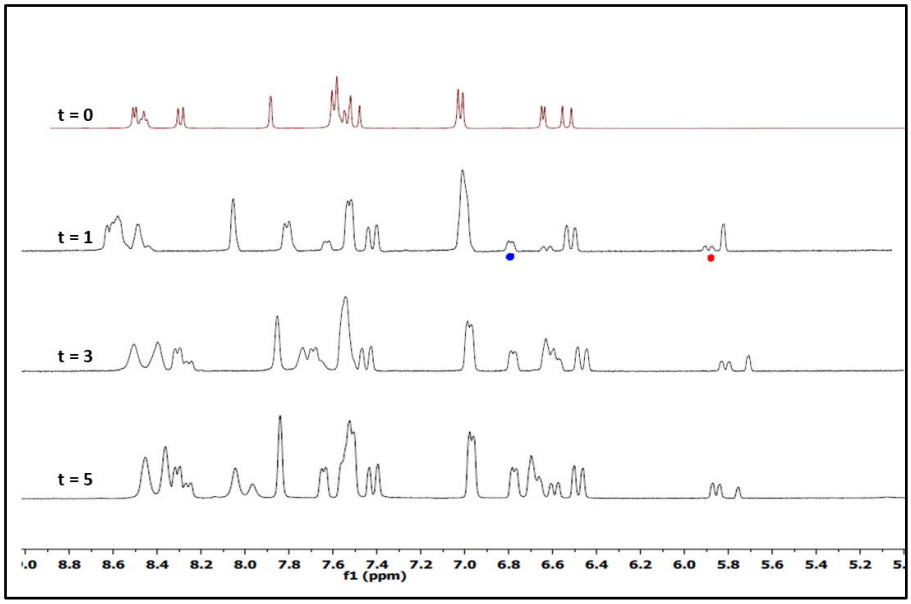

Figure 28: *Time (t) course study of the photoisomerization of* ***19a/19b*** *as monitored by 400 MHz* ^{1}*H NMR spectroscopy.*

The time-course study demonstrated the conversion of the trans isomer to the emergence of cis isomer. This was evidenced by the gradual appearance of mixtures of both trans and cis representative signals. A doublet signal at δ 6.46 ppm with a coupling constant of 15.7 Hz was identified for the trans isomer at t = 0. The new olefinic proton double indicating the presence of cis isomer appeared more upfield at δ 5.82 ppm with a coupling constant of 12.1 Hz. The coupling constant of the trans isomer is higher than the cis isomer because the C-H bond is parallel, so orbital overlap is greater. The results are consistent with the reported chemical shifts and coupling constants of cis-trans isomers observed elsewhere.[83–85]

The plots in **Figure 32** highlight the olefinic proton region of interest, a cis isomer at (5.82 ppm, *J*=12.1 Hz) and trans isomer peak (6.46 ppm, *J*= 15.7 *Hz*). The peak height of both cis and trans signals could allow the determination of the relative amounts of these two materials. Although after several hours of exposure to the UV light, the intensity of the trans-isomer does not change much, the cis isomer increases with time.

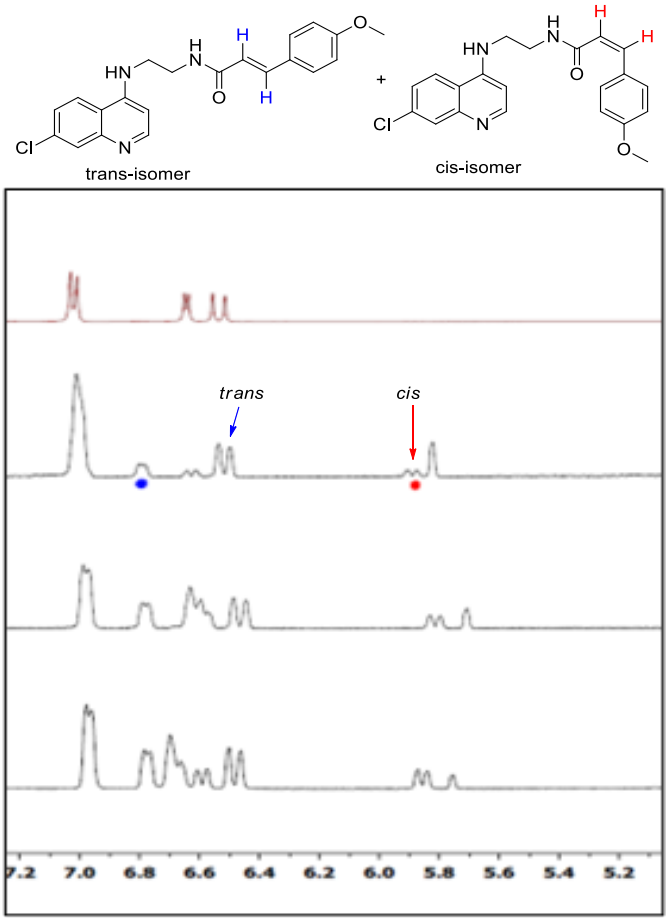

Figure 29: *Time course study demonstrating the appearance of the cis olefinic proton 5.82 ppm.*

The results showed that UV-geometrical isomerization via artificial light exposure is a viable method for increasing the isomerization of synthetic compounds. Moreover, this method is portrayed as advantageous because it does not alter the natural molecule, which may affect absorption across lipophilic cell membranes through simple passive processes. The UHPLC-QTOF-MS chromatographs analysis demonstrated how cinnamic acids influence the polarity of their conjugated compounds. The results demonstrated a commendable approach to the development of new chloroquinoline analogues that can counteract malaria resistance due to their ease of synthesis, high recovery yields, and photo isomerism properties with more polar geometrical isomers.

CHAPTER 4

ANTIPLASMODIAL ACTIVITES OF CINNAMOYL-CHLOROQUINE HYBRIDS

4.1 ANTIPLASMODIAL ACTIVITIES

4.1.1. Introduction

The rise in malaria cases is linked to various factors such as the emergence and spread of drug-resistant parasites. It is crucial to find new approaches to fight the disease since affordable drugs that are on the market today are becoming less effective.[86] Current efforts are focused on discovering and developing hybrid antimalarial drugs.

In line with one of the aims of this project, new cinnamoyl chloroquinoline hybrids synthesized in this work were submitted for antiplasmodial screening at University of Cape Town's H3D labs. The *trans* analogues **18-36** together with their respective mixtures with *cis* isomers (due to irradiation) **18a-36a** were evaluated for their antiplasmodial activities.

The test samples were performed at 2 µM concentration over 72 hours against the wild-type drug sensitive strain (Nf54) and K1 resistant strain of the human malaria parasite *Plasmodium falciparum*.

4.2. Method

Continuous cultures of asexual erythrocyte stages of *P. falciparum* were maintained using the method described by Trager and Jensen (1976)[87] with minor modifications. Quantitative assessment of antiplasmodial activity in vitro was determined via the parasite lactate dehydrogenase assay using the method described by Makler et al (1993),[88] in which parasite viability is determined colourimetrically using the breakdown of a dye by metabolic enzymes of the glycolytic pathway taking place in living parasites as a marker for survival.

The test samples were prepared to a 10 mmol/L stock solution in 100% DMSO. Samples were tested as a suspension if not completely dissolved. Further dilutions to the desired starting concentration were freshly prepared in growth media on each occasion of the experiment. The standard antimalarial drugs chloroquine (CQ was used as the reference drug in all experiments. All compounds were tested for IC_{50} in a 96-well plate to determine the efficacy at 2 µM concentration. The same dilution technique was used for all samples. Chloroquine was tested from a starting

concentration of 1 µg/mL. The highest concentration of solvent to which the parasites were exposed was <0.5% and has no measurable effect on the parasite viability.

The assay plate was incubated at 37 ˚C for 72 h in a sealed gas chamber under 3% O_2 and 4% CO_2 with the balance being N_2. After 72 h, the wells in the assay plate were gently resuspended, and 15nL from each well was transferred to a duplicate plate containing 80nL of Malstat reagent and 20 nL of nitro blue tetrazolium solution in each well. Plates were left to develop for 20 minutes in the dark and then absorbance of each well was quantified using a spectrophotometer at 620nM wavelength.

The remaining population of parasites at 2 µM concentration of the test compound was determined by comparing the absorbance of each well to the absorbance of a well containing the drug-free control.

4.3. Results and discussion

The activities of these compounds were influenced by various factors such as modifications of the chain length of the linker and the specific R groups attached to the cinnamoyl moiety. The analogues hybridized two known pharmacological scaffolds (dichloroquinoline and cinnamic acid) into one compound with the aim of getting better activity from their individual drugs. These modifications can affect their pharmacological properties, including their ability to inhibit the growth of the malaria parasite.

4.3.1 Evaluation of antiplasmodial activities of compounds 18-36.

Tables 12, 13 and **14** provide information on the antiplasmodial activities of various compounds against the chloroquine sensitive (NF54) and resistant (K1) strains of the parasite. The compounds are characterized by different R groups and chain lengths.

- R group represents the substituent on the cinnamoyl moiety. Chain length refers to the length of the alkyl chain attached to the quinoline ring and cinnamoyl moiety.
- The IC_{50} values are the inhibitory concentration required for 50% growth inhibition. The lower IC_{50} values suggest a better antiplasmodial activity.

- The Resistance Index (RI) gives an indication of how well the compounds perform against the resistant strain compared to the sensitive strain. It is a measure of the compound's effectiveness against the resistant strain (K1) relative to the sensitive strain (NF54) and is calculated as a ratio of the K1 result to the NF54 result.
- A resistance index closer to 1.5 signifies equal potency against both NF54 and K1 strains, whereas a value below 1.5 indicates greater efficacy against the CQ-resistant strain than the CQ-sensitive strain. If the resistance index is above 1.5, it suggests that the compound being used is less effective against the CQ-resistant strain than the CQ-sensitive strain.
- In all experiments, the standard antimalarial drug chloroquine (CQ) was used as the reference, with IC50 values of 0.006 µM for the NF54 strain and 0.178 µM for the K1 strain.

4.3.1.1 Antiplasmodial activities of compounds with alkyl carbon chain linker (n=2) (18-26) against sensitive Strain (NF54) and *resistant strain (K1).*

Table 12 exhibits the antiplasmodial activities of compounds **18-26** against both the sensitive strain (NF54) and the resistant strain (K1) of *Plasmodium falciparum*. Generally, compounds containing the Ph-4-OCH_3, Ph-4-Cl, and Ph-4-H groups showed strong antiplasmodial activity against both sensitive and resistant strains Compounds **18-24**, linked by an ethane-1,2-diamine linker, showed different levels of antiplasmodial activity against NF54 and K1 strains. Compound **26** and its isomer **26i** showed higher potency against both strains, with IC_{50} values of 0.032 µM, comparable to CQ (0.006 µM) on the sensitive strain but more potent to CQ against chloroquine-resistant (CQR) strain with an IC_{50} of 0.044 µM. Compound **19**, with *p*-methoxy group, amongst compounds with propane-1,2-diamine linker exhibited better activities with of 0.086 µM and 0.090 µM against NF54 and K1, respectively.

A branched linker in this series appears to improve antiplasmodial activity, as evidenced by compound **26** (NF54: 0.032 µM and K1: 0.044 µM) exhibiting greater activity than compound 20 (NF54: 0.534 µM and K1: 0.108 µM). Notably, compound **20** with a Ph-4-Cl R group demonstrates substantial activity against the sensitive NF54 strain with an IC_{50} of 0.534 µM, but even more impressively, it exhibits a very low IC_{50}

of 0.108 µM against the resistant K1 strain, suggesting potential efficacy in overcoming resistance. Compound **18**, containing a Ph-4-H group, exhibits promising antiplasmodial activity against both NF54 and K1 strains, with IC_{50} values of 0.129 µM and 0.165 µM, respectively. The Mixture of trans/cis isomers **20c** and **22e**, which are isomers of **20** and **22**, shows equal efficacy with lower IC_{50} of 0.052 µM against K1, indicating enhanced efficacy. Notably, several compounds displayed lower IC_{50} values than chloroquine against the resistant strain, indicating potential efficacy. Many compounds displayed lower IC_{50} values against the K1 strain than chloroquine, suggesting possible efficacy against resistant strains.

Compound **20** shows a RI of 0.420, suggesting higher potency against the resistant strain than the sensitive strain. Similarly, compounds **20c** and **23** exhibit RIs of 0.182 and 0.370, respectively, indicating improved efficacy against the resistant strain. On the other hand, compounds **21d** and **22** show higher RIs than 1.5, indicating lower effectiveness against the resistant strain in comparison to the sensitive strain.

Table 12**: Antiplasmodial activities of cinnamoyl chloroquinoline hybrids **(18-26).

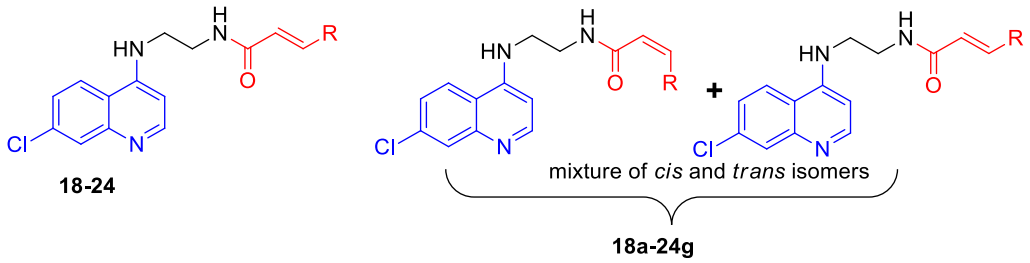

Compound	R group	Chain length	IC_{50} (µM)		Resistance index (RI)
			Sensitive strain (NF54)	Resistant strain (K1)	
CQ			0,006	0,178	29,598
18	Ph-4-H	2	0,129	0,165	1,281
18a	Ph-4-H	2	0,284	0,372	1,307
19	Ph-4-OCH_3	2	0,086	0,090	1,046
19b	Ph-4-OCH_3	2	0,474	0,199	0,420
20	Ph-4-Cl	2	0,534	0,108	0,203
20c	Ph-4-Cl	2	0,285	0,052	0,182
21	Ph-4-F	2	0,193	0,137	0,711

21d	Ph-4-F	2	0,059	0,161	2,716
22	Ph-4-NO_2	2	0,261	0,405	1,554
22e	Ph-4-NO_2	2	0,040	0,052	1,317
23	Furan	2	0,153	0,057	0,370
23f	Furan	2	0,288	0,271	0,942
24	benzo[d][1,3]dioxole	2	0,323	0,238	0,736
24g	benzo[d][1,3]dioxole	2	0,101	0,099	0,974
Propane-1,2-diamine linker 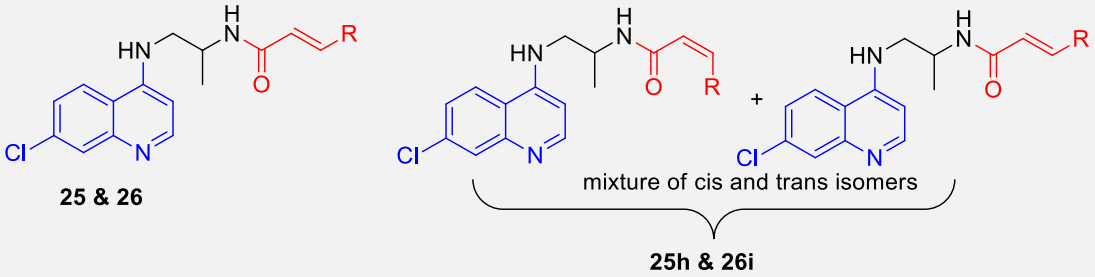					
25	Ph-4-H	2	0,281	0,296	1,053
25h	Ph-4-H	2	0,157	0,171	1,091
26	Ph-4-Cl	2	0,032	0,044	1,386
26i	Ph-4-Cl	2	0,107	0,118	1,096

4.3.1.2 Antiplasmodial activities of compounds with alkyl carbon chain linker (n=3) (28 and 29) against sensitive (NF54) and resistant Strain (K1).

The antiplasmodial activities of compounds **28-29** against the sensitive strain (NF54) and resistant strain (K1) of *Plasmodium falciparum* are shown in (**Table 13**). Compound **28**, featuring an unsubstituted benzyl group (Ph-4-H), exhibited higher activity than **29** with IC_{50} values of 0.086 µM for the NF54 strain and 0.100 µM for the K1 strain. By contrast, compound **28a**, a mixture of *trans/cis* isomers with identical substituents, exhibited higher IC_{50} values of 0.215 µM for NF54 and 0.338 µM for K1, indicating decreased antiplasmodial activity. Compound **29**, which has a phenyl group with a 4-methoxy substituent, showed lower activity with IC_{50} values of 0.117 µM for NF54 and 0.574 µM for K1. Similarly, compound **29b**, a mixture of *trans/cis* isomers with a 4-methoxy (4-OCH_3) substituent, showed IC_{50} values of 0.113 µM for NF54 and 0.174 µM for K1. When comparing the results, it is evident that compounds **28** and **28a** showed relatively lower IC_{50} values against both strains, indicating their potential as effective antimalarial agents. Compound **29** showed higher resistance index of

4.928, this indicates a significant decrease in activity compared to the control drug (CQ).

***Table 13**: Antiplasmodial activities of cinnamoylated chloroquinoline **28** and **29**.*

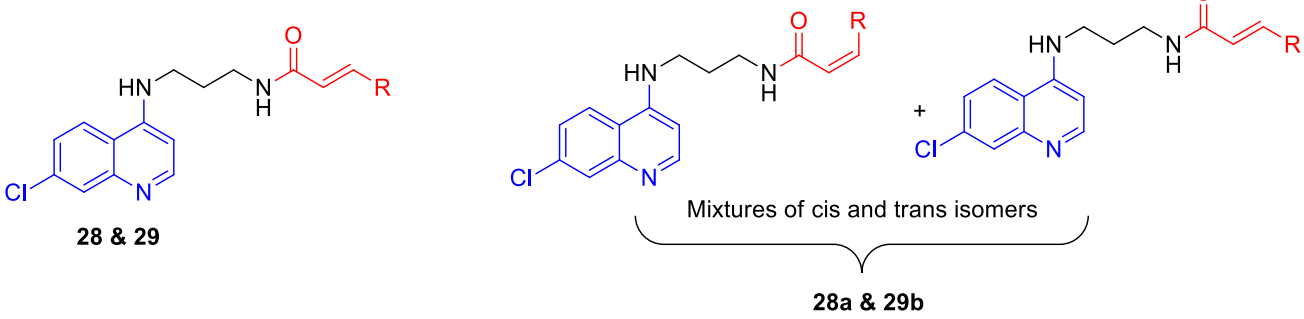

			IC_{50}(µM)		
Compound	**R group**	**Chain length**	**Sensitive strain (NF54)**	**Resistant strain (K1)**	**Resistance index (RI)**
CQ			0,006	0,178	29,598
28	Ph-4-H	3	0,086	0,100	1,172
28a	Ph-4-H	3	0,215	0,338	1,574
29	Ph-4-OCH_3	3	0,117	0,574	4,928
29b	Ph-4-OCH_3	3	0,113	0,174	1,541

4.3.1.3 Antiplasmodial activities of compounds with alkyl carbon chain linker (n=6) (30-36) against sensitive strain (NF54) and resistant Strain (K1).

Generally, looking at the extended carbon chain linker. It was discovered that the analogues of this series were showing high potency (**Table 14**). Notably, compounds **32**, **34** and **35** were the most active of the compounds of this series with IC_{50} values of 0.012 µM, 0.036 µM and 0.037 µM, respectively. Furthermore, with the same analogues it was seen that the mixtures of both isomers (**32c**, **34e** and **35f**) also exhibited good potency against the CQ sensitive (NF54) strain. Both **32**, **34** and **35** showed better activity than chloroquine with IC_{50} 0.009 µM, 0.043 µM and 0.090 µM respectively against the CQ-resistant strain (K1). This demonstrates that the chloroquine (IC_{50}: 0.178 µM) is more resistant than these compounds.

However, some compounds displayed higher IC_{50} values, indicating reduced efficacy. For instance, compound **33d**, with a fluorine substituent on the pazra position of the phenyl, demonstrated an IC_{50} value of 0.051 µM against NF54 but a significantly higher value of 0.242 uM against K1 compared to 0.178 µM of chloroquine (CQ). This indicates that the presence of a fluorine group has a negative impact on the two strains. Compounds **33d** and **35** exhibited resistance indices of 4.700 and 2.424, respectively, indicating less potency against the chloroquine-resistant strain. The control drug chloroquine (CQ) showed a resistance index of 29.598, suggesting resistance of p.falciparum to chloroquine.

Compounds **35** and **36** with furan and benzo[d][1,3]dioxole moieties, respectively, showed promising antiplasmodial activities. However, the furan-containing compound **35** had a lower IC_{50} against both strains compared to the benzo[d][1,3]dioxole-containing compound **36**. This suggests that the specific chemical structure of the aromatic ring attached to the alkyl carbon chain may influence the antiplasmodial activity.

***Table 14**: Antiplasmodial activities of cinnamoylated chloroquinoline **30-36**.*

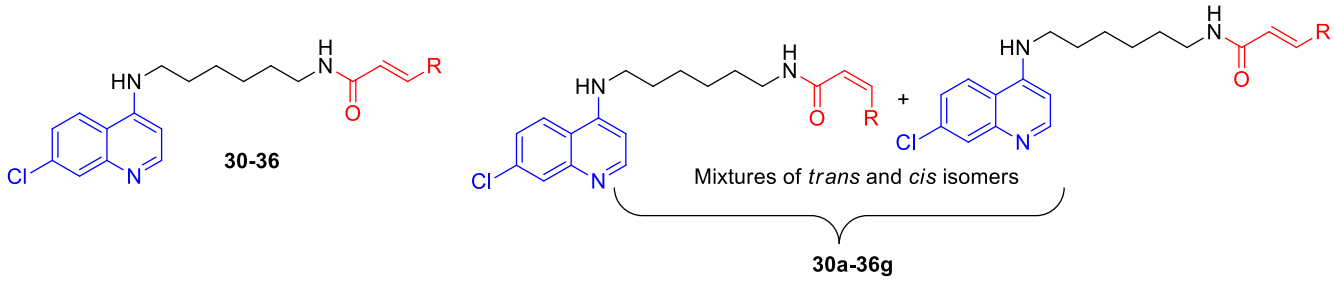

			IC_{50} (µM)		
Compound	**R group**	**Chain length**	**Sensitive strain (NF54)**	**Resistant strain (K1)**	**Resistance index (RI)**
CQ			0,006	0,178	29,598
30	Ph-4-H	6	0,172	0,069	0,403
30a	Ph-4-H	6	0,269	0,151	0,563
31	Ph-4-OCH_3	6	0,113	0,125	1,104
31b	Ph-4-OCH_3	6	0,119	0,110	0,927

32	Ph-4-Cl	6	0,012	0,009	0,717
32c	Ph-4-Cl	6	0,074	0,061	0,829
33	Ph-4-F	6	0,168	0,199	1,189
33d	Ph-4-F	6	0,051	0,242	4,700
34	Ph-4-NO_2	6	0,036	0,043	1,216
34e	Ph-4-NO_2	6	0,036	0,065	1,812
35	Furan	6	0,037	0,090	2,424
35f	Furan	6	0,015	0,020	1,291
36	benzo[d][1,3]dioxole	6	0,101	0,095	0,934
36g	benzo[d][1,3]dioxole	6	0,117	0,097	0,830

4.4 Summary and Conclusion

In summary, the study investigated the antiplasmodial activities of cinnamoyl chloroquinoline hybrids with alkyl carbon chain linkers of different lengths (n=2, n=3, and n=6) against both sensitive (NF54) and resistant (K1) strains of *Plasmodium falciparum*. Compounds **18-26** with a chain length of 2 exhibited promising results, with some analogues displaying lower IC_{50} values lower than chloroquine against the resistant strain, suggesting potential efficacy. Compounds with branched linkers, such as compound **26**, showed improved antiplasmodial activity compared to linear counterparts like compound **20**. Compounds **28** and **28a**, with a chain length of 3, demonstrated potential effectiveness, while compound **29** exhibited a higher resistance index, indicating reduced activity against the resistant strain. Compounds **30-36** with a chain length of 6 showed overall high potency, with compounds **32**, **34**, and **35** being the most active.

Most of the compounds showed higher activity against the CQ-resistant (K1) strain compared to the CQ-sensitive (NF54) strain. Compounds from the n=2, 3, and 6 series with various substituents exhibited high activity against the CQ-resistant strain as compared to CQ, with exception of compounds **22**, **24**, **25**, **28a**, **29**, **33,** and **33d**. Compound **18-36** were compared, revealing that a hexyl linker is more favourable than ethyl and propyl linkers for better antiplasmodial activity.

The impact of the R groups was analysed, revealing that for compounds with a chain length of n=2, the activity followed a specific order: OCH_3>

H>furan>F>NO_2>benzo[d][1,3]dioxole>Cl .Surprisingly, the order changed significantly when the carbon chain extended to n=6, revealing the following trend: Cl>NO2>Furan>benzo[d][1,3]dioxole>OCH3>F>H. This emphasized the importance of the linker, facilitating in the development of potent antimalarial hybrid compounds to combat drug resistance. Compounds with branched alkyl carbon chains exhibited higher activity in the presence of chlorine compared to those with simple linear alkyl carbon chain.

The study showed that the mixtures containing cis and trans isomers were generally more effective in some compounds than the original trans cinnamoyl-chloroquine hybrids. This indicates that the isomerization process improved the pharmacological properties of the compounds. The increased activities seen in the mixtures may be due to the unique characteristics of cis isomers. These isomers frequently exhibit unique biological activity compared to their trans counterparts due to differences in their spatial configurations. Thus, these results show how the isomerization concept could be a powerful new tool in the fight against drug resistance and used as “smart drugs”.

These findings contribute valuable insights into these hybrid compounds, laying the groundwork for potential development of more effective antimalarial agents. Further research may delve into optimizing these structures for excellent efficacy and reduced resistance. It is important to note that these conclusions are based on *in vitro* assay, and additional assays and studies would be necessary for a comprehensive evaluation of the antiplasmodial potential of these compounds.

CHAPTER 5

CONCLUSION AND FUTURE WORK

5. CONCLUSION

This chapter looks at the general conclusion of this MSc project. This project explored a series of cinnamoyl-chloroquine hybrids. The chemistry, photoisomerization and antiplasmodial activities of the target synthesized compounds were well studied and gave interesting results.

5.1 Synthesis of cinnamoyl-chloroquine hybrids

Three series of nineteen hybrid cinnamoyl chloroquinoline hybrids **18-36** were successfully synthesized by employing known conventional methods. These compounds were variously modified at different positions as outlined in the aims section representing diversity of substitution.

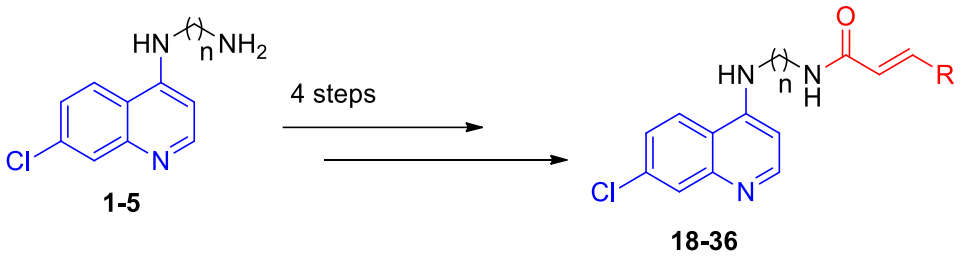

***Scheme 14**: A general synthesis of cinnamoylated chloroquinoline hybrids.*

Four steps were followed en route to these compounds **18-36**, with overall yields of 24-74%. The key steps included (i) the nucleophilic (Cl) substitution, (ii) acyl chloride formation and (iii) conjugation reactions. A direct conjugation of cinnamic acids with 4-aminochloroquinolines by coupling agents as reported by *Perez et al* was problematic, hence the option to generate acyl chlorides which were used without further purification. Modifications of a range of carbon chain (with lengths 2-6) linkers as well as different R- groups substituted at the cinnamoyl ring afforded a range of compounds.

5.2 Photoisomerization

Cinnamoyl chloroquinoline hybrids have characteristics of being photo-pharmacological agents. These characteristics are brought by olefinic protons in the cinnamic acid moiety. These types of compounds have photoactive group that when light is absorbed at a desired wavelength, the molecular structure is reorganized into a different isomer.

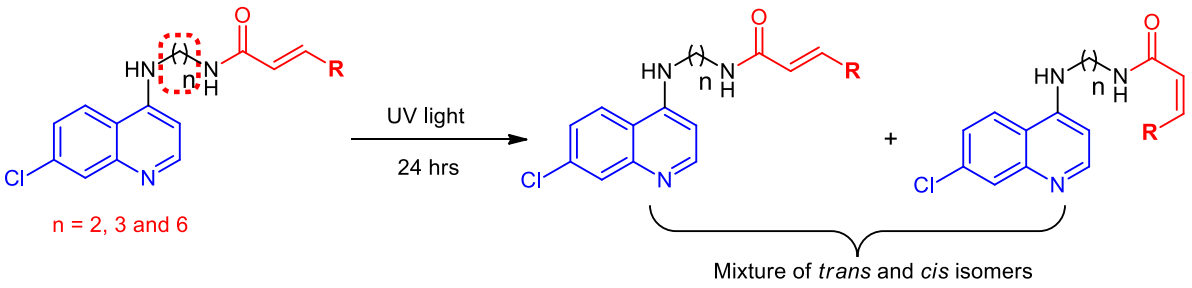

***Scheme 15**: Schematic representation showing both trans and cis structures after UV irradiation.*

Through chromatographic mass spectrometry (LC-MS), these isomers have been shown to result in a remarkable polarity change. When compounds **18-36** were subjected to UV-induced photoisomerization for 24 hours, LC-Q-TOF-MS/MS analyses of the photo-products revealed the emergence of *cis* isomer which eluted before its synthesized *trans* counterpart, suggesting a reduced polarity. The polarity of the compounds was significantly influenced by the nature of the substituent attached to the phenyl ring. For example, the presence of electron-withdrawing groups such as Cl, NO_2, and F resulted in increased polarity as exhibited in compounds **20a, 20b, 22a, 22b, 26a, 26b, 28a, 28b, 31a, 31b, 33a** and **33b**. In contrast, electron donating group OCH_3, as found in compounds (**18a, 18b, 25a, 25b, 27a, 27b**) appeared to reduce polarity. The concept of photoisomerization of cinnamoyl chloroquinoline hybrids were virtually validated by the measurement of the transformation of trans to cis isomers using ^1H NMR.

5.3 Antiplasmodial activities

The project investigated the antiplasmodial activities of the synthesized compounds against wild-type drug-sensitive strain (NF54) and multidrug-resistant strain (K1) of the human malaria parasite *Plasmodium falciparum*. It was found that most of the compounds with longer alkyl carbon chain linker had higher the antiplasmodial activity than their counterparts with shorter carbon chain. Most of the test compounds showed higher activity against the CQ-resistant (K1) strain compared to the CQ-sensitive (NF54) strain. Remarkably, the activity of compound **32** (9 nM) was more potent than the activity of 11 nM of compound **C6-c** that was obtained by *Perez et al* [67] against the chloroquine resistant malaria strain (K1).

5.4 Overall conclusion of the project

In conclusion, this MSc project successfully synthesized and characterized nineteen cinnamoyl-chloroquine hybrids. The study explored photoisomerization characteristics and identified them as potential photo-pharmacological agents. The compounds showed significant polarity changes upon UV-induced photoisomerization, and their antiplasmodial activities were investigated against drug-sensitive (NF54) and multidrug-resistant (K1) Plasmodium falciparum strains. Compounds with longer alkyl carbon chain linkers showed higher antiplasmodial activity and hexyl linker is more favourable than ethyl and propyl linkers for higher antiplasmodial activity. The findings provide valuable insights for further research.

5.5 Future work

The future work of this project aims to further investigate the isomerization process and its impact on the biological activities of cinnamoyl-chloroquine hybrids. The focus will be on isolating and characterizing individual *trans* and *cis* isomers to find out which one of the two isomers would exhibit better antiplasmodial activity than the other. Advanced analytical techniques for separation, purification and characterization, such as preparative high-performance liquid chromatography (p-HPLC) and nuclear magnetic resonance (NMR) spectroscopy will be used. Furthermore, selected compounds will be used to conduct *in vivo* experiments to assess the compounds' efficacy and safety in a whole organism.

CHAPTER 6

EXPERIMENTAL

6.1 General Information

Reactions were performed using conventional methods. All reagents and solvents were used as received without further purification. Chemicals and solvents used in this project were purchased from chemical suppliers like Merck and Sigma Aldrich. Toluene and anhydrous dichloromethane (DCM) were freshly distilled and stored over 4Å molecular sieves.

A Bruker Optics 7.0 Alpha Fourier transformed Infrared (FTIR) spectrophotometer was used to study the functional group and chemical structure of the materials. The absorptions were reported using the wavenumber scale in the 500-4000 cm^{-1} range. Proton nuclear magnetic resonance (^{1}H NMR; 400 MHz) and carbon nuclear magnetic resonance (^{13}C NMR; 101MHz) spectra were recorded in dimethyl sulfoxide (DMSO-d_6) on Bruker spectrometer. Chemical shifts were reported in a δ scale in ppm and proton peaks were presented in the following order of multiplicity; s=singlet, d = doublet, t=triplet, q=quartet, quin=quintet, sept=septet, dd = doublet of doublets, dt = doublet of triplets, m=multiplet, and br=broad signal. All melting points of synthesized compounds were determined by Electrothermal 9200 Büchi LABOTEC melting point (M-560) using capillary tubes.

Merck Silica gel 60 (particle size 0.063-0.200 mm) was used as the adsorbent for conventional column chromatography, with a silica to compound ratio of 30:1 by mass. The silica was packed into a suitable size column and products were purified by elution process, using suitable solvent ratio mixtures. An analytical thin-layer chromatography (TLC) pre-coated with silica gel 60F254 aluminum plates (Merck) was performed to monitor reactions and to ensure separation of compounds after column and flash chromatography. Spectroline American UV (E NF-240C/FE) with maximum (230V and 0.17A) was used for detection of compounds at 254 nm A 2013 Buchi Rotary Evaporator (B-491) with 1700W power and 220-240 Hz volts was used for removal of solvents and purification of some solvents via distillation process. The compounds prepared were named in the following experimental sections according to IUPAC systematic nomenclature using Chem Draw ultra 2010 Cambridge software version 12.0.0.

UV irradiation

Cinnamoyl chloroquinoline hybrids (**18**-**36**) were dissolved in ethanol inside centrifuge tubes. The solution of cinnamoyl chloroquinoline hybrids was placed in a Spectroline UV lamp operating at 245 nm with an intensity of 390 µW/cm^2. UV irradiation was conducted for 24 h, and aliquots (100 µL) were taken at 24 h post irradiation. UV treated samples were filtered in amber vials and subjected to UHPLC-QTOF-MS.

MS/MS experiments

Tandem MS (MS/MS) experiments, typical mass accuracies with a mass error below 1 ppm was obtained using a mass calibration solution of sodium iodide (NaI). High resolution was obtained for MS and (MS/ MS) experiments using a mass-to-ratio (m/z) range of 100-1000. Argon gas was used as a collision gas for (MS/MS) experiments along with MSE mode using collision energy ramp of 12 eV to 25 eV for generation of fragments.

6.2 Experimental Details

6.2.1 General synthesis of the amination of 4,7-dichloroquinoline

A mixture of 4,7-dichloroquinoline (1 equiv.) and diaminoalkane (5 equiv.) was heated slowly from room temperature to 80 °C for 1 h while stirring under inert atmosphere and thereafter the temperature was increased to 165 °C for 8 h with continued stirring to drive the reaction to completion. The reaction mixture was cooled to room temperature and taken up in dichloromethane. The organic layer was successively washed with 5% aq $NaHCO_3$ followed by water wash and then finally with brine. The organic extract was dried over anhydrous Na_2SO_4, filtered and concentrated under reduced pressure. The products were used further without purifications. Following this general method, the following compounds were synthesized.[89]

6.2.1.1. Synthesis of N-(7- Chloroquinoline-4-yl) ethyl-diamine (1)

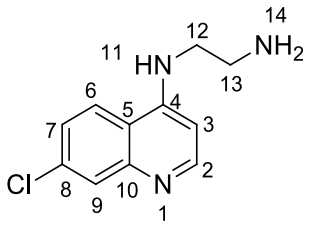

1

4.7-dichloroquinoline (1.05 g, 5.30 mmol) and 1,2-ethanediamine (3.06 g, 3.54 ml, 53.01 mmol**)** afforded **1** as yellow solid (0.27 g, 23%).

^{1}H NMR (400 MHZ, DMSO-d$_6$) δ 8.37 (d, *J* = 5.4 Hz, 1H, H-2), 8.27 (d, *J* = 9.0 Hz, 1H, H-6), 7.78 (d, *J* = 2.2 Hz, 1H, H-9), 7.43 (dd, *J* = 9.0, 2.2 Hz, 1H, H-7), 7.28 (br t, 1H, NH-11), 6.49 (d, *J* = 5.5 Hz, 1H, H-3), 3.38 (br s, 2H, NH_2-14), 3.26 (dd, *J* = 11.6, 6.2 Hz, 1H, H-12), 2.81 (t, *J* = 6.5 Hz, 1H, H-13). **^{13}C NMR (101 MHz, DMSO-d$_6$)** δ 152.3 (C-4), 150.8 (C-2), 149.4 (C-10), 133.8 (C-8), 127.81 (C-9), 124.5 (C-6), 124.5 (C-7), 117.8 (C-5), 99.2 (C-3), 46.4 (C-12), 40.5 (C-13).

6.2.1.2. Synthesis of N^1-(7-chloroquinolin-4-yl) propane-1,3-diamine (2)

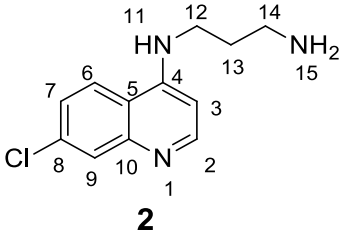

2

4.7-dichloroquinoline (3.0 g, 15.10 mmol) and 1,3-propanediamine (6.64 ml, 5 equiv., 75,50 mmol) afforded **2** as yellow solid (3.16 g, 89%).

^{1}H NMR (400 MHz, DMSO-d$_6$) δ 8.38 (d, *J* = 5.5 Hz, 1H, H-2), 8.24 (d, *J* = 9.0 Hz, 1H, H-6), 7.78 (d, *J* = 1.6 Hz, 1H, H-9), 7.67 – 7.48 (m, 1H, NH-11), 7.42 (dd, *J* = 8.9, 2.0 Hz, 1H, H-7), 6.45 (d, *J* = 5.4 Hz, 1H, H-3), 3.31 (t, *J* = 6.8 Hz, 2H, H-12), 2.99 (br s, 2H, NH_2-15), 2.68 (t, *J* = 6.5 Hz, 2H, H-14), 1.79 – 1.65 (m, 2H, H-13). **^{13}C NMR (101 MHz, DMSO-d$_6$)** δ 152.4 (C-4), 150.6 (C-2), 149.5 (C-10), 133.8 (C-8), 127.9 (C-9), 124.5 (C-6), 124.4 (C-7), 117.9 (C-5), 99.0 (C-3), 41.07 (C-12), 39.3 (C-14), 31.5 (C-13).

6.2.1.3. Synthesis of N^1-(7-chloroquinolin-4-yl) propane-1,2-diamine (3)

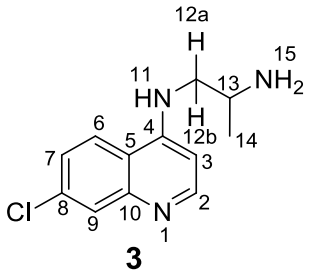

3

4.7-dichloroquinoline (4.0 g, 20.20 mmol) and propane-1,2-diamine (7.74 ml, 4,5 equiv., 90.90 mmol) afforded **3** as a yellow solid (3.52g, 74%).

^{1}H NMR (400 MHz, DMSO) δ 8.37 (d, *J* = 5.4 Hz, 1H, H-2), 8.30 (d, *J* = 9.0 Hz, 1H, H-6), 7.78 (d, *J* = 2.1 Hz, 1H, H-3), 7.43 (dd, *J* = 8.9, 2.1 Hz, 1H, H-7), 7.28 (br s, 1H, NH-11), 6.49 (d, *J* = 5.4 Hz, 1H, H-3), 3.13 (dd, *J* = 9.5, 3.5 Hz, 1H,H-13), 2.78 (dd, *J* = 12.8, 6.0 Hz, 1H, H-12a), 2.64 (dd, *J* = 12.9, 5.9 Hz, 1H, H-12b), 1.20 (br d, *J* = 6.4 Hz, 2H, NH_2-15), 1.06 (d, *J* = 5.6 Hz, 3H, H-14). **^{13}C NMR (101 MHz, DMSO)** δ 151.8 (C-4), 150.3 (C-2), 149.1 (C-10), 133.4 (C-8), 127.5 (C-9), 124.1 (C-6), 123,9 (C-7), 117.4 (C-5), 98.9 (C-3), 51.2 (C-12), 45.1 (C-13), 21.6 (C-14).

6.2.1.4. Synthesis of N^1-(7-chloroquinolin-4-yl)-N3-methylpropane-1,3-diamine (4)

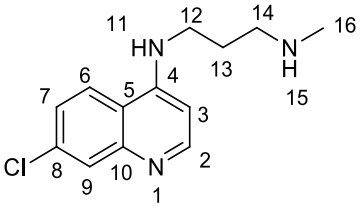

4

4.7-dichloroquinoline (5.0 g, 25.20 mmol) and N^1-methylpropane-1,3-diamine (10.52 mL, 4,5 equiv., 100.80 mmol) afforded **4** as a pale-yellow solid (3.52g, 79%).

^{1}H NMR (400 MHz, DMSO) δ 8.38 (d, *J* = 5.4 Hz, 1H, H-2), 8.20 (d, *J* = 9.0 Hz, 1H, H-6), 7.78 (d, *J* = 1.9 Hz, 1H, H-9), 7.54 (br s, 1H, NH-11), 7.43 (dd, *J* = 8.9, 1.9 Hz, 1H, H-7), 6.44 (d, *J* = 5.5 Hz, 1H, H-3), 3.30 (t, *J* = 6.8 Hz, 2H, H-12), 3.14 (br s, 1H, H-15), 2.58 (t, *J* = 6.5 Hz, 2H, H-14), 2.29 (s, 3H, H-16), 1.78 (quint, *J* = 6.7 Hz, 2H, H-13). **^{13}C NMR (101 MHz, DMSO)** δ 151.9 (C-4), 150.1 (C-2), 149.1 (C-10), 133.3 (C-8), 127.5 (C-9), 123.9 (C-C-6), 123.9 (C-7), 117.5 (C-5), 98.5 (C-3), 49.4 (C-14), 41.1 (C-12), 36.1 (C-16), 27.6 (C-13).

5.1.2.5. Synthesis of N^1-(7-chloroquinolin-4-yl)hexane-1,6-diamine (5)

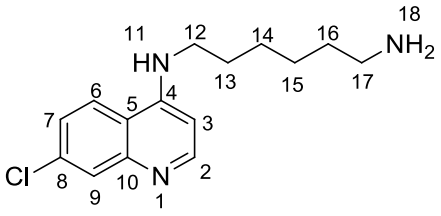

5

4.7-dichloroquinoline (7.61 g, 38.4mmol) and 1,6-hexanediamine (44.66 g, 53.17 mL, 384.32 mmol) afforded **5** as a yellow solid (6.04g, 57%).

^{1}H NMR (400 MHZ, DMSO-d$_6$) δ 8.33 (d, *J* = 5.4 Hz, 1H, H-2), 8.22 (d, *J* = 9.0 Hz, 1H, H-6), 7.74 (d, *J* = 10.6 Hz, 1H, H-9), 7.31 (d, *J* = 9.0 Hz, 1H, H-7), 7.21 (br s, 1H, NH-11), 6.35 (d, *J* = 5.5 Hz, 1H, H-3), 3.26 – 3.17 (m, 1H, H-11), 3.02 (dd, *J* = 12.2, 6.6 Hz, 1H, H-16), 2.54 (dd, *J* = 14.0, 6.9 Hz, 1H, H-15), 1.65 (dd, *J* = 13.7, 6.7 Hz, 1H, H-12), 1.37 (dd, *J* = 12.9, 6.5 Hz, 1H, H-13), 1.28 – 1.16 (m, 1H, H-14). **^{13}C NMR (101 MHz, DMSO-d$_6$)** δ 169.7 (C-4), 152.0 (C-2), 150.7 (C-10), 149.3 (C-8), 133.9 (C-9),

127.7 (C-6), 124.9 (C-7), 117.9 (C-5), 98.7 (C-3), 41.8 (C-12), 33.4 (C-17), 29.5 (C-13), 28.2 (C-16), 27.1 (C-14), 26.6 (C-15).

6.2.2. General Synthesis Procedures for Cinnamic Acid Derivatives

While some of the cinnamic acids (unsubstituted and substituted) used were readily available from the suppliers, others were synthesized from the lab as follows:

The malonic acid (2.2 equiv.), aromatic aldehyde (1.0 equiv.), piperidine (0.2 equiv.) and pyridine (5.7 equiv.) as solvent were added to 250 ml reaction flask and the mixtures was refluxed for 6 hours. The reaction was monitored by thin layer chromatography (10% MeOH/EtOAc) and after its completion it was added to 600 mL beaker which contained 400 mL distilled water to form precipitations. The solutions were acidified by HCl to pH 2-3, followed by stirring at room temperatures for 2 hours. The precipitates were filtered and obtained solids were dried.[90]

6.2.2.1. Synthesis of 4-Nitrocinnamic acid (6)

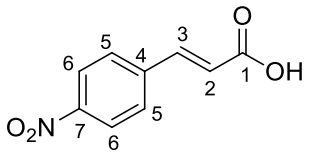

6

4-nitrobenzaldehyde (1.0 g; 6.60 mmol), malonic acid (1.51 g; 14.50 mmol), and piperidine (0.13 ml; 1.30 mmol) in pyridine (5 ml) afforded **6** as a pale-yellow solid (1.07 g, 84%).

^{1}H NMR (400 MHz, DMSO-d$_6$) δ 12.70 (br s, 1H, OH), 8.22 (d, *J* = 8.7 Hz, 2H, H-6), 7.96 (d, *J* = 8.7 Hz, 2H, H-5), 7.68 (d, *J* = 16.1 Hz, 1H, H-3), 6.73 (d, *J* = 16.1 Hz, 1H, H-2). **^{13}C NMR (101 MHz, DMSO-d$_6$)** δ 167.0 (C-1), 147.9 (C-7), 141.3 (C-3), 140.7 (C-4), 129.3 (C-5), 123.9 (C-6), 123.6 (C-2).

6.2.2.2. Synthesis of (E)-3-(4-chlorophenyl) acrylic acid (7)

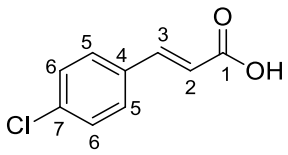

7

4-chlorobenzaldehyde (5.0 g; 35.60 mmol), malonic acid (8.14 g; 78.30 mmol), and piperidine (0.70 ml; 7.10 mmol) in pyridine (10 ml) afforded **7** as a white solid (6.32 g, 97%).

^{1}H NMR (400 MHz, DMSO-d$_6$) δ 12.47 (br s, 1H, OH), 7.71 (d, *J* = 8.3 Hz, 2H, H-5), 7.58 (d, *J* = 16.0 Hz, 1H, H-3), 7.46 (d, *J* = 8.3 Hz, 2H, H-6), 6.55 (d, *J* = 16.0 Hz, 1H, H-2). **^{13}C NMR (101 MHz, DMSO-d$_6$)** δ 167.4 (C-1), 142.5 (C-3), 134.7 (C-7), 133.2 (C-4), 129.9 (C-5), 128.9 (C-6), 120.1 (C-2).

6.2.2.3. Synthesis of (E)-3-(4-fluorophenyl) acrylic acid (8)

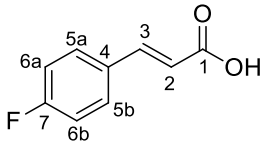

8

4-fluorobenzaldehyde (2.50 g; 20.10 mmol), malonic acid (4.61 g; 44.30 mmol), and piperidine (0.40 ml; 4 mmol) in pyridine (10 ml) afforded **8** as a white solid (1.95 g; 17.77 mmol, 88%).

^{1}H NMR (400 MHz, DMSO) δ 12.67 (s, 1H, OH), 8.01 (dd, *J* = 8.4, 5.7 Hz, 1H, H-5a), 7.77 (dd, *J* = 8.4, 5.7 Hz, 1H, H-5b), 7.59 (d, *J* = 16.1 Hz, 1H, H-3), 7.33 (t, *J* = 8.8 Hz, 1H, H-6a), 7.26 (t, *J* = 8.7 Hz, 1H, H-6b), 6.50 (d, *J* = 16.0 Hz, 1H, H-2). **^{13}C NMR (101 MHz, DMSO-d$_6$)** δ 167.9 (C-1), 162.2 (C-7) 143.2 (C-3), 132.6 (d, *J* = 9.5 Hz, C-4), 131.0 (d, *J* = 8.4 Hz, C-5), 119.6 (C-2), 116.2 (d, *J* = 5.1 Hz, C-6).

6.2.2.4. Synthesis of (E)-3-(furan-2-yl) acrylic acid (9)

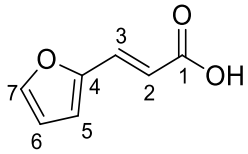

9

Furfural (2.0 g; 20.08 mmol), malonic acid (4.77 g; 45.80 mmol), and piperidine (0.41 ml; 4.50 mmol) in pyridine (10 ml) afforded **9** as a dark brown solid (2.60 g, 90%).

^{1}H NMR (400 MHz, DMSO-d$_6$) δ 12.45 (br s, 1H, OH), 7.83 (s, 1H, H-7), 7.41 (d, *J* = 15.8 Hz, 1H, H-3), 6.93 (s, 1H, H-5), 6.63 (s, 1H, H-6), 6.17 (d, *J* = 15.8 Hz, 1H, H-2).

^{13}C NMR (101 MHz, DMSO) δ 167.5 (C-1), 150.4 (C-4), 145.8 (C-7), 130.9 (C-3), 116.0 (C-2), 115.6 (C-5), 112.8 (C-6).

6.2.2.4. Synthesis of (E)-3-(benzo[d][1,3] dioxol-5-yl)acrylic acid (10)

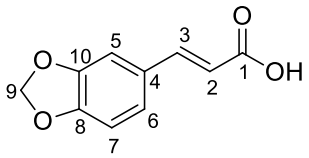

10

Piperonal (5.0 g; 30.10 mmol), malonic acid (6.87 g; 66.20 mmol), and piperidine (0.59 ml; 6.02 mmol) in pyridine (10 ml) afforded **10** as black solid (4.68 g, 81%).

^{1}H NMR (400 MHz, DMSO-d$_6$) δ 12.26 (br s, 1H, OH), 7.50 (d, *J* = 15.9 Hz, 1H, H-3), 7.36 (d, *J* = 1.2 Hz, 1H, H-5), 7.15 (dd, *J* = 8.1, 1.3 Hz, 1H, H-6), 6.93 (d, *J* = 7.9 Hz, 1H, H-7), 6.39 (d, *J* = 15.9 Hz, 1H, H-2), 6.06 (s, 2H, H-9). **^{13}C NMR (101 MHz, DMSO-D$_6$)** δ 167.9 (C-1), 149.2 (C-10), 148.1 (C-8), 143.9 (C-3), 128.7 (C-4), 124.7 (C-6), 117.1 (C-2), 108.5 (C-7), 106.7 (C-5), 101.6 (C-9).

6.2.3. Chlorination of trans-cinnamic acids

6.2.3.0 General Procedure of synthesizing acyl halides

To a round bottom flask dry toluene (20 ml), $SOCl_2$ (5 equiv) and a few drops of DMF (enough to dissolve the reaction mixture) was added with 1.0 equiv of cinnamic acid. The reaction was stirred at room temperature for 8 hours. The progress of the reactions was monitored by (TLC). After completion, the solvent was evaporated from the mixture under reduced pressure using a rotary evaporator. The residues were dissolved in dry toluene, and the solvent evaporated again. The products were used in further reactions without purification. Using this general method, the following compounds were synthesized.[53]

6.2.3.1 Synthesis of (E)-3-Phenylacryloyl chloride (11)

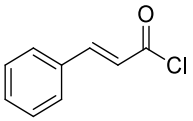

11

Trans cinnamic acid (1.0 g, 6.75 mmol), dry toluene (15 ml), $SOCl_2$ (2.46 ml, 33.75 mmol) and a few drops of DMF afforded **11** as a yellow residue (1.45 ml, 76%).

6.2.3.2. Synthesis of (E)-3-(4-methoxyphenyl)-acryloyl chloride (12)

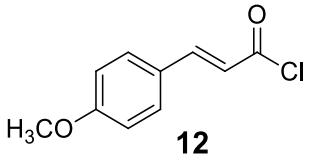

12

4-methoxy-Cinnamic acid (1.0 g, 5.61 mmol), dry toluene (15 ml), $SOCl_2$ (3.07 ml, 28.06 mmol) and a few drops of DMF afforded **12** as a brown residue (0.87 g, 79%).

6.2.3.3 Synthesis of (E)-3-(4-chlorophenyl)acryloyl chloride (13)

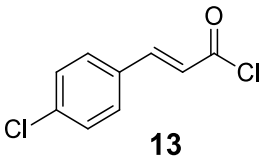

13

4-chloro cinnamic acid (1.0 g, 5.48 mmol), dry toluene (15 ml), $SOCl_2$ (2.0 ml, 27.38 mmol) and a few drops of DMF afforded **13** as a yellow residue (0.80 g, 73%).

6.2.3.4 Synthesis of (E)-3-(4-nitrophenyl)acryloyl chloride (14)

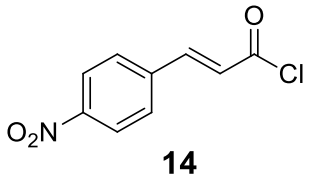

14

4-nitro cinnamic acid (1.07 g; 5.52 mmol), dry toluene (15 ml), $SOCl_2$ (2.0 ml, 27.38 mmol) and a few drops of DMF afforded **14** as a light-yellow residue (1.06 g, 85%).

6.2.3.5. Synthesis of (E)-3-(4-fluorophenyl)acryloyl chloride (15)

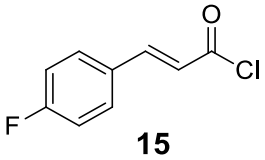

15

4-fluoro cinnamic acid (1.95 g; 17.77 mmol,), dry toluene (15 ml), $SOCl_2$ (4.28 ml, 58.70 mmol) and a few drops of DMF afforded **15** as a brown solid (2.06 g, 95%).

6.2.3.6. Synthesis of (E)-3-(furan-2-yl)acryloyl chloride (16)

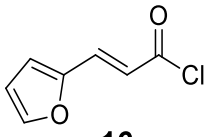

16

(E)-3-(furan-2-yl)acrylic acid (5.0 g; 36.20 mmol,), dry toluene (20 ml), $SOCl_2$ (13.20 ml, 181.0 mmol) and a few drops of DMF afforded **16** as a brown residue (5.55 g, 97%).

6.2.3.7. Synthesis of (E)-3-(benzo[d][1,3]dioxol-5-yl)acryloyl chloride (17)

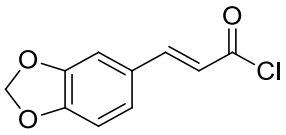

17

(E)-3-(benzo[d][1,3]dioxol-5-yl)acrylic acid (4.68 g; 24.37 mmol) dry toluene (20 ml), $SOCl_2$ (14.50 ml, 121.90 mmol) and a few drops of DMF afforded **17** as a black residue (5.55 g, 97%).

6.2.4 General Procedure for the synthesis of cinnamoyl chloroquinoline hybrids (18-36).

6.2.4.0 Conjugation of Acyl Halides and N-(7-Chloroquinoline 4yl) alkyl-diamine.

A mixture of *N*-(7- chloroquinoline 4yl) alkyl-diamine (1.0 equiv), triethylamine (TEA) (3.0 equiv) and dry DCM was stirred at room temperature for 15 minutes. Thereafter, the solution of acyl halide and dry DCM was added dropwise. The resulting reaction mixture was at stirred at room temperature for 24 hours with round bottom flask covered with aluminium foil (light protected). The progress of the reaction was monitored TLC (20% MeOH/EtOAc). After completion, the solvent was evaporated from the mixture under reduced pressure. The residue was dissolved in ethyl acetate/ NaOH (5%) mixture (1:1). The reaction was worked up by liquid-liquid extraction using 5% NaOH and washed with water. The organic layer was dried over anhydrous sodium sulphate (Na_2SO_4), filtered and excess solvent was removed under reduced pressure and the products were purified by column and flash chromatography using 5-20% (v/v)

ethyl acetate/ methanol. Using this method, the following compounds were synthesized.[53]

6.2.4.1. Synthesis of N-(2-((6-chloronaphthalen-1-yl) amino) ethyl) cinnamamide (18)

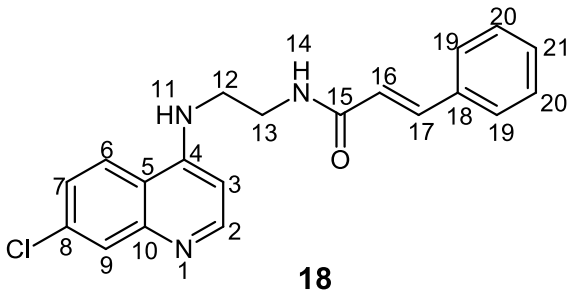

18

The compound **18** was obtained from trans-cinnamoyl chloride (**11)** (0.34 g, 2.02 mmol) and N^1-(7-chloroquinolin-4-yl) ethane-1,2-diamine (**1)** (1.32 g, 1.62 mmol) in 0.33 g (59%) as a light-yellow solid; mp. 252-258 °C.

^{1}H NMR (400 MHZ, DMSO-d$_6$) δ 8.51 – 8.38 (m, 2H, H-2, NH-14), 8.22 (d, *J* = 9.0 Hz, 1H-H-6), 7.79 (s, 1H, H-9), 7.57 (d, *J* = 6.8 Hz, 2H, H-19), 7.54 – 7.44 (m, 4H, H-20, H-7, NH-11), 7.37 – 7.21 (m, 2H, H-17, H-21), 6.70 (d, *J* = 15.8 Hz, 1H, H-16), 6.53 (d, *J* = 5.4 Hz, 1H, H-3), 3.47 – 3.36 (m, 4H, H-12, H-13). **^{13}C NMR (101 MHz, DMSO-d$_6$)** δ166.2 (C-15), 152.4 (C-2), 150.5 (C-4), 149.5 (C-10), 139.4 (C-17), 135.3 (C-18), 133.9 (C-8), 130.0 (C-21), 129.4 (C-20), 128.0 (C-19), 127.9 (C-9), 124.7 (C-6), 124.5 (C-7), 122.39 (C-16), 117.9 (C-5), 99.1 (C-3), 42.7 (C-12), 37.9 (C-13). **IR (cm^{-1})**: 3316 (N-H stretch), 2954 (C-H stretch), 1657 (C=O), 1622 (C=N), 1550 (C=C), 1222 (C-N). **HRMS (ESI-TOF+)**: *m/z* Calculated for $C_{21}H_{19}ClN_2O$: 351.8294; found: 352.1383 (M+H).

6.2.4.2. Synthesis of (E)-N-(2-((6-chloronaphthalen-1-yl) amino) ethyl)-3-(4-methoxyphenyl) acrylamide (19)

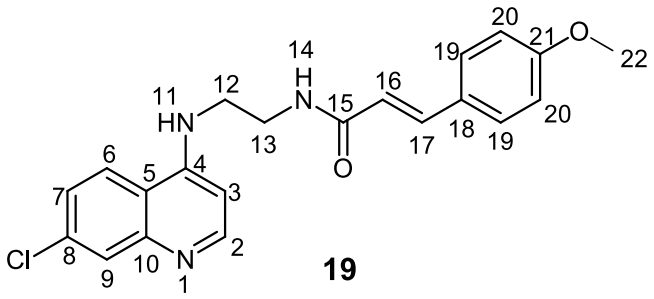

19

The compound **19** was obtained from trans-4-methoxy cinnamoyl chloride (**12**) (0.33 g, 1.70 mmol) and N^1-(7-chloroquinolin-4-yl)ethane-1,2-diamine (**1**) (0.30 g, 1.35 mmol) in 0.35 g (68%) as a light-yellow solid; mp. 235-236°C.

^{1}H NMR (400 MHZ, DMSO-d_6) δ 8.41 (d, *J* = 5.3 Hz, 1H, H-2), 8.36 (br t, *J* = 5.4 Hz, 1H, H-14), 8.20 (d, *J* = 9.0 Hz, 1H, H-6), 7.80 (s, 1H, H-9), 7.52 (d, *J* = 8.6 Hz, 1H, H-19), 7.45 (m, 2H, H-7, NH-11), 7.42 (d, *J* = 15.8 Hz, 1H, H-17), 6.96 (d, *J* = 8.4 Hz, 2H, H-20), 6.60 (d, *J* = 5.4 Hz, 1H, H-3), 6.49 (d, *J* = 15.7 Hz, 1H, H-16), 3.77 (s, 3H, H-22), 3.50 – 3.45 (m, 2H, H-12), 3.44 – 3.37 (m, 2H, H-13). **^{13}C NMR (101 MHz, DMSO-d_6)** δ 166.5 (C-15), 160.8 (C-21), 152.4 (C-2), 150.5 (C-4), 149.5 (C-10), 139.2 (C-17), 133.9 (C-8), 129.6 (C-19), 127.9 (C-9), 127.8 (C-18), 124.7 (C-6), 124.4 (C-7), 119.8 (C-16), 117.9 (C-5), 114.8 (C-20), 99.1 (C-3), 55.7 (C-22), 42.8 (C-12), 37. 9 (C-13). **IR (cm^{-1})**: 3318 (N-H stretch), 2907 (C-H stretch), 1663 (C=O), 1366 (C-O), 1287 (C-N). **HRMS(ESI-TOF+)**: *m/z* Calculated for $C_{22}H_{21}ClN_2O_2$: 381.8554; found: 382.1443 (M+H).

6.2.4.3. Synthesis of (E)-N-(2-((6-chloronaphthalen-1-yl) amino) ethyl)-3-(4-chlorophenyl) acrylamide (20)

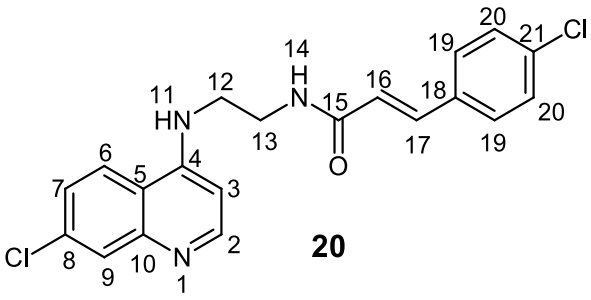

20

The compound **20** was obtained from 4-chlorocinnamoyl chloride (**13**) (0.34 g, 1.70 mmol) and N^1-(7-chloroquinolin-4-yl)ethane-1,2-diamine (**1**) (0.3 g, 1.30 mmol) in 0.33 g (63%) as a yellow solid; mp. 251-252°C.

^{1}H NMR (400 MHZ, DMSO-d_6) δ 8.43 (dd, *J* = 13.1, 5.4 Hz, 2H, NH-14, H-2), 8.22 (d, *J* = 9.1 Hz, 1H, H-6), 7.80 (d, *J* = 1.6 Hz, 1H, H-9), 7.61 (d, *J* = 8.4 Hz, 1H, H-19), 7.51 – 7.47 (m, 3H, NH-11, H-7, H-17), 7.45 (d, *J* = 3.1 Hz, 2H, H-20), 6.64 (d, *J* = 15.8 Hz, 1H, H-16), 6.60 (d, *J* = 5.4 Hz, 1H, H-3), 3.55 – 3.44 (m, 2H, H-12), 3.44 – 3.39 (m, 2H, H-13). **^{13}C NMR (101 MHz, DMSO-d_6)** δ 165.9 (C-15), 152.4 (C-2), 150.5 (C-4), 149.4 (C-10), 138.0 (C-17), 134.4 (C-8), 134.2 (C-21), 133.9 (C-8), 129.7 (C-19), 129.4 (C-20), 127.9 (C-9), 124.6 (C-6), 124.4 (C-7), 123.2 (C-16), 117.8 (C-5), 99.1 (C-3),

42.6 (C-12), 37.9 (C-13). **IR (cm-1)**: 3327 (N-H stretch), 2926 (C-H stretch), 1665 (C=O), 1343 (C-N) and 492 (C-Cl). **HRMS(ESI-TOF+)**: *m/z* Calculated for $C_{21}H_{18}Cl_2N_2O$: 386.2745; found: 387.0855 (M+H).

6.2.4.4. Synthesis of (E)-N-(2-((7-chloroquinolin-4-yl)amino)ethyl)-3-(4-fluorophenyl)acrylamide (21)

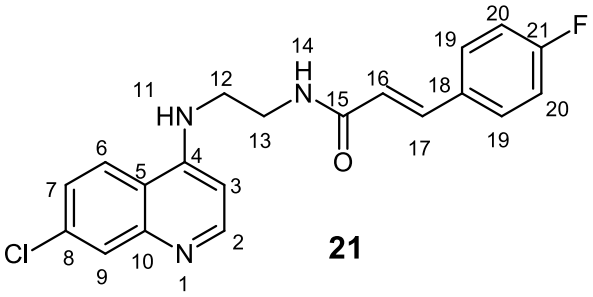

21

The compound **21** was obtained from trans-4-fluoro cinnamoyl chloride (**15**) (1.04 g, 5.6 mmol) and N^1-(7-chloroquinolin-4-yl)ethane-1,2-diamine (**1**) (1 g, 4.5 mmol) in 0.63 g (38%) as a light-yellow solid; mp. 246-249°C.

^{1}H NMR (400 MHz, DMSO-d_6) δ 8.74 (br t, *J* = 5.5 Hz, 1H, NH-14), 8.41 (d, *J* = 5.4 Hz, 1H, H-2), 8.37 (br t, *J* = 5.6 Hz, 1H, NH-11), 8.20 (dd, *J* = 9.1, 1.7 Hz, 1H, H-6), 7.98 – 7.85 (m, 1H, H-17), 7.79 (d, *J* = 2.1 Hz, 1H, H-9), 7.71 – 7.57 (m, 1H, H-16), 7.52 – 7.41 (m, 3H, H-7, H-19), 7.27 (dt, *J* = 23.9, 8.9 Hz, 2H, H-20), 6.71 – 6.45 (m, 1H, H-3), 3.46 (m, 4H, H-12, H-13). **^{13}C NMR (101 MHz, DMSO-d_6)** δ 165.7 (C-15), 162.0 (d, $J_{C\text{-}F}$ = 107.3 Hz, C-21), 152.0 (C-2), 150.1 (C-4), 149.1 (C-10), 137.8 (C-17), 133.5 (C-8), 131.47 (d, $J_{C\text{-}F}$ = 2.9 Hz, C-18), 129.8 (d, $J_{C\text{-}F}$ = 8.5 Hz, C-19), 127.6 (C-9), 124.2 (C-6), 123.9 (C-7), 121.9 (C-16), 117.5 (C-5), 115.9 (d, $J_{C\text{-}F}$ = 21.8 Hz, C-20), 98.7 (C-2), 42.3 (C-12), 37.5 (C-13). **IR (cm^{-1})**: 3330 (N-H stretch), 2939 (C-H stretch), 1667 (C=O), 1586 (C=N), 1532 (C=O), 1225 (C-N) and 513 (C-F**). HRMS(ESI-TOF+)**: *m/z* Calculated for $C_{20}H_{17}ClFN_3O$: 369.8199; found: 370.1126 (M+H).

6.2.4.5. Synthesis of (E)-N-(2-((7-chloroquinolin-4-yl)amino)ethyl)-3-(4-nitrophenyl)acrylamide (22)

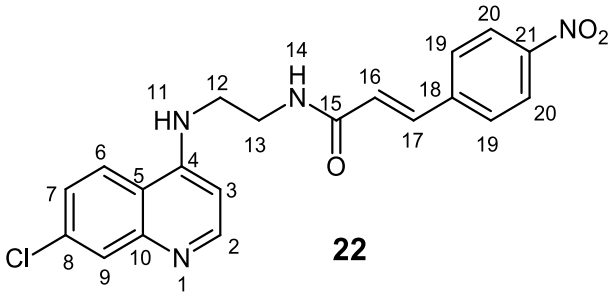

22

The compound **22** was obtained from (*E*)-3-(4-nitrophenyl)acryloyl chloride (**14**) (1.19 g, 5.6 mmol) and N^1-(7-chloroquinolin-4-yl) ethane-1,2-diamine (**1**) (1 g, 4.5 mmol) in 0.72 g (41%) as brown solid; mp. 241-243°C.

^{1}H NMR (400 MHz, DMSO-d$_6$) δ 8.55 (br t, *J* = 5.5 Hz, 1H, NH-14), 8.43 (d, *J* = 4.6 Hz, 1H, H-2), 8.26 (d, *J* = 8.7 Hz, 2H, H-20), 8.23 (d, *J* = 9.0 Hz, 1H, H-6), 7.85 (d, *J* = 8.7 Hz, 2H, H-19), 7.81 (d, *J* = 1.7 Hz, 1H, H-9), 7.59 (d, *J* = 15.9 Hz, 1H, H-17), 7.49 (td, *J* = 8.6, 3.5 Hz, 2H, NH-11, H-7), 6.84 (d, *J* = 15.9 Hz, 1H, H-16), 6.62 (d, *J* = 5.5 Hz, 1H, H-3), 3.55 – 3.43 (m, 4H, H-12 & H-13). **^{13}C NMR (101 MHz, DMSO-d6)** δ 165.5 (C-15), 152.4 (C-2), 150.5 (C-4), 149.5 (C-10), 148.0 (C-21), 141.9 (C-18), 137.1 (C-17), 133.9 (C-8), 129.1 (C-19), 128.0 (C-9), 126.7 (C-6), 124.6 (C-7), 124.6 (C-20), 124.4 (C-16), 117.9 (C-5), 99.2 (C-3), 42.6 (C-12), 38.0 (C-13). **IR (cm^{-1})**: 3333 (N-H stretch), 2983 (C-H stretch), 1666 (C=O), 1558 (C=N), 1516 (C=O), 1339 (C-N) and 1299-1225 (N-O). **HRMS(ESI-TOF+)**: *m/z* Calculated for $C_{20}H_{17}ClN_4O_3$: 396.8270; found: 397.1194 (M+H).

6.2.4.6. Synthesis of (E)-N-(2-((7-chloroquinolin-4-yl)amino)ethyl)-3-(furan-2-yl)acrylamide (23)

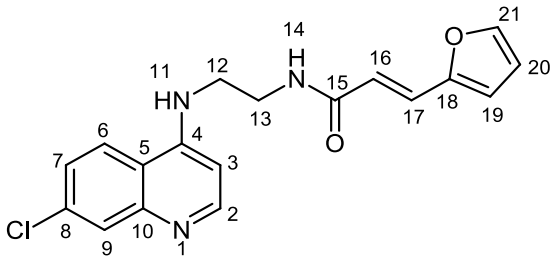

23

The compound **23** was obtained from (*E)*-3-(furan-2-yl)acryloyl chloride (**16)** (0.88 g, 5.6 mmol) and N^1-(7-chloroquinolin-4-yl) ethane-1,2-diamine (**1**) (1.0 g, 4.5 mmol) in 0.64 g (42%) as a brown solid; mp. 240-242°C.

^{1}H NMR (400 MHz, DMSO-d$_6$) δ 8.42 (d, *J* = 5.5 Hz, 1H, H-2), 8.28 (br t, *J* = 5.6 Hz, 1H, NH-14), 8.21 (d, *J* = 9.0 Hz, 1H, H-6), 7.80 (d, *J* = 2.2 Hz, 1H, H-21), 7.52 (br t, *J* = 5.0 Hz, 1H, NH-11), 7.47 (dd, *J* = 9.0, 2.3 Hz, 1H, H-7), 7.39 (d, *J* = 15.7 Hz, 1H, H-17), 7.16 (d, *J* = 1.6 Hz, 1H, H-9), 7.07 (dd, *J* = 8.1, 1.5 Hz, 1H, H-20), 6.94 (d, *J* = 7.9 Hz, 1H, H-19), 6.60 (d, *J* = 5.5 Hz, 1H, H-3), 6.47 (d, *J* = 15.7 Hz, 1H, 16), 3.55 – 3.42 (m, 4H, H-12; H-13). **^{13}C NMR (101 MHz, DMSO-d$_6$)** δ 165.6 (C-15), 151.9 (C-2), 150.9 (C-4), 150.1 (C-18), 149.1 (C-10), 144.8 (C-21), 133.5 (C-8), 127.5 (C-17), 126.3 (C-9), 124.2 (C-16), 123.9 (C-6), 119.2 (C-7), 117.5 (C-5), 113.9 (C-19), 112.4 (C-20), 98.7 (C-3), 42.3 (C-12), 37.5 (C-13). **IR (cm^{-1})**: 3324 (N-H stretch), 2983 (C-H stretch), 1666 (C=O), 1586 (C=N), 1533 (C=C), 1238 (C-N) and 1136 (C-O). **HRMS(ESI-TOF+)**: *m/z* Calculated for $C_{18}H_{16}ClN_3O_2$: 341.7915; found: 342.1032 (M+H).

6.2.4.7. Synthesis of (E)-3-(benzo[d][1,3]dioxol-5-yl)-N-(2-((7-chloroquinolin-4-yl)amino)ethyl)acrylamide (24)

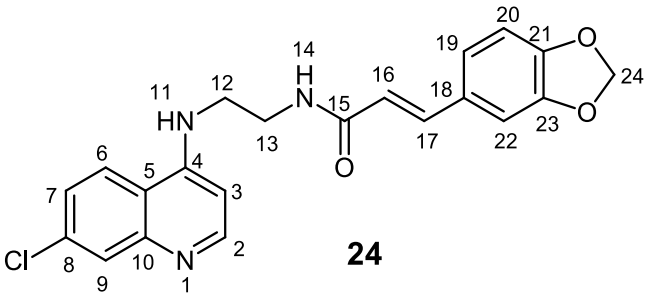

24

The compound **24** was obtained from (E)-3-(benzo[d][1,3]dioxol-5-yl)acryloyl chloride (**17)** (2.27 g, 10.80 mmol) and N^1-(7-chloroquinolin-4-yl) ethane-1,2-diamine (**1**) (1.90 g, 8.6 mmol) in 1.85 g (54%) as a brown solid; mp. 252-254°C.

^{1}H NMR (400 MHz, DMSO-d$_6$) δ 8.42 (d, *J* = 5.5 Hz, 1H, H-2), 8.30 (br t, *J* = 5.6 Hz, 1H, NH-14), 8.21 (d, *J* = 9.2 Hz, 1H, H-6), 7.80 (d, *J* = 2.1 Hz, 1H, H-9), 7.54 (br t, *J* = 5.1 Hz, 1H, NH-11), 7.48 (dd, *J* = 8.9, 2.2 Hz, 1H, H-7), 7.39 (d, *J* = 15.7 Hz, 1H, H-17), 7.17 (d, *J* = 1.3 Hz, 1H, H-22), 7.08 (dd, *J* = 8.1, 1.3 Hz, 1H, H-19), 6.94 (d, *J* = 8.1 Hz, 1H, H-20), 6.61 (d, *J* = 5.5 Hz, 1H, H-3), 6.48 (d, *J* = 15.8 Hz, 1H, H-16), 6.06 (s, 2H, H-24), 3.56 – 3.44 (m, 4H, H-12 & H-13). **^{13}C NMR (101 MHz, DMSO-d6)** δ 166.0 (C-15), 151.7 (C-2), 150.2 (C-4), 148.8 (C-10), 148.5 (C-23), 147.9 (C-21), 138.8

(C-17), 133.5 (C-8), 129.2 (C-18), 127.3 (C-9), 124.2 (C-6), 123.9 (C-19), 123.3 (C-6), 120.0 (C-16), 117.4 (C-5), 108.6 (C-20), 106.2 (C-22), 101.4 (C-24), 98.7 (C-3), 42.4 (C-12), 37.5 (C-13). **IR (cm^{-1})**: 3310 (N-H stretch), 2986 (C-H stretch), 1686 (C=O), 1618 (C=N), 1488 (C=C), 1245 (C-N) and 1035 (C-O). **HRMS(ESI-TOF+)1q**: *m/z* Calculated for $C_{21}H_{18}ClN3O_3$: 395.8389; found: 396.1240 (M+H).

6.2.4.8. Synthesis of N-(1-((7-chloroquinolin-4-yl)amino)propan-2-yl)cinnamamiden (25).

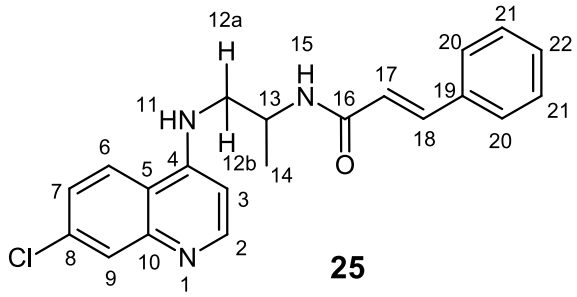

25

The compound **25** was obtained from trans cinnamoyl chloride (**11**) (2.13 g, 10.6 mmol) and *N*^{1}-(7-chloroquinolin-4-yl) propane-1,2-diamine (**3**) (2.01 g, 8.50 mmol) in 1.69 g (50%) as a white solid; mp. 152-153°C.

^{1}H NMR (400 MHz, DMSO-d$_6$) δ 8.41 (d, *J* = 5.3 Hz, 1H, H-2), 8.23-8.16 (m, 2H, H-6, NH-15), 7.79 (d, *J* = 1.8 Hz, 2H, H-9), 7.56 (d, *J* = 7.0 Hz, 2H, H-20), 7.53 – 7.32 (m, 6H, H-21, H-18, H-7, H-22, NH-11), 6.74 (d, *J* = 5.4 Hz, 1H, H-3), 6.64 (d, *J* = 15.9 Hz, 1H, H-17), 4.24 (dt, *J* = 13.4, 6.7 Hz, 1H, H-13), 3.43 (dd, *J* = 12.5, 6.4 Hz, 1H, H-12a), 3.22 (dd, *J* = 13.2, 6.4 Hz, 1H, H-12b), 1.22 (d, *J* = 6.6 Hz, 3H, H-14). **^{13}C NMR (101 MHz, DMSO-d$_6$)** δ 165.2 (C-16), 151.9 (C-2), 150.1 (C-4), 149.1 (C-10), 138.9 (C-18), 134.9 (C-19), 133.4 (C-8), 129.5 (C-9), 128.9 (C-21), 127.5 (C-22), 127.6 (C-20), 124.2 (C-6), 123.9 (C-7), 122.1 (C-17), 117.4 (C-5), 98.9 (C-3), 47.9 (C-12), 43.6 (C-13), 18.0 (C-14).). **IR (cm^{-1})**: 3329 (N-H stretch), 3048 (C-H stretch), 1659 (C=O), 1622 (C=N), 1537.19 (C=C), 1137.7 (C-N). **HRMS(ESI-TOF+)**: *m/z* Calculated for $C_{21}H_{20}ClN_3O$:365.8560; found: 366.1375 (M+H).

6.2.4.9. Synthesis of (E)-3-(4-chlorophenyl)-N-(1-((7-chloroquinolin-4-yl)amino)propan-2-yl)acrylamide (26)

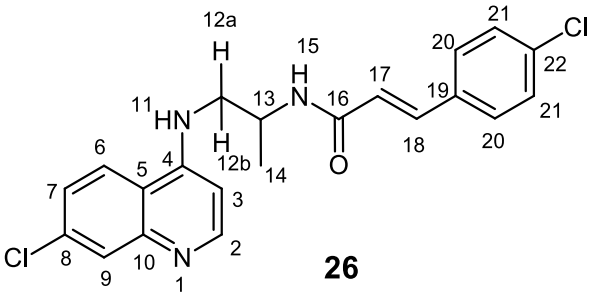

26

The compound **26** was obtained from trans-4-chloro cinnamoyl chloride (**13**) (2.13 g, 10.6 mmol) and N^1-(7-chloroquinolin-4-yl) propane-1,2-diamine (**3**) (2.01 g, 8.5 mmol) in 1.64 g (48%) as a white solid; mp. 237-240°C.

^{1}H NMR (400 MHz, DMSO-d$_6$) δ 8.41 (d, *J* = 5.4 Hz, 1H, H-2), 8.27 (d, *J* = 7.3 Hz, 1H, H-6), 8.22 (br d, *J* = 9.0 Hz, 1H, NH-15), 7.80 (d, *J* = 2.2 Hz, 1H, H-9), 7.59 (d, *J* = 8.6 Hz, 2H, H-20) , 7.53 – 7.40 (m, 6H, H-18, H-21, H-7, H-8, NH-11), 6.73 (d, *J* = 5.5 Hz, 1H, H-3), 6.65 (d, *J* = 15.9 Hz, 1H, H-17), 4.25 (dt, *J* = 13.6, 6.8 Hz, 1H, H-13), 3.34 – 3.16 (m, 2H, H-12a, H-12b), 1.23 (d, *J* = 6.7 Hz, 3H, H-14). **^{13}C NMR (101 MHz, DMSO-D$_6$)** δ 165.0 (C-16), 151.9 (C-2), 150.2 (C-4), 149.1 (C-10), 137.6 (C-18), 133.9 (C-8), 133.8 (C-22), 133.4 (C-19), 129.2 (C-20), 128.9 (C-21), 127.5 (C-9), 124.2 (C-6), 123.8 (C-7), 122.9 (C-17), 117.4 (C-5), 98.9 (C-3), 47.9 (C-12), 43.7 (C-13), 17.9 (C-14). **IR (cm^{-1})**: 3325 (N-H stretch), 2852 (C-H stretch), 1656 (C=O), 1625 (C=N), 1575 (C=C), 1367 (C-O), 1235 (C-N), 848 (C-Cl). **HRMS(ESI-TOF+)**: *m/z* Calculated for $C_{21}H_{19}Cl_2N_3O$:400.3011; found: 401.1014 (M+H).

6.2.4.10. Synthesis of (E)-N-(1-((7-chloroquinolin-4-yl)amino)propan-2-yl)-3-(4-methoxyphenyl)acrylamide (27)

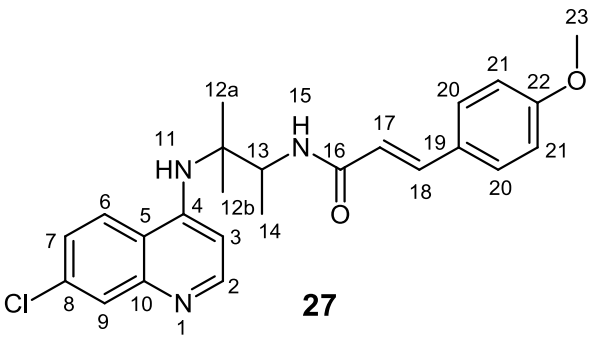

27

The compound **27** was obtained from trans-4-methoxy cinnamoyl chloride (**12**) (2.09 g, 5.3 mmol) and N^1-(7-chloroquinolin-4-yl) propane-1,2-diamine (**3**) (2.0 g, 8.50 mmol) in 46% as a brown solid; mp. 212-216°C.

^{1}H NMR (400 MHz, DMSO-d$_6$) δ 8.43 (d, *J* = 5.3 Hz, 1H, H-2), 8.24 (d, *J* = 9.1 Hz, 1H, H-6), 8.17 (d, *J* = 7.5 Hz, 1H, NH-15), 7.81 (d, *J* = 2.2 Hz, 1H, H-9), 7.57 – 7.50 (m, 3H, NH-11, H-20). 7.48 (dd, *J* = 8.8, 2.3 Hz, 1H, H-7), 7.45 (d, *J* = 15.2 Hz, 1H, H-18), 6.99 (d, *J* = 8.8 Hz, 2H, H-21), 6.74 (d, *J* = 5.5 Hz, 1H, H-3), 6.51 (d, *J* = 15.8 Hz, 1H, H-17), 4.26 (dt, *J* = 13.5, 6.8 Hz, 1H, H-13), 3.80 (s, 3H, H-23), 3.36 – 3.09 (m, 2H, H-12a, H-12b), 1.23 (d, *J* = 6.7 Hz, 3H, H-14). **^{13}C NMR (101 MHz, DMSO-d$_6$)** δ 165.6 (C-16), 160.4 (C-22), 152.0 (C-2), 150.2 (C-4), 149.1 (C-10), 138.8 (C-18), 133.5 (C-8), 129.2 (C-20), 127.6 (C-9), 127.5 (C-19), 124.3 (C-6), 123.9 (C-7), 119.9 (C-17), 117.4 (C-5), 114.4 (C-21), 99.0 (C-3), 55.3 (C-23), 48.2 (C-12), 43.6 (C-13), 18.1 (C-14). **IR (cm^{-1})**: 3351 (N-H stretch), 3062 (C-H stretch), 1644 (C=O), 1367 (C-O), 1248 (C-N). **HRMS(ESI-TOF+)**: *m/z* Calculated for $C_{22}H_{22}ClN_3O_2$:395.8820; found: 396.1823 (M+H).

6.2.4.11. Synthesis of N-(3-((7-chloroquinolin-4-yl) amino)propyl) cinnamamide (28)

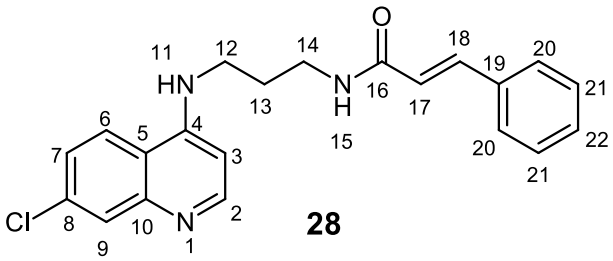

28

The compound **28** was obtained from trans-cinnamoyl chloride (**11**) (1.32 g, 7.9 mmol) and N^1-(7-chloroquinolin-4-yl)propane-1,3-diamine (**2**) (0.5 g, 4.0 mmol) in 0.90 g (54%) as a white solid; mp. 190-196 °C.

^{1}H NMR (400 MHz, DMSO-d$_6$) δ 8.39 (d, *J* = 5.4 Hz, 1H, H-2), 8.26 (m, 2H, H-6, NH-15), 7.79 (d, *J* = 2.2 Hz, 1H, H-9), 7.56 (d, *J* = 6.8 Hz, 2H, H-20), 7.48 – 7.32 (m, 6H, H-21, H-18, H-7, H-22, NH-11), 6.64 (d, *J* = 15.8 Hz, 1H, H-17), 6.49 (d, *J* = 5.5 Hz, 1H, H-3), 3.33 (dd, *J* = 12.6, 6.6 Hz, 2H, H-12; H-14), 1.87 (p, *J* = 6.8 Hz, 2H, H-13). **^{13}C NMR (101 MHz, DMSO-d$_6$)** δ 165.2 (C-16), 151.9 (C-2), 150.1 (C-4), 149.0 (C-10), 138.6 (C-18), 134.9 (C-19), 133.4 (C-8), 129.4 (C-9), 128.9 (C-20), 127.5 (C-21), 127.4 (C-22), 124.1 (C-6), 124.0 (C-7) 122.2 (C-17), 117.5 (C-5), 98.7 (C-3), 40.1 (C-

14), 36.7 (C-12), 27.9 (C-13). **IR (cm^{-1})**: 3337 (N-H stretch), 3048 (C-H stretch), 1659 (C=O), 1622 (C=N), 1537.19 (C=C), 1137.7 (C-N). **HRMS(ESI-TOF+)**: *m/z* Calculated for $C_{21}H_{20}ClN_3O$:365.8560; found: 366.1408 (M+H).

6.2.4.12. Synthesis of (E)-N-(3-((7-chloroquinolin-4-yl)amino)propyl)-3-(4-methoxyphenyl)acrylamide (29)

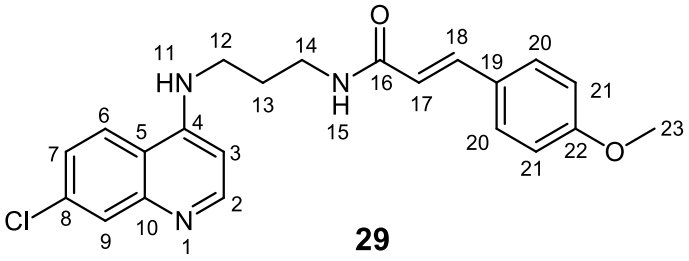

29

The compound **29** was obtained from trans-4-methoxy cinnamoyl chloride (**12**) (1.36 g, 6.90 mmol) and N^1-(7-chloroquinolin-4-yl)propane-1,3-diamine (**2**) (1.0 g, 4,6 mmol) in 0.95 g (52%) as a white solid; mp. 196-198°C.

^{1}H NMR (400 MHz, DMSO) δ 8.39 (d, *J* = 4.8 Hz, 1H, H-2), 8.26 (d, *J* = 9.1 Hz, 1H, H-6), 8.15 (br t, *J* = 5.6 Hz, 1H, NH-15), 7.79 (d, *J* = 2.0 Hz, 1H, H-9), 7.50 (d, *J* = 8.8 Hz, 2H, H-20), 7.45 (dd, *J* = 9.0, 2.2 Hz, 1H, H-7), 7.39 (d, *J* = 15.8 Hz, 1H, H-18), 7.34 (br t, *J* = 5.3 Hz, 1H, NH-11), 6.96 (d, *J* = 8.8 Hz, 2H, H-21), 6.49 (d, *J* = 15.8 Hz, 1H, H-17), 6.50 (d, *J* = 5.5 Hz, 1H, H-3), 3.77 (s, 3H, H-23), 3.37 – 3.24 (m, 4H, H-12, H-14), 1.86 (p, *J* = 6.8 Hz, 2H, H-13). **^{13}C NMR (101 MHz, DMSO-d$_6$)** δ 166 (C-16), 160.8 (C-22), 152.4 (C-2), 150.5 (C-4), 149.5 (C-10), 138.8 (C-18), 133.9 (C-8), 129.5 (C-20), 127.9 (C-9), 124.6 (C-6), 124.5 (C-7), 120.2 (C-17), 118.0 (C-5), 114.8 (C-21), 99.2 (C-3), 55.7 (C-23), 49.1 (C-14), 41.3 (C-12), 28.4 (C-13). **IR (cm^{-1})**: 3351 (N-H stretch), 3062 (C-H stretch), 1644 (C=O), 1367 (C-O), 1248 (C-N). **HRMS(ESI-TOF+)**: *m/z* Calculated for $C_{22}H_{22}ClN_3O_2$:395.8820; found: 396.1820 (M+H).

6.2.4.13. Synthesis of N-(6-((7-chloroquinolin-4-yl) amino) hexyl) cinnamamide (30)

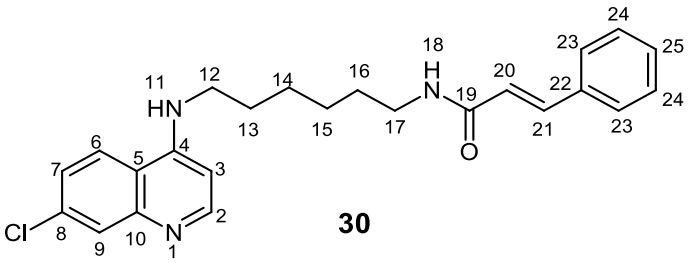

30

The compound **30** was obtained from trans-cinnamoyl chloride (**11**) (0.44 g, 4.32 mmol) and N^1-(7-chloroquinolin-4-yl)hexane-1,6-diamine (**5**) (0.40 g, 1.44 mmol) in 0.41 g (70%) as a yellow solid; mp. 174-175°C.

^{1}H NMR (400 MHZ, DMSO-d$_6$) δ 8.38 (d, *J* = 5.3 Hz, 1H, H-2), 8.28 (d, *J* = 9.0 Hz, 1H, H-6), 8.13 (br t, *J* = 5.3 Hz, 1H, NH-18), 7.78 (d, *J* = 1.8 Hz, 1H, H-9), 7.55 (d, *J* = 7.3 Hz, 2H, H-23), 7.47 – 7.35 (m, 5H, H-7, H-21, H-24, H-25), 7.32 (br t, *J* = 5.1 Hz, 1H, NH-11), 6.63 (d, *J* = 15.8 Hz, 1H, H-20), 6.46 (d, *J* = 5.5 Hz, 1H, H-3), 3.26 (dd, *J* = 12.7, 6.6 Hz, 2H, H-12), 3.22 – 3.13 (m, 2H, H-17), 1.66 (dd, *J* = 14.0, 7.0 Hz, 2H, H-13), 1.47 (dd, *J* = 13.6, 6.8 Hz, 2H, H-16), 1.38 (t, *J* = 10.6 Hz, 2H, H-15), 1.34 – 1.28 (m, 2H, H-14). **^{13}C NMR (101 MHz, DMSO-d$_6$)** δ 165.3 (C-19), 152.3 (C-2), 150.5 (C-4), 149.4 (C-10), 138.8 (C-21), 135.4 (C-22), 133.8 (C-8), 129.8 (C-25), 129.3 (C-24), 127.9 (C-23), 127.8 (C-9), 124.5 (C-6), 124.4 (C-7), 122.7 (C-20), 117.9 (C-5), 99.0 (C-3), 42.8 (C-12), 39.1 (C-17), 29.5 (C-13), 28.1 (C-16), 26.8 (C-15), 26.7 (C-14)**. IR (cm^{-1})**: 3359 (N-H stretch), 2929 (C-H stretch), 1664 (C=O), 1537 (C=C), 1331 (C-N). **HRMS(ESI-TOF+)**: *m/z* Calculated for $C_{24}H_{26}ClN_3O$:407.9357; found: 408.1963 (M+H).

6.2.4.14 Synthesis of (E)-N-(6-((7-chloroquinolin-4-yl) amino) hexyl)-3-(4-methoxyphenyl) acrylamide (31)

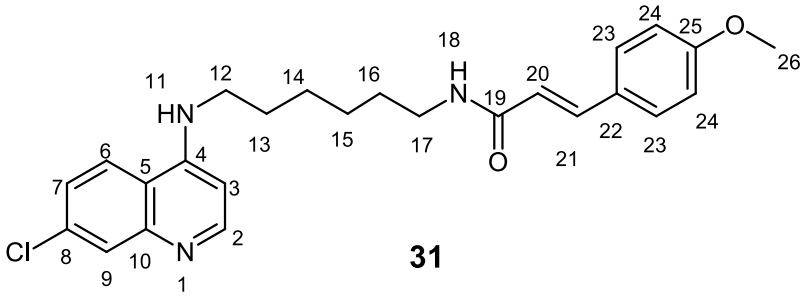

31

The compound **31** was obtained from trans-4-methoxy cinnamoyl chloride (**12**) (0.51 g, 1.84 mmol) and N^1-(7-chloroquinolin-4-yl)hexane-1,6-diamine (**5**) (0.45 g, 2.30 mmol) in 0.60 g (74%) as a light-yellow solid; mp. 107-109°C.

^{1}H NMR (400 MHZ, DMSO-d$_6$) δ 8.38 (d, *J* = 5.2 Hz, 1H, H-2), 8.28 (d, *J* = 9.0 Hz, 1H, H-6), 8.04 (br t, *J* = 5.3 Hz, 1H, NH-18), 7.78 (d, *J* = 1.8 Hz, 1H, H-9), 7.50 (d, *J* = 8.6 Hz, 2H, H-23), 7.43 (dd, *J* = 9.0, 1.8 Hz, 1H, H-7), 7.35 (d, *J* = 15.9 Hz, 1H, H-21), 7.31 (br t, *J* = 4.9 Hz, 1H, NH-11), 6.96 (d, *J* = 8.5 Hz, 2H, H-24), 6.47 (d, *J* = 15.6 Hz, 1H, H-20), 6.44 (d, *J* = 5.2 Hz, 1H, H-3), 3.78 (s, 1H, H-26), 3.25 (dd, *J* = 12.6, 6.6 Hz,

2H, H-12), 3.17 (dd, *J* = 12.6, 6.5 Hz, 2H, H-17), 1.64 (dd, *J* = 13.6, 6.7 Hz, 2H, H-13), 1.46 (dd, *J* = 13.1, 6.5 Hz, 2H, H-16), 1.36-1.30 (m, 4H, H-15, H-14**). ^{13}C NMR (101 MHz, DMSO-d$_6$)** δ 165.6 (C-19), 160.7 (C-25), 152.3 (C-2), 150.5 (C-4), 149.5 (C-10), 138.5 (C-21), 133.8 (C-8), 129.4 (C-23), 127.9 (C-9), 127.8 (C-6), 124.5 (C-7), 124.4 (C-20), 120.3 (C-5), 117.9 (C-24), 116.9 (C-5), 114.8 (C-26), 99.0 (C-3), 55.6 (C-12), 42.8 (C-17), 29.6 (C-13), 28.1 (C-16), 26.8 (C-15), 26.7 (C-14). **IR (cm^{-1})**: 3355 (N-H stretch), 2905 (C-H stretch), 1657 (C=O), 1373 (C-O), 1250 (C-N**). HRMS(ESI-TOF+)**: *m/z* Calculated for $C_{25}H_{28}ClN_3O_2$: 437.9617; found: 438.1980 (M+H).

6.2.4.15 Synthesis of (E)-3-(4-chlorophenyl)-N-(6-((7-chloroquinolin-4-yl) amino) hexyl) acrylamide (32)

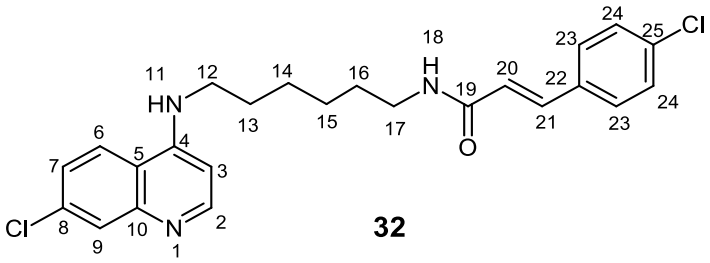

32

The compound **32** was obtained from 4-chloro-cinnamoyl chloride (**13**) (0.45 g, 2.27 mmol) and N^1-(7-chloroquinolin-4-yl)hexane-1,6-diamine (**5**) (0.50 g, 1.81 mmol) in 0.48 g (60%) as a yellow solid; mp. 183-185°C.

^{1}H NMR (400 MHZ, DMSO-d$_6$) δ 8.37 (d, *J* = 5.2 Hz, 1H, H-2), 8.28 (d, *J* = 9.1 Hz, 1H H-6), 8.17 (br t, *J* = 5.4 Hz, 1H, NH-18), 7.78 (d, *J* = 1.7 Hz, 1H, H-9), 7.58 (d, *J* = 8.4 Hz, 2H, H-23), 7.49 – 7.40 (m, 3H, H-24, H-7), 7.40 (d, *J* = 15.7 Hz, 1H, H-21), 7.31 (br t, *J* = 4.8 Hz, 1H, NH-11), 6.62 (d, *J* = 15.8 Hz, 1H, H-20), 6.44 (d, *J* = 5.4 Hz, 1H, H-3), 3.24 (dd, *J* = 12.4, 6.5 Hz, 2H), 3.18 (q, *J* = 6.5 Hz, 3H), 1.70 – 1.59 (m, 2H), 1.46 (dd, *J* = 13.6, 7.0 Hz, 2H). 6.50 – 6.42 (m, 2H, H-12), 3.25 (d, *J* = 5.5 Hz, 2H, H-17), 3.21 – 3.10 (m, 2H, H-13), 1.65 (dd, *J* = 13.7, 6.8 Hz, 2H, H-16), 1.53 – 1.28 (m, 4H, H-15, H-14). **^{13}C NMR (101 MHz, DMSO-d$_6$)** δ 165.1 (C-19), 152.35 (C-4), 150.5 (C-2), 149.5 (C-10), 137.5 (C-21), 134.3 (C-8), 134.2 (C-25), 133.8 (C-22), 129.6 (C-23), 129.4 (C-24), 127.8 (C-9), 124.5 (C-6), 124.4 (C-7), 123.6 (C-20), 117.9 (C-5), 99.0 (C-3), 42.8 (C-12), 39.1 (C-17), 29.5 (C-13), 28.1 (C-16), 26.8 (C-15), 26.7 (C-14). **IR (cm^{-1})**: 3344 (N-H stretch), 2928 (C-H stretch), 1665 (C=O), 1315 (C-N) and 491 (C-Cl**). HRMS(ESI-TOF+)**: *m/z* Calculated for $C_{24}H_{25}Cl_2N_3O$: 442.3808; found: 443.1484 (M+H).

6.2.4.16 Synthesis of (E)-N-(6-((7-chloroquinolin-4-yl)amino)hexyl)-3-(4-fluorophenyl)acrylamide (33)

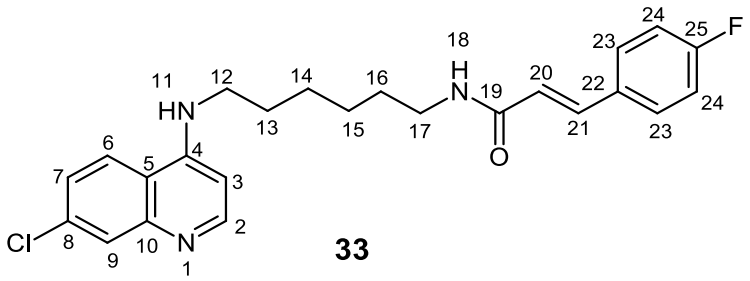

33

The compound **32** was obtained from trans-4-fluoro cinnamoyl chloride (**15**) (0.83 g, 4.5 mmol) and N^1-(7-chloroquinolin-4-yl)hexane-1,6-diamine (**5**) (1.02 g, 3.6 mmol) in 0.38 g (25%) as a light-yellow solid; mp. 150-153°C.

^{1}H NMR (400 MHz, DMSO-D$_6$) δ 8.46 (br t, *J* = 5.5 Hz, 1H, NH-18), 8.37 (d, *J* = 5.3 Hz, 1H, H-2), 8.27 (d, *J* = 9.1 Hz, 1H, H-6), 8.09 (br t, *J* = 5.6 Hz, 1H, NH-11), 7.77 (d, *J* = 2.2 Hz, 1H, H-9), 7.60 (dd, *J* = 8.7, 5.6 Hz, 2H, H-23), 7.43 (dd, *J* = 6.0, 3.0 Hz, 2H, H-24), 7.40 (d, *J* = 9.8 Hz, 1H, H-21), 7.32 – 7.19 (m, 1H, H-7), 6.56 (d, *J* = 15.8 Hz, 1H, H-20), 6.44 (d, *J* = 5.5 Hz, 1H, H-3), 3.29 – 3.21 (m, 2H, H-6), 3.22 – 3.12 (m, 2H, H-17), 1.72 – 1.60 (m, 2H, H-13), 1.47 (dd, *J* = 13.9, 7.0 Hz, 2H, H-16), 1.46 – 1.25 (m, 4H, H-14, H-15). **^{13}C NMR (101 MHz, DMSO-D$_6$)** δ 164.8 (C-19),161.6 (d, J_{C-F} = 159.3 Hz, C-25), 151.9 (C-2), 150.1 (C-4), 149.1 (C-10), 137.2 (C-21), 133.4 (C-8), 131.6 (d, J_{C-F} = 2.9 Hz, C-22), 129.6 (d, J_{C-F} = 8.5 Hz, C-23), 127.5 (C-9), 124.1 (C-6), 123.9 (C-7), 122.3 (C-20), 117.5 (C-5), 115.9 (d, J_{C-F} = 21.7 Hz, C-24), 98.6 (C-3), 42.4 (C-12), 38.7 (C-17), 29.2 (C-13), 27.8 (C-16), 26.4 (C-14), 26.3 (C-15). **IR (cm^{-1})**: 3346 (N-H stretch), 2977 (C-H stretch), 1636 (C=O), 1680 (C=N), 1508 (C=O), 1315 (C-N) and 501 (C-F). **HRMS(ESI-TOF+)**: *m/z* Calculated for $C_{24}H_{25}ClFN_3O$: 425.9262; found: 426.1751 (M+H).

6.2.4.17 Synthesis of (E)-N-(6-((7-chloroquinolin-4-yl)amino)hexyl)-3-(4-nitrophenyl)acrylamide (34)

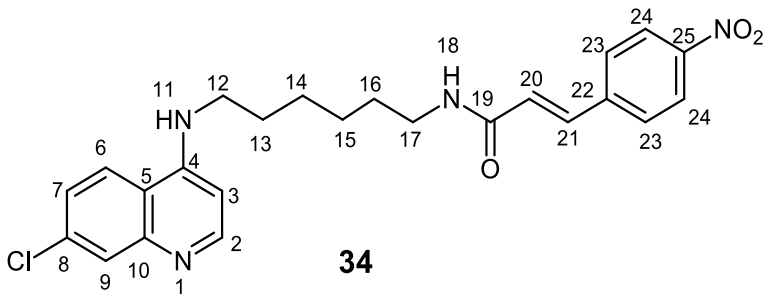

34

The compound **34** was obtained from (*E*)-3-(4-nitrophenyl)acryloyl chloride (**14**) (0.95 g, 4.5 mmol) and N^1-(7-chloroquinolin-4-yl)hexane-1,6-diamine (**5**) (1.01 g, 3.6 mmol) in 0.75 (46%) as brown solid; mp. 136-140°C.

^{1}H NMR (400 MHz, DMSO-d$_6$) δ 8.40 (d, *J* = 5.4 Hz, 1H, H-2), 8.34 – 8.27 (m, 2H, H-6, NH-18), 8.25 (d, *J* = 8.8 Hz, 2H, H-24), 7.82 (d, *J* = 8.8 Hz, 2H, H-23), 7.79 (d, *J* = 1.8 Hz, 1H, H-9), 7.54 (d, *J* = 15.8 Hz, 1H, H-21), 7.45 (dd, *J* = 8.9, 2.1 Hz, 1H, H-7), 7.34 (br t, *J* = 5.1 Hz, 1H, NH-11), 6.83 (d, *J* = 15.9 Hz, 1H, H-20), 6.46 (d, *J* = 5.5 Hz, 1H, H-3), 3.31 – 3.17 (m, 4H, H-12, H-17), 1.74 – 1.60 (m, 2H, H-13), 1.57 – 1.45 (m, 2H, H-16), 1.48 – 1.30 (m, 6H, H-14, H-15)**. ^{13}C NMR (101 MHz, DMSO-D$_6$)** δ 164.6 (C-19), 152.3 (C-2), 150.6 (C-4), 149.5 (C-10), 147.9 (C-25), 142.1 (C-22), 136.6 (C-21), 133.9 (C-8), 128.9 (C-23), 127.8 (C-9), 127.1 (C-6), 124.6 (C-7), 124.5 (C-24), 124.4 (C-20), 117.9 (C-5), 99.0 (C-3), 42.8 (C-12), 39.2 (C-17), 29.5 (C-13), 28.2 (C-16), 26.8 (C-14), 26.7 (C-15). **IR (cm^{-1})**: 3289 (N-H stretch), 2932 (C-H stretch), 1650 (C=O), 1607 (C=N), 1510 (C=C), 1337 (C-N) and 1838 (N-O). **HRMS(ESI-TOF+)**: *m/z* Calculated for $C_{24}H_{25}ClN_4O_3$:452.9333; found: 453.1696 (M+H).

6.2.4.18 Synthesis of (E)-N-(6-((7-chloroquinolin-4-yl)amino)hexyl)-3-(furan-2-yl)acrylamide (35)

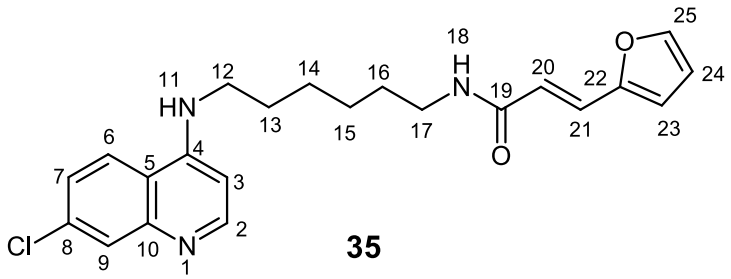

35

The compound **35** was obtained from (*E*)-3-(furan-2-yl)acryloyl chloride (**16)** (0.70 g, 4.5 mmol) and N^1-(7-chloroquinolin-4-yl)hexane-1,6-diamine (**5**) (1.0 g, 3.6 mmol) in 0.53 g (41%) as a brown solid; mp. 120-123°C.

^{1}H NMR (400 MHz, DMSO-d$_6$) δ 8.37 (d, *J* = 5.4 Hz, 1H, H-2), 8.28 (d, *J* = 9.0 Hz, 1H, H-6), 8.14 (br t, *J* = 5.6 Hz, 1H, NH-18), 7.78 (d, *J* = 2.2 Hz, 1H, H-25), 7.74 (d, *J* = 1.5 Hz, 1H, H-9), 7.42 (dd, *J* = 9.0, 2.1 Hz, 1H, H-7), 7.34 (br t, *J* = 5.0 Hz, 1H, NH-11), 7.22 (d, *J* = 15.7 Hz, 1H, H-21), 6.74 (d, *J* = 3.3 Hz, 1H, H-23), 6.56 (dd, *J* = 3.3, 1.8 Hz, 1H, H-24), 6.44 (d, *J* = 5.7 Hz, 1H, H-3), 6.43 (d, *J* = 15.2 Hz, 1H, H-20), 3.36 – 3.10 (m, 4H, H-12, H-17), 1.76 – 1.52 (m, 2H, H-13), 1.51 – 1.25 (m, 6H, H-16, H-14,

H-15). **^{13}C NMR (101 MHz, DMSO-d$_6$)** δ 165.2 (C-19), 152.1 (C-2), 151.5 (C-4), 150.7 (C-22), 149.3 (C-10), 145.1 (C-25), 133.9 (C-8), 127.7 (C-21), 126.3 (C9), 124.6 (C-20), 124.5 (C-6), 120.1 (C-7), 117.9 (C-5), 113.9 (C-23), 112.8 (C-24), 99.0 (C-3), 42.8 (C-12), 39.1 (C-17), 29.6 (C-13), 28.2 (C-16), 26.8 (C-14), 26.7 (C-15). **IR (cm^{-1})**: 3284 (N-H stretch), 2928 (C-H stretch), 1656 (C=O), 1575 (C=N), 1450 (C=C), 1230 (C-N) and 1136 (C-O). **HRMS(ESI-TOF+)**: *m/z* Calculated for $C_{22}H_{24}ClN_3O_2$:397.8979; found: 398.1678 (M+H).

6.2.4.19 Synthesis of (E)-3-(benzo[d][1,3]dioxol-5-yl)-N-(6-((7-chloroquinolin-4-yl)amino)hexyl)acrylamide (36)

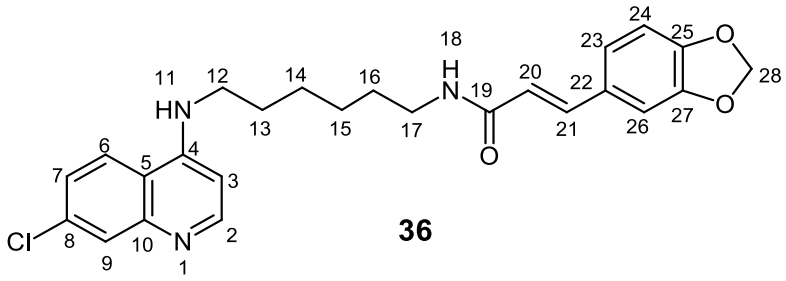

36

The compound **36** was obtained from *(E)*-3-(benzo[d][1,3]dioxol-5-yl)acryloyl chloride (**17)** (1.33 g, 6.3 mmol) and N^1-(7-chloroquinolin-4-yl)hexane-1,6-diamine (**5**) (1.40 g, 5.0 mmol) in 1.23 g (54%) as a brown solid, mp 168-170°C.

^{1}H NMR (400 MHz, DMSO-d$_6$) δ 8.37 (d, *J* = 5.4 Hz, 1H, H-2), 8.28 (d, *J* = 9.0 Hz, 1H, H-6), 8.00 (t, *J* = 5.7 Hz, 1H, NH-18), 7.77 (d, *J* = 2.2 Hz, 1H, H-9), 7.43 (dd, *J* = 8.9, 2.1 Hz, 1H, H-7), 7.39 – 7.23 (m, 2H, NH-11; H-21), 7.12 (d, *J* = 1.5 Hz, 1H, H-26), 7.04 (dd, *J* = 8.1, 1.4 Hz, 1H, H-23), 6.93 (d, *J* = 7.9 Hz, 1H, H-24), 6.45 (dd, *J* = 10.6, 5.1 Hz, 2H, H-3 & H-20), 6.05 (s, 2H, H-28), 3.31 – 3.20 (m, 2H, H-12), 3.20 – 3.10 (m, 2H, H-17), 1.73 – 1.57 (m, 2H, H-13), 1.55 – 1.40 (m, 2H, H-16), 1.41 – 1.26 (m, 4H, H-14, H-15). **^{13}C NMR (101 MHz, DMSO-d6)** δ 165.0 (C-19), 151.7 (C-2), 150.2 (C-4), 148.9 (C-10), 148.3 (C-27), 147.9 (C-25), 138.2 (C-21), 133.4 (C-8), 129.4 (C-22), 127.3 (C-9), 124.1 (C-6), 123.9 (C-23), 123.1 (C-7), 120.5 (C-20), 117.4 (C-5), 108.5 (C-24), 106.1 (C-26), 101.4 (C-28), 98.6 (C-3), 42.4 (C-12), 38.6 (C-17), 29.2 (C-13), 27.7 (C-16), 26.3 (C-14), 26.2 (C-15). **IR (cm^{-1})**: 3343 (N-H stretch), 2930 (C-H stretch), 1620 (C=O), 1444 (C=N), 1388 (C=C), 1247 (C-N) and 1038 (C-O. **HRMS(ESI-TOF+)**: *m/z* Calculated for $C_{25}H_{26}ClN_3O_3$:451.9452; found: 452.1746 (M+H).

7. REFERENCES

(1) Kondaparla, S.; Debnath, U.; Soni, A.; Dola, V. R.; Sinha, M.; Srivastava, K.; Puri, S. K.; Katti, S. B. Synthesis, Biological Evaluation, and Molecular Modeling Studies of Chiral Chloroquine Analogues as Antimalarial Agents. *Antimicrob. Agents Chemother.* **2018**, *62* (12).

(2) Neafsey, D. E.; Taylor, A. R.; MacInnis, B. L. Advances and Opportunities in Malaria Population Genomics. *Nat. Rev. Genet.* **2021**, *22* (8), 502–517.

(3) Sato, S. Plasmodium—a Brief Introduction to the Parasites Causing Human Malaria and Their Basic Biology. *J. Physiol. Anthropol.* **2021**, *40* (1), 1–13.

(4) World Health Organization. WOrld Malaria Report 2015; Geneva: *World Health Organization.* **2015**.

(5) World Health Organization. World Malaria Report 2022; Geneva: *World Health Organization*. **2022**.

(6) World Health Organization. World Malaria Report 2019; Geneva: *World Health Organization*. **2019**.

(7) World Health Organization. Word Malaria Report 2021; Geneva: *World Health Organization.* **2021**.

(8) World Health Organization. World Malaria Report 2023; Geneva: *World Health Organization*. **2023**

(9) Sinha, M.; Dola, V. R.; Soni, A.; Agarwal, P.; Srivastava, K.; Haq, W.; Puri, S. K.; Katti, S. B. Bioorganic & Medicinal Chemistry Synthesis of Chiral Chloroquine and Its Analogues as Antimalarial Agents. *Bioorg. Med. Chem.* **2014**, *22* (21), 5950–5960.

(10) Nasir, S. M. I.; Amarasekara, S.; Wickremasinghe, R.; Fernando, D.; Udagama, P. Prevention of Re-Establishment of Malaria: Historical Perspective and Future Prospects. *Malar. J.* **2020**, *19* (1), 1–16.

(11) Fornace, K. M.; Zorello Laporta, G.; Vythilingham, I.; Chua, T. H.; Ahmed, K.; Jeyaprakasam, N. K.; de Castro Duarte, A. M. R.; Amir, A.; Phang, W. K.;

Drakeley, C.; Sallum, M. A. M.; Lau, Y. L. Simian Malaria: A Narrative Review on Emergence, Epidemiology and Threat to Global Malaria Elimination. *Lancet Infect. Dis.* **2023**, *23* (12), e520–e532.

(12) Gething, P. W.; Elyazar, I. R. F.; Moyes, C. L.; Smith, D. L.; Battle, K. E.; Guerra, C. A.; Patil, A. P.; Tatem, A. J.; Howes, R. E.; Myers, M. F.; George, D. B.; Horby, P.; Wertheim, H. F. L.; Price, R. N.; Müeller, I.; Baird, J. K.; Hay, S. I. A Long Neglected World Malaria Map: Plasmodium Vivax Endemicity in 2010. *PLoS Negl. Trop. Dis.* **2012**, *6* (9).

(13) Price, R. N.; Commons, R. J.; Battle, K. E.; Thriemer, K.; Mendis, K. Plasmodium Vivax in the Era of the Shrinking P. Falciparum Map. *Trends Parasitol.* **2020**, *36* (6), 560–570.

(14) Battle, K. E.; Lucas, T. C. D.; Nguyen, M.; Howes, R. E.; Nandi, A. K.; Twohig, K. A.; Pfeffer, D. A.; Cameron, E.; Rao, P. C.; Casey, D.; Gibson, H. S.; Rozier, J. A.; Dalrymple, U.; Keddie, S. H.; Collins, E. L.; Harris, J. R.; Guerra, C. A.; Thorn, M. P.; Bisanzio, D.; Fullman, N.; Huynh, C. K.; Kulikoff, X.; Kutz, M. J.; Lopez, A. D.; Mokdad, A. H.; Naghavi, M.; Nguyen, G.; Shackelford, K. A.; Vos, T.; Wang, H.; Lim, S. S.; Murray, C. J. L.; Price, R. N.; Baird, J. K.; Smith, D. L.; Bhatt, S.; Weiss, D. J.; Hay, S. I.; Gething, P. W. Mapping the Global Endemicity and Clinical Burden of Plasmodium Vivax, 2000–17: A Spatial and Temporal Modelling Study. *Lancet* **2019**, *394* (10195), 332–343.

(15) Loeffel, M.; Ross, A. *The Relative Impact of Interventions on Sympatric Plasmodium Vivax and Plasmodium Falciparum Malaria: A Systematic Review*; **2022**; Vol. 16.

(16) Morrison, L.; Zembower, T. R. Antimicrobial Resistance. *Gastrointest. Endosc. Clin. N. Am.* **2020**, *30* (4), 619–635.

(17) Winzeler, E. A. Malaria Research in the Post-Genomic Era. *Nature* **2008**, *455* (7214), 751–756.

(18) Parhizgar, A. R. Introducing New Antimalarial Analogues of Chloroquine and Amodiaquine: A Narrative Review. *Iranian Journal of Medical Sciences*. **2017**, pp 115–128.

(19) Kaur, K.; Jain, M.; Reddy, R. P.; Jain, R. Quinolines and Structurally Related Heterocycles as Antimalarials. *Eur. J. Med. Chem.* **2010**, *45* (8), 3245–3264.

(20) Antoine C. Banet, P. E. B. *Antimalarial Drug Research and Development*; Nova Science Publishers, Inc. Nova Biomedical New York, 2013.

(21) Shibeshi, M. A.; Kifle, Z. D.; Atnafie, S. A. Antimalarial Drug Resistance and Novel Targets for Antimalarial Drug Discovery. *Infect. Drug Resist.* **2020**, *13*, 4047–4060.

(22) Baird, J. K.; Hoffman, S. L. Primaquine Therapy for Malaria. *Clin. Infect. Dis.* **2004**, *39* (9), 1336–1345.

(23) Baird, K. J.; Maguire, J. D.; Price, R. N. Diagnosis and Treatment of Plasmodium Vivax Malaria. In *Advances in Parasitology*; Elsevier, 2012; Vol. 80, pp 203–270.

(24) Chu, C. S.; White, N. J. The Prevention and Treatment of Plasmodium Vivax Malaria. *PLoS Med.* **2021**, *18* (4 April), 1–21.

(25) WHO. Artemisinin Resistance and Artemisinin-Based Combination Therapy Efficacy. *Who* **2019**, *2018* (August), 10.

(26) Shibeshi, W.; Baye, A. M.; Alemkere, G.; Engidawork, E. Efficacy and Safety of Artemisinin-Based Combination Therapy for the Treatment of Uncomplicated Malaria in Pregnant Women: A Systematic Review and Meta-Analysis. *Ther. Clin. Risk Manag.* **2021**, *17*, 1353–1370.

(27) White, N. J. Artemisinin Resistance - The Clock Is Ticking. *Lancet* **2010**, *376* (9758), 2051–2052. https://doi.org/10.1016/S0140-6736(10)61963-0.

(28) Ouji, M.; Augereau, J. M.; Paloque, L.; Benoit-Vical, F. Plasmodium Falciparum Resistance to Artemisinin-Based Combination Therapies: A Sword of Damocles in the Path toward Malaria Elimination. *Parasite* **2018**, *25*.

(29) Roux, A. T.; Maharaj, L.; Oyegoke, O.; Akoniyon, O. P.; Adeleke, M. A.; Maharaj, R.; Okpeku, M. Chloroquine and Sulfadoxine–Pyrimethamine Resistance in Sub-Saharan Africa—A Review. *Front. Genet.* **2021**, *12* (June).

(30) Hyde, J. E. Drug-Resistant Malaria - An Insight. *FEBS J.* **2007**, *274* (18), 4688–4698.

(31) Grynberg, S.; Lachish, T.; Kopel, E.; Meltzer, E.; Schwartz, E. Artemether-Lumefantrine Compared to Atovaquone-Proguanil as a Treatment for Uncomplicated Plasmodium Falciparum Malaria in Travelers. *Am. J. Trop. Med. Hyg.* **2015**, *92* (1), 13–17.

(32) Prasad Raiguru, B.; Panda, J.; Mohapatra, S.; Nayak, S. Recent Developments in the Synthesis of Hybrid Antimalarial Drug Discovery. *Bioorg. Chem.* **2023**, *139* (June), 106706.

(33) Vandekerckhove, S.; D'Hooghe, M. Quinoline-Based Antimalarial Hybrid Compounds. *Bioorganic Med. Chem.* **2015**, *23* (16), 5098–5119.

(34) Claudio Viegas-Junior; Eliezer J. Barreiro; Carlos Alberto Manssour Fraga. Molecular Hybridization: A Useful Tool in the Design of New Drug Prototypes. *Curr. Med. Chem.* **2007**, *14* (17), 1829–1852.

(35) Abu Almaaty, A. H.; Elgrahy, N. A.; Fayad, E.; Abu Ali, O. A.; Mahdy, A. R. E.; Barakat, L. A. A.; Behery, M. El. Design, Synthesis and Anticancer Evaluation of Substituted Cinnamic Acid Bearing 2-Quinolone Hybrid Derivatives. *Molecules* **2021**, *26* (16).

(36) Srivastava, V.; Lee, H. Chloroquine-Based Hybrid Molecules as Promising Novel Chemotherapeutic Agents. *Eur. J. Pharmacol.* **2015**, *762*, 472–486.

(37) Walsh, J.; Bell, A. Hybrid Drugs for Malaria. *Curr. Pharm. Des.* **2009**, *15* (25), 2970–2985.

(38) Morphy, R.; Rankovic, Z. Designed Multiple Ligands. An Emerging Drug Discovery Paradigm. *J. Med. Chem.* **2005**, *48* (21), 6523–6543.

(39) Szumilak, M.; Wiktorowska-Owczarek, A.; Stanczak, A. Hybrid Drugs—a Strategy for Overcoming Anticancer Drug Resistance? *Molecules* **2021**, *26* (9), 1–31.

(40) Gediya, L. K.; Njar, V. C. Promise and Challenges in Drug Discovery and Development of Hybrid Anticancer Drugs. *Expert Opin. Drug Discov.* **2009**, *4* (11), 1099–1111.

(41) Marchesi, E.; Perrone, D.; Navacchia, M. L. Molecular Hybridization as a Strategy for Developing Artemisinin-Derived Anticancer Candidates.

Pharmaceutics **2023**, *15* (9).

(42) Kim, J.; Tan, Y. Z.; Wicht, K. J.; Erramilli, S. K.; Dhingra, S. K.; Okombo, J.; Vendome, J.; Hagenah, L. M.; Giacometti, S. I.; Warren, A. L.; Nosol, K.; Roepe, P. D.; Potter, C. S.; Carragher, B.; Kossiakoff, A. A.; Quick, M.; Fidock, D. A.; Mancia, F. Structure and Drug Resistance of the Plasmodium Falciparum Transporter PfCRT. *Nature* **2019**, *576* (7786), 315–320.

(43) Ch'Ng, J. H.; Mok, S.; Bozdech, Z.; Lear, M. J.; Boudhar, A.; Russell, B.; Nosten, F.; Tan, K. S. W. A Whole Cell Pathway Screen Reveals Seven Novel Chemosensitizers to Combat Chloroquine Resistant Malaria. *Sci. Rep.* **2013**, *3*, 1–9.

(44) Agrawal, P.; Manjithaya, R.; Surolia, N. Autophagy-Related Protein PfATG18 Participates in Food Vacuole Dynamics and Autophagy-like Pathway in Plasmodium Falciparum. *Mol. Microbiol.* **2020**, *113* (4), 766–782.

(45) Aliyu, A. W.; Mustaffa, K. M. F.; Yew, L. C.; Hou, L. J. Chloroquine Bioconjugates and Hybrid Compounds: Past and Recent Developments in Combatting Chloroquine Resistant Malaria. *Trop. J. Pharm. Res.* **2021**, *20* (12), 2663–2674.

(46) Kiarie, W. C.; Wangai, L.; Agola, E.; Kimani, F. T.; Hungu, C. Chloroquine Sensitivity: Diminished Prevalence of Chloroquine-Resistant Gene Marker Pfcrt-76 13 Years after Cessation of Chloroquine Use in Msambweni, Kenya. *Malar. J.* **2015**, *14* (1), 1–7.

(47) Lödige, M.; Lewis, M. D.; Paulsen, E. S.; Esch, H. L.; Pradel, G.; Lehmann, L.; Brun, R.; Bringmann, G.; Mueller, A. K. A Primaquine-Chloroquine Hybrid with Dual Activity against Plasmodium Liver and Blood Stages. *Int. J. Med. Microbiol.* **2013**, *303* (8), 539–547.

(48) Oliveira, R.; Miranda, D.; Magalhães, J.; Capela, R.; Perry, M. J.; O'Neill, P. M.; Moreira, R.; Lopes, F. From Hybrid Compounds to Targeted Drug Delivery in Antimalarial Therapy. *Bioorganic Med. Chem.* **2015**, *23* (16), 5120–5130.

(49) Guzman, J. D. *Natural Cinnamic Acids, Synthetic Derivatives and Hybrids with Antimicrobial Activity*; **2014**; Vol. 19.

(50) Lingbeck, J. M.; O'Bryan, C. A.; Martin, E. M.; Adams, J. P.; Crandall, P. G.

Sweetgum: An Ancient Source of Beneficial Compounds with Modern Benefits. *Pharmacogn. Rev.* **2015**, *9* (17), 1–11.

(51) Silva, A. T.; Bento, C. M.; Pena, A. C.; Figueiredo, L. M.; Prudêncio, C.; Aguiar, L.; Silva, T.; Ferraz, R.; Gomes, M. S.; Teixeira, C.; Gomes, P. Cinnamic Acid Conjugates in the Rescuing and Repurposing of Classical Antimalarial Drugs. *Molecules* **2020**, *25* (1), 1–15.

(52) Ruwizhi, N.; Aderibigbe, B. A. Cinnamic Acid Derivatives and Their Biological Efficacy. *Int. J. Mol. Sci.* **2020**, *21* (16), 1–36.

(53) Pavić, K.; Perković, I.; Gilja, P.; Kozlina, F.; Ester, K.; Kralj, M.; Schols, D.; Hadjipavlou-Litina, D.; Pontiki, E.; Zorc, B. Design, Synthesis and Biological Evaluation of Novel Primaquine-Cinnamic Acid Conjugates of the Amide and Acylsemicarbazide Type. *Molecules* **2016**, *21* (12).

(54) Chhabra, N.; Aseri, M.; Padmanabhan, D. A Review of Drug Isomerism and Its Significance. *Int. J. Appl. Basic Med. Res.* **2013**, *3* (1), 16.

(55) Katsonis, N.; Lubomska, M.; Pollard, M. M.; Feringa, B. L.; Rudolf, P. Synthetic Light-Activated Molecular Switches and Motors on Surfaces. *Prog. Surf. Sci.* **2007**, *82* (7–8), 407–434.

(56) Wang, R.; Yang, W.; Fan, Y.; Dehaen, W.; Li, Y.; Li, H.; Wang, W.; Zheng, Q.; Huai, Q. Design and Synthesis of the Novel Oleanolic Acid-Cinnamic Acid Ester Derivatives and Glycyrrhetinic Acid-Cinnamic Acid Ester Derivatives with Cytotoxic Properties. *Bioorg. Chem.* **2019**, *88* (April), 102951.

(57) Guo, S.; Zhen, Y.; Zhu, Z.; Zhou, G.; Zheng, X. Cinnamic Acid Rescues Behavioral Deficits in a Mouse Model of Traumatic Brain Injury by Targeting MiR-455-3p/HDAC2. *Life Sci.* **2019**, *235* (1), 116819.

(58) Wiesner, J.; Mitsch, A.; Wißner, P.; Jomaa, H.; Schlitzer, M. Structure - Activity Relationships of Novel Anti-Malarial Agents. Part 2: Cinnamic Acid Derivatives. *Bioorganic Med. Chem. Lett.* **2001**, *11* (3), 423–424.

(59) Chang, S. T.; Chen, P. F.; Chang, S. C. Antibacterial Activity of Leaf Essential Oils and Their Constituents from Cinnamomum Osmophloeum. *J. Ethnopharmacol.* **2001**, *77* (1), 123–127.

(60) Wen, A.; Delaquis, P.; Stanich, K.; Toivonen, P. Antilisterial Activity of Selected Phenolic Acids. *Food Microbiol.* **2003**, *20* (3), 305–311.

(61) Alves, M. J.; Ferreira, I. C. F. R.; Froufe, H. J. C.; Abreu, R. M. V.; Martins, A.; Pintado, M. Antimicrobial Activity of Phenolic Compounds Identified in Wild Mushrooms, SAR Analysis and Docking Studies. *J. Appl. Microbiol.* **2013**, *115* (2), 346–357.

(62) Schmidt, Erich, Stefanie Bail, Susanne Mirjam Friedl, Leopold Jirovetz, Gerhard Buchbauer, Jürgen Wanner, Zapryana Denkova, Alexander Slavchev, Albena Stoyanova, and M. G. Antimicrobial Activities of Single Aroma Compounds. *Nat. Prod. Commun.* **2010**, *1* (4), 9–12.

(63) Ugazio, E.; Carlotti, M. E.; Sapino, S.; Trotta, M.; Vione, D.; Minero, C. Photodegradation of Cinnamic Acid in Different Media. *J. Dispers. Sci. Technol.* **2008**, *29* (5), 641–652.

(64) Pérez, B.; Teixeira, C.; Gut, J.; Rosenthal, P. J.; Gomes, J. R. B.; Gomes, P. Cinnamic Acid/Chloroquinoline Conjugates as Potent Agents against Chloroquine-Resistant Plasmodium Falciparum. *ChemMedChem* **2012**, *7* (9), 1537–1540.

(65) Pérez, B. C.; Teixeira, C.; Figueiras, M.; Gut, J.; Rosenthal, P. J.; Gomes, J. R. B.; Gomes, P. Novel Cinnamic Acid/4-Aminoquinoline Conjugates Bearing Non-Proteinogenic Amino Acids: Towards the Development of Potential Dual Action Antimalarials. *Eur. J. Med. Chem.* **2012**, *54*, 887–899.

(66) Pérez, B. C.; Teixeira, C.; Albuquerque, I. S.; Gut, J.; Rosenthal, P. J.; Gomes, J. R. B.; Prudeîncio, M.; Gomes, P. N-Cinnamoylated Chloroquine Analogues as Dual-Stage Antimalarial Leads. *J. Med. Chem.* **2013**, *56* (2), 556–567.

(67) Gayam, V.; Ravi, S. Cinnamoylated Chloroquine Analogues: A New Structural Class of Antimalarial Agents. *Eur. J. Med. Chem.* **2017**, *135*, 382–391.

(68) Assaleh, M. H.; Jeremić, S.; Cvijetić, I.; Marinković, A.; Prlainović, N. In Vitro Activity of Novel Cinnamic Acids Hydrazides against Clinically Important Pathogens. *J. Mol. Struct.* **2022**, *1262*.

(69) Li, X.; Sheng, J.; Huang, G.; Ma, R.; Yin, F.; Song, D.; Zhao, C.; Ma, S. Design,

Synthesis and Antibacterial Activity of Cinnamaldehyde Derivatives as Inhibitors of the Bacterial Cell Division Protein FtsZ. *Eur. J. Med. Chem.* **2015**, *97*, 32–41.

(70) Smit, F. J.; N'Da, D. D. Synthesis, in Vitro Antimalarial Activity and Cytotoxicity of Novel 4-Aminoquinolinyl-Chalcone Amides. *Bioorganic Med. Chem.* **2014**, *22* (3), 1128–1138.

(71) Lee, S. Chemical Structure Elucidation of an Unknown Compound By Direct Analysis in Real-Time Mass Spectrometry and Nuclear Magnetic Resonance Spectroscopy, **2019**.

(72) Hand, E. S.; Belmore, K. A.; Kispert, L. D. The Effect of Electron-Donating and Electron-Withdrawing Substituents on 1H-and 13C-NMR Chemical Shifts of Novel 7′-aryl-substituted 7′-apo-β-carotenes. *Helv. Chim. Acta* **1993**, *76* (5), 1928–1938.

(73) Kabanda, M. M.; Nemudzivhadi, A. I.; Bvumbi, M. V.; Madala, N. E. Rationalizing the Formation of Quasi-Molecular Anions Due to Tautomerization of Chloroquine-Cinnamide Hybrid Molecule during Analysis by Electrospray Ionization (ESI) – Mass Spectrometry (MS) and through Density Functional Theory (DFT) Calculations. *J. Mol. Struct.* **2023**, *1291*.

(74) Allegretti, P.; Schiavonni, M.; Castro, E.; Furlong, J. Tautomeric Equilibria Studies by Mass Spectrometry. *Nat. Preced.* **2008**, 1–76.

(75) Chiu, F. C. K.; Lo, C. M. Y. Observation of Amide Anions in Solution by Electrospray Ionization Mass Spectrometry. *J. Am. Soc. Mass Spectrom.* **2000**, *11* (12), 1061–1064.

(76) Masike, K.; Dubery, I.; Steenkamp, P.; Smit, E.; Madala, E. Revising Reverse-Phase Chromatographic Behavior for Efficient Differentiation of Both Positional and Geometrical Isomers of Dicaffeoylquinic Acids. *J. Anal. Methods Chem.* **2018**, *2018*.

(77) Velema, W. A.; Szymanski, W.; Feringa, B. L. Photopharmacology: Beyond Proof of Principle. *J. Am. Chem. Soc.* **2014**, *136* (6), 2178–2191.

(78) Kobauri, P.; Dekker, F. J.; Szymanski, W.; Feringa, B. L. Rational Design in Photopharmacology with Molecular Photoswitches. *Angew. Chemie - Int. Ed.*

2023, *62* (30).

(79) Zhu, J.; Sun, X.-W.; Yang, X.; Yu, S.-N.; Liang, L.; Chen, Y.-Z.; Zheng, X.; Yu, M.; Yan, L.; Tang, J.; Zhao, W.; Yang, X.-J.; Wu, B. In Situ Photoisomerization of an Azobenzene-Based Triple Helicate with a Prolonged Thermal Relaxation Time. *Angew. Chemie Int. Ed.* **2023**, *202314510*.

(80) Rickhoff, J.; Arndt, N. B.; Böckmann, M.; Doltsinis, N. L.; Ravoo, B. J.; Kortekaas, L. Reversible, Red-Shifted Photoisomerization in Protonated Azobenzenes. *J. Org. Chem.* **2022**, *87* (16), 10605–10612.

(81) Abd El-Raouf, O. M.; El-Sayed, E. S. M.; Manie, M. F. Cinnamic Acid and Cinnamaldehyde Ameliorate Cisplatin-Induced Splenotoxicity in Rats. *J. Biochem. Mol. Toxicol.* **2015**, *29* (9), 426–431.

(82) Salum, M. L.; Erra-Balsells, R. High Purity Cis-Cinnamic Acid Preparation for Studying Physiological Role of Trans-Cinnamic and Cis-Cinnamic Acids in Higher Plants. *Environ. Control Biol.* **2013**, *51* (1), 1–10.

(83) Li, Y. S.; Escobar, L.; Zhu, Y. J.; Cohen, Y.; Ballester, P.; Rebek, J.; Yu, Y. Relative Hydrophilicities of Cis and Trans Formamides. *Proc. Natl. Acad. Sci. U. S. A.* **2019**, *116* (40), 19815–19820.

(84) Matsuhira, T.; Yamamoto, H.; Okamura, T. A.; Ueyama, N. Manipulation of an Intramolecular NH ⋯ O Hydrogen Bond by Photoswitching between Stable E/Z Isomers of the Cinnamate Framework. *Org. Biomol. Chem.* **2008**, *6* (11), 1926–1933.

(85) Rodríguez, R. B.; Iguchi, D.; Erra-Balsells, R.; Laura Salum, M.; Froimowicz, P. Design and Effects of the Cinnamic Acids Chemical Structures as Organocatalyst on the Polymerization of Benzoxazines. *Polymers (Basel).* **2020**, *12* (7), 1–11.

(86) Sinha, S.; Medhi, B.; Sehgal, R. Challenges of Drug-Resistant Malaria. *Parasite* **2014**, *21*.

(87) WILLIAM TRAGER JAMES B. JENSEN. Human Malaria Parasites in Continuous Culture. *J. Natl. Med. Assoc.* **1976**, *68* (6), 530–533.

(88) Makler MT, Ries JM, Williams JA, Bancroft JE, Piper RC, Gibbins BL, H. D.

Parasite Lactate Dehydrogenase as an Assay for Plasmodium Falciparum Drug Sensitivity. *Am. J. Trop. Med. Hyg.* **1993**, *48(6)* (June), 739–741.

(89) Kondaparla, S.; Manhas, A.; Dola, V. R.; Srivastava, K.; Puri, S. K.; Katti, S. B. Design, Synthesis and Antiplasmodial Activity of Novel Imidazole Derivatives Based on 7-Chloro-4-Aminoquinoline. *Bioorg. Chem.* **2018**, *80* (March), 204–211.

(90) Çalışkan, E.; Biryan, F.; Koran, K.; Akman, F.; Görgülü, A. O.; Çetin, A. Synthesis of Cinnamoyl-Amino Acid Ester Derivatives and Structure-Activity Relationship Based on Thermal Stability, Dielectric, and Theoretical Analysis. *ChemistrySelect* **2022**, *7* (20).

CHAPTER 8

APPENDIX

Journal of Molecular Structure 1291 (2023) 136014

Contents lists available at ScienceDirect

Journal of Molecular Structure

journal homepage: www.elsevier.com/locate/molstr

Rationalizing the formation of quasi-molecular anions due to tautomerization of chloroquine-cinnamide hybrid molecule during analysis by electrospray ionization (ESI) – mass spectrometry (MS) and through density functional theory (DFT) calculations

Mwadham Mwombeki Kabanda [a,*], Anza Imanuel Nemudzivhadi [a], Mpelegeng Victoria Bvumbi [a], Ntakadzeni Edwin Madala [b,*]

[a] Department of Chemistry, Faculty of Science, Engineering and Agriculture, Private Bag X 5050, Thohoyandou 0950 South Africa
[b] Department of Biochemistry and Microbiology, Faculty of Science, Engineering and Agriculture, Private Bag X 5050, Thohoyandou 0950 South Africa

ARTICLE INFO

Keywords:
Amide
Imidic
Tautomerization
Electrospray ionization
Mass spectrometry
DFT

ABSTRACT

Molecules that contain amide groups often have interesting biological and pharmacological properties. However, analysing these molecules using electrospray ionization (ESI) - mass spectrometry (MS) can be a challenging scientific endeavour due to their chargeability, particularly in negative ESI mode. In this study, a newly synthesized anti-malarial compound, N-(2-((6-chloronaphthalen-1-yl) amino) ethyl) cinnamamide, and its structural analogues were observed to generate strong quasi-molecular anions during ESI-MS, despite not being predisposed to anion formation based on their structural configuration. To uncover the mechanism underlying this anion formation, density functional theory calculations were performed, revealing that the formation of the anions is attributed to the imidic tautomer generated at the ESI chamber/probe's ion source. This leads to ionization occurring on the newly formed OH resulting from the enolization of the imidic form of the molecule.

A snapshot of the article that was published from the miscellaneous work done on the compounds.

8. Selected ^{1}H, ^{13}C, dept NMR, IR spectra and Chromatograms and their respective Mass Spectra.

8.1 ^{1}H, ^{13}C, DEPT NMR spectra, IR, Chromatogram and mass spectrum of (E)-N-(2-((6-chloronaphthalen-1-yl) amino) ethyl)-3-(4- methoxyphenyl) acrylamide (19)

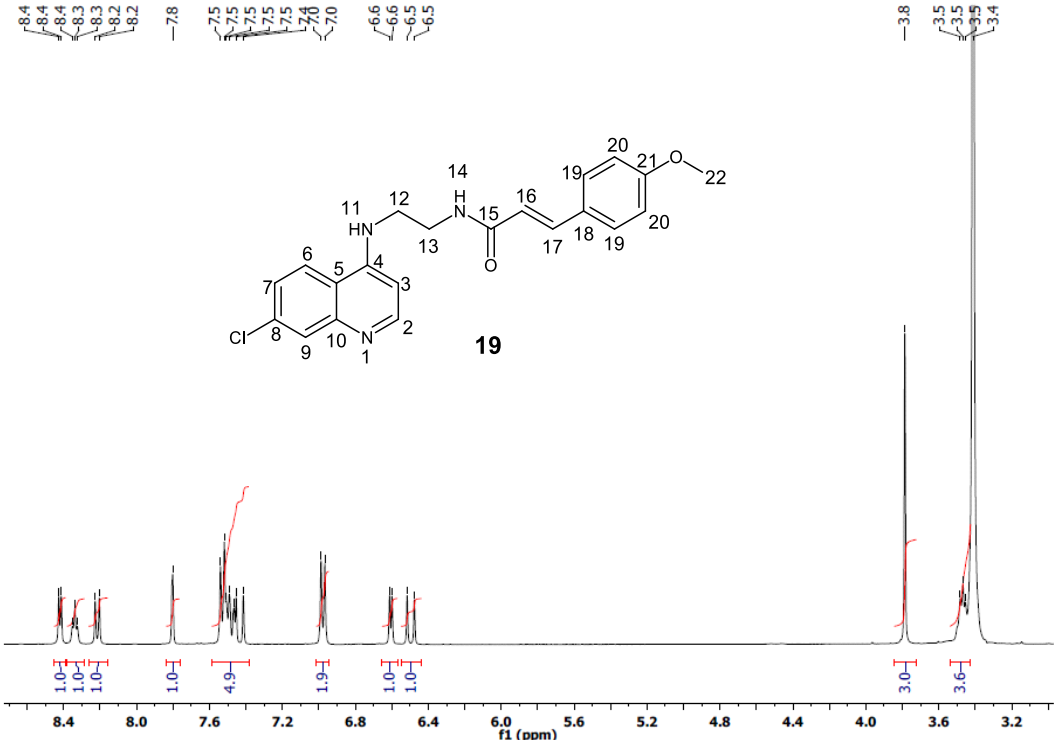

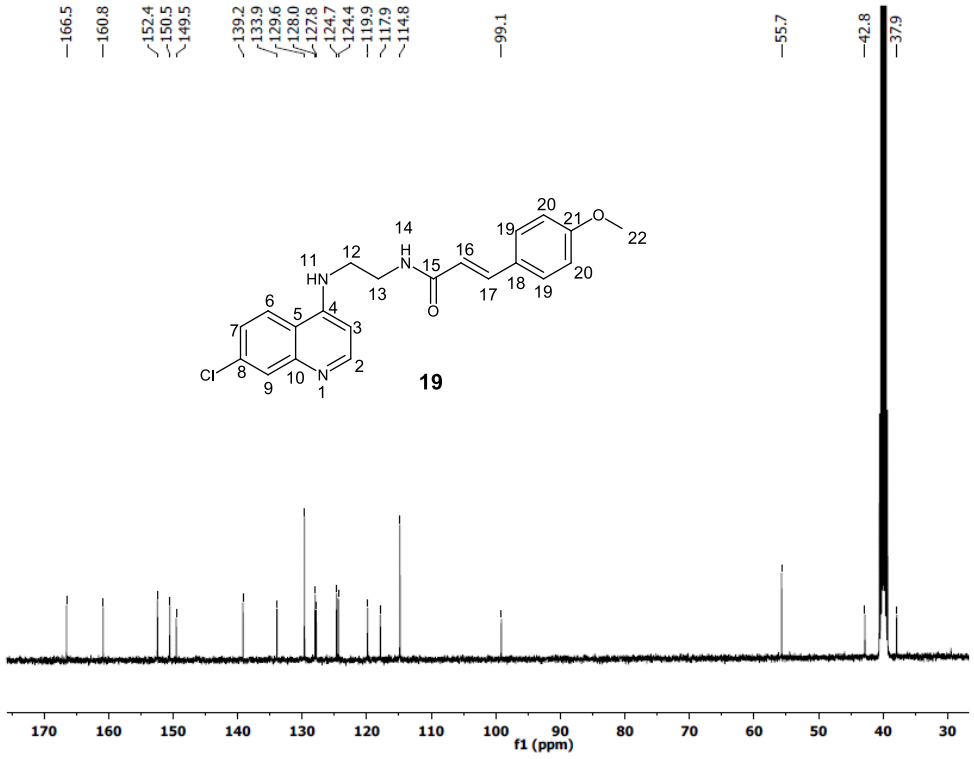

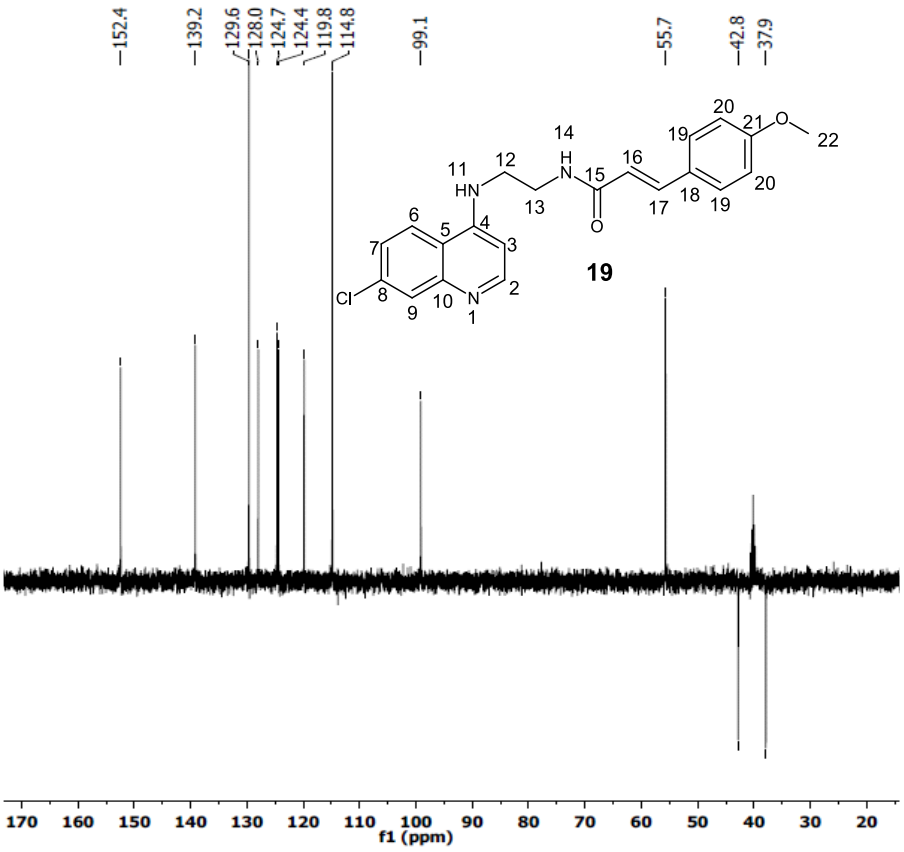

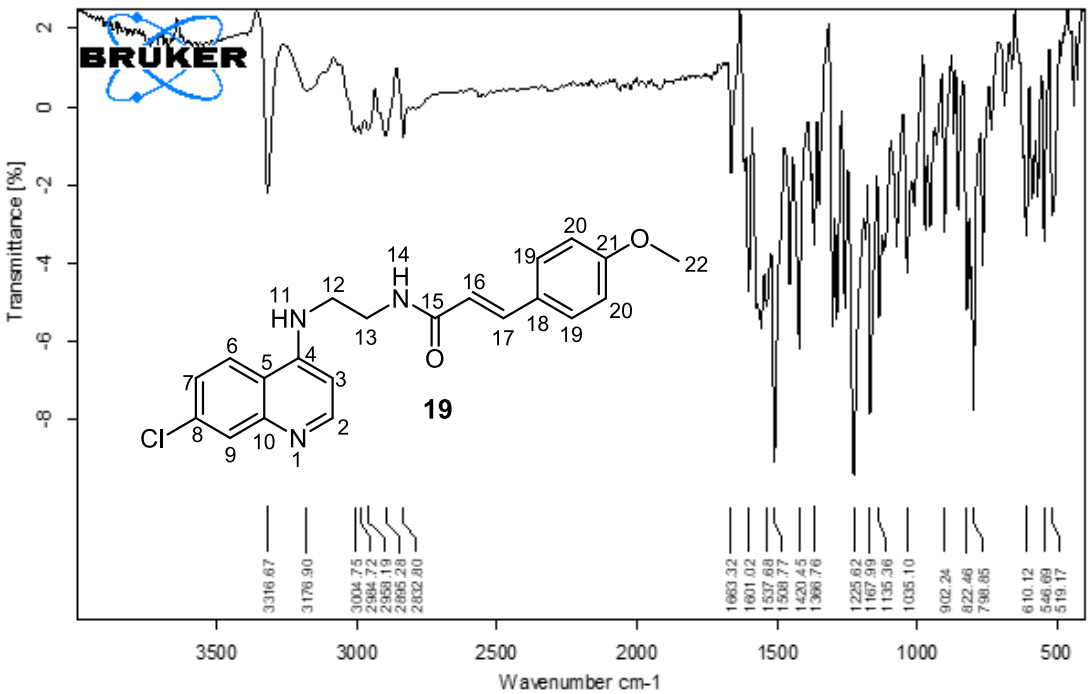

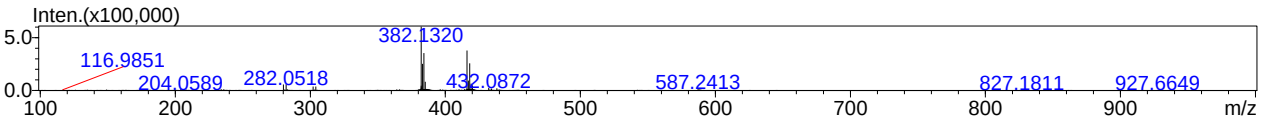

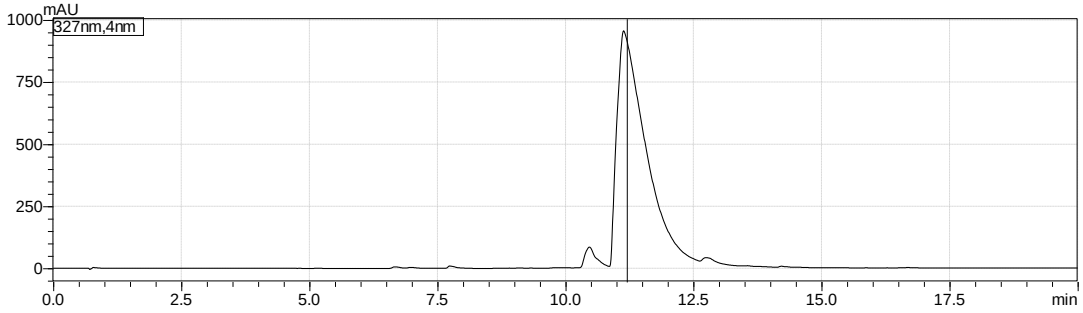

8.2. IR, Chromatogram and Mass spectrum of (E)-N-(2-((7-chloroquinolin-4-yl)amino)ethyl)-3-(furan-2-yl)acrylamide (23)

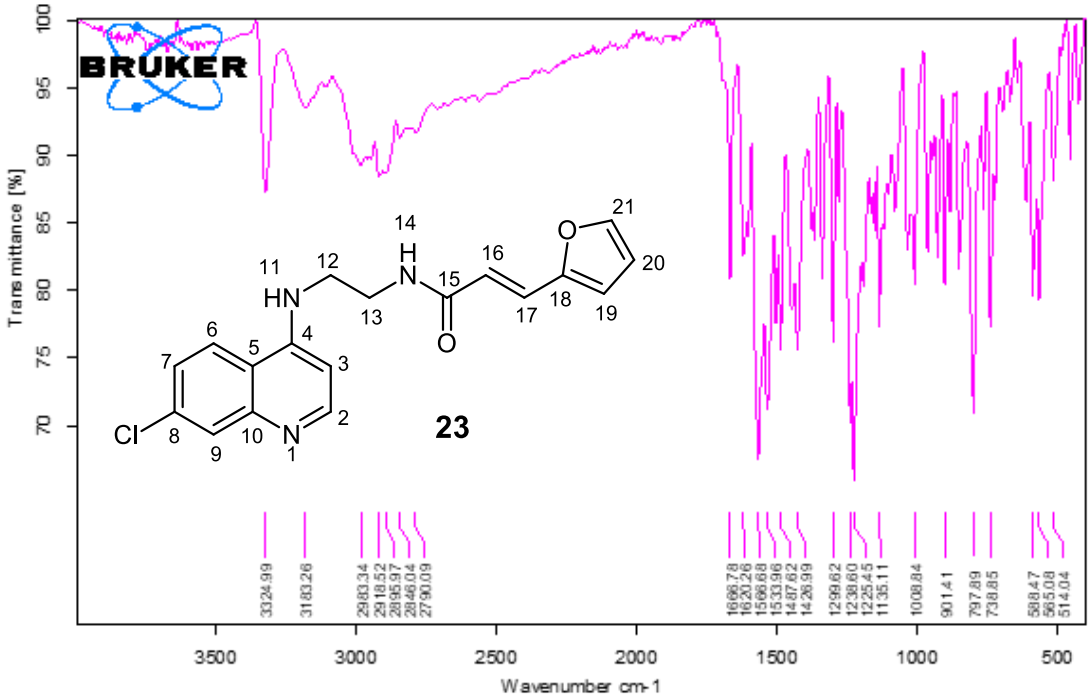

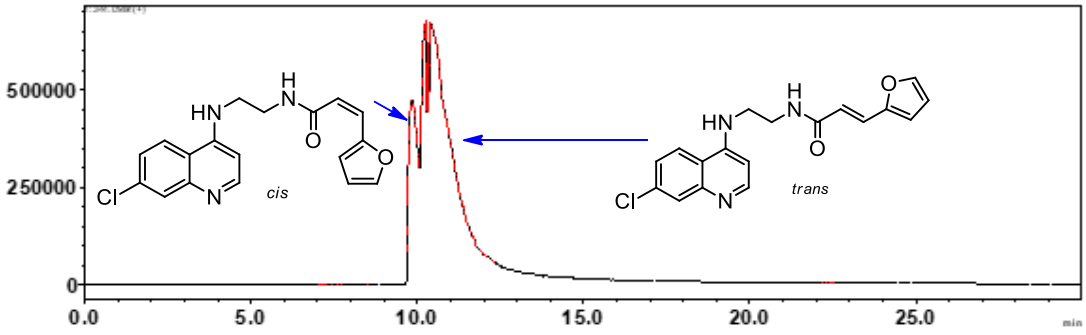

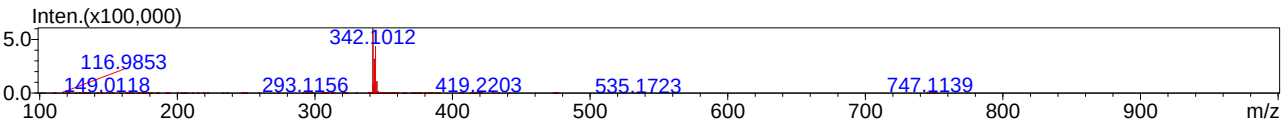

8.3 ^{1}H, ^{13}C, DEPT NMR spectra, IR, Chromatogram and mass spectrum of (E)-3-(benzo[d][1,3]dioxol-5-yl)-N-(2-((7-chloroquinolin-4-yl)amino)ethyl)acrylamide (24)

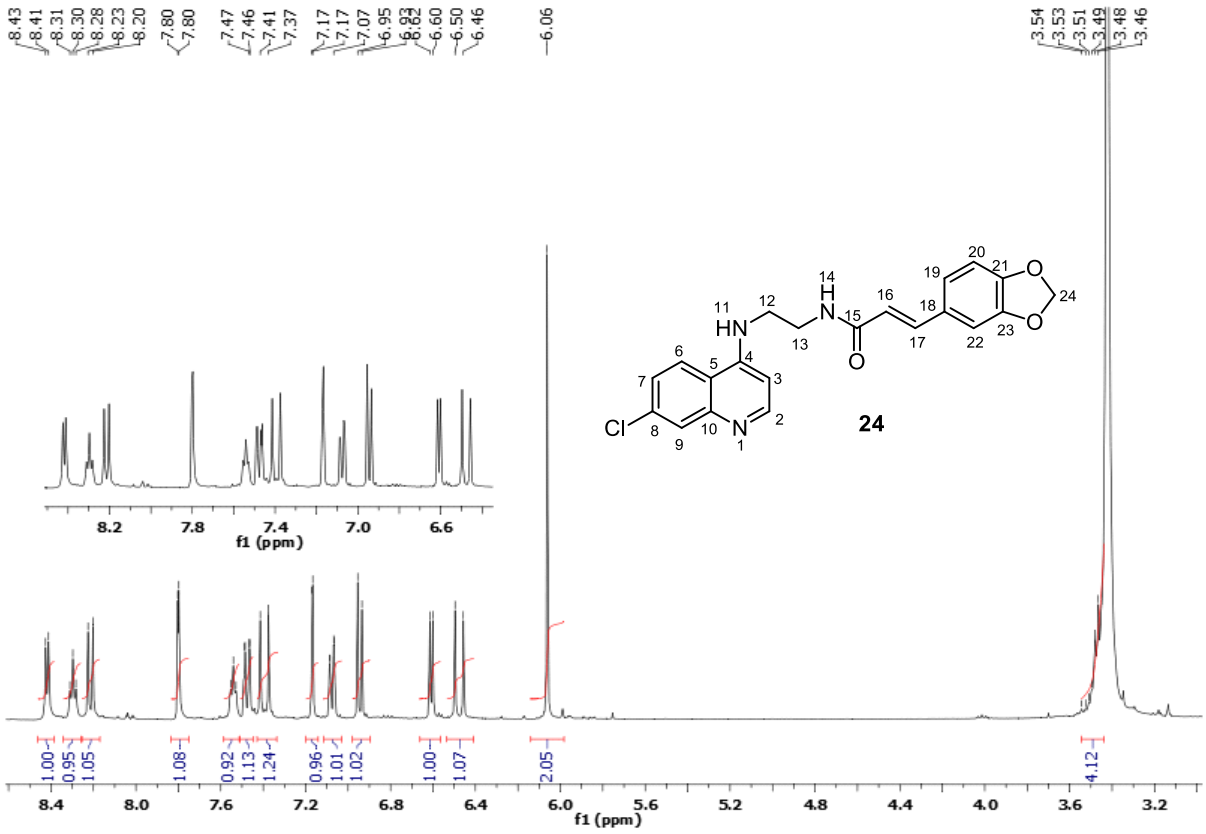

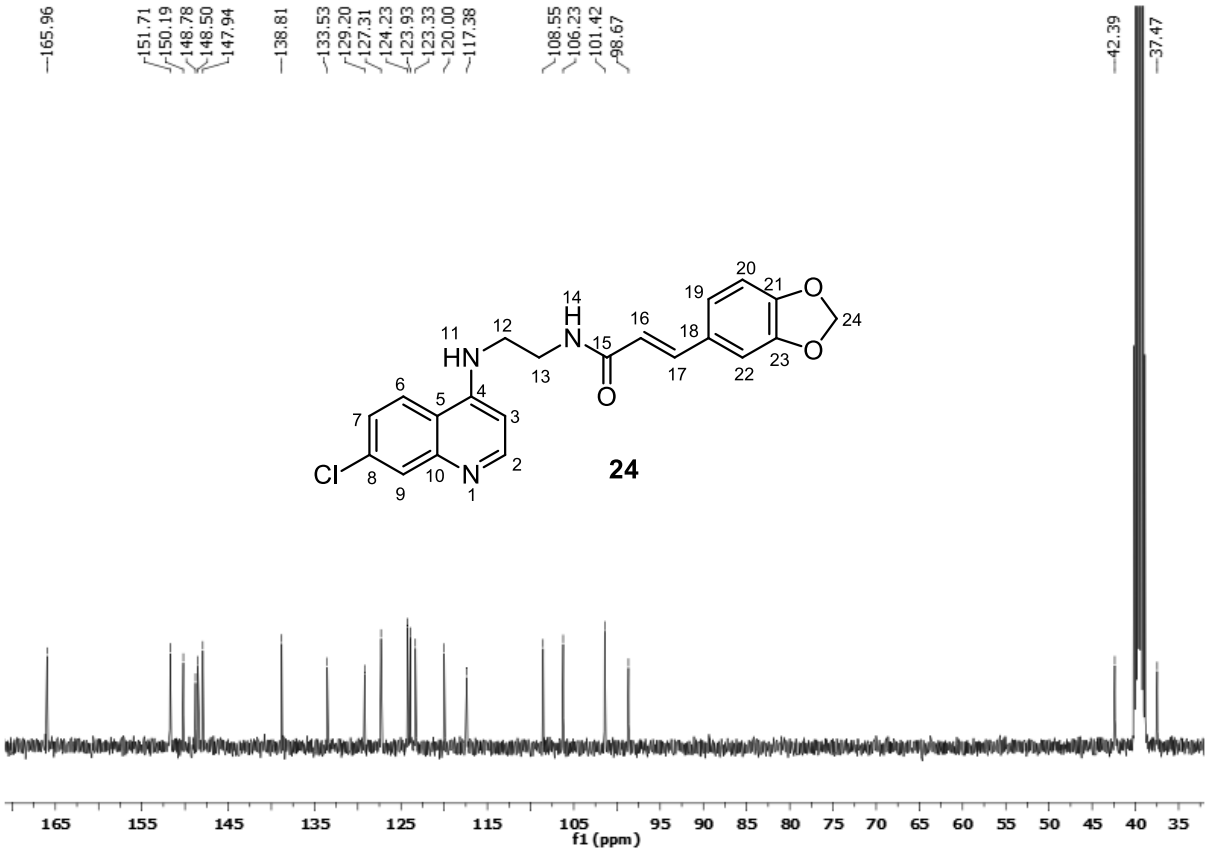

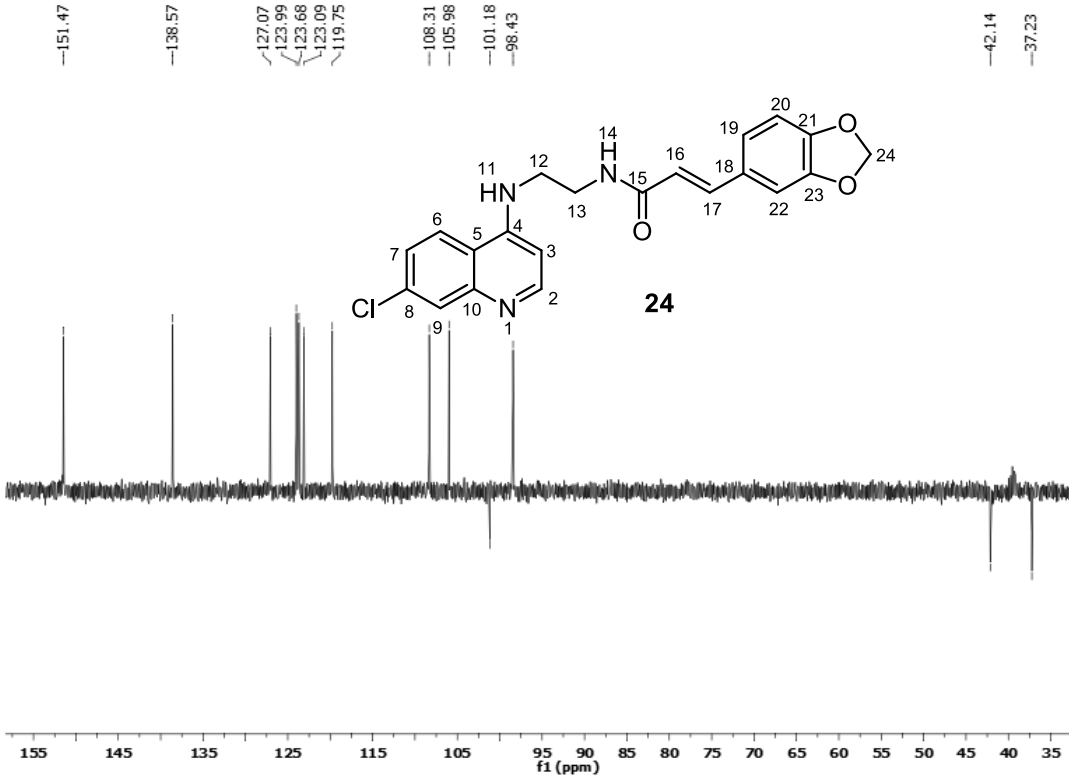

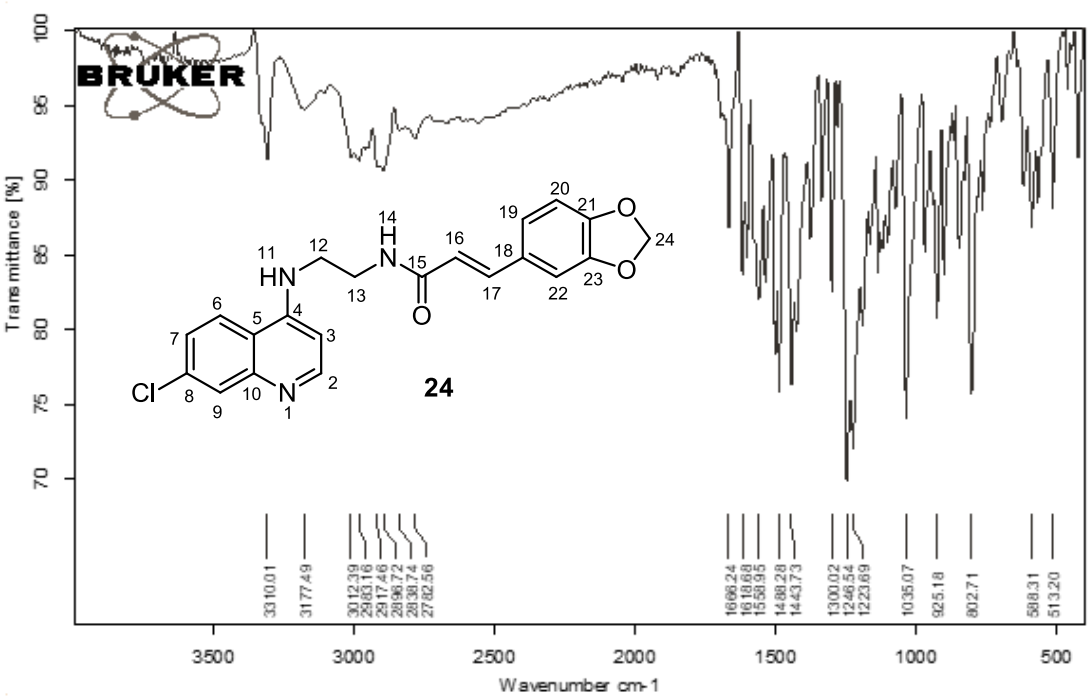

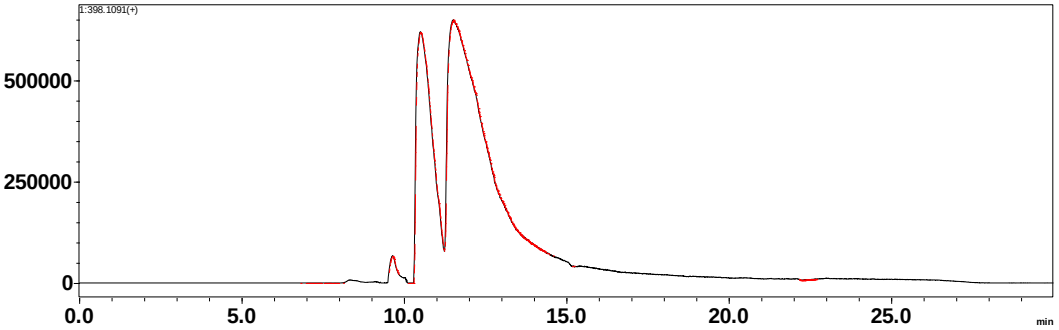

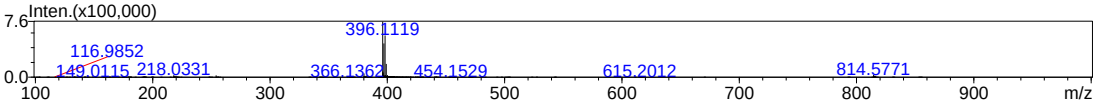

8.4 IR, Chromatogram and Mass spectrum of N-(1-((7-chloroquinolin-4-yl)amino)propan-2-yl)cinnamamiden (25).

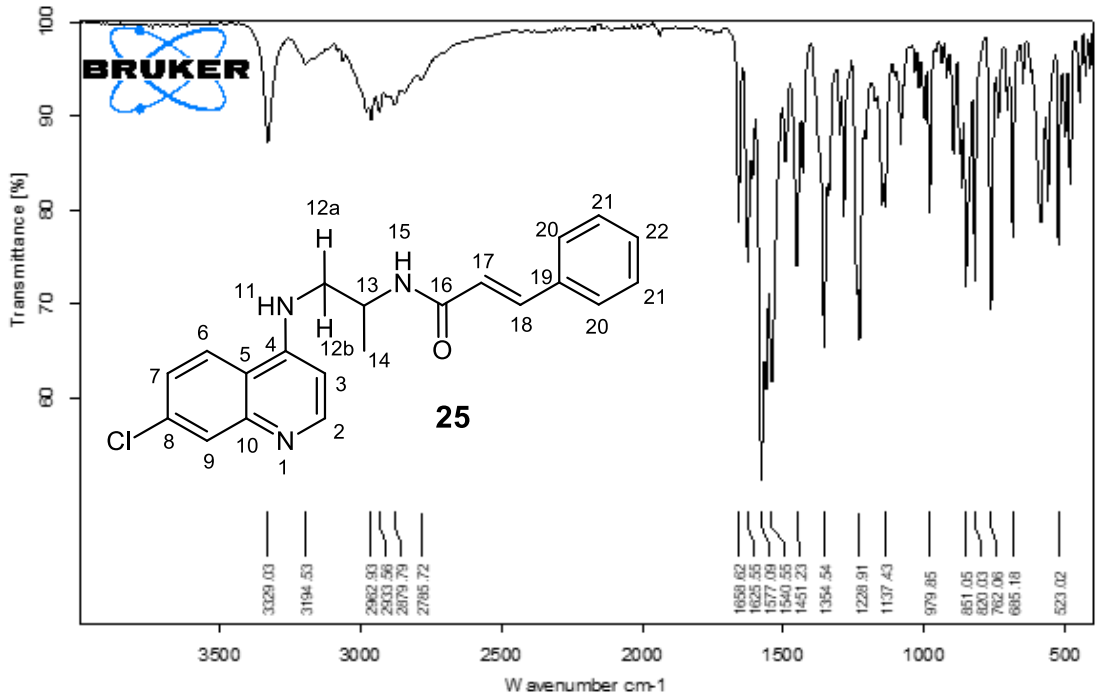

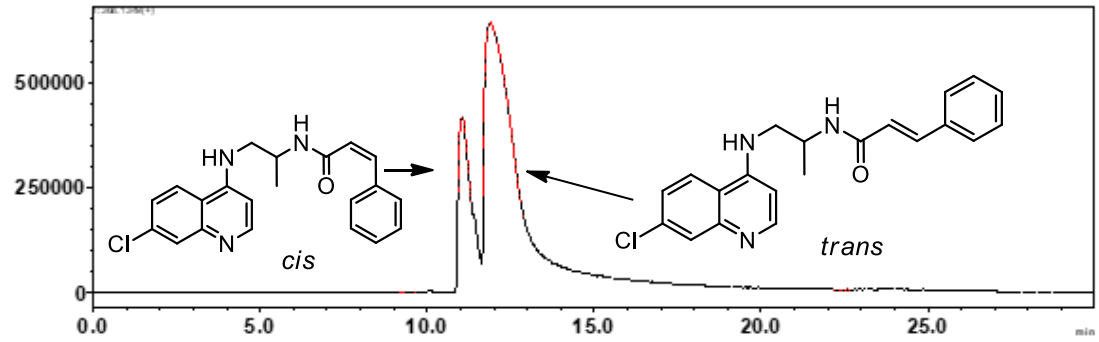

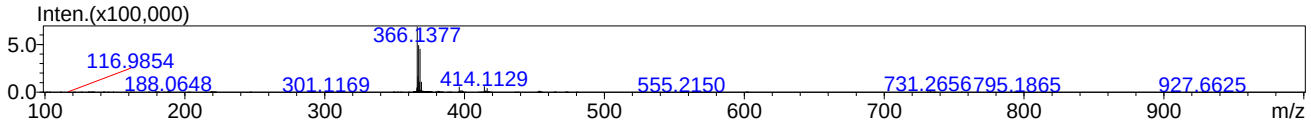

8.5 ^{1}H, ^{13}C and DEPT NMR spectra of N^{1}-(7-chloroquinolin-4-yl) propane-1,2-diamine (3)

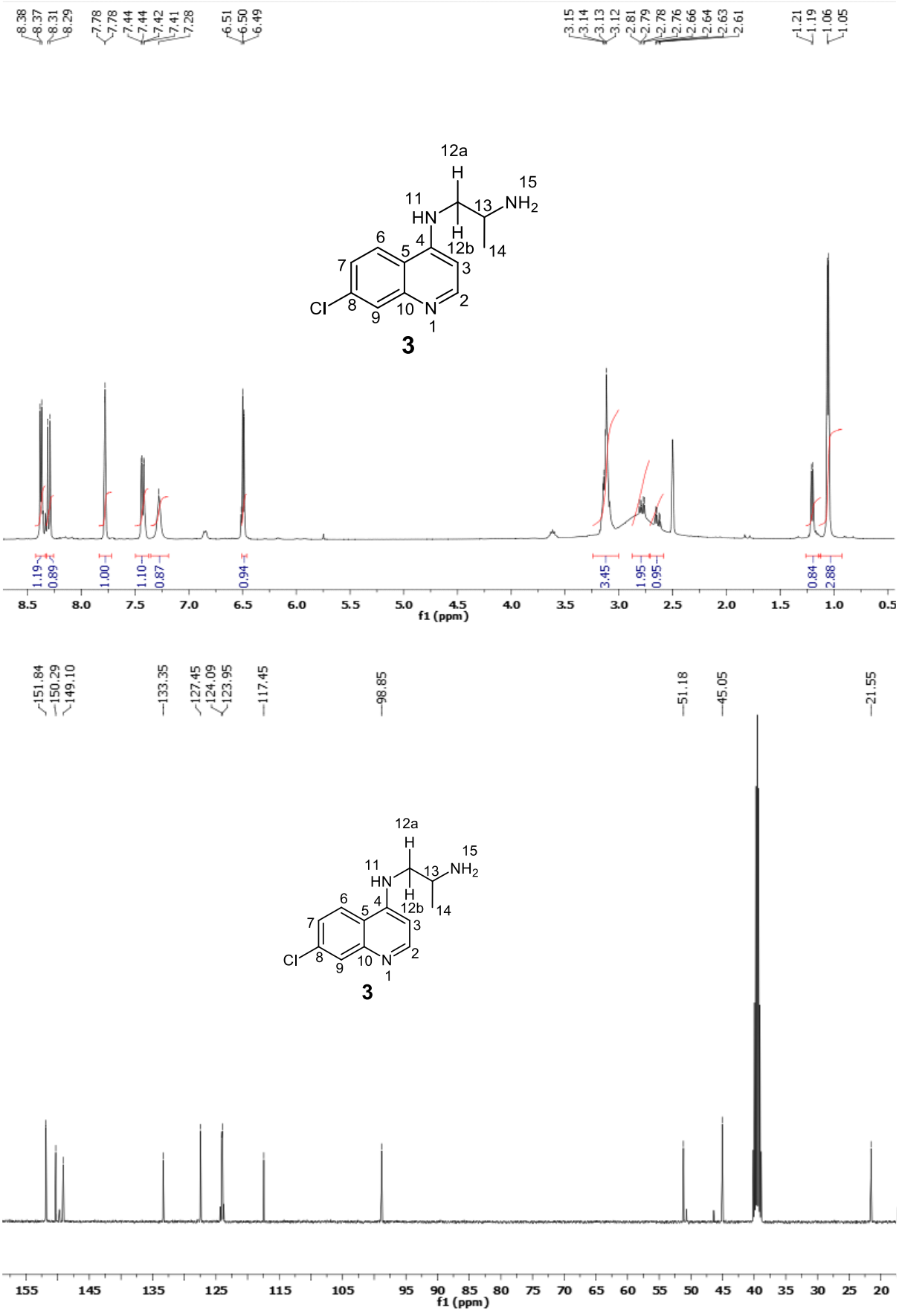

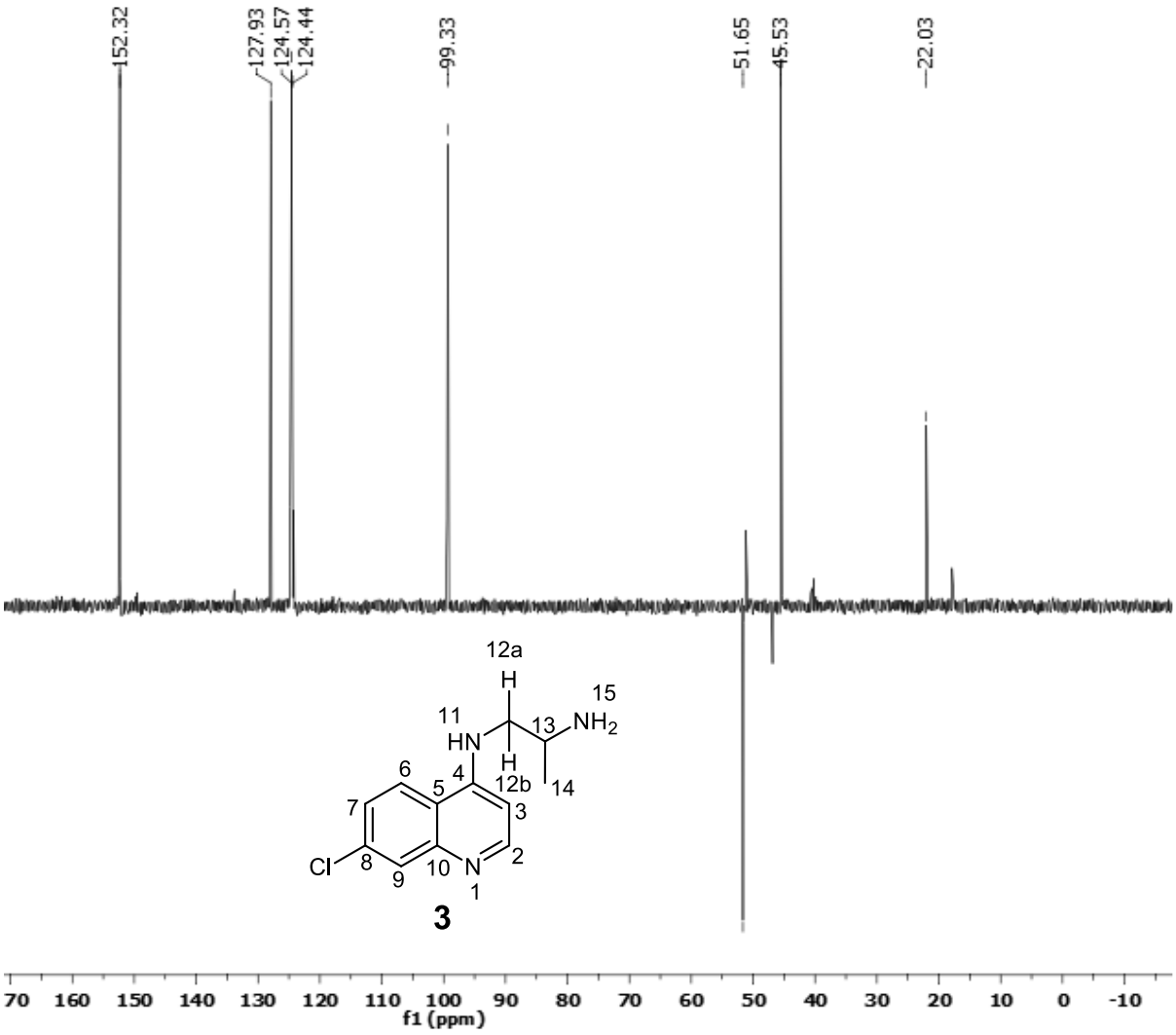

8.6 1H, 13C, DEPT NMR spectra, IR, Chromatogram and mass spectrum of (E)-3-(4-chlorophenyl)-N-(1-((7-chloroquinolin-4-yl)amino)propan-2-yl)acrylamide (26)

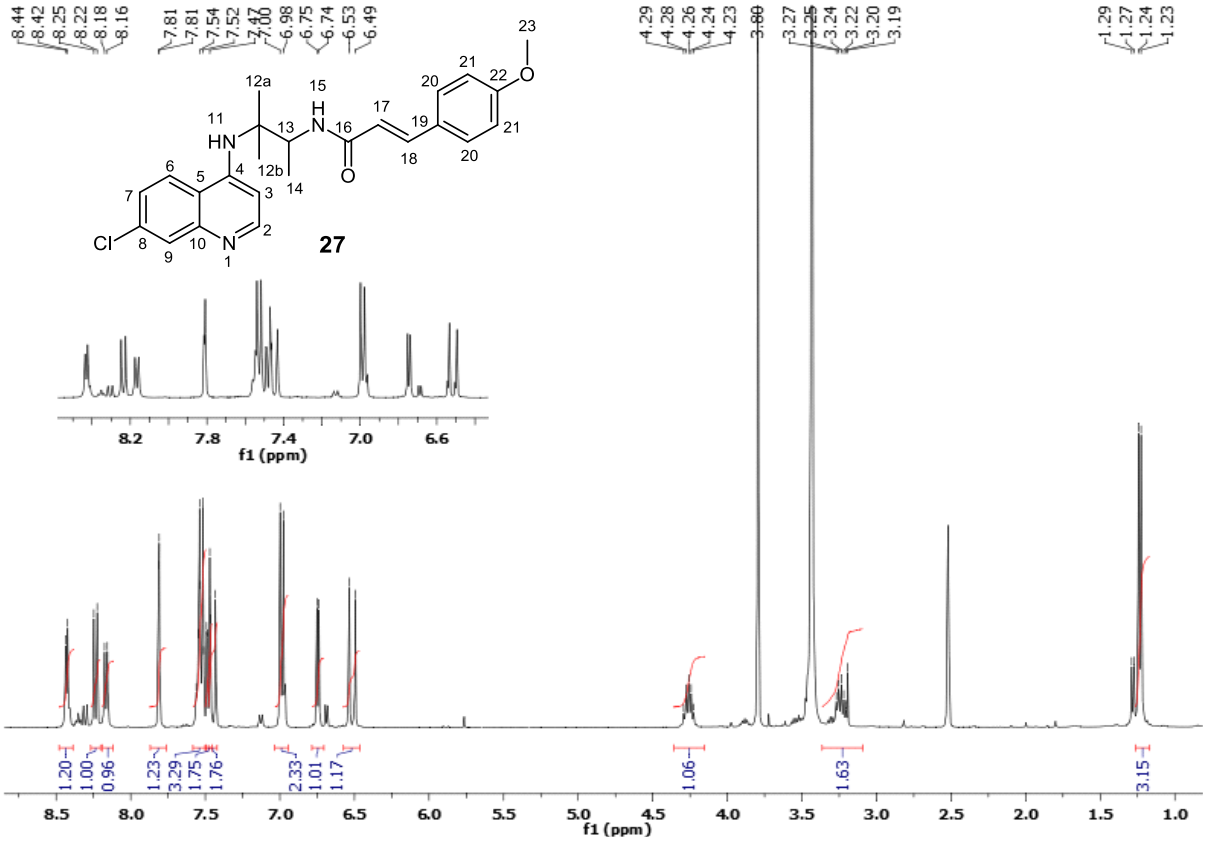

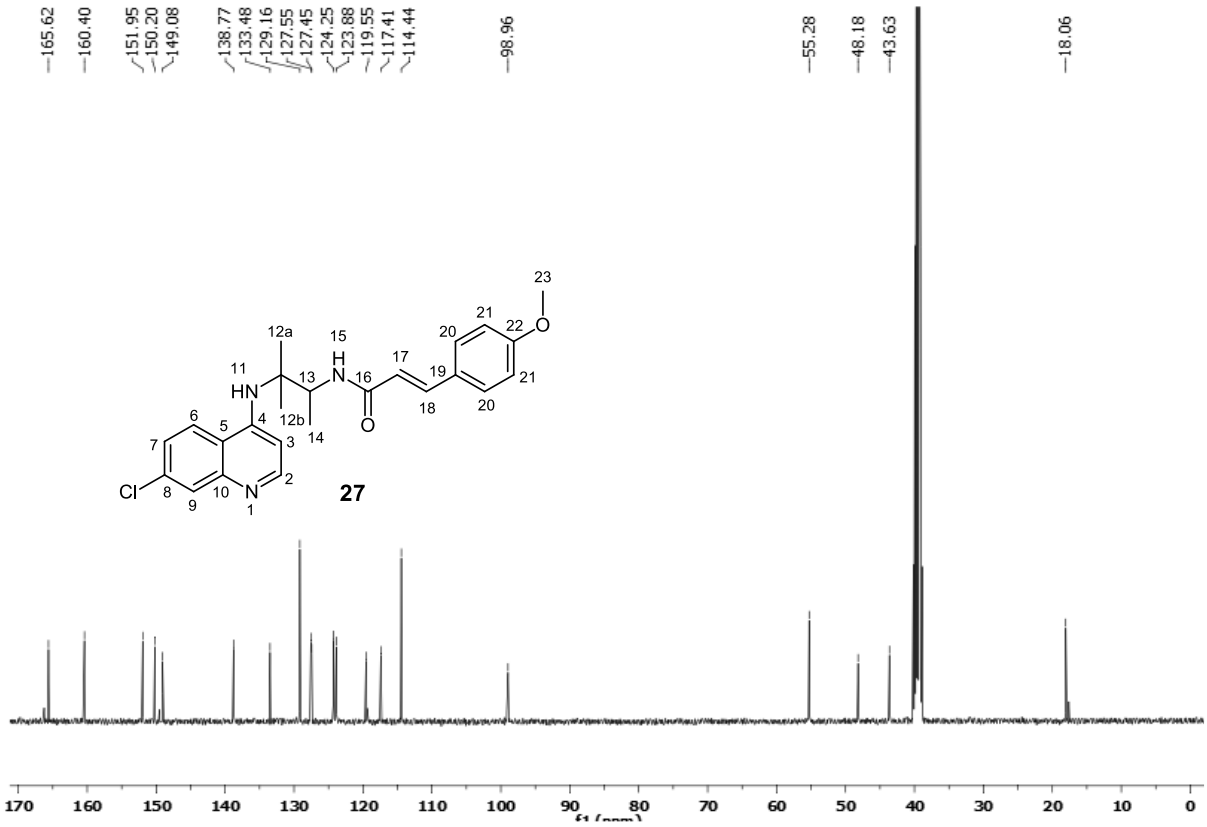

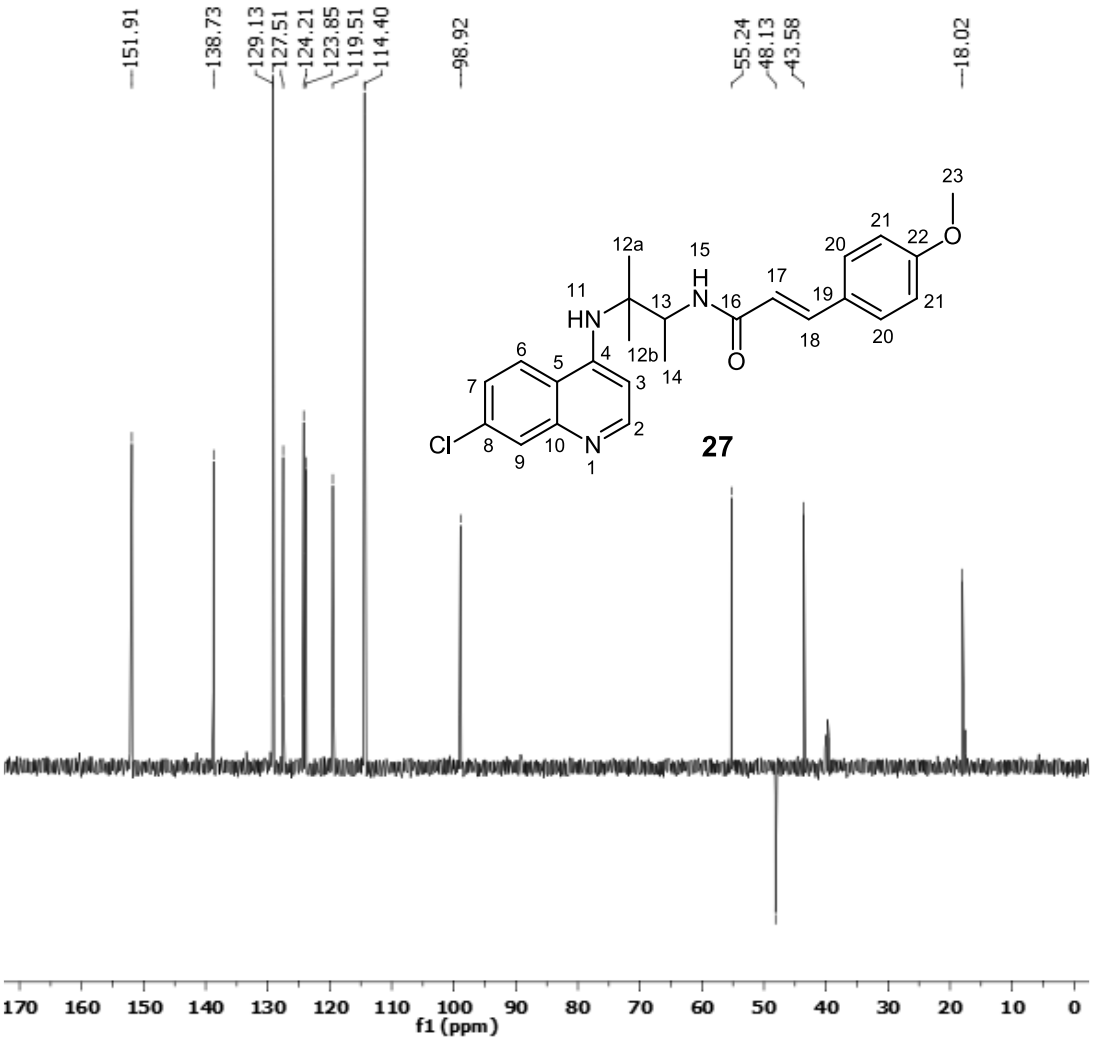

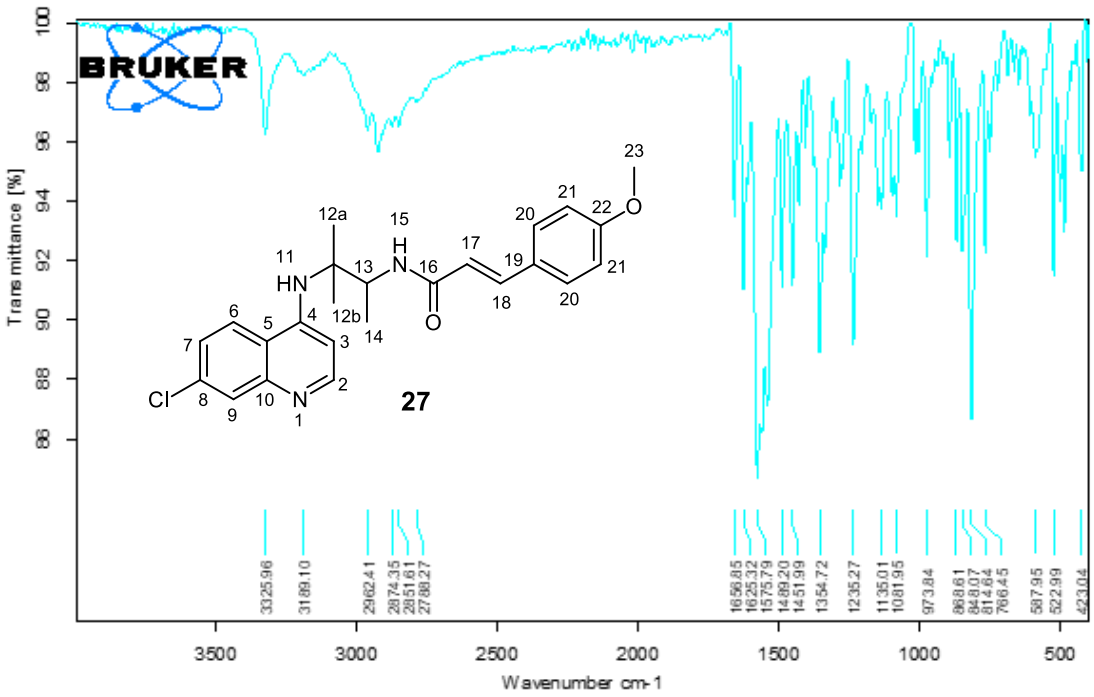

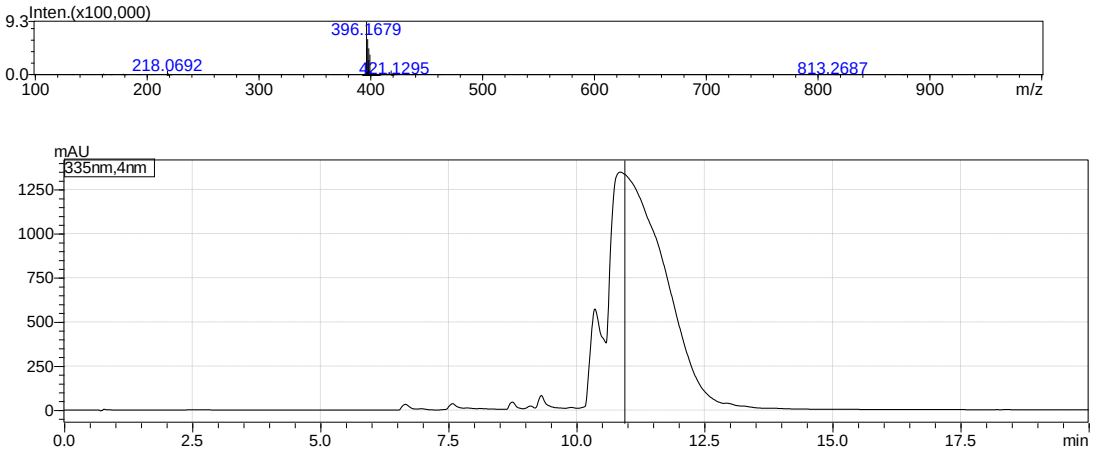

8.7 ^{1}H, ^{13}C and DEPT NMR spectra of N^{1}-(7-chloroquinolin-4-yl) propane-1,3-diamine (2)

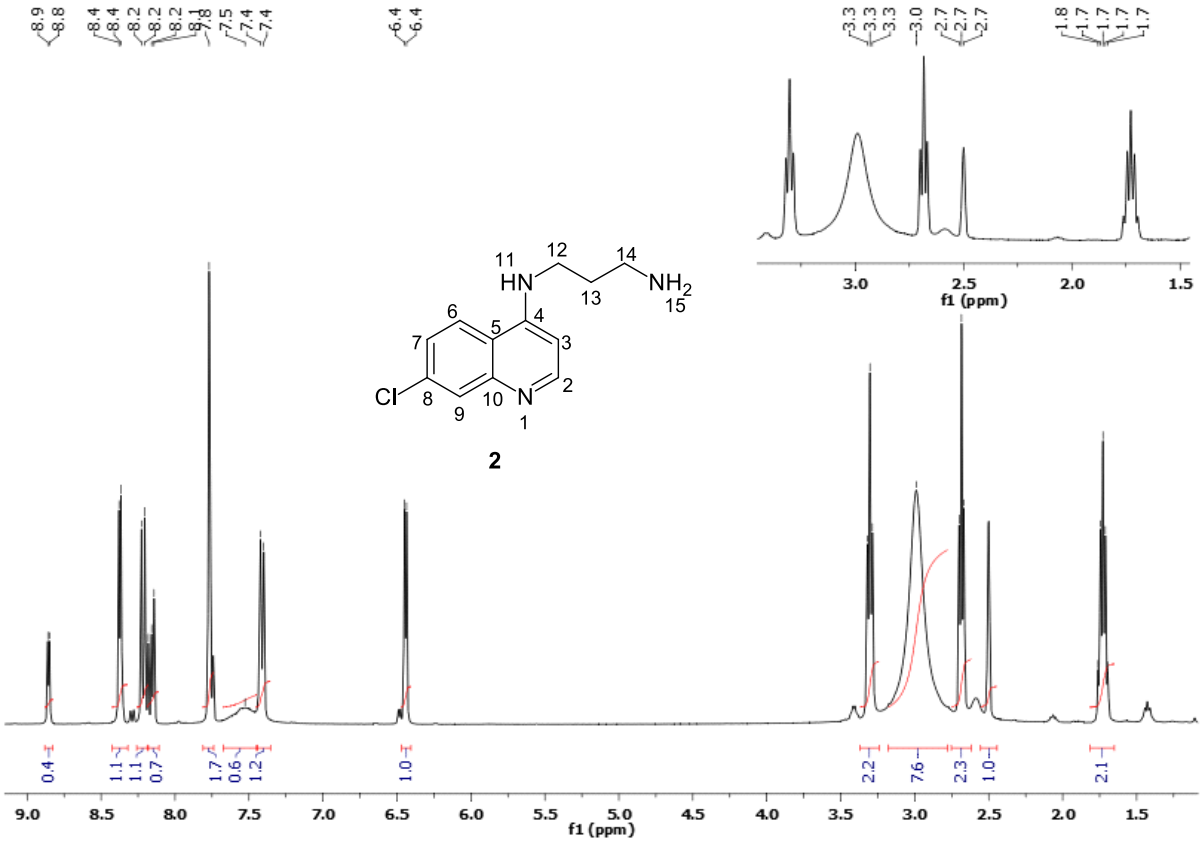

2

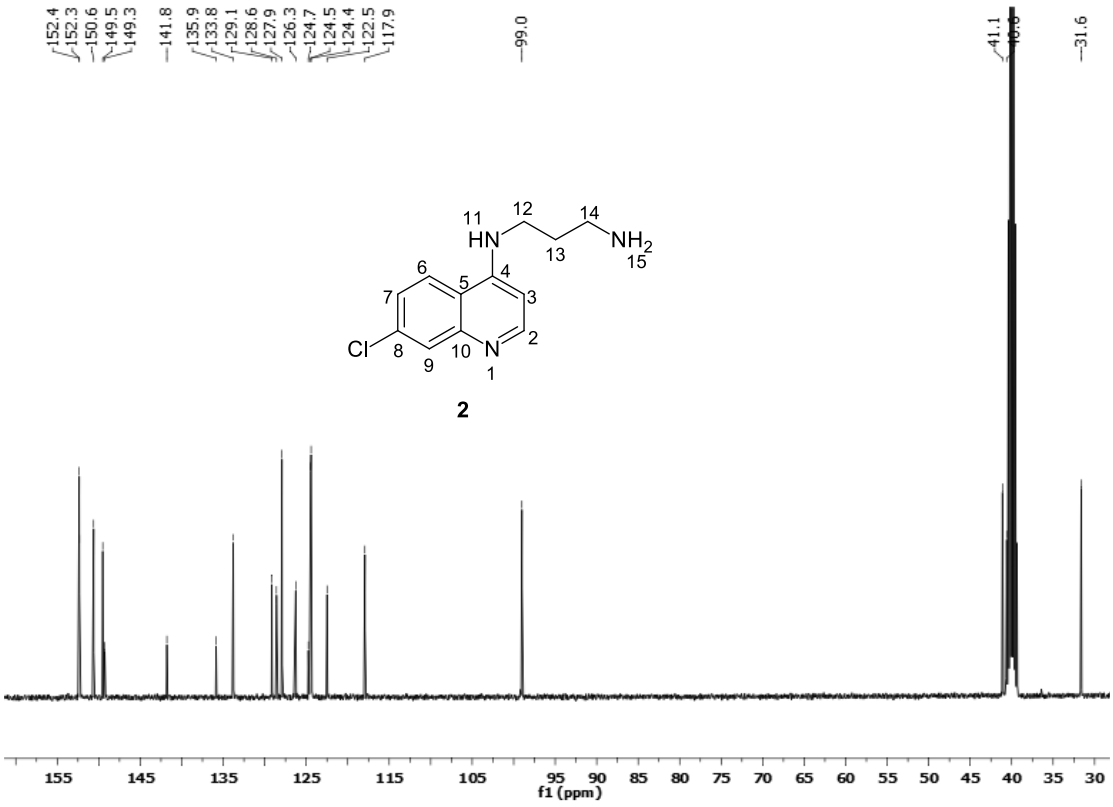

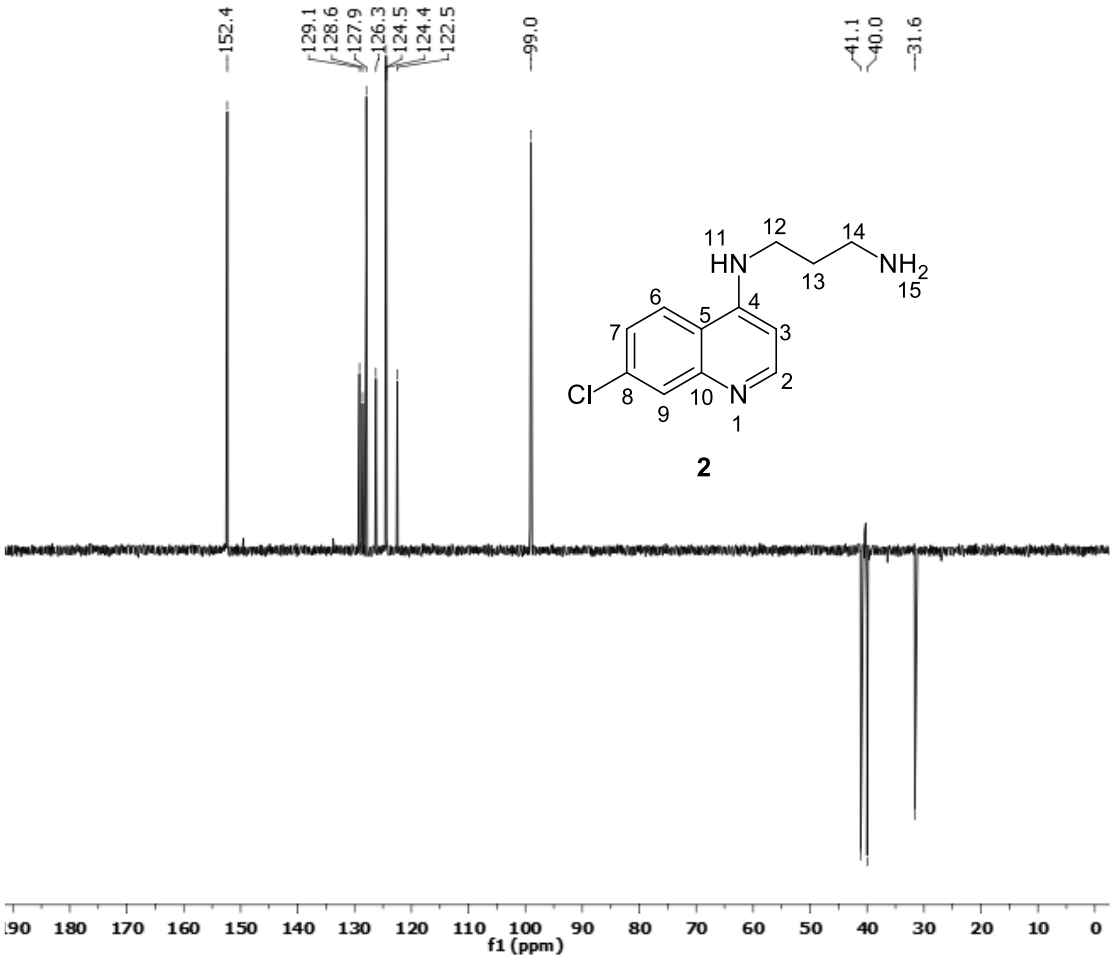

8.8 1H, 13C, DEPT NMR spectra, IR, Chromatogram and mass spectrum of (E)-N-(3-((7-chloroquinolin-4-yl)amino)propyl)-3-(4-methoxyphenyl)acrylamide (29)

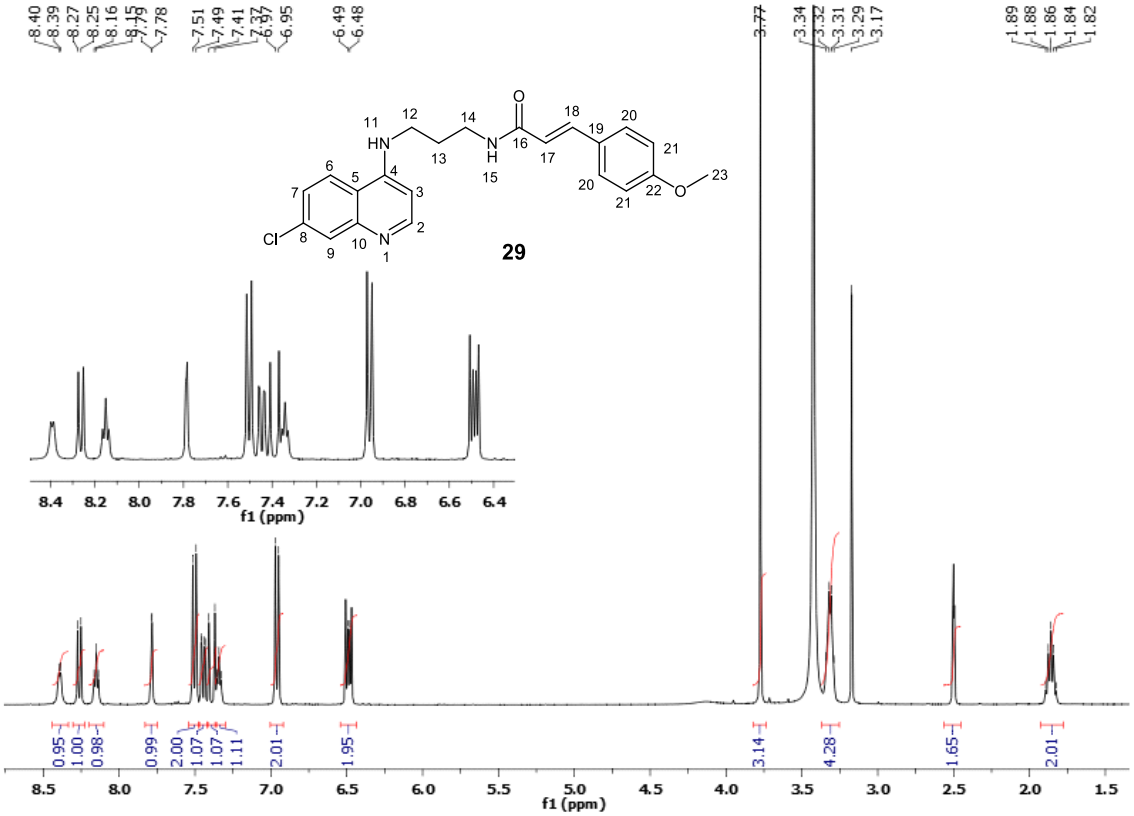

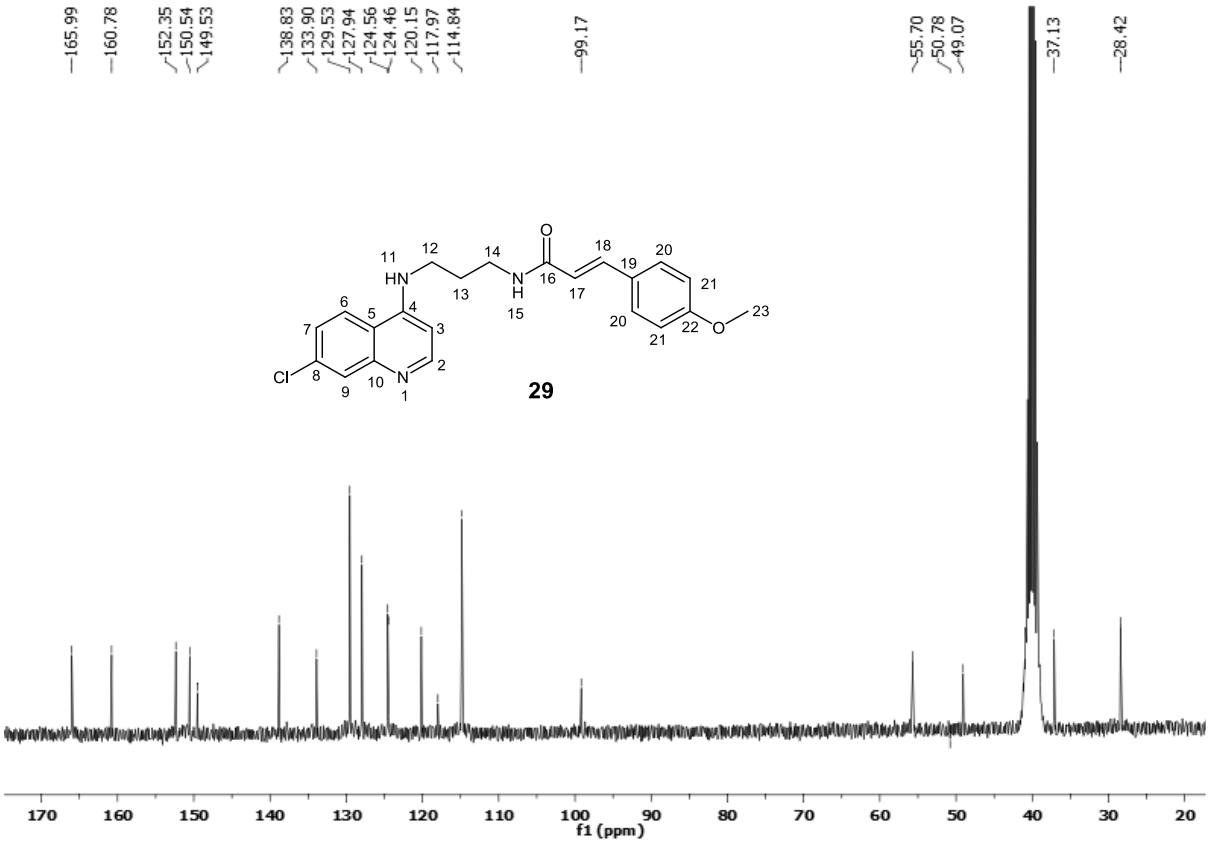

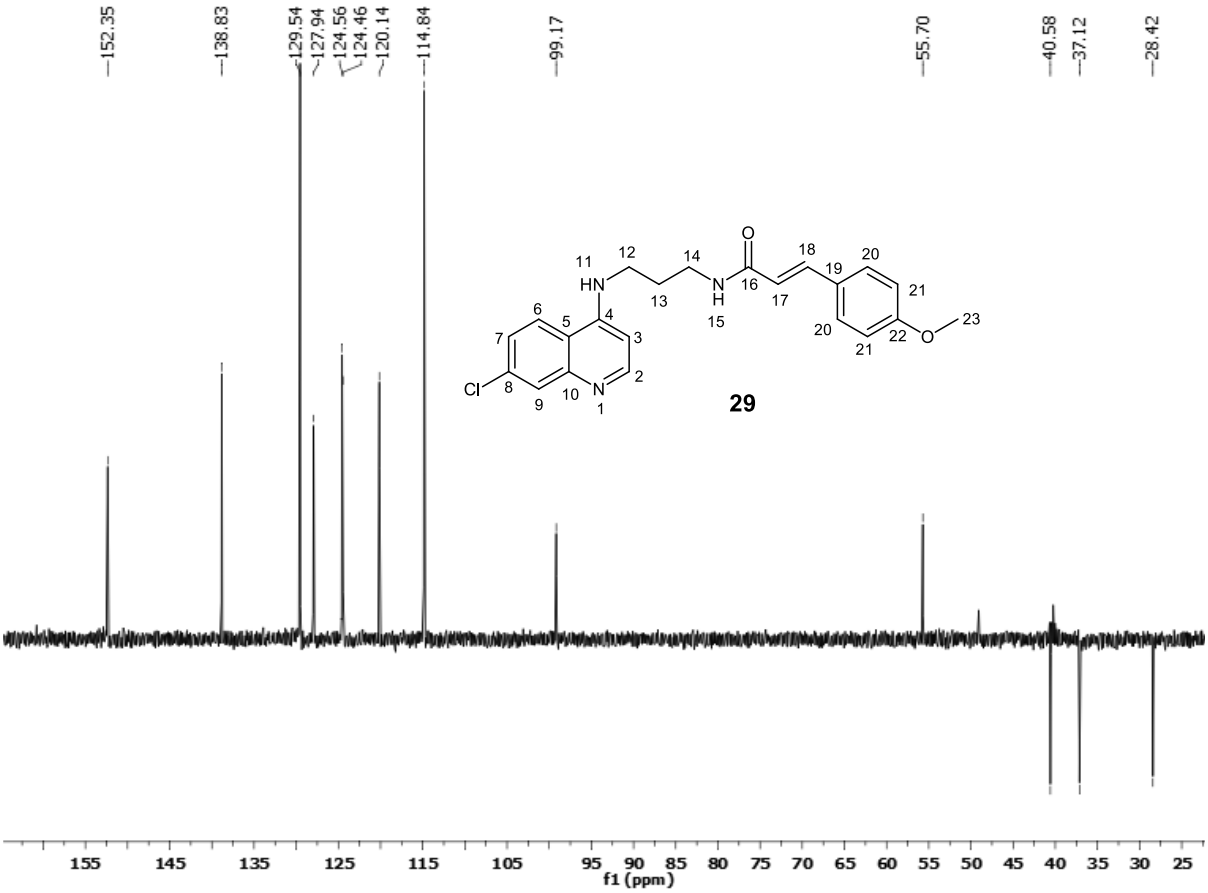

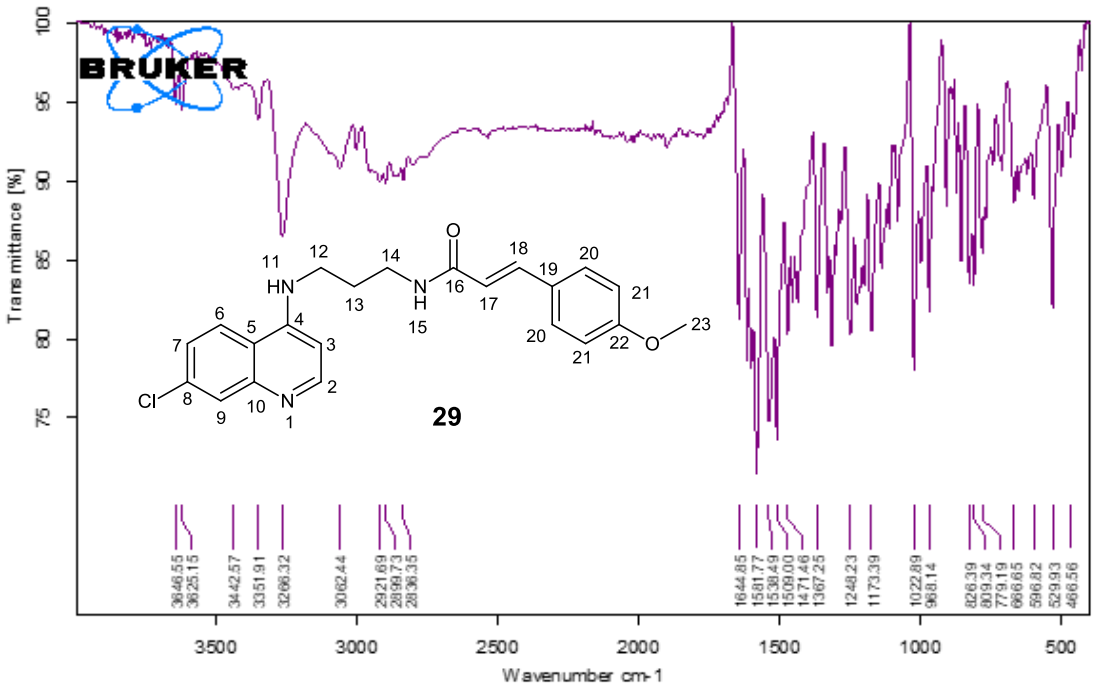

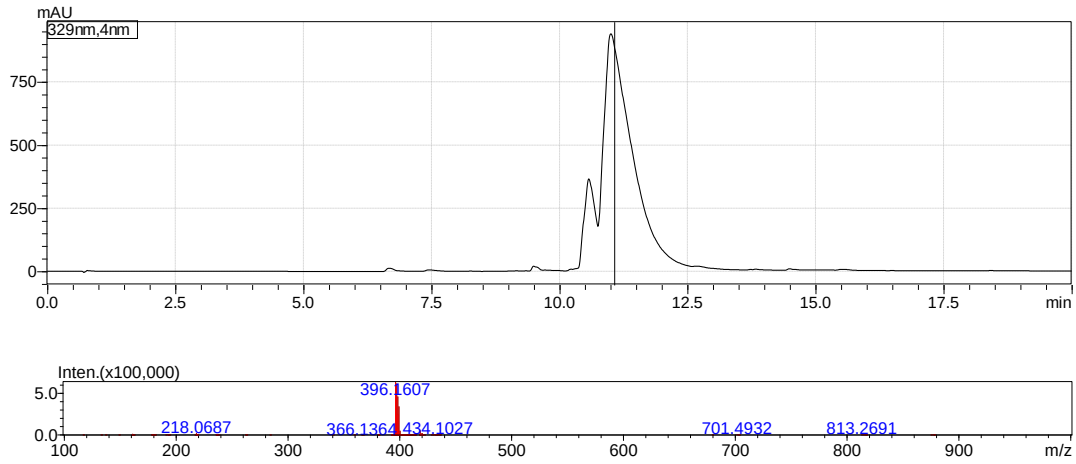

8.9 ^{1}H, ^{13}C and DEPT NMR spectra of N^{1}-(7-chloroquinolin-4-yl)hexane-1,6-diamine (5)

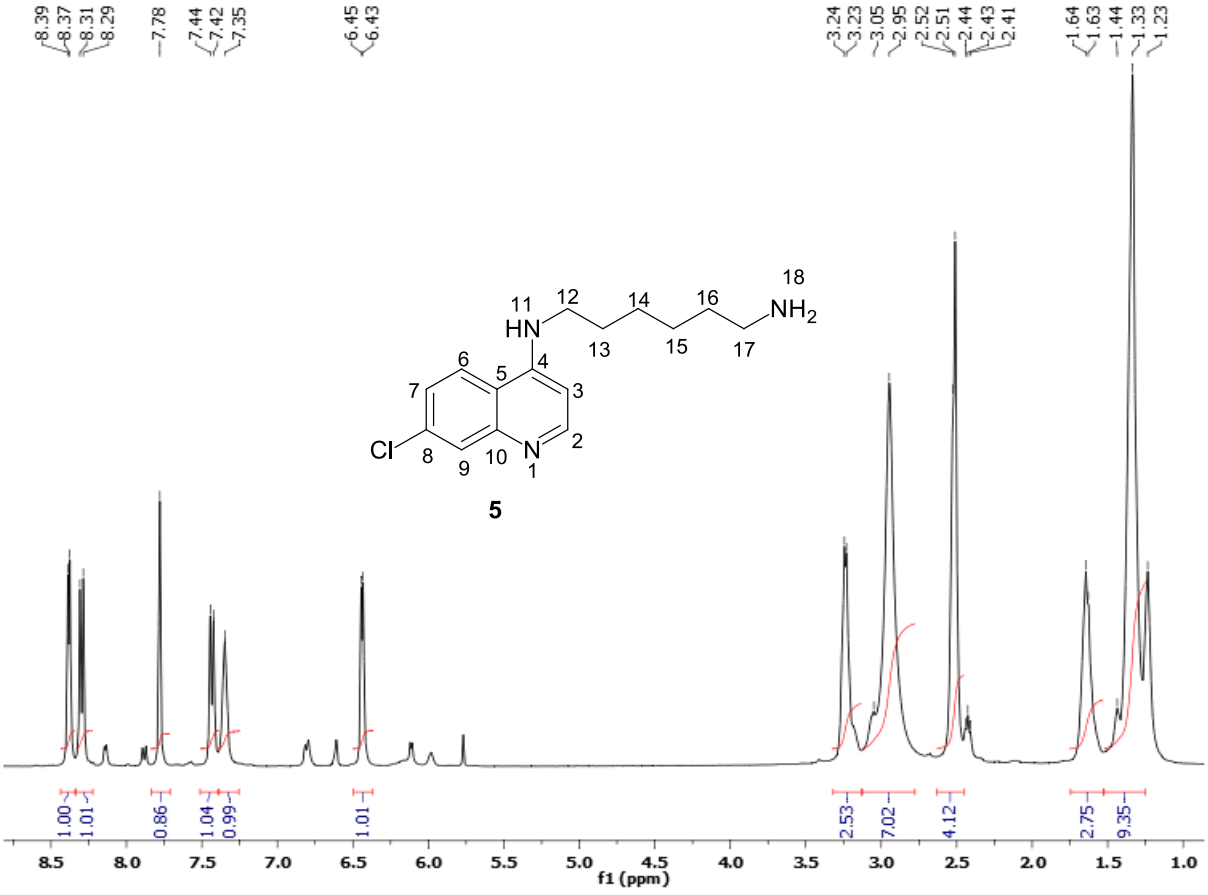

5

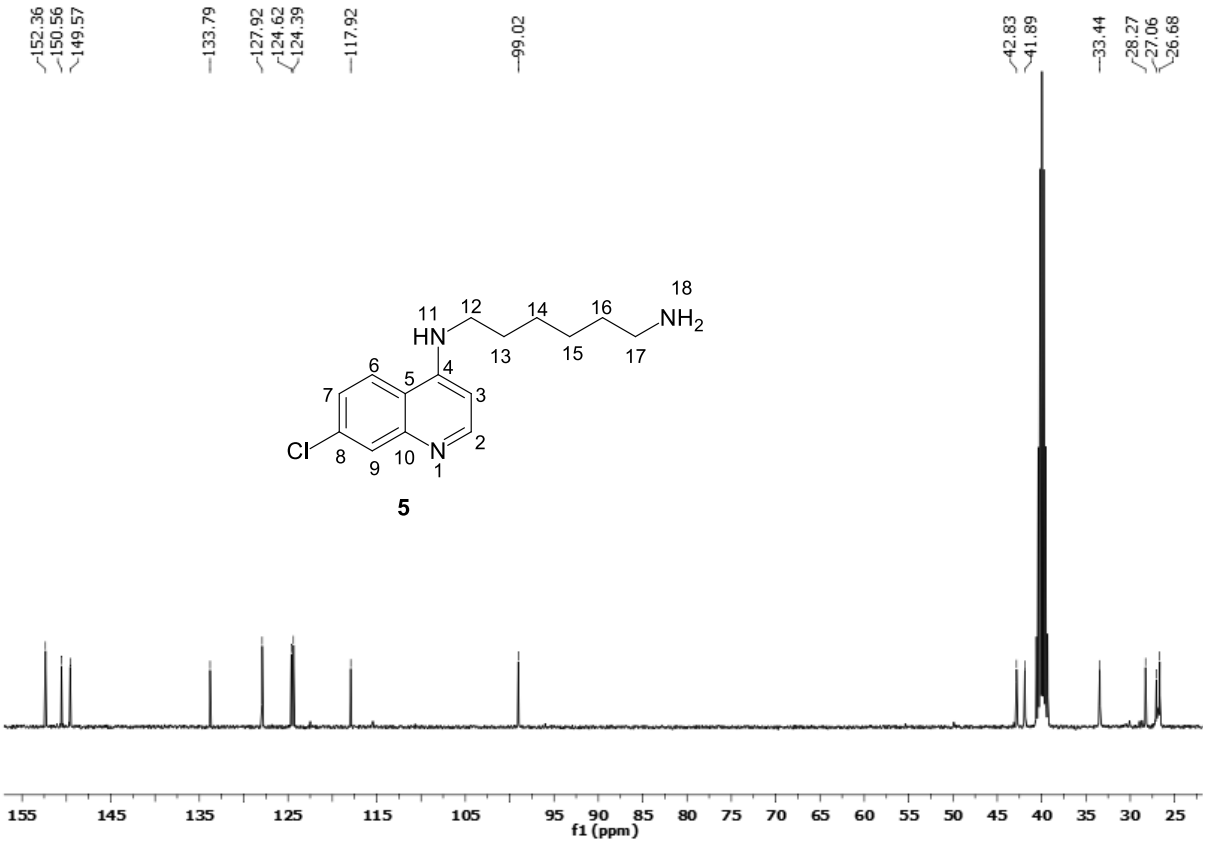

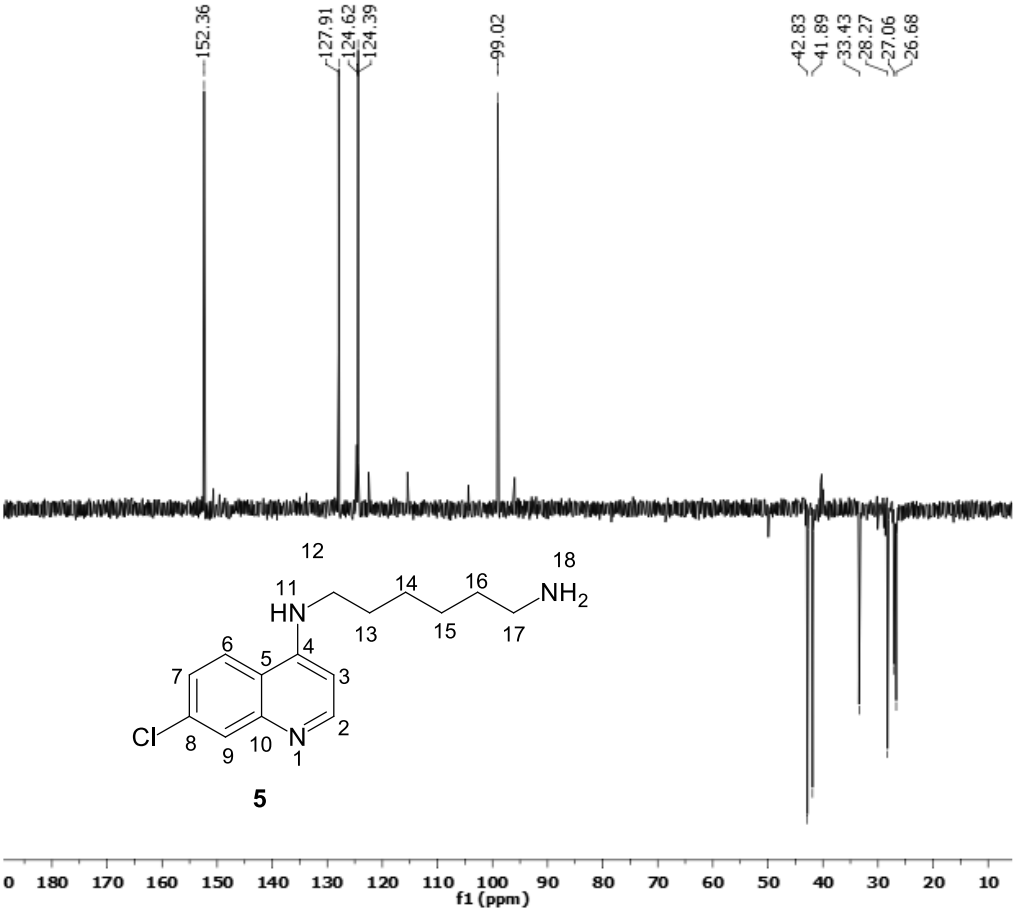

8.10 ^{1}H, ^{13}C, DEPT NMR spectra, IR, Chromatogram and mass spectrum of (E)-3-(4-chlorophenyl)-N-(6-((7-chloroquinolin-4-yl) amino) hexyl) acrylamide (32)

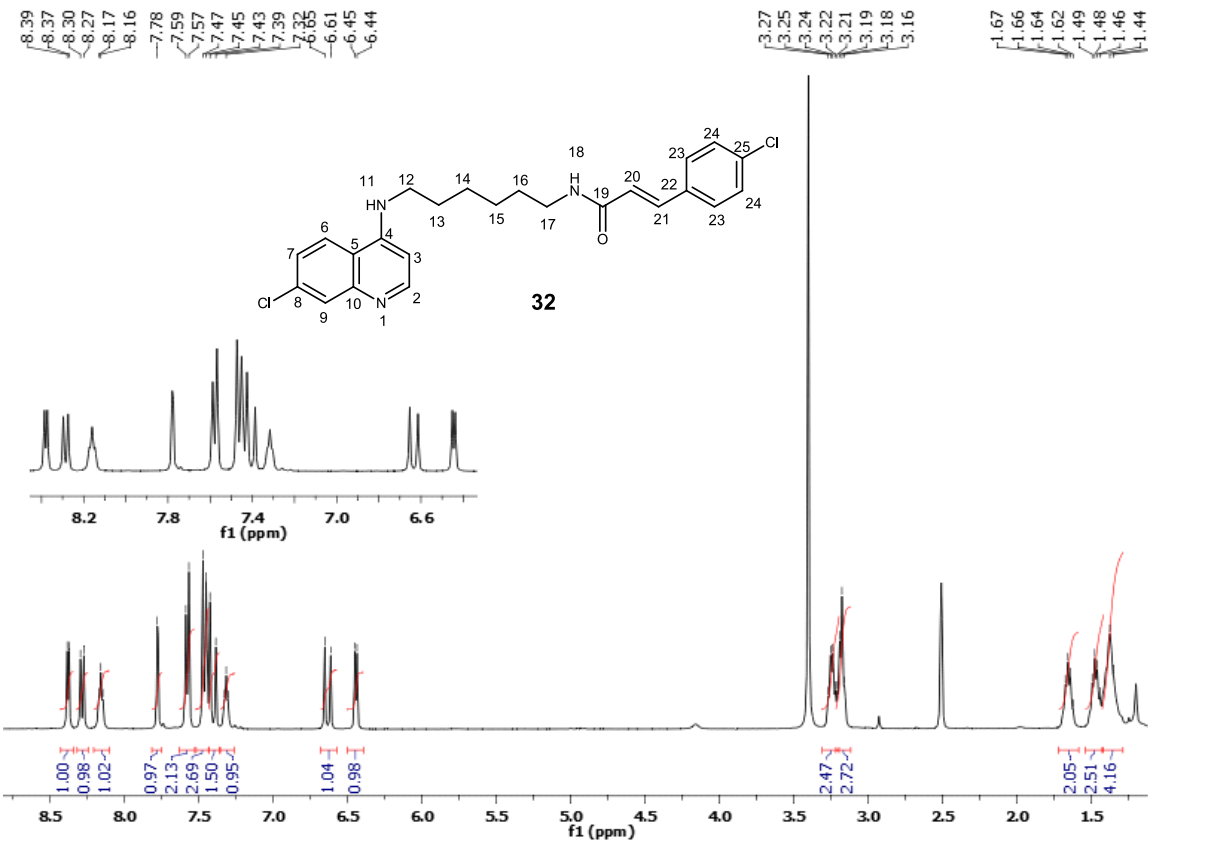

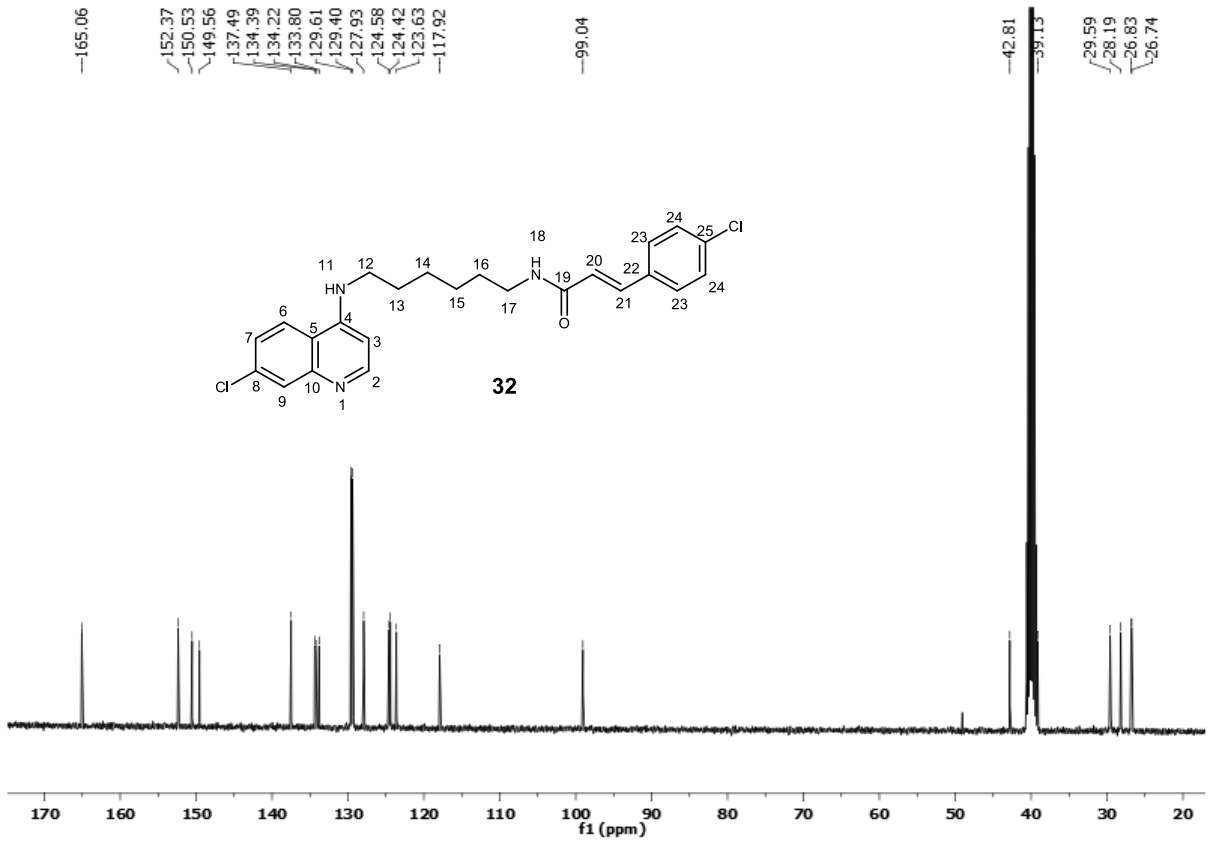

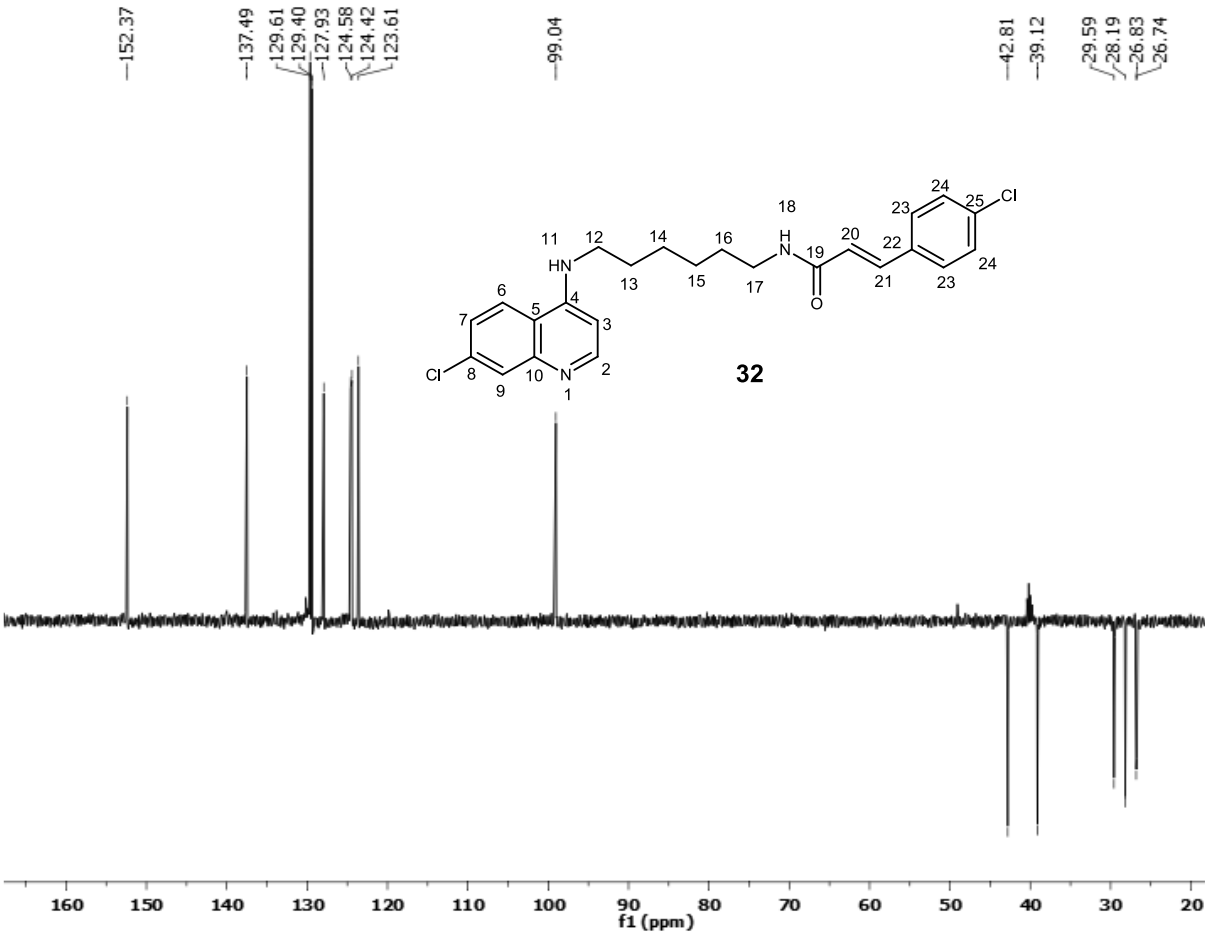

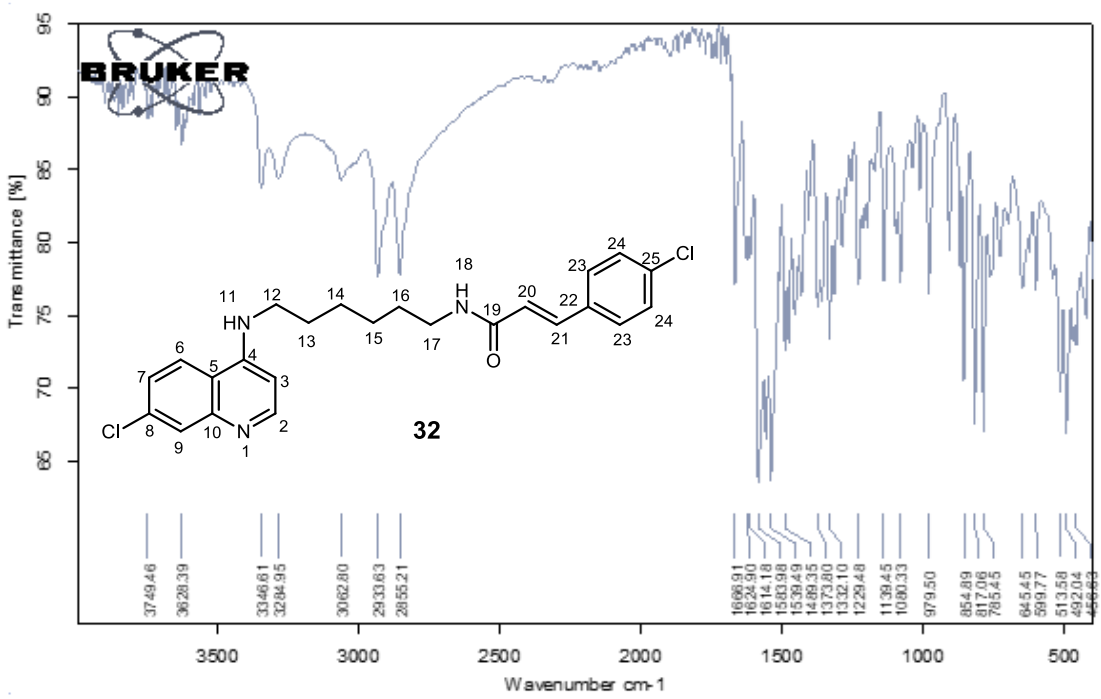

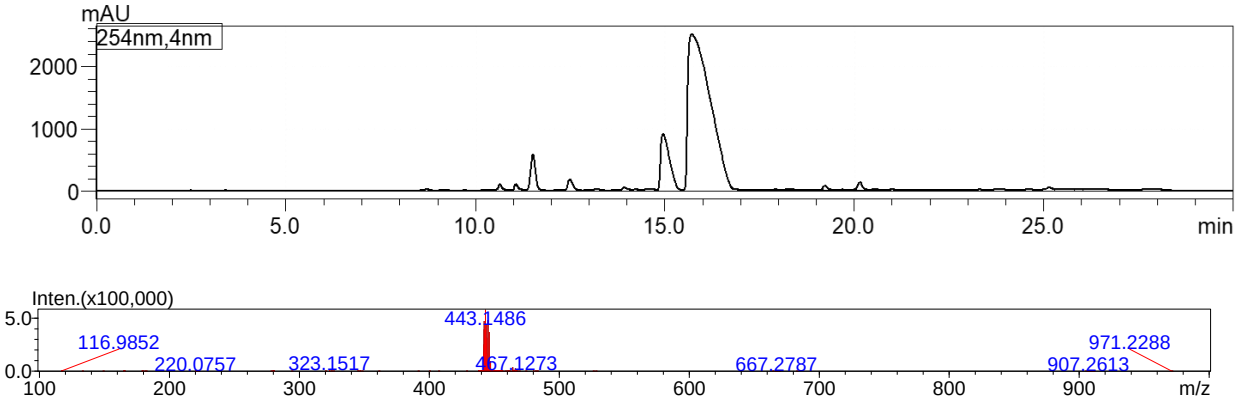

8.11, 13C, DEPT NMR spectra, IR, Chromatogram and mass spectrum of (E)-N-(6-((7-chloroquinolin-4-yl)amino)hexyl)-3-(4-nitrophenyl)acrylamide (34)

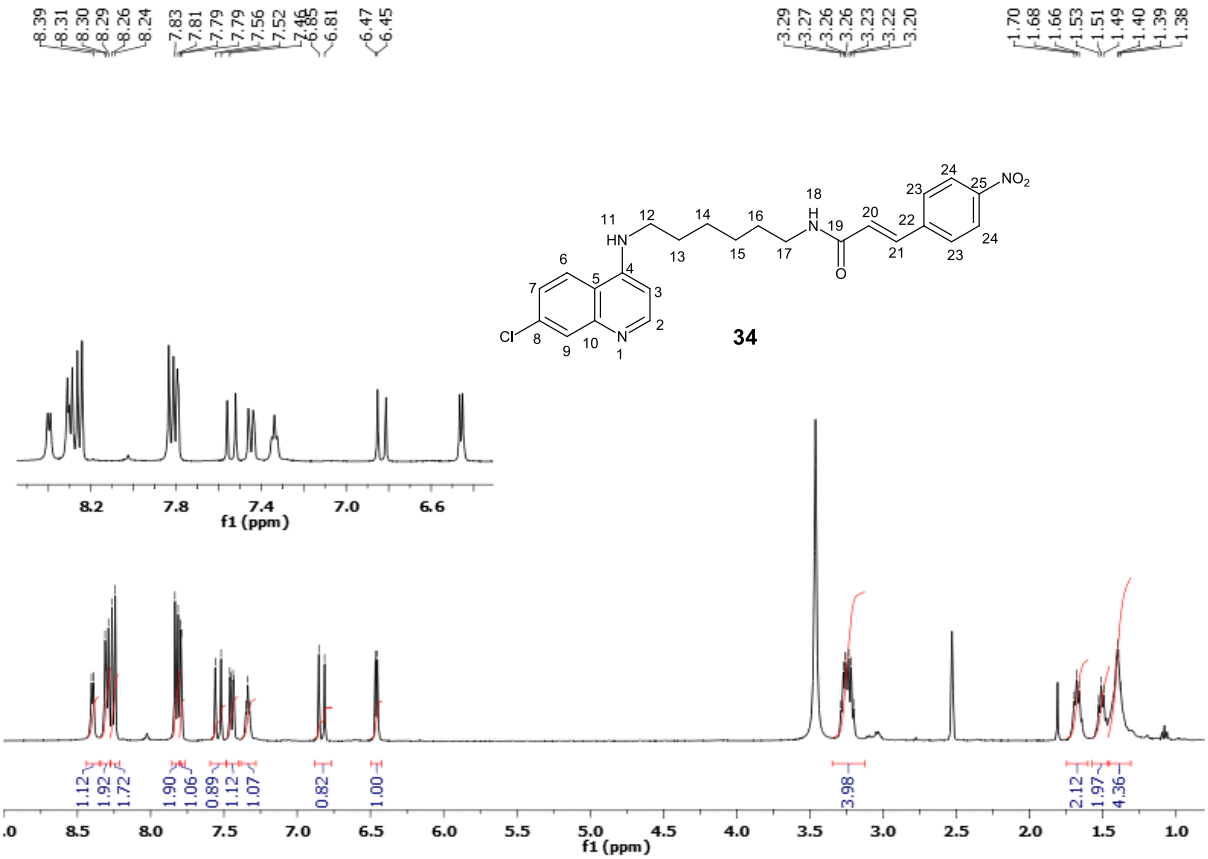

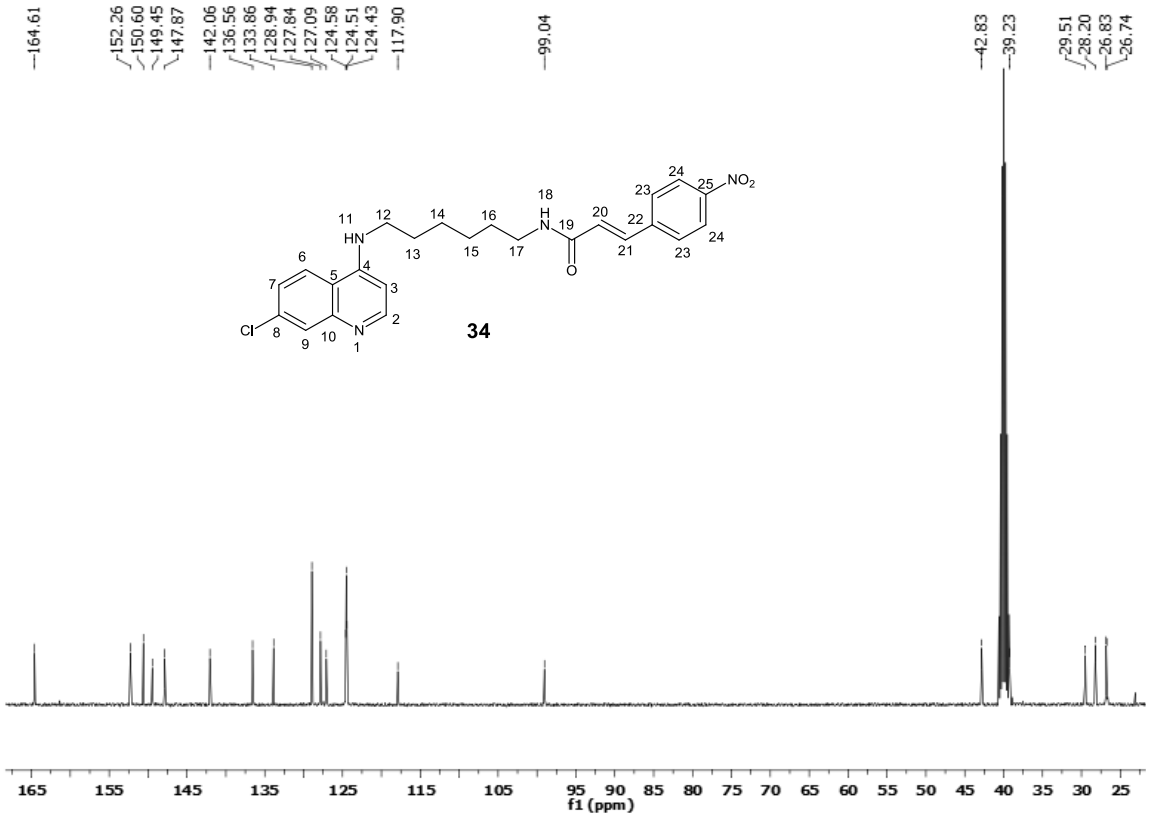

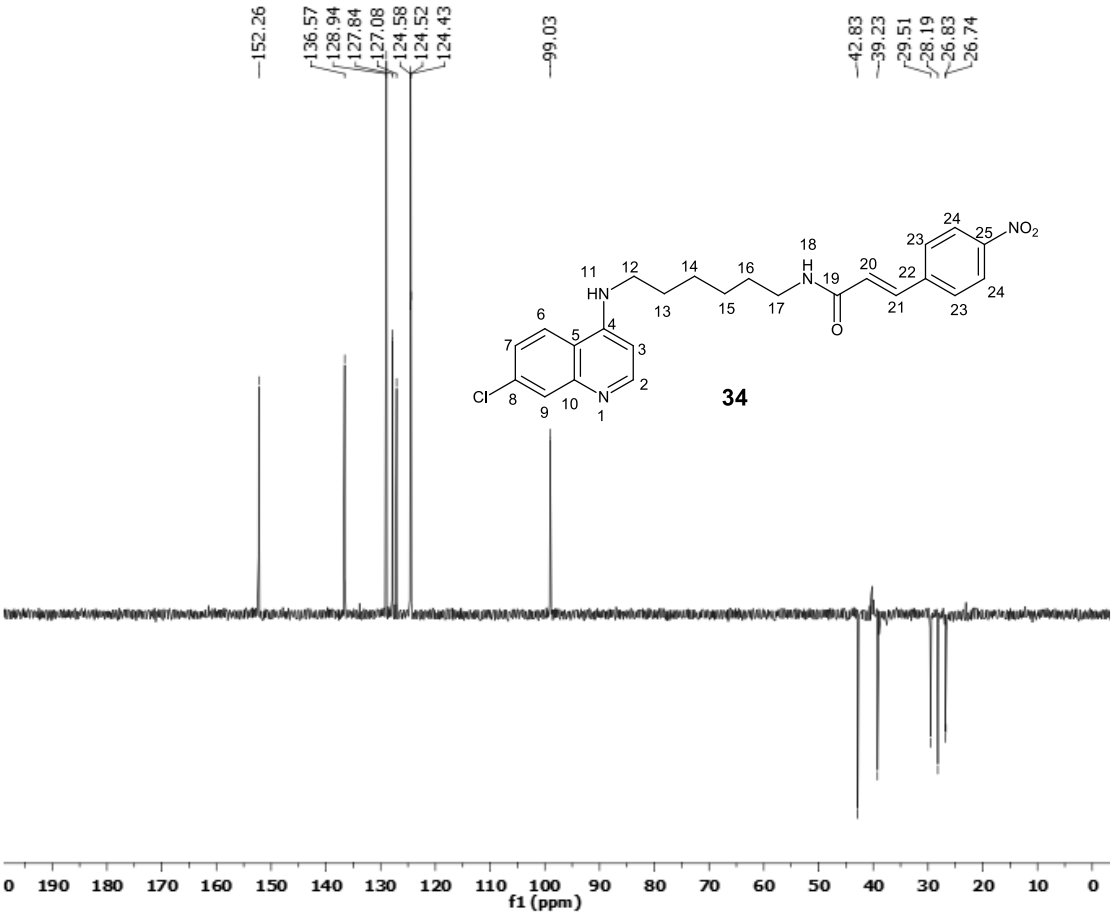

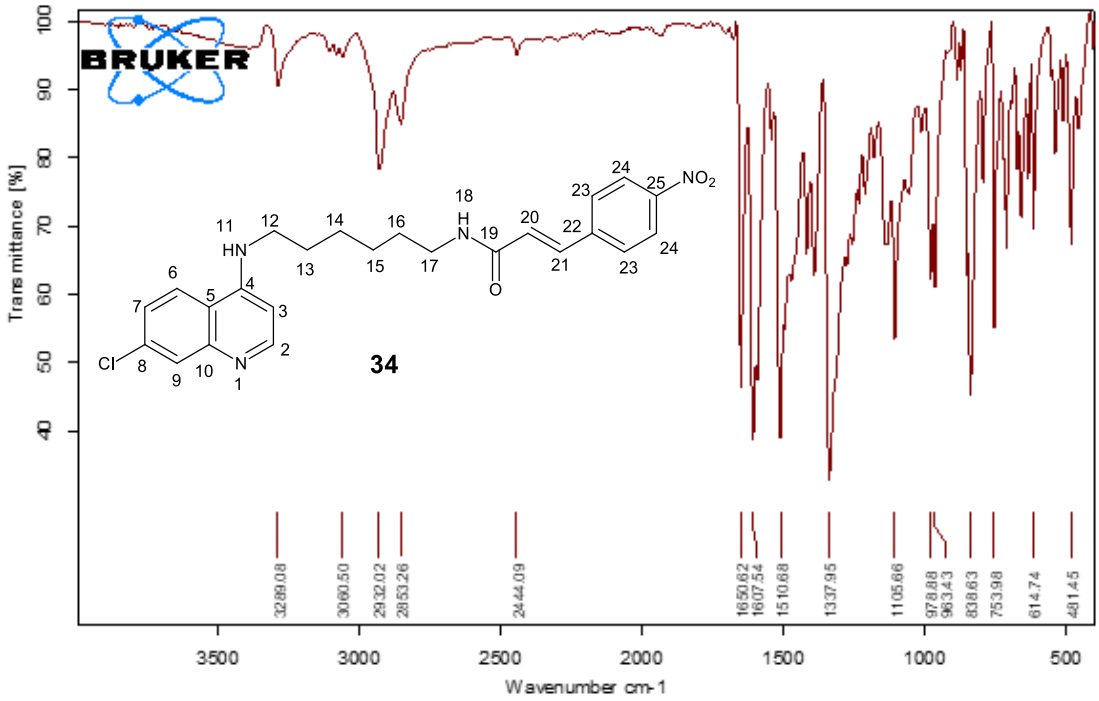

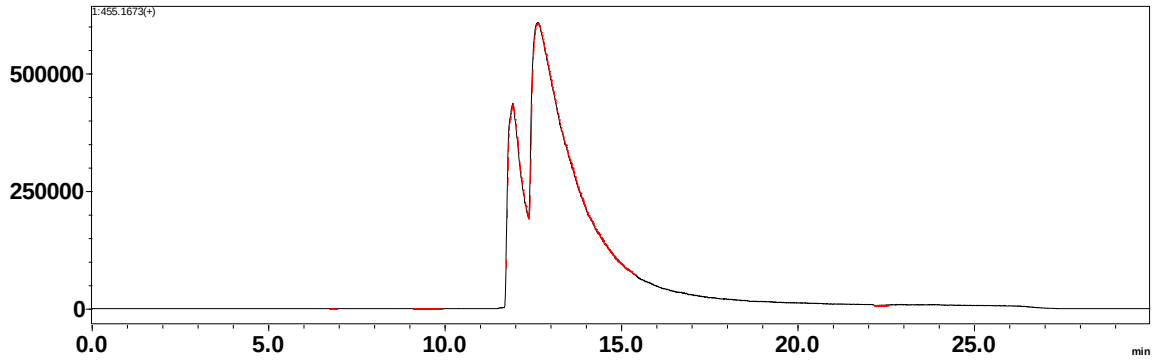

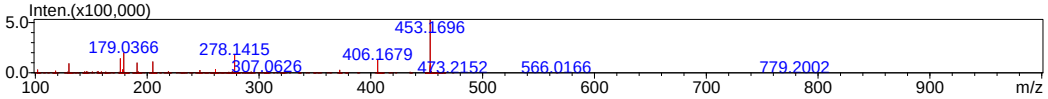

8.12 1H, 13C, DEPT NMR spectra, IR, Chromatogram and mass spectrum of (E)-3-(benzo[d][1,3]dioxol-5-yl)-N-(6-((7-chloroquinolin-4-yl)amino)hexyl)acrylamide (36)